

2010

Synthesis of Novel Glycosylidene-Based Quinolines

Peter H. Dobbelaar
Seton Hall University

Follow this and additional works at: <https://scholarship.shu.edu/dissertations>

 Part of the [Organic Chemistry Commons](#)

Recommended Citation

Dobbelaar, Peter H., "Synthesis of Novel Glycosylidene-Based Quinolines" (2010). *Seton Hall University Dissertations and Theses (ETDs)*. 1483.
<https://scholarship.shu.edu/dissertations/1483>

Synthesis of Novel Glycosylidene-Based Quinolines

A Dissertation

In The Department of Chemistry and Biochemistry submitted
to the faculty of the Graduate School of Arts and Sciences
in partial fulfillment of the requirements for the

degree of

Doctor of Philosophy

In Chemistry

At

Seton Hall University

by

Peter H. Dobbelaar

May 2010

We certify that we have read this thesis and that in our opinion it is adequate in scientific scope and quality as a dissertation for the degree of Doctor of Philosophy.

APPROVED

Signature Cecilia H. Marzabadi, Ph.D.
Dr. Cecilia H. Marzabadi, Advisor

Signature John R. Sowa
Dr. John R. Sowa, Reader

Signature Stephen P. Kelty
Dr. Stephen P. Kelty, Reader and Department Chair
Approved for the Department of Chemistry and Biochemistry

Acknowledgements

I owe a debt of gratitude to my graduate advisor, Dr. Cecilia H. Marzabadi, for her guidance during my studies at Seton Hall University. In addition, I am also grateful for the support of my supervisors, Maryadele J. O'Neil and Patricia E. Heckelman, both of *The Merck Index*, as well as Dr. Cherie B. Koch, my previous supervisor and a former *Merck Index* editor. Their backing was pivotal in obtaining financial assistance through The Merck Research Laboratories Doctoral Program. I thank the past and present leadership of Merck's Department of Medicinal Chemistry, Rahway, NJ for the permission to use their laboratory facilities. I also gratefully acknowledge my Merck sponsor, Dr. Vincent J. Colandrea of Merck Research Laboratories, for his willingness to serve as a mentor and aid in my educational and scientific development. I deeply appreciate the expertise of the following scientists of Merck Research Laboratories: Drs. George A. Doss and Mikhail Reibarkh for both NMR and molecular modeling assistance, Dr. Charles W. Ross III and Kithsiri B. Herath for mass spectrometry support, Eric C. Streckfuss and Craig K. Esser for chromatography suggestions, Dr. R. Scott Hoerrner for assistance with high pressure hydrogenolysis experiments, Dorothy A. Levorse for salt stoichiometry and pKa analysis, and Dr. Yan Lin for discussions involving sugar chemistry. I acknowledge Rita A. Nacchio-Wells and the Merck library staff for the prompt retrieval of non-electronic references. I am grateful to the National Cancer Institute for testing several compounds in their *in vitro* cancer screens. I also thank my friends, Patrick J. Pollard, J.D. and Chris L. Franklin, for their particularly useful discussions as well as Jeremy M. West for technical support. Finally, as I have become

increasingly driven to complete this project, I now understand why so many authors acknowledge the patient understanding of family. I thank my mother, Janet C. Dobbelaar, for encouraging me to continue my education. I dedicate this work to the memory of my grandparents, Janet and Robert O. Schlenker.

Inspiration
Spoken by a True Leader – A Leader of
Character, Competence, and Courage

“Hang tough! Never, ever give up.”

Major Richard D. Winters, Ret.
Easy Company, 506th Parachute Infantry Regiment
101st Airborne Division, US Army
Band of Brothers, WWII

Table of Contents

Acknowledgements	iii
Inspiration	v
List of Tables	ix
List of Schemes	xi
List of Figures	xiii
Abstract	xv
Chapter 1. The Properties and Biological Significance of Carbohydrates	
1. Overview and Historical Perspective	1
2. Physical and Chemical Properties	3
3. Biological Relevance	7
4. Therapeutic Applications	14
5. Glycosidase Inhibitors	18
6. Industrial Importance of Carbohydrates	21
7. Summary	22
Chapter 2. Synthesis of Glucose-Derived Quinolines	
1. Introduction	24
2. Background	
a. Glycals and Spiroanellation Chemistry	33
b. Synthesis of Quinolines Via the Povarov Reaction	39

3. Results	
a. Synthesis of Starting Materials	46
b. Catalyst Screening	47
c. Structural Determination	49
d. Reaction Optimization	53
e. Evaluation of Substituent Effects	62
f. Deprotection Attempts	67
4. Summary	75

Chapter 3. Reaction Scope Expansion

1. Introduction	77
2. Background	
a. Biological Relevance of Arabinose and Galactose	78
b. Scope Expansion Rationale	80
c. Reaction Stereochemistry	81
3. Results	
a. <i>exo</i> -Glycal Dienophiles	83
b. Azadienes	91
c. Further Transformations of Sugar-Derived Quinolines	94
d. Stereochemistry of the Povarov Addition Reaction	99
4. Summary	108

Chapter 4. Biological Evaluation of Selected Compounds	
1. Introduction	110
2. Background	
a. Physiochemical Properties	111
b. Anticancer Screening	113
3. Results	
a. Physiochemical Properties Assessment	114
b. <i>in vitro</i> Anticancer Activity	117
4. Summary	121
Chapter 5. Conclusions	
1. Summary	122
2. Experimentals	126
3. References	149
4. Appendix (NMR spectra)	157

List of Tables

Table 2.0. Catalyst and reaction condition screening.

Table 2.1. Spectral analysis for the spiroanellated tetrahydroquinoline **87Major**.

Table 2.2. Spectral analysis for the spiroanellated tetrahydroquinoline **87Minor**.

Table 2.3. Spectral analysis for the open-ring glycosylidene-derived quinoline **88a**.

Table 2.4. Screening of Povarov reaction conditions involving catalysis by $\text{Sc}(\text{OTf})_3$ at various temperatures.

Table 2.5. Reaction optimization experiments involving addition of molecular sieves and/or 2,6-di-*tert*-butyl-4-methylpyridine **92**.

Table 2.6. Reaction optimization experiments involving a microwave reactor.

Table 2.7. Examination of the electronic effect of *para*-substituted, benzaldehyde-derived imines on the one-pot synthesis of glycosylidene-based quinolines.

Table 2.8. Examination of the electronic effect of *para*-substituted, aniline-derived imines on the one-pot synthesis of glycosylidene-based quinolines.

Table 2.9. Hydrogen balloon debenzylation experiments.

Table 2.10. High pressure, high temperature debenzylation experiments.

Table 2.11. Transfer hydrogenation debenzylation experiments.

Table 2.12. Debzylation experiments utilizing chemical methods.

Table 3.0. Synthesis of arabinose-derived quinolines.

Table 3.1. Synthesis of galactose-derived quinolines.

Table 3.2. Catalyst and reaction condition screening with azobenzene **100**.

Table 3.3. Quinoline *N*-methylation attempts.

Table 3.4. Glycosylation attempts.

Table 3.5. Molecular modeling calculations for both the observed and potential Povarov reaction products.

Table 3.6. Stereoselective reaction condition screening.

Table 4.0. Calculated physiochemical properties of novel glycosylidene-derived quinolines.

Table 4.1. Results from the NCI60 human tumor cell line anticancer drug screen assay.

List of Schemes

- Scheme 1.0. Chemical equations for the processes of (a) photosynthesis and (b) respiration.
- Scheme 2.0. Knapp's approach toward carbohydrate-fused thiazolines.
- Scheme 2.1. DeCastro and Marzabadi's synthesis of oxazoline-fused carbohydrates.
- Scheme 2.2. Talisman and Marzabadi's synthesis of carboethoxy cyclopropanated carbohydrates.
- Scheme 2.3. Somsak's synthesis of an analogue of 2-thiohydantocidin.
- Scheme 2.4. Synthesis of furanoid spironucleosides of oxazolidine-2-thiones and oxazinane-2-thiones.
- Scheme 2.5. Generalized Povarov reaction sequence.
- Scheme 2.6. Currently postulated, non-concerted mechanism for the Povarov reaction illustrated with $\text{BF}_3 \cdot \text{Et}_2\text{O}$ as the Lewis acid catalyst.
- Scheme 2.7. Multicomponent reactions involving glycal addition reported by Jiminez and colleagues.
- Scheme 2.8. First reported Povarov reaction utilizing a glycal derivative as the activated alkene.
- Scheme 2.9. Preparation of quinoline **80**.
- Scheme 2.10. Preparation of glucose-fused quinoline **82**.
- Scheme 2.11. Synthesis of the essential *exo*-glycal intermediate.
- Scheme 2.12. Synthesis of benzanilines.
- Scheme 2.13. Benzyl ether deprotection of glucose-based quinoline **88a**.
- Scheme 3.0. Ishanti and Kobayashi's stereoselective Povarov reaction.
- Scheme 3.1. Synthesis of the arabinose-derived *exo*-glycal.
- Scheme 3.2. Synthesis of the arabinose-spiroanellated tetrahydroquinoline.

Scheme 3.3. Debenzylation of arabinose-based quinolines **110a** and **110b**.

Scheme 3.4. Synthesis of the galactose-derived *exo*-glycal.

Scheme 3.5. Debenzylation of galactose-based quinoline **115a**.

Scheme 3.6. Povarov reaction attempts with ethenyl *exo*-glycal **118**.

Scheme 3.7. Povarov reaction attempts with imine **99**.

Scheme 3.8. Formation of the hydrochloride salt of **93a**.

Scheme 3.9. Deprotection of spiroanellated tetrahydroquinoline **87Major**.

List of Figures

Figure 1.0. Structural representations of D-glucose.

Figure 1.1. Mutarotation of glucose in water at 31 °C.

Figure 1.2. Equilibrium chair conversions of glucose.

Figure 1.3. Practical illustration of the anomeric effect.

Figure 1.4. Glucose-based storage carbohydrates.

Figure 1.5. Repeating units of polysaccharide polymers used by organisms for structural support.

Figure 1.6. Structural representations of (a) a generic nucleotide and (b) nucleotide sugars.

Figure 1.7. Several carbohydrate-based therapeutics.

Figure 1.8. Macrolide antibiotics.

Figure 1.9. Anticancer and antiviral carbohydrate-based drugs.

Figure 1.10. Generic illustration of the activity of a glycosidase enzyme.

Figure 1.11. Carbohydrate-based glycosidase inhibitors.

Figure 1.12. Azasugar glycosidase inhibitors.

Figure 2.0. Carbohydrate-based diabetes drugs.

Figure 2.1. Examples of carbohydrate-spiro heterocycles with glycosidase inhibitory activity.

Figure 2.2. Examples of carbohydrate-fused or C-linked heterocycles with glycosidase inhibitory activity.

Figure 2.3. Structural representation of quinoline.

Figure 2.4. Medicinally significant quinoline-based compounds.

Figure 2.5. *Stauranthus* quinoline alkaloids.

Figure 2.6. Quinoline-glucose hybrids evaluated as DNA intercalators.

Figure 2.7. Structural representation of a generic glycal.

Figure 2.8. Comparison of generic *endo*- and *exo*-glycals.

Figure 2.9. Diastereomers resulting from Povarov condensations with dihydrofuran and dihydropyran.

Figure 2.10. Tentative structural assignment of Povarov reaction side-products.

Figure 2.11. Structure of the organic base, 2,6-di-*tert*-butyl-4-methylpyridine.

Figure 2.12. Tentative structural assignments of the products formed from reaction conditions in (a) entries 1-5 and (b) entries 6-9 of Table 2.10.

Figure 3.0. Arabinose and an antiviral derivative.

Figure 3.1. Structures of galactose and the disaccharide, lactose.

Figure 3.2. Alternate azadienes.

Figure 3.3. Structures of the chiral ligands, BINAP and BINOL.

Abstract

Synthesis of Novel Glycosylidene-Based Quinolines

Peter H. Dobbelaar

Doctor of Philosophy in Chemistry

Seton Hall University

Dr. Cecilia H. Marzabadi, Advisor

Carbohydrates and their derivatives are involved in a wide array of biological processes and are crucial for the survival of living entities. As a result, sugar-based compounds have become attractive scaffolds for drug design. In addition, quinoline derivatives have shown promise in the treatment of numerous health conditions such as cancer and life-threatening infections and are therefore of interest from a therapeutic point of view. Consequently, we desired to prepare molecules that contained carbohydrates conjugated to these heterocycles. Such novel sugar-derived quinoline compounds were anticipated to have pharmacological activity as anticancer DNA intercalating agents. Based upon common structural features, we surmised that they may also possess glycosidase inhibitory activity.

The focal point of our research was to determine a synthetic route for the preparation of novel sugar-based quinolines. We have developed a facile, one-pot method based upon the Povarov reaction to prepare C-glycosylated quinolines. We have determined that this reaction proceeds through sugar-spiroanellated tetrahydroquinoline

intermediates. These compounds subsequently oxidize and undergo sugar ring opening to form the fully aromatized quinolines. Extensive catalyst screening and reaction optimization studies were conducted, and NMR experiments have confirmed the structures of both the spiro and open-ring sugar-linked quinolines. This one-pot methodology has been efficiently employed with several sugar *exo*-glycals and a series of *para*-substituted benzanilines to prepare novel open-ring, glycosylidene-derived quinolines. Deprotection experiments were carried out in order to determine conditions to remove the benzyl protective groups. The successful debenylation chemistry demonstrates that this one-pot, scandium triflate-catalyzed Povarov reaction followed by manganese dioxide oxidation is an expeditious way to obtain novel C-glycosylated quinolines.

The physiochemical and anticancer properties of several carbon-linked sugar-derived quinolines have been assessed. Results from computer calculations lead us to predict that the debenzylated compounds should exhibit favorable bioavailability. Some of the glucose analogues have been tested in the NCI60 human tumor cell line anticancer screen. Although several cell lines experienced modest growth inhibition, the glycosylidene-based quinolines do not possess sufficient anticancer activity to warrant dose titration studies.

Chapter 1

The Properties and Biological Significance of Carbohydrates

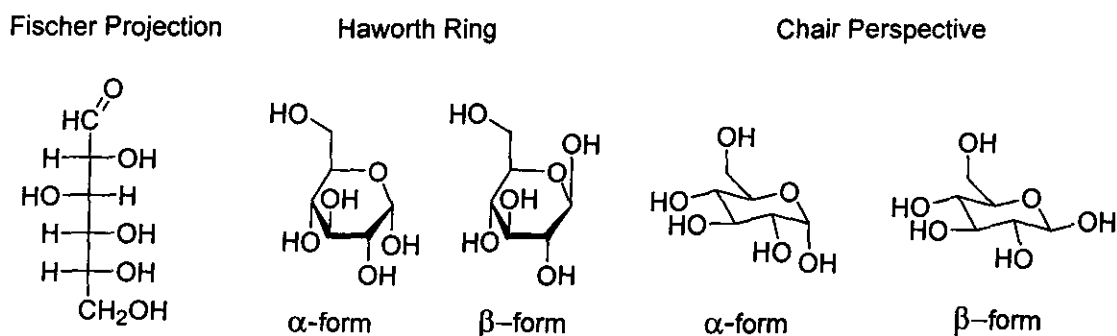
1.1. Overview and Historical Perspective

Carbohydrates are the most abundant biomolecules on Earth. Saccharides and their derivatives are involved in a wide array of biological processes and are therefore crucial for the survival of living entities. Carbohydrates are a unique family of polyfunctional molecules, and the chemistry of these compounds can be enormously complex. They exist as monosaccharide building blocks that are linked together in almost limitless ways to form oligosaccharides and polysaccharides. Most monosaccharides are predominately cyclized polyhydroxy aldehydes and ketones with the general formula $C_n(H_2O)_n$. Even the simplest monosaccharides possess multiple asymmetric carbons, resulting in a variety of isomers.¹ Although the stereoisomeric diversity and oftentimes problematic chemistry of carbohydrates present numerous challenges, their widespread presence in biological systems makes them attractive targets for continued research, especially in the field of therapeutics.² In addition, carbohydrate products are utilized in the food, clothing, and agrochemical industries.³ Today a renewed focus on carbohydrates is necessary to understand the relevance of the interrelationships among many disciplines of science, including organic chemistry, cellular and molecular biology, and biochemistry.

The significance of carbohydrates has been recognized for hundreds of years, dating back to the times of the Persians and Arabians. These ancient civilizations were familiar with grape sugar, which centuries later was given its current name, glucose, by Dumas in 1838. Despite methodical studies by both Dumas and Kekule, it was the pioneering work of the German scientist Emil Fischer in the late 19th and early 20th centuries that rapidly advanced the ever-growing field of carbohydrate chemistry.³

Emil Fischer was the key figure in the development of carbohydrate chemistry because he was instrumental in the transformation of the field from a study of syrups and gums to an accepted scientific discipline. Fischer established the fundamental groundwork that provides the basis of carbohydrate chemistry. He successfully elucidated the structure of D-(+)-glucose by utilizing both chemical reactivity observations as well as polarimetric methods. Several depictions of the structure of glucose⁴ are illustrated in Figure 1.0. One such structural representation, the Fischer projection, is named in his honor. In recognition of his achievement for the structural work surrounding glucose, Fischer was awarded the second Nobel Prize for Chemistry in 1902.³

Figure 1.0. Structural representations of D-glucose.

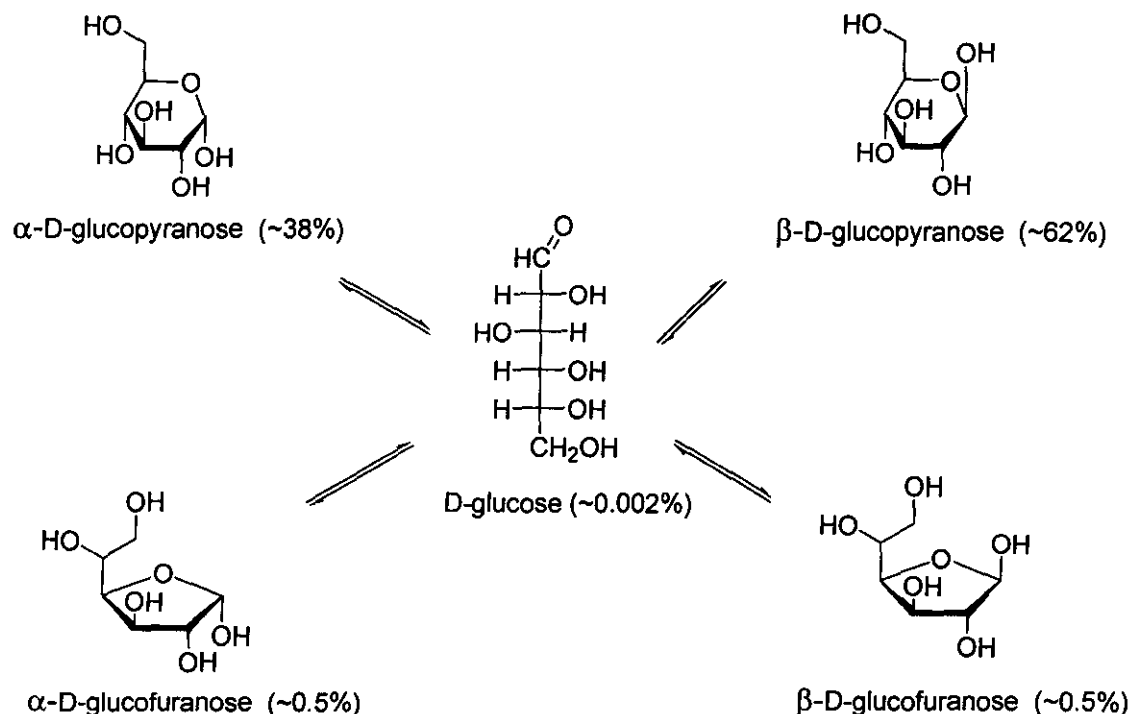


The knowledge associated with the field of carbohydrates has expanded rapidly since Fischer's early studies. Other scientists, such as Hudson and Haworth, have also made key contributions to this area of chemistry. Prior to the 1970s, carbohydrate chemistry was considered to be an isolated field of study practiced by specialists. Since that time, this discipline has been mainstreamed into the realm of organic chemistry, and many of the resulting developments have been the work of organic chemists.⁵

1.2. Physical and Chemical Properties

Carbohydrates possess several unique physical and chemical properties that differentiate them from other types of organic compounds. One such property is the phenomenon of mutarotation, which was first observed by Fischer's students, Deidi and Heinz, in 1891.⁵ Mutarotation is the change in optical rotation of a monosaccharide solution over time as an equilibrium is reached between the cyclic hemiacetal or hemiketal form and the linear aldose or ketose containing the free carbonyl group. Six-membered cyclic pyranoses and five-membered furanoses usually predominate over their linear form counterparts in solution. In addition, cyclic pyranose and furanose anomers also exist, and these isomers differ by the configuration of the hydroxyl group at the anomeric carbon. Each isomer has its own characteristic optical rotation, and the rotation of the solution therefore changes until equilibrium is established between the interconverting forms.³ Figure 1.1 illustrates the process of mutarotation with D-glucose.⁶

Figure 1.1. Mutarotation of glucose in water at 31 °C.



Another equilibrium process that is characteristic of sugars is the conformational conversion of the cyclic ring. Much like cyclohexane, monosaccharides can undergo an equilibrium between chair conformations. Figure 1.2 illustrates the process with β -D-glucose. The preferred 4C_1 conformation has all of the hydroxyl substituents in the equatorial position. Upon conversion via a boat conformation, the 1C_4 form has all of the hydroxyl groups in the axial position. From an energetics perspective, the 4C_1 conformation is significantly more stable.⁵ However, a stereoselective effect exists that causes a heteroatomic substituent to favor the axial orientation instead of the equatorial orientation. This tendency for the formation of the α -anomer is known as the anomeric effect. This effect, originally noted by Edward⁷ and later extensively studied by

Lemieux,⁸ virtually ensures that an electronegative atom at the anomeric carbon will take the axial position as illustrated in Figure 1.3. Although the anomeric effect has many potential theoretical explanations, its influence is important for determining the energetics as well as the three-dimensional shape of many polysaccharides. Therefore, the anomeric effect impacts both the molecular configuration and biological function of sugar derivatives.⁵

Figure 1.2. Equilibrium chair conversions of glucose.

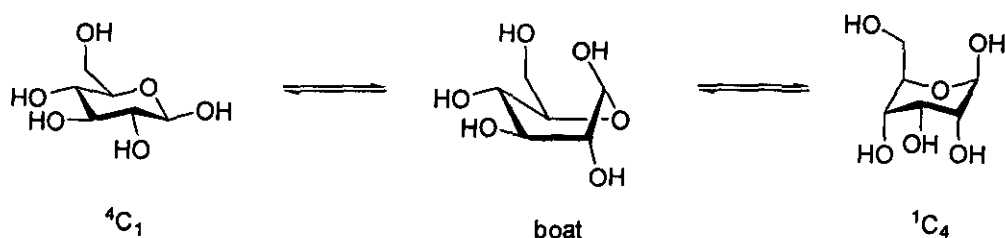


Figure 1.3. Practical illustration of the anomeric effect.



Several monosaccharides are readily obtainable from the environment, but many carbohydrates are not available in bulk quantities from natural sources. This requires that chemists must turn to synthesis as an alternate means of supply. However, the reactivity

of the functional groups of carbohydrates renders their synthetic manipulations particularly challenging. The free hydroxyl groups help to make the sugar water soluble and frequently have an undesired effect on the intended reaction.⁵ As a consequence, protecting groups are often introduced to mask particular functionalities during a reaction. The use of protective groups is essential to ensure that the desired chemical reaction occurs at the desired atom. Commonly, hydroxyl groups are protected as esters and acetates as well as benzyl and silyl ethers. The appropriate protecting group is usually chosen based upon the subsequent reaction sequence, and includes such considerations as sterics, robustness, and removal conditions.⁹ The site or location of transformation is also an issue that needs to be considered, especially since sugars contain numerous stereocenters. Although the utilization of protecting groups is necessary to carry out chemistry on carbohydrates, it adds extra steps to the synthetic sequence. Common problems associated with protection and deprotection chemistry also include additional purifications and the potential for loss of material. As a direct result of the challenges posed by both stereochemistry and protection/deprotection chemistry, the development of the field of carbohydrate chemistry was slower than other scientific disciplines.

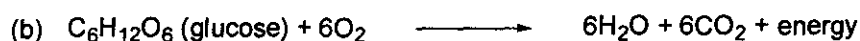
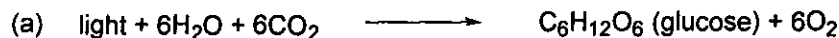
The chemistry of sugars is exceedingly complex, and carbohydrate chemists need to evaluate a variety of properties when designing syntheses and conducting structural analyses. In addition to potential conformational changes, chemists must carefully consider protection strategies to mask hydrophilic hydroxyl groups. Reaction conditions must preserve stereochemistry while avoiding epimerization and unwanted side reactions such as ring opening events. In addition, carbohydrate chemists have come to realize that

the three dimensional properties of sugars are essential from a biochemical perspective. Modern analytical methods can determine the position and configuration of linkages between monosaccharide units while glycosylation chemistry exists to synthesize oligosaccharides in a stereoselective manner. These techniques now permit a laboratory synthesis that produces the same compound as the natural preparation. This crucial development allows for a more systematic study of the biological properties of sugars.⁶

1.3. Biological Relevance

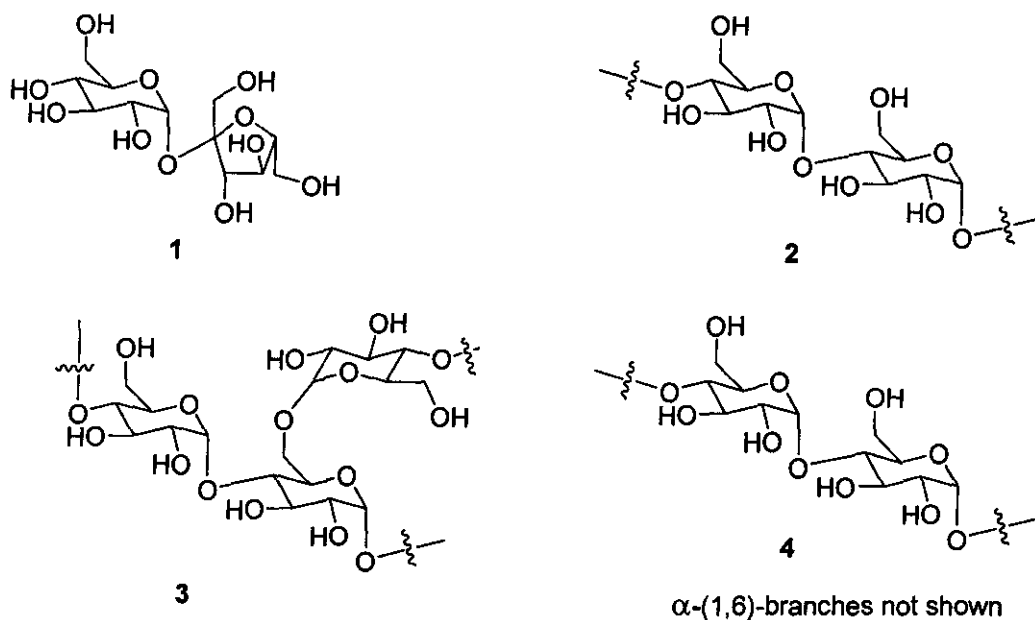
Carbohydrates are a diverse and versatile class of functional natural products, and their primary significance is attributed to their major importance in numerous, crucial biological functions. Many processes required to maintain life, such as biochemical reactions, involve carbohydrates and their derivatives. D-glucose is central to several of these pathways. For example, it is the major fuel of most organisms and occupies an essential position in both anabolic and catabolic reactions. Glucose is relatively rich in energy, and it is a remarkably versatile building block for more complex biomolecules. Glucose is the key product of photosynthesis carried out by plants in which energy from the sunlight is converted into chemical bonds (Scheme 1.0a). It is also the essential starting material for respiration, the process by which energy stored in chemical bonds is extracted by animals (Scheme 1.0b). These complimentary metabolic pathways required for living organisms to sustain life are therefore dependent upon glucose.¹

Scheme 1.0. Chemical equations for the processes of (a) photosynthesis and (b) respiration.



In addition to catabolic processes that break down compounds, glucose is also involved in anabolic pathways responsible for the synthesis of important biomolecules. For instance, glucose may be stored as sucrose **1** or more complex polysaccharides in both higher plants and animals (Figure 1.4).¹ Sucrose, commonly known as table sugar, is the most abundant disaccharide in the biological world.¹⁰ Starch, a mixture of the α -amylose **2** and amylopectin **3** polysaccharides, is used in plants for energy storage and is concentrated in roots, tubers, rhizomes, fruits, and seeds. Glycogen **4** is a non-linear polymer of D-glucose that is the mammalian counterpart to starch. It is primarily stored in the muscle and liver.⁵ Compounds such as sucrose, starch, and glycogen are examples of abundant energy storage carbohydrates, and their widespread presence in nature indicates that glucose storage is an important strategy for both plants and animals.

Figure 1.4. Glucose-based storage carbohydrates.



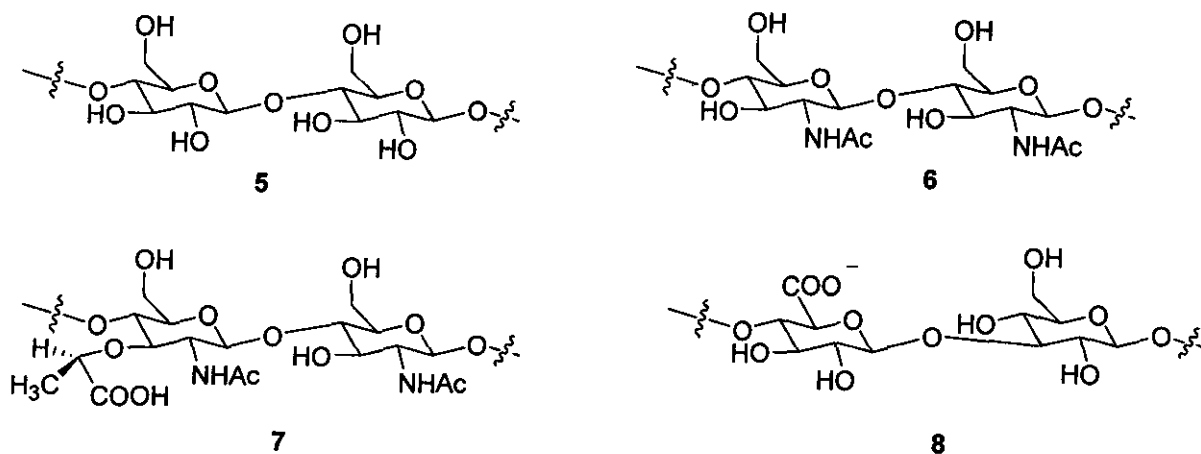
The regulation of blood glucose levels in humans is a significant physiological process required to properly maintain carbohydrate homeostasis. In addition to its role as the principle source of energy for the cells and tissues of the body, glucose is also the primary energy source for the brain. The human body is dependent upon glucose availability for both physical and psychological processes. The uptake of glucose from the blood is regulated by the hormone insulin. This polypeptide is produced by pancreatic β -cells and is released into the bloodstream in response to rising glucose concentrations. Insulin also triggers the conversion of glucose into the polysaccharide glycogen. Glucagon is a polypeptide hormone produced by the α -cells of the pancreas, and it acts in a manner opposite to that of insulin. When low blood concentrations of glucose and insulin are detected, glucagon stimulates hepatic glucose output via the breakdown of glycogen. An individual's inability to regulate glucose levels may result in

diabetes mellitus, a globally prevalent health condition. Diabetes is a chronic metabolic disorder characterized by high blood glucose levels, and it is usually the result of defective insulin secretion or function. Both insulin and glucagon hold crucial functions as hormones involved in feedback loops responsible for the regulation of glucose in the bloodstream through the modulation of its metabolic pathways.¹

Aside from their involvement in energetic pathways necessary for the maintenance of homeostasis in living entities, carbohydrates also play a key role in providing structural support for viable organisms (Figure 1.5). For instance, cellulose **5** is the main component of the cell wall of plants and is the most abundant polymer on Earth. Cellulose is a linear polysaccharide that consists of D-glucose units joined by β -1,4-glycoside bonds. Although humans do not have the enzyme required for the digestion of cellulose, many bacteria have the β -glycosidases necessary to break down the cellulose in wood and other plant material. Chitin **6**, on the other hand, is the cellulose of the animal world. Chitin is a polymer of *N*-acetyl-D-glucosamine that is present in the hard exoskeletons of insects, the shells of crustaceans, and the cell walls of many mushrooms. The cell wall of many bacteria consists of murein **7**, an aminosugar polymer commonly called peptidoglycan. It contains *N*-acetyl-D-glucosamine and *N*-acetyl-D-muraminic acid polysaccharide units cross-linked by short peptide chains. In multicellular animals, the extracellular matrix holds together cells and provides a medium for the diffusion of substances. It is composed of an interlocking network of heteropolysaccharides known as glycosaminoglycans. Hyaluronic acid **8** is a key component of the extracellular matrix as well as cartilage and tendons.⁶ From these examples, it is apparent that many organisms synthesize functional carbohydrate-based

polymers not only to provide structural support, but also to create a barrier from the external environment.

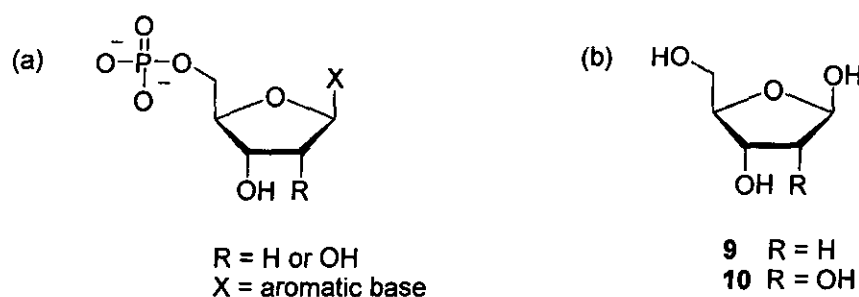
Figure 1.5. Repeating units of polysaccharide polymers used by organisms for structural support.



Sugars are also key structural components of nucleic acids, a class of biomolecules that serve to carry out a diverse set of functions in the cell. These nucleotide polymers consist of three types of monomer units: a pentose sugar, a phosphoric acid functionality component, and a heterocyclic aromatic amine base derived from either purine or pyrimidine (Figure 1.6a). The sugar for deoxyribonucleic acids (DNA) is 2-deoxy-D-ribose **9** while D-ribose **10** is the sugar for ribonucleic acids (RNA) (Figure 1.6b). DNA is the biopolymer that functions as the carrier of genetic information, and messenger RNA is the intermediate that conveys this coded genetic information from DNA to the ribosomes for protein synthesis. In addition, nucleotides also are incorporated into enzyme cofactors, serve as cellular secondary messengers, and store chemical energy in the form of adenosine triphosphate (ATP).¹ There is

considerable overlap in both the roles and functions of the different classes of biomolecules, as sugars are integrated into the structure of nucleic acids which are, in turn, directly linked to proteins.

Figure 1.6. Structural representations of (a) a generic nucleotide and (b) nucleotide sugars.



Many carbohydrates in the cell are covalently bound to a protein or lipid, and these carbohydrate containing biomolecules are located primarily on the cell surfaces. Such hybrid molecules, known as glycoconjugates, are the subject of a field of study now referred to as glycobiology. The importance of glycobiology has been established only in the last quarter century after scientists have studied the role that these molecules play in cellular processes. However, glycobiology has quickly become an active and exciting area of biochemistry, despite the fact that the biological advantages to linking oligosaccharides to proteins and lipids are still not fully understood. Although many theories have been proposed, it is evident that oligosaccharides mediate specific events and modulate biological processes.¹¹

Glycoproteins and glycolipids are crucial to a variety of diverse roles, including cell signal transduction, cellular recognition, and the initiation of both bacterial and viral

infections. For instance, oligosaccharide labels on glycoconjugates influence levels of circulating hormones and blood cells as well as the rate of peptide hormone degradation.¹ Many cell surface and extracellular proteins contain oligosaccharides that are recognized by lectins. These plasma membrane lectins, commonly referred to as selectins, bind to carbohydrate chains in the extracellular matrix or on the surface of other cells in order to mediate recognition, communication, and adhesion. In addition, the binding of both bacterial and viral pathogens to their desired cellular targets occurs via lectins.¹² This is true for such pathogens as *Vibrio cholera* and *Bordetella pertussis*. The sugar coatings of plasma membrane bound proteins are for self-recognition purposes, and they act as biochemical markers, or antigenic determinants, in the blood group substances. The lipopolysaccharides on the outer membranes of *Escherichia coli* and *Salmonella typhimurium* are the targets of the vertebrate immune system in response to bacterial infections.¹ These diverse and varied examples indicate that organisms are reliant upon oligosaccharides and glycoconjugates to conduct the essential cellular processes of recognition, adhesion, and communication.

The growing appreciation for the importance of oligosaccharides and their derivatives has resulted in a vast amount of information that suggests they are involved in processes that are both trivial and crucial for the survival of organisms. Carbohydrate functions include energy regulation and homeostasis, structural support, and cellular communication. These important findings have led to the elucidation of biosynthetic reactions and enzyme control mechanisms. Numerous fundamental discoveries by primary investigators have resulted in many significant developments in medicinal chemistry. As the roles that carbohydrates play in biological processes and diseases

become better understood, tremendous opportunities exist for the development of new carbohydrate therapeutics.¹¹ Areas of focus include, but are not limited to, bacterial and viral infections, cancer, immunity, and metabolic disorders such as diabetes and obesity.¹³

1.4. Therapeutic Applications

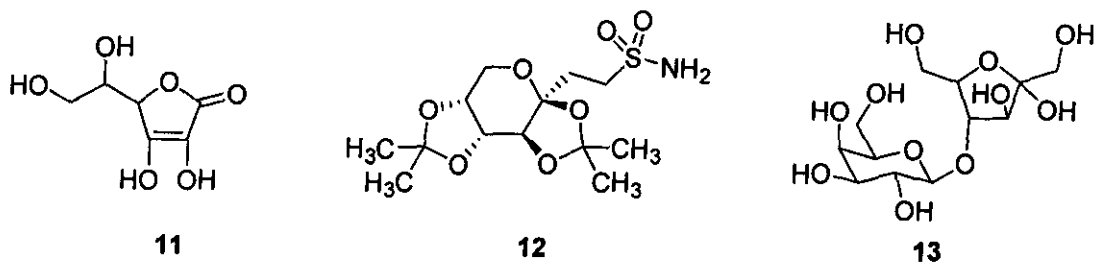
The pharmacokinetic properties of absorption, distribution, biotransformation, and excretion are important areas of focus in the field of drug discovery, especially when dealing with sugar-based compounds.¹⁴ Incorporation of a sugar moiety onto a drug candidate often impacts the compound's physiochemical properties.¹⁵ Furthermore, many natural products, including those with a saccharide moiety, can typically be modified into drug-like molecules with favorable absorption and metabolic properties. In fact, the biological prevalence and favorable bioavailability of carbohydrates make stable sugar derivatives attractive scaffolds for drug design.²

The ability to generate structure activity relationship (SAR) data while balancing stability, solubility, molecular weight, lipophilicity, and metabolism is extremely important in the hit to lead process. Although high throughput methodology and combinatorial libraries hold many advantages for drug discovery, natural product modification has the potential to provide improved structural diversity. Often, sugar-based compounds have enhanced activity against the specified target. In many cases, this can be attributed to structural similarities to endogenous ligands, especially if the ligand possesses a carbohydrate moiety.² Therefore, molecules with a carbohydrate scaffold are

excellent targets for new chemical entities with potentially favorable pharmacological properties.

A variety of natural products and derivatives of natural products that contain a carbohydrate moiety have shown utility in the treatment of human medical conditions. Several therapeutically beneficial compounds (Figure 1.7) can be classified as derivatives of structurally simple carbohydrates. For instance, one such example is the physiological antioxidant, ascorbic acid **11**. This monosaccharide, also known as vitamin C, is an important dietary supplement that is necessary to prevent the deficiency syndrome scurvy.¹⁶ The sulfamate substituted monosaccharide, topiramate **12**, is a structurally distinct antiepileptic that is also used to treat migraine headaches.¹⁷ Yet another illustration of a structurally simple carbohydrate-based therapeutic compound is the synthetic disaccharide, lactulose **13**. This compound is composed of lactose and glucose and has been used as a treatment for both hepatic coma and chronic constipation.⁴

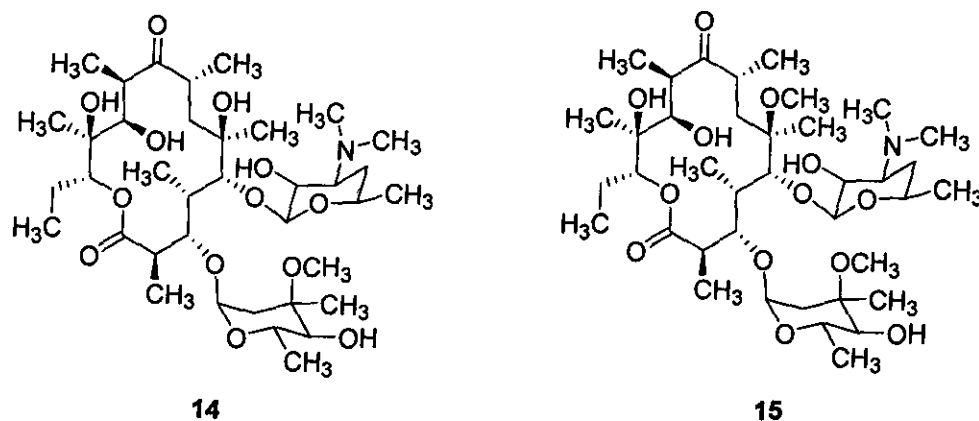
Figure 1.7. Several carbohydrate-based therapeutics.



Natural products that contain a carbohydrate component also serve as important antibiotics. Macrolide antibiotics (Figure 1.8), produced as secondary metabolites of soil

microorganisms, are polyfunctional molecules that contain at least one aminosugar. The natural product erythromycin **14** is one of the first known macrolides and has been an effective treatment for a variety of bacterial infections.¹⁸ The semisynthetic macrolide clarithromycin **15** is a well-tolerated derivative of erythromycin that exhibits similar activity against pathogenic bacteria.¹⁹ These representative macrolides are just a sampling of the diversity of carbohydrate-based antibiotics and illustrate the potential benefit of natural product modification. Other examples of antibiotic classes that consist of a carbohydrate-based scaffold include aminoglycosamides, avermectins, and analogues of streptomycin.¹³

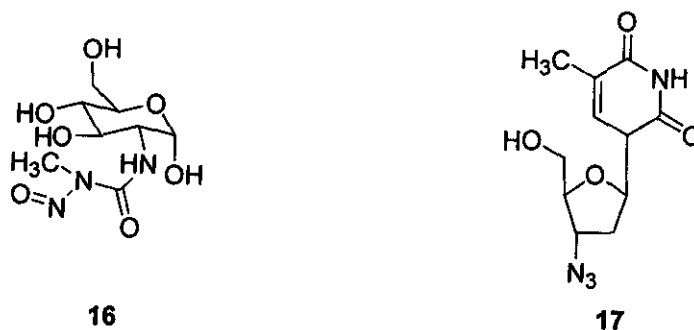
Figure 1.8. Macrolide antibiotics.



Carbohydrate-based natural products and their synthetic derivatives are also useful in the treatment of potentially fatal diseases such as cancer and HIV (Figure 1.9). Streptozocin **16** is a glucose derivative isolated from the fermentation broth of *Streptomyces achromogenes*. This compound is an antineoplastic and diabetogenic

agent.²⁰ Azidothymidine 17, commonly referred to as AZT, is a pyrimidine nucleoside analogue. This synthetic pentose derivative is a reverse transcriptase inhibitor that is prescribed as an antiretroviral.²¹ The functional specialization of these and other biologically active carbohydrate derivatives has brought about improved treatments for both cancer and life-threatening viral infections.

Figure 1.9. Anticancer and antiviral carbohydrate-based drugs.

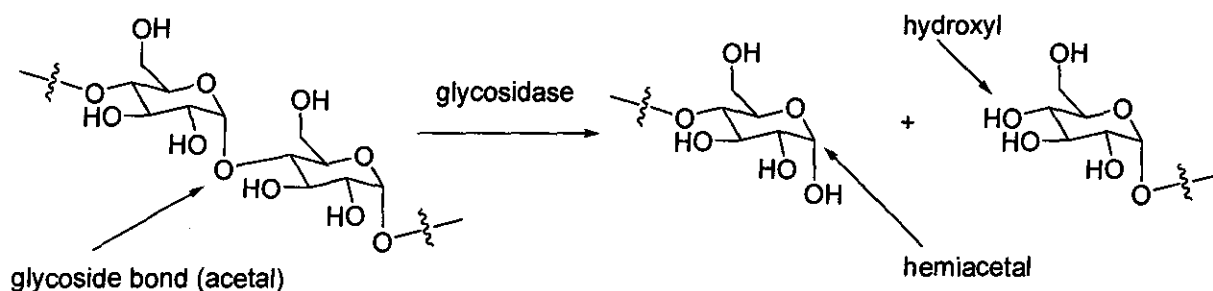


Carbohydrate-based therapeutics are well known for their ability to successfully treat human disease. The provided examples illustrate the fact that carbohydrate derivatives possess the biological activity as well as the pharmacokinetic properties necessary to be beneficial drugs. The study of natural products and their synthetic derivatives has been crucial for the development of novel antibacterial, antiviral, and anticancer agents. Sugar-based compounds must be utilized in the exploitation of both new and existing targets in order to discover future novel medicines.

1.5. Glycosidase Inhibitors

Perhaps one of the most promising areas of research involving carbohydrates is the study of glycosidase inhibitors. Both pharmaceutical companies and academic laboratories have recognized the importance of glycosidase inhibitors because of their biological relevance. Glycosidases are enzymes which catalyze glycosidic bond hydrolysis (Figure 1.10). A glycoside bond is a covalent linkage between two monosaccharide units that results in the formation of an acetal from the hemiacetal of one sugar and the hydroxyl group of another sugar molecule.¹ Currently there are more than 2,000 identified glycoside hydrolases which are classified into 97 different families.²² The sheer number of presently known glycosidases indicates that these enzymes impact numerous, crucial biological functions and thus warrant further study.

Figure 1.10. Generic illustration of the activity of a glycosidase enzyme.

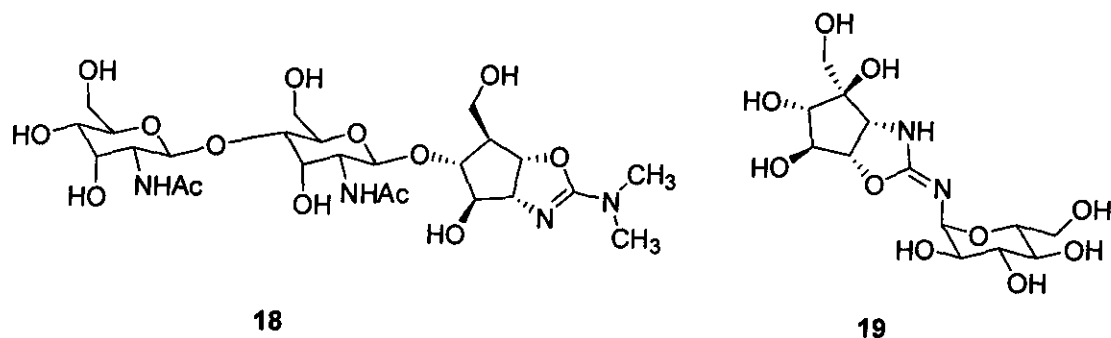


Glycosidases are central to a wide variety of biological anabolic and catabolic processes, such as digestion, the synthesis of glycoproteins, the catabolism of glycoconjugates, quality control of the endoplasmic reticulum (ER), and ER-associated

degradation of glycoproteins. The blockade or modulation of these functions may prove beneficial from a therapeutic point of view.²³ Small molecules designed as reversible or irreversible inhibitors could slow down or prevent glycoside bond hydrolysis and thus modify a specific biochemical process. Potent synthetic glycosidase inhibitors show promise as fungicides and insecticides in the agricultural industry. Successfully designed inhibitors have the potential to treat numerous metabolic and genetic disorders such as diabetes, obesity, and lysosomal storage diseases. They can also be used as therapeutic agents for cancer as well as viral, bacterial, and fungal infections.²⁴

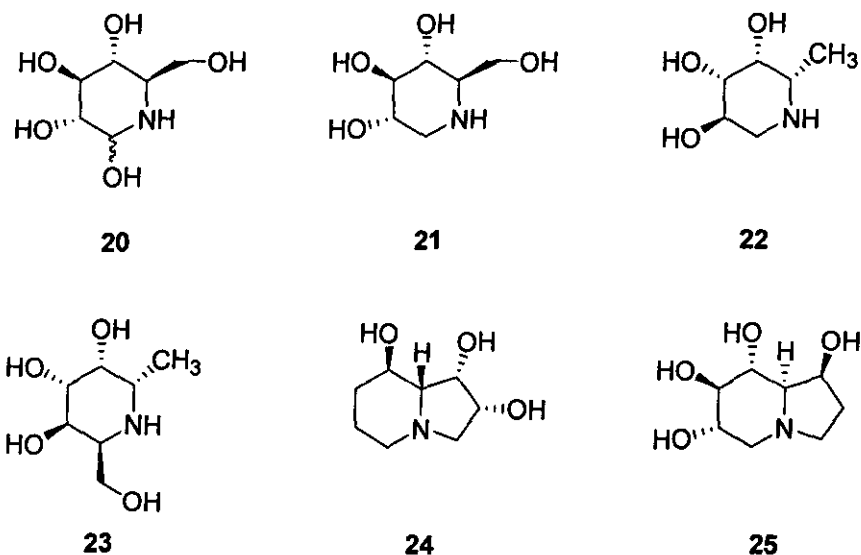
Allosamidin²⁵ **18** and trehazolin²⁶ **19** (Figure 1.11) are both heterocycle bearing carbohydrates with strong inhibitory activity toward chitinases. These compounds are capable of inhibiting the biosynthesis of the polysaccharide chitin and have been utilized as agricultural insecticides and fungicides. The inhibitory activity of these compounds has been correlated with their ability to mimic the glycoside hydrolysis transition state. In addition, the heterocycle portion of the molecule aids in the binding process through hydrogen bonding to amino acid residues within the active site of the enzyme pocket. Studies surrounding both allosamidin and trehazolin demonstrate that the disruption of chitin biosynthesis can have profound biological effects.²⁷

Figure 1.11. Carbohydrate-based glycosidase inhibitors.



Many potent glycosidase inhibitors are classified as azasugars (Figure 1.12), a group of carbohydrate derivatives in which the ring oxygen is replaced by nitrogen. This class of polyhydroxypiperdines and polyhydroxypyrrolidines is represented by compounds derived from nojirimycin²⁸ **20** and its close analogue, the reduced form, 1-deoxynojirimycin²⁹ **21**. Other related derivatives such as deoxyfuconojirimycin³⁰ **22** and α -homofuconojirimycin³¹ **23** are highly potent fucosidase inhibitors that are implicated in disruption of *N*-glycoprotein processing.³² These targets may be exploited for the treatment of HIV infection. Swainsonine **24** is an α -D-mannosidase inhibitor with antineoplastic activity.³³ A similar compound, castanospermine **25**, is an α - and β -glucosidase inhibitor with antiviral activity.³⁴ This group of naturally occurring and synthetically modified azasugars shows further potential as an important category of carbohydrate-based therapeutics.

Figure 1.12. Azasugar glycosidase inhibitors.



Virtually all living organisms have the need to break down complex sugars. In addition to polysaccharide digestion, glycoside hydrolases are involved in a plethora of biomolecule modification processes. Many potent natural product derivatives that contain a carbohydrate scaffold are known to inhibit these enzymes. As a result of their biological importance and potential to treat diseases, the study of carbohydrate-based glycosidase inhibitors has emerged as an important area of research.

1.6. Industrial Importance of Carbohydrates

The study of carbohydrates is required for many disciplines other than for the purpose of developing new therapeutics. One such area is human nutrition and its application to the agricultural industry. Carbohydrates are one of the most important energy providers among the macronutrients. Foods high in starch include breads, pastas,

beans, potatoes, and cereals.⁵ Carbohydrates therefore comprise an important dietary staple and are essential for the maintenance of human health through proper nutrition.

Other industries with a substantial economic impact are also reliant upon chemical processes involving carbohydrates as the precursors to commercial products. The textile and paper industries, for instance, are two examples that are heavily based on the glucose-derived polysaccharide, cellulose. Textiles, which are used to make clothing and other garments, utilize cotton as the essential natural product starting material. The cellulose of the cotton is chemically modified to form both rayon and acetate rayon. In addition, the papermaking process, which dates back to 2nd century China, also makes use of carbohydrate plant material. In the pulping process, the lignin is separated from the cellulose fibers. These fibers then undergo further chemical treatments to make paper.¹⁰ Clearly carbohydrate natural products play an important part in fulfilling many basic needs in everyday society, and continued research is necessary to ensure that the industrial processes are efficient and sustainable.

1.7. Summary

Carbohydrates comprise the most common class of biomolecules found in nature. The word carbohydrate is derived from the observation that simple sugars are hydrates of the element carbon, and the term now encompasses monosaccharides, oligosaccharides, and polysaccharides as well as their derivatives. Multiple stereocenters and numerous functional groups make carbohydrates a diverse class of structurally unique compounds. The primary significance of carbohydrates lies in their major functional importance in

biological entities. Glucose is a biologically prominent monosaccharide involved in energetic as well as metabolic pathways. One of the most influential discoveries surrounding carbohydrates is the relevance of glycoconjugates. All organisms, ranging from primitive unicellular microbes to complex mammals, depend on carbohydrates and glycoconjugates to maintain life.

The previous underestimation of the biological significance of carbohydrates initially resulted in a lack of research attention. Progress in understanding the relationship between carbohydrate structure and function has been slow in comparison to other classes of biomolecules because the synthesis of carbohydrates for biochemical studies is problematic. In particular, synthetic carbohydrate chemistry is challenging due to issues involving stereochemistry as well as the selective protection and deprotection of saccharide building blocks. Despite these difficulties, carbohydrates are now known to be a diverse class of compounds with numerous functions that have far-reaching biological implications. The recent substantial interest in sugars has marked the start of increased exploration of carbohydrate drug candidates as therapeutics for a wide array of medical conditions. Both simple and complex carbohydrates have shown promise to treat human diseases such as cancer, diabetes, and infections. In addition to therapeutics, carbohydrates have a firm footing in the agricultural, clothing, and paper industries, and our modern society is heavily dependent upon carbohydrate-derived products. As a result of the prevalence and documented importance of carbohydrates, there is a significant future for basic research involving carbohydrates.

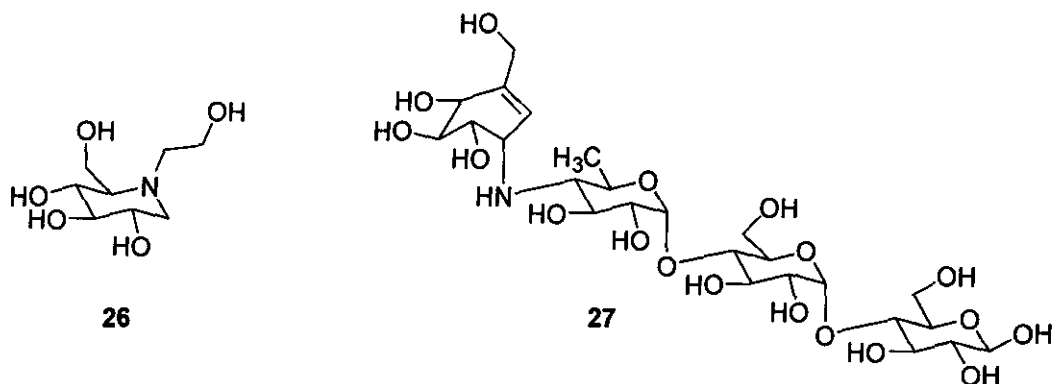
Chapter 2

Synthesis of Glycosylidene-Based Quinolines

2.1. Introduction

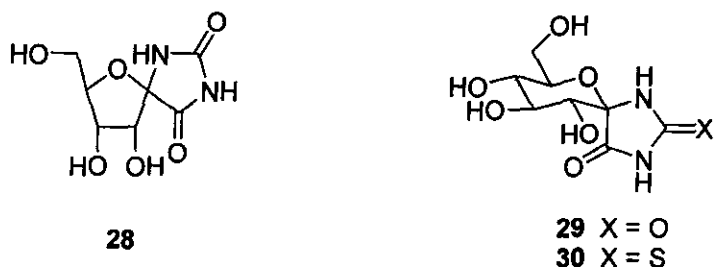
The significance of carbohydrates in the maintenance of homeostasis cannot be overstated, and the biological roles played by carbohydrates in living systems are too important to be neglected. Although numerous prescription medicines are available for the treatment of human diseases, medicinal chemists are continuously searching for compounds with improved efficacy. In addition, stable sugar derivatives have become attractive scaffolds for drug design due to their favorable pharmacokinetic properties. Natural product derivitization remains a viable drug discovery strategy, and a potentially promising target to exploit is the class of enzymes known as glycosidases. Several effective prescription medications are classified as sugar-based glycosidase inhibitors. For instance, the azasugar miglitol³⁵ **26** is an inhibitor of α -glucosidase, and the carbohydrate-based glycosidase inhibitor acarbose³⁶ **27**, is an excellent inhibitor of α -amylase. Both of these carbohydrate-based glycosidase inhibitors (Figure 2.0) have successfully made it to market as approved therapies for the management of diabetes. Such examples illustrate the potential that sugar-derived compounds hold for the improvement of human health.

Figure 2.0. Carbohydrate-based diabetes drugs.



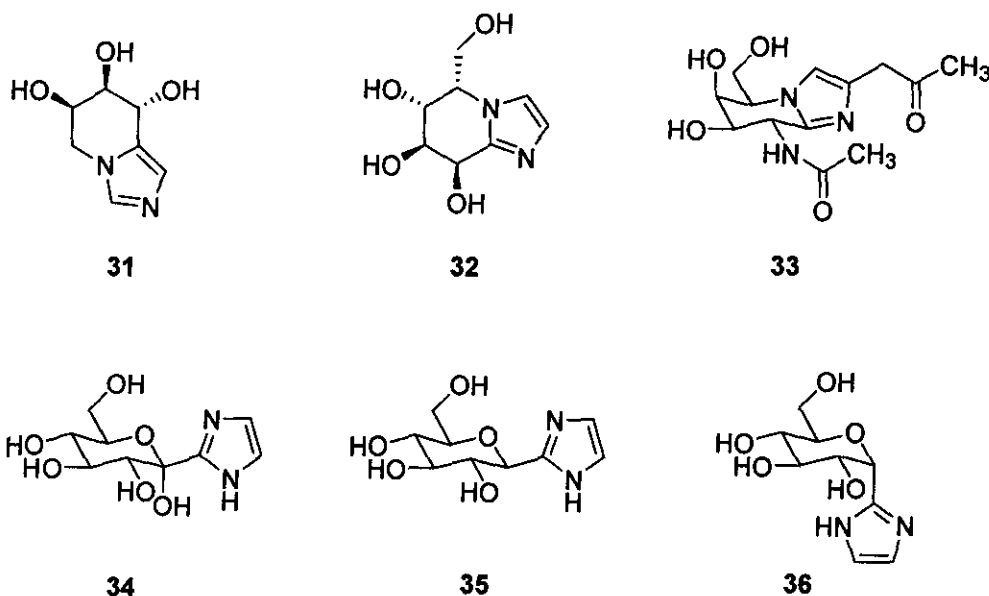
A survey of the structures of known glycosidase inhibitors indicates that many of these molecules possess both a carbohydrate moiety and an aromatic heterocycle. In numerous examples, the heterocycle is linked to the anomeric carbon in some manner (Figure 2.1). For instance, the spiro-compound, (+)-hydantocidin³⁷ **28**, has generated substantial interest due to its activity as a herbicide. Modification of this structurally unusual spironucleoside has resulted in D-glucopyranosylidene-spiro-hydantocidin analogues.³⁸ The glucose-based hydantocidin **29** possesses potent inhibitory activity towards muscle glycogen phosphorylase. The thio analogue **30** is also a potent inhibitor of glycogen phosphorylases a and b from both muscle and liver. These glycosylidene-spiro heterocycles have been the subject of research attention due to their biological activities and unique structures.

Figure 2.1. Examples of carbohydrate-spiro heterocycles with glycosidase inhibitory activity.



In addition to carbohydrates with spiro-heterocycles, numerous saccharides that contain a fused or C-linked heterocycle have also been characterized as glycosidase inhibitors (Figure 2.2). A common motif of monosaccharide derivatives **31**³⁹, **32**⁴⁰, and **33**⁴¹ is an imidazole ring fused to the sugar. Imidazolyl C-glucopyranosides **34**, **35**, and **36** are also carbohydrate-linked heterocycles that inhibit glycoside hydrolases.⁴² These compounds illustrate the common theme that many glycosidase inhibitors are sugar-based heterocycles. In addition, this sampling of compounds, when evaluated in combination with the spiro examples, helps to indicate the observation that strategies within nature are conservative and structural patterns are often repeated.

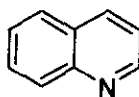
Figure 2.2. Examples of carbohydrate-fused or C-linked heterocycles with glycosidase inhibitory activity.



Aside from imidazole rings, other heteroaromatics are widely distributed among natural products and their synthetic derivatives. For instance, one such example is the class of compounds derived from quinoline 37 (Figure 2.3). Structurally, quinoline consists of a benzene ring fused to a pyridine ring. The synthesis of quinolines and their substituted derivatives has been a subject of great importance in the field of organic chemistry. Numerous preparative methods for the formation of quinolines have been determined since the late 1880s. Some of the most popular and widely used name reactions to synthesize quinolines include: (a) Camps synthesis; (b) Combes synthesis; (c) Doebner-Miller reaction; (d) Friedlander synthesis; (e) Knorr synthesis; (f) Niementowski reaction; (g) Pfitzinger reaction; (h) Pomeranz-Fritsch reaction; (i) Pictet-Spengler synthesis; (j) Riehm synthesis; and (k) Skraup reaction.⁴ These well-known

examples of quinoline preparations indicate that the synthesis of this functional group has been a critical objective for chemists.

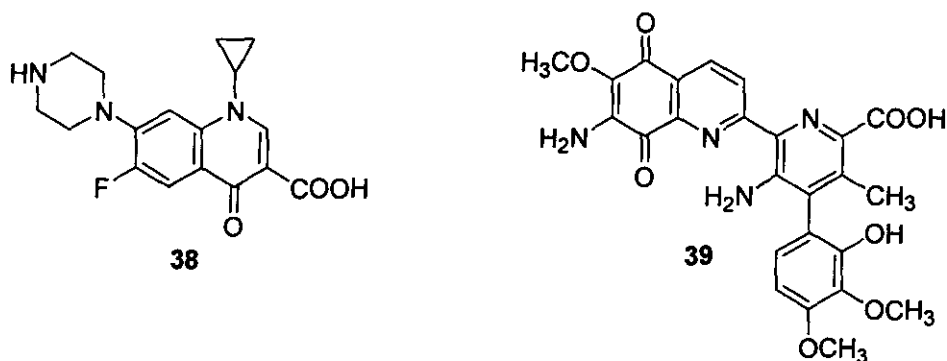
Figure 2.3. Structural representation of quinoline.



37

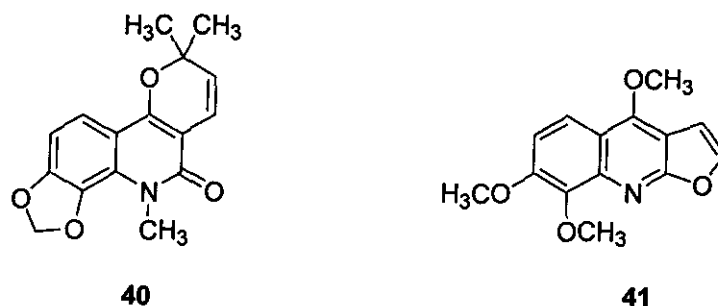
Developments in the area of quinoline chemistry are also due, in part, to the biological activities of their derivatives.⁴³ Accordingly, this group of compounds is of interest from a therapeutic point of view. This structural class includes fluoroquinolone antibiotics such as ciprofloxacin⁴⁴ 38 and antitumor alkaloids related to streptonigrin⁴⁵ 39 (Figure 2.4). In fact, many compounds containing a quinoline ring have the ability to bind to DNA. The planar aromatic system enables binding by insertion between the DNA base pairs. Such intercalating agents often possess anticancer properties.⁴⁶ Other therapeutic areas in which quinoline derivatives have shown promising activity include asthma,⁴⁷ Alzheimers' disease,⁴⁸ and AIDS.⁴⁹

Figure 2.4. Medicinally significant quinoline-based compounds.



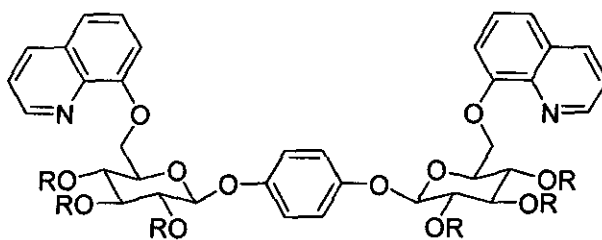
A number of quinoline alkaloid natural products and their derivatives have displayed cytotoxic activity. Planar aromatic heterocycles function as intercalating antitumor agents by forming a ternary cleavable complex with DNA and various DNA polymerases such as topoisomerases.⁵⁰ Intercalators are among some of the most important compounds that reversibly interact with the double helix of DNA. Currently, intercalation is thought to be the binding model of choice for planar aromatics with a sufficiently large area and favorable steric properties.⁵¹ In particular, compounds such as the *Stauranthus* quinoline alkaloids stauranthine **40** and skimmianine **41** were shown to interactively dock consistently into DNA (Figure 2.5). Molecular modeling studies suggest that the docked orientations are electronically and energetically favorable. These theoretical experiments provide further validation for the potential of quinolines as DNA intercalators.⁵²

Figure 2.5. *Stauranthus* quinoline alkaloids.



A study has recently been published in which Li and colleagues synthesized and evaluated quinoline-glucose hybrids as potential DNA intercalators. Specifically, these compounds were designed to be bisintercalators because higher DNA binding capacity, slower dissociation rate, and improved sequence selectivity can be achieved when multiple intercalating functionalities are included in a ligand. Carbohydrate-derived quinolines **42** and **43** are examples of synthetic hybrids in which quinoline is linked to the sugar's C6 hydroxyl group (Figure 2.6). Preliminary binding assays suggest that these compounds could bind to calf-thymus DNA through intercalation. In addition, both **42** and **43** exhibited moderate cytotoxicity against human breast cancer cell lines. While it is hypothesized that the quinoline groups are intercalating with the DNA, the researchers suggested that glucose groups may also help to regulate the interaction between the compound and the DNA duplex.⁵³ This study on quinoline-glucose hybrids further reinforces the potential application of glucose-derived heterocycles as DNA intercalators.

Figure 2.6. Quinoline-glucose hybrids evaluated as DNA intercalators.



42 R = Ac

43 R = H

The observation that many small carbohydrate-based aromatics possess activity against a variety of targets sparked our synthetic interest in this area. We desired to make glucose derivatives with a quinoline heterocycle linked to the sugar's anomeric carbon. We felt that glucose was an ideal choice for the sugar scaffold due to its role as a monomer in complex polysaccharides as well as its documented importance in numerous biological pathways. Quinoline was selected as the heterocycle portion of the molecule because of the biological activity associated with this functionality. Heteroaromatics such as quinolines serve as bioisosteres for other substituents and can often improve upon biological activity and metabolic properties of the resulting compound.² We theorized that combining these structural motifs and incorporating both a sugar and aromatic heterocycle would provide for a stable compound. Furthermore, if the quinoline and sugar were appended via carbon-carbon bonds (rather than carbon-oxygen bonds), this would impart an additional measure of stability to the molecule from endogenous glycosidases in the body. We also hypothesized that incorporation of a sugar would not only facilitate drug delivery, but may also aid in the DNA intercalation process as well.

We surmised that the sugar moiety could help to stabilize DNA binding by interacting with the sugar-phosphate backbone once the quinoline has come in contact with the DNA.

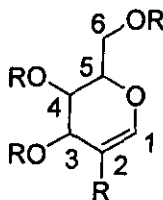
Carbohydrates and their derivatives are crucial for the survival of living entities because of their integral involvement in life sustaining processes. As a result of the biological prevalence and bioavailability of carbohydrates, stable sugar derivatives present themselves as potentially favorable platforms for drug design. In fact, monosaccharides have long been known as biologically relevant scaffolds.² Despite the volume of literature published on carbohydrate derivatives, it is surprising to note that no groups have cited examples of synthetic glycosylidene-spiro aromatic heterocycles. In addition, carbohydrate-derived quinolines represent a unique and potentially beneficial class of compounds. We feel that these novel types of glycosylidene-based heterocycles are particularly valuable targets. This project is worthy of study because it creates the opportunity for us to develop and apply some new synthetic methodology. We surmise that compounds with this novel structural motif can be accessed through a variation of the Povarov reaction with an *exo*-glycal. In addition, we predict that some of these compounds may possess pharmacological activity. The structural motifs of both a carbohydrate moiety and a heterocycle are prevalent throughout biological systems, and our proposed targets combine these common themes associated with some antitumor DNA intercalating agents as well as glycosidase inhibitors. Finally, we anticipate that our synthetic sugar derivatives also have the potential to act as antiviral, antifungal, or antibacterial agents.

2.2. Background

a. Glycals and Spiroanellation Chemistry

Glycals are cyclic vinyl ether derivatives of sugars that contain a double bond between carbon atoms 1 and 2 of the ring (Figure 2.7). These 1,2 unsaturated sugars are either commercially available or easily prepared from 1-halogeno sugars. Manipulations of this double bond have been utilized in many syntheses, thereby making glycals useful starting materials. Addition reactions have been employed in the preparation of carbohydrate-based compounds, including fused heterocycles. A survey of the current scientific literature pertaining to the chemistry of glycals indicates that some of these synthetic strategies may prove useful when applied to sugars with double bonds at other positions of the molecule.⁵⁴

Figure 2.7. Structural representation of a generic glycal.

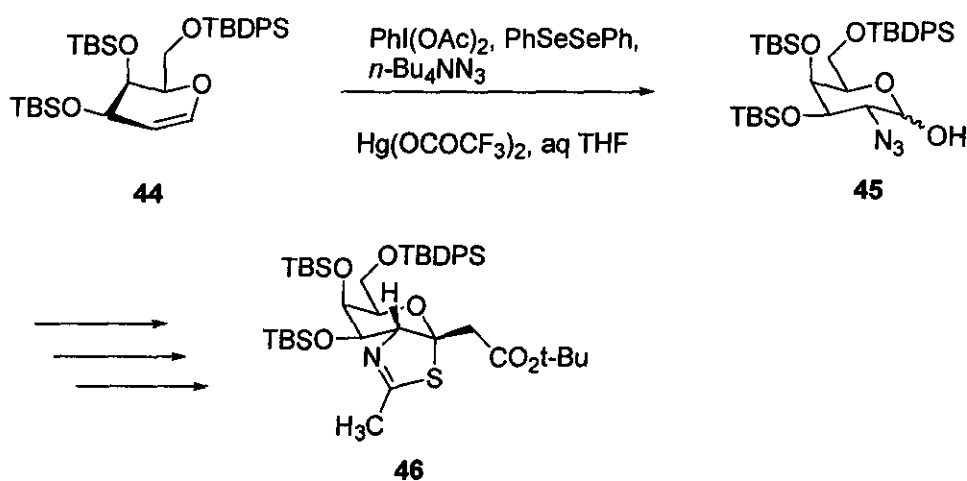


glycal = 1,2 unsaturated sugar

An example of glycal chemistry involving a heterocyclic fused sugar system is illustrated by the work carried out by Professor Knapp and colleagues. His group attempted the synthesis of carbohydrate-fused thiazoline derivatives through the use of a protected glycal (Scheme 2.0). Their work with galactal derivative **44** ultimately led to

the synthesis of thiazoline **46** through azido intermediate **45**.⁵⁵ However, the cyclization step was problematic and subject to side reactions. In addition to these shortcomings, the reaction sequence was lengthy. Other approaches by Knapp have resulted in the preparation of heterocyclic products that were limited to substituted thiazolines.⁵⁶

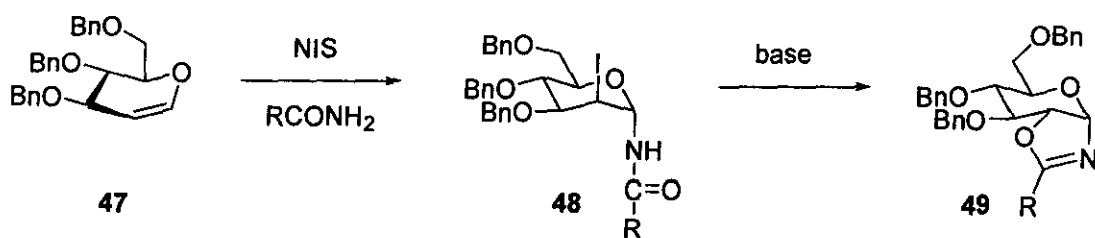
Scheme 2.0. Knapp's approach toward carbohydrate-fused thiazolines.



Upon careful review of the procedures utilized by Knapp and colleagues, the research group of Professor Marzabadi became interested in developing a general method which would not limit the type of heterocycle fused to the monosaccharide. Marzabadi and DeCastro predicted that carbohydrate-fused heterocycles could be accessed from 2-iodo-glycosylamides.⁵⁷ They revisited the haloglycosylation chemistry developed by Lemieux⁵⁸ and Thiem,⁵⁹ and ultimately applied the principle of alkoxyhalogenation to glycal **47** in the synthesis of *trans*-diaxial iodo-glycosylamide **48** (Scheme 2.1). This intermediate was then cyclized under basic conditions to form fused heterocycle **49**.⁶⁰ DeCastro and Marzabadi's efforts have resulted in the preparation of a series of

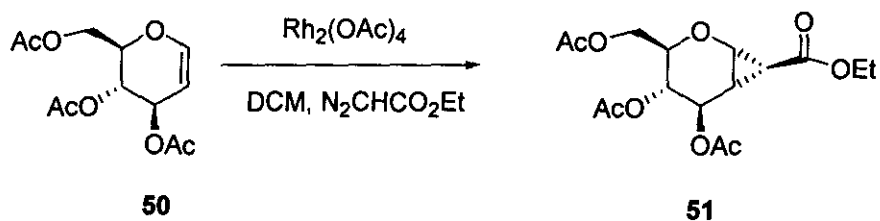
heterocycles, and this approach also succeeded in the synthesis of selected urea oxazolines and thiazolines. A major advantage of this chemistry is that it is general enough to allow for the synthesis of both oxazolines and thiazolines.⁵⁷ These heterocycles are accessible in two steps from protected glycals. In comparison, Knapp's chemistry permits substituted thiazolines only. DeCastro and Marzabadi's novel approach to carbohydrate-fused heterocycles is a general strategy that is more streamlined than Knapp's synthetic sequence.

Scheme 2.1. DeCastro and Marzabadi's synthesis of oxazoline-fused carbohydrates.



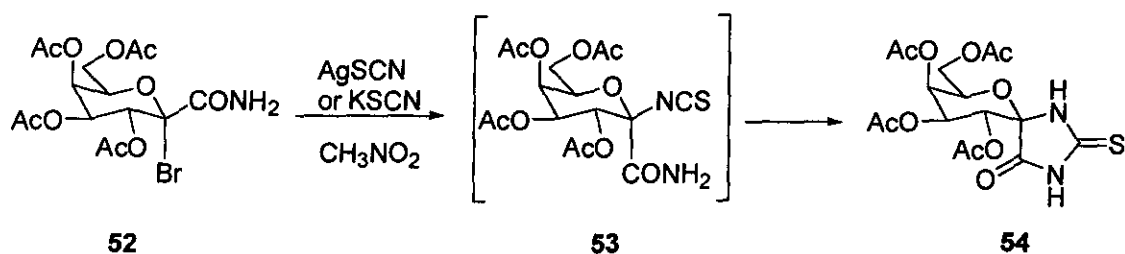
In addition to carbohydrate-fused heterocycles, the Marzabadi group has also focused on cyclopropanated carbohydrate derivatives. Talisman and Marzabadi have synthesized a series of compounds based on glycal addition chemistry (Scheme 2.2). Specifically, carboethoxy cyclopropanated carbohydrate **51** was accessed through the reaction of 1,2 unsaturated glycal **50** with a rhodium-derived carboxy carbene. Additional transformations further functionalized this carboethoxy derivative, and similar chemistry was applied to synthesize carbomethoxy cyclopropanated carbohydrates as well.⁶¹ This route marks another application of the strategy of glycal addition in the synthesis of carbohydrate-based derivatives.

Scheme 2.2. Talisman and Marzabadi's synthesis of carboethoxy cyclopropanated carbohydrates.



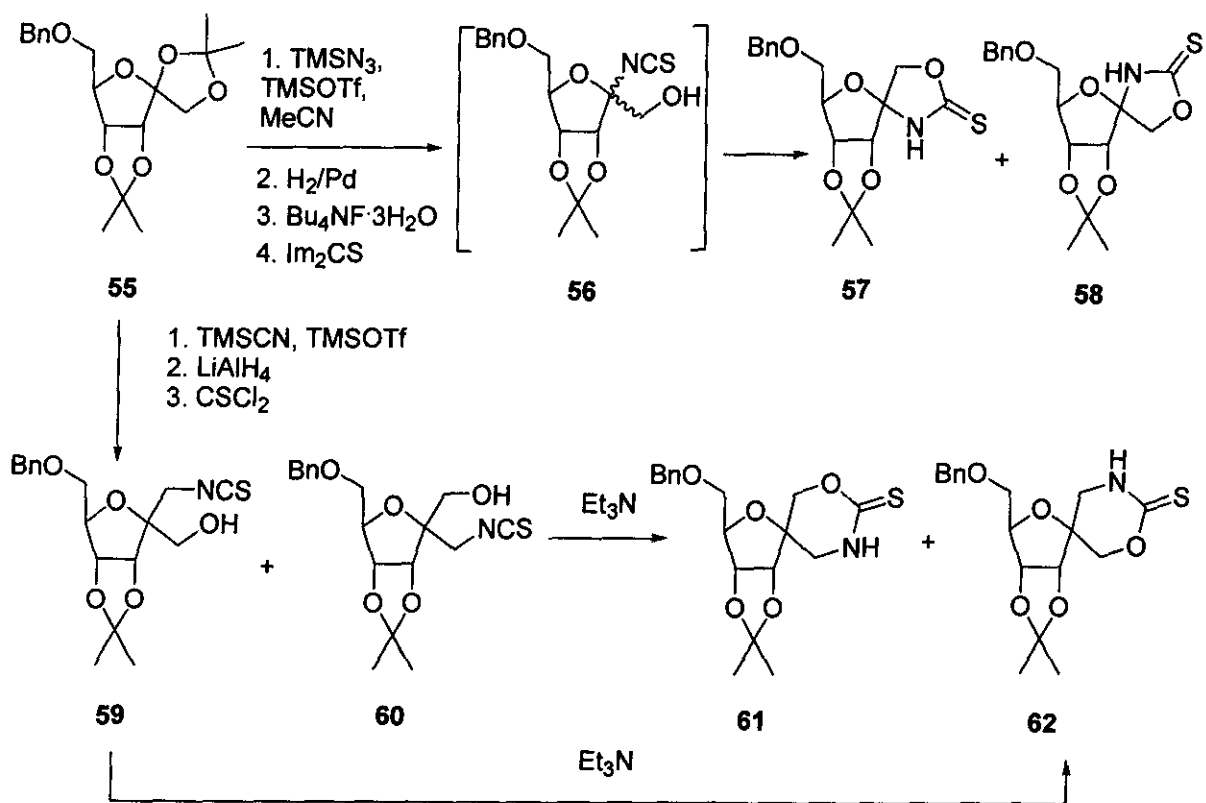
The synthetic studies surrounding glycosylidene-spiroanellated heterocycles were of particular interest to us because relatively few published examples targeting spiro-heterocycles exist. Somsak, Osz, and colleagues have described the synthesis of a pyranose ring version of 2-thiohydantocidin **54** (Scheme 2.3). The 1,1-disubstituted glycosyl compound **52** was the key intermediate in the synthesis. Displacement of the bromo group with the thiocyanate ion followed by ring closure of **53** yielded the desired spiro compound **54**.⁶² The group further elaborated upon this strategy of cyclizing 1,1-disubstituted glycosyl derivatives, and they successfully synthesized several glycosylidene-spiroanellated-thiazolidene and -thiazoline analogues.⁶³

Scheme 2.3. Somsak's synthesis of an analogue of 2-thiohydantocidin.



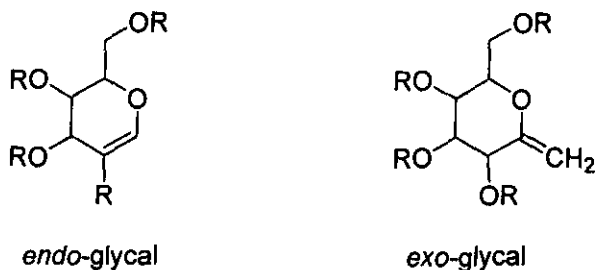
Gasch and colleagues have also verified that isothiocyanato sugar derivatives have proven useful in the synthesis of both furanoid spiro-nucleosides of oxazolidine-2-thiones and oxazinane-2-thiones (Scheme 2.4). In the case of spirooxazolidine-2-thiones, the resulting isothiocyanate intermediate **56** spontaneously cyclizes to give isomeric products **57** and **58**. However, base-catalyzed intramolecular cycloaddition of the isothiocyanates **59** and **60** is required to obtain spirooxazines **61** and **62**, respectively. A similar reaction sequence has been utilized to access the pyranose analogues of these spiroannellated heterocycles.⁶⁴

Scheme 2.4. Synthesis of furanoid spironucleosides of oxazolidine-2-thiones and oxazinane-2-thiones.



Although several research groups have synthesized glycosylidene-spiroannellated heterocycles, no published examples have been reported that include aromatic heterocycles. In addition, the sequences to access these spiro-heterocycles are rather lengthy and involve difficult chemistry. We desired to work in the area of glucose-derived spiro-aromatic heterocycles, with the goal of synthesizing novel compounds through the development of a facile synthetic sequence. Given the Marzabadi group's reliance on glycols as essential starting materials, we surmised that *exo*-glycols may prove useful for the project. *exo*-Glycols can be classified as C-glycosylidenes that are olefinic sugars with an *exo*-cyclic double bond at the anomeric center (Figure 2.8). Specifically, the *exo*-glycol double bond is a highly reactive functional group due to the presence of the ring oxygen substituent.⁵⁴ We decided to exploit the reactivity of the olefinic system, and we therefore embarked upon the development of a general strategy to synthesize sugar-based quinolines.

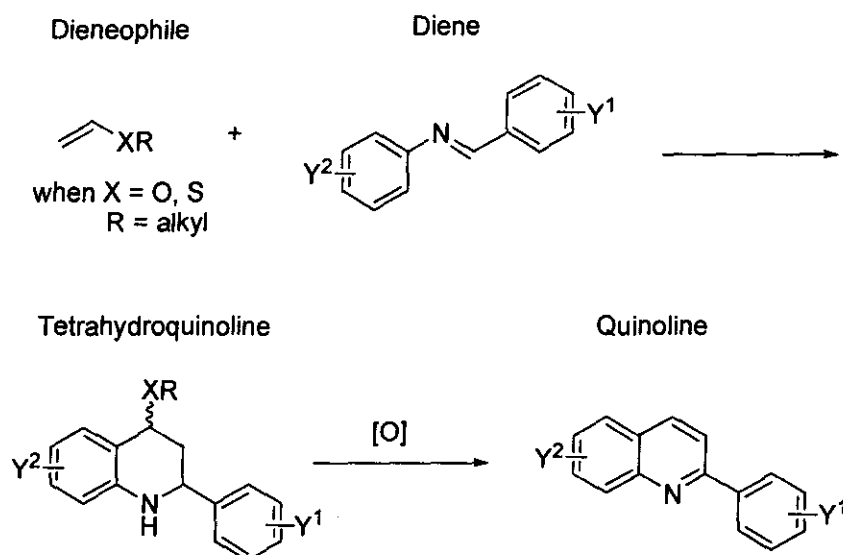
Figure 2.8. Comparison of generic *endo*- and *exo*-glycols.



b. Synthesis of Quinolines Via the Povarov Reaction

Despite the multitude of publications covering quinolines, we chose to focus our work on applications of the Povarov reaction. We hypothesized that a variation of the Povarov reaction could allow us access to glycosylidene-spiroannellated quinolines. In the 1960s, Povarov and colleagues described an addition reaction between an aromatic Schiff base and activated alkene to give tetrahydroquinolines⁶⁵ (Scheme 2.5). This type of cyclization reaction has also been referred to in the scientific literature as the aza-Diels-Alder reaction as well as the imino-Diels-Alder reaction. Electron-rich vinyl ethers or alkyl vinyl sulfides are the activated alkenes (dienophiles) that react with derivatives of benzaniline (dienes). The original Lewis acid catalyst for the transformation was $\text{BF}_3 \cdot \text{Et}_2\text{O}$ while the solvent of choice was benzene. Povarov and colleagues also reported that these tetrahydroquinoline products could subsequently be oxidized to the corresponding fully aromatized dihydroquinolines with the elimination of the alkoxy or alkyl sulfide group.

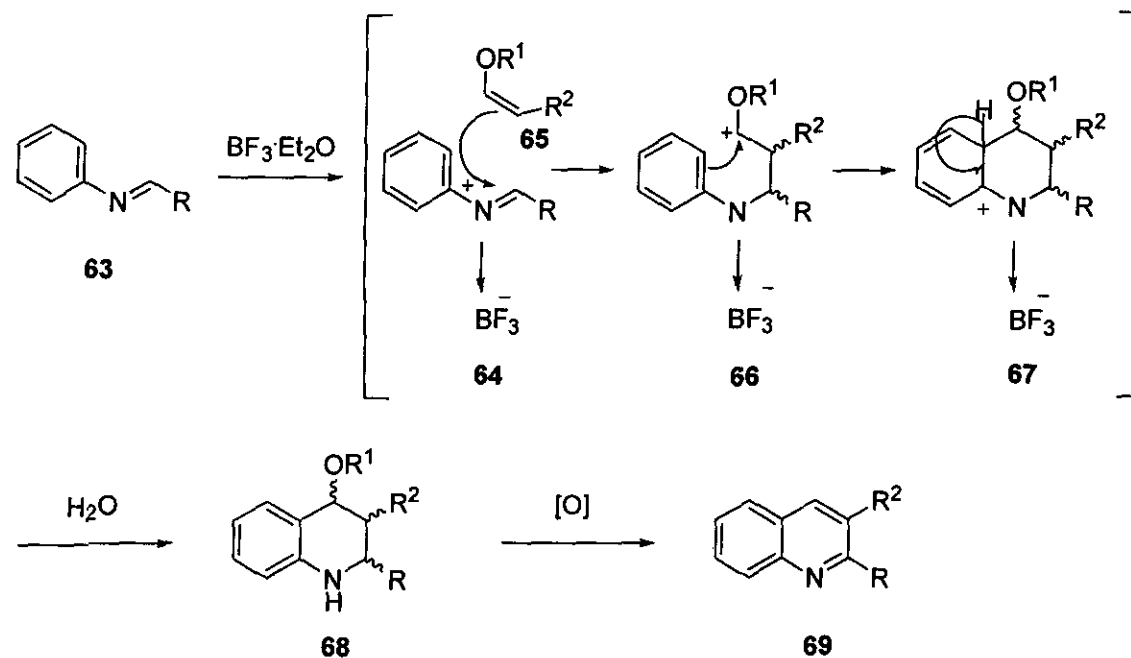
Scheme 2.5. Generalized Povarov reaction sequence.



Despite only modest yields at best, interest in the Povarov reaction was rekindled in the 1990s. A critical objective for the advancement of this reaction's utility was the determination of conditions leading to increased reaction yields. Recent publications have documented the usefulness of the Povarov reaction,⁶⁶ and new catalysts have led to improved preparation conditions.⁶⁷ Specifically advantageous catalysts include the lanthanide triflates, Sc(OTf)₃ and Yb(OTf)₃, while the new solvent of choice for the reaction is acetonitrile. This is likely due to the fact that both the substrates and catalysts are easily soluble in this solvent. Procedures involving three component syntheses as well as combinatorial methods on solid supports have also led to enhanced yields. The Povarov reaction has now grown into a popular and useful strategy for the preparation of substituted tetrahydroquinolines.⁶⁶

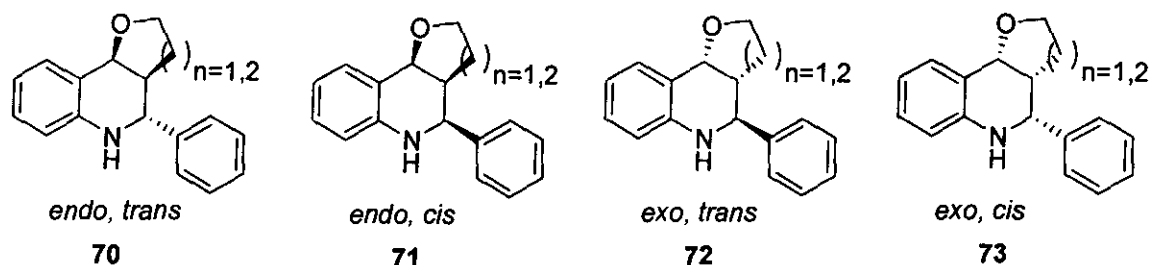
Previously Povarov and colleagues made the assumption that the reaction of activated alkenes and aromatic Schiff bases occurred via a conjugated [4+2] cycloaddition.⁶⁵ Recently, however, the mechanism for this process has been debated. Experiments in which the ionic intermediates were captured by nucleophiles and subsequently characterized have been performed.⁶⁸ These results call into question the prevailing thought of a concerted pathway and instead suggest that a stepwise reaction mechanism is more probable. Although there does not appear to be one generic mechanism to explain all reactions of this class, a majority of chemists now acknowledge that the Povarov reaction proceeds through a stepwise mechanism. In the currently postulated, non-concerted reaction mechanism⁶⁶ (Scheme 2.6), the Lewis acid catalyst $\text{BF}_3 \cdot \text{Et}_2\text{O}$ first complexes to the nitrogen of imine **63**, resulting in formation of iminium ion intermediate **64** in which the nitrogen atom bears a positive charge. The electrons from the activated alkene **65** then react with compound **64** to create a bond which couples the two compounds together, resulting in the formation of intermediate **66**. The second ring of compound **67** is created by electrophilic attack of the ortho carbon of the aniline, and a bond is formed between the phenyl ring directly attached to the nitrogen atom and the carbon atom bearing the positive charge. Next, hydrogen elimination re-aromatizes the aniline-derived phenyl ring. Trace quantities of water are required to break the complex between the nitrogen atom and the Lewis acid catalyst. The tetrahydroquinoline product mixture **68** results once this complex is broken. If desired, treatment of the reaction products with oxidizing agents (*e.g.* KMnO_4 , *p*-toluenesulfonic acid, or atmospheric oxygen) may aid in the elimination of the alkoxy or alkyl sulfide group to give the fully aromatized dihydroquinoline **69**.

Scheme 2.6. Currently postulated, non-concerted mechanism for the Povarov reaction illustrated with $\text{BF}_3 \cdot \text{Et}_2\text{O}$ as the Lewis acid catalyst.



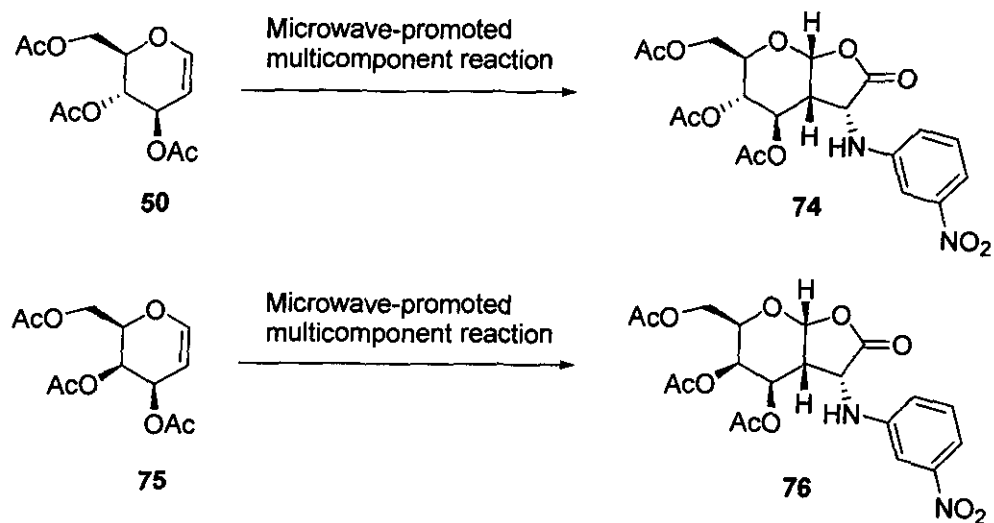
The tetrahydroquinolines formed under Povarov reaction conditions possess several asymmetric carbons. The ratio of diastereomers formed is often dependent upon a variety of factors, including the reaction conditions as well as the substrates, catalyst, and solvent.⁶⁹ For instance, in situations when the activated alkene is a dihydrofuran or dihydropyran derivative, three chiral centers are formed during the reaction (Figure 2.9). In a majority of cases, the annulation proceeds in such a way that typically only four diastereomers can result. While the *endo,trans* **70** and *endo,cis* **71** isomers predominate, the *exo,trans* **72** and *exo,cis* **73** isomers are almost never formed in appreciable quantities.⁷⁰ The preferential formation of diastereomers during the annulation of an alkene and benzaniline adds a unique stereochemical aspect to the Povarov reaction.

Figure 2.9. Diastereomers resulting from Povarov condensations with dihydrofuran and dihydropyran.

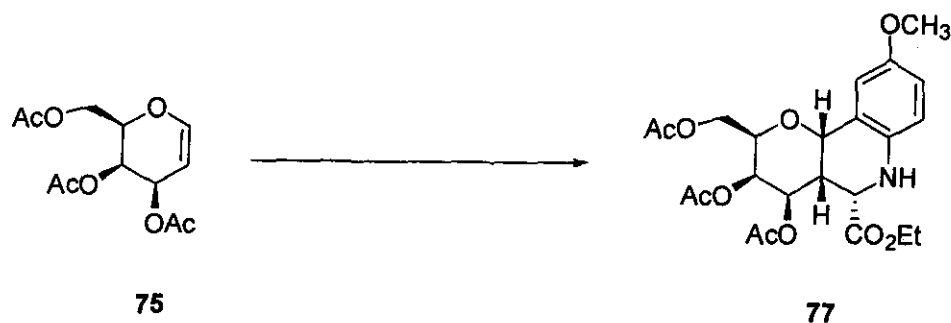


Our interest in the Povarov reaction was sparked by a recent publication that reported cycloaddition chemistry involving a protected glycal as a scaffold. However, this report is the only known example of Povarov glycal cycloaddition chemistry published to date. Jiminez and colleagues performed multicomponent Povarov reactions utilizing tri-*O*-acetyl-*D*-glucal **50** and tri-*O*-acetyl-*D*-galactal **75**, and the research group synthesized glycosylidene-fused compounds **74** and **76** from these starting reagents (Scheme 2.7). Reactions with these protected glycals displayed excellent facial selectivity. Although reaction times were quite long (two weeks) and yields were low (<40%) when the experiments were conducted at 40 °C, microwave irradiation increased the yields of the reaction, lowered the reaction time to two minutes, and enhanced stereoselectivities to 99:1. The researchers did not observe Ferrier-type rearrangements or ring-opening transformations that are common in acid-promoted reaction conditions with glycals. In addition, the research team also synthesized galactose-derived tetrahydroquinoline **77** (Scheme 2.8).⁷¹ This example is the first sugar-fused quinoline synthesized via the Povarov reaction to be reported in the scientific literature. Despite this group's success, it is surprising to note that they have yet to report additional work in this area.

Scheme 2.7. Multicomponent reactions involving glycal addition reported by Jiminez and colleagues.



Scheme 2.8. First reported Povarov reaction utilizing a glycal derivative as the activated alkene.

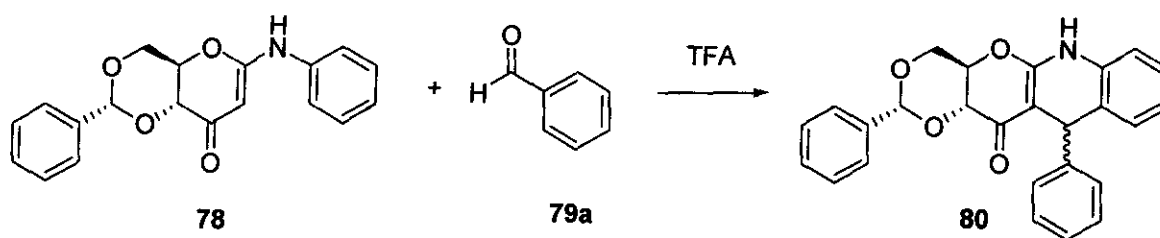


Several other groups have made efforts focused on the synthesis of sugar-based quinolines via addition reactions. For instance, Scheffler and colleagues have prepared sugar-anellated dihydroquinoline **80** through the condensation of **78** with benzaldehyde **79a** (Scheme 2.9).⁷² In addition, Yadav and coworkers reported the synthesis of glucose-fused tetrahydroquinoline **82**. This high yielding, stereoselective synthesis involved a

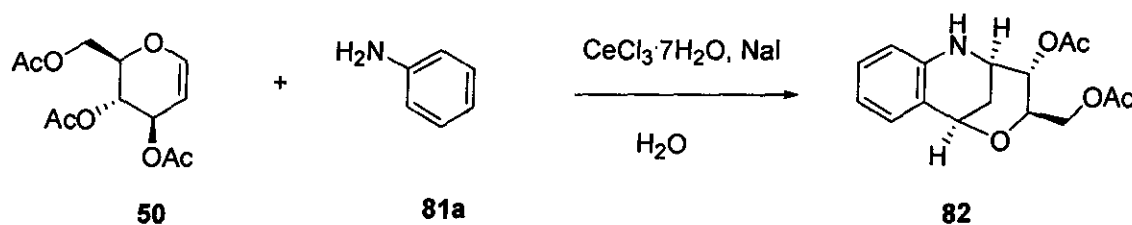
Lewis acid catalyzed cycloaddition of aniline **81a** with *endo*-glycal **50** (Scheme 2.10).⁷³

These reports denote examples within the scientific literature that most closely resemble our proposed area of study focusing on the preparation of sugar-based quinolines.

Scheme 2.9. Preparation of quinoline **80**.



Scheme 2.10. Preparation of glucose-fused quinoline **82**.



The application of the Povarov reaction to glycols, as reported by Jiminez and colleagues, motivated us to focus on this reaction with *exo*-glycols. To the best of our knowledge, syntheses involving the Povarov reaction with *exo*-glycols have not yet been described. In an effort to overcome this limitation, we embarked upon studies to identify reaction conditions that would allow us access to our target compounds. This research project idea would also nicely complement the previous interests of the Marzabadi group,

namely addition reactions and the synthesis of carbohydrate-derived heterocycles and carbocycles. A program of study focused on the Povarov reaction with *exo*-glycals is worthy of research attention because it will allow for the likely expansion of the scope of this reaction strategy. Finally, the resulting synthetic products have the potential to possess biological activity.

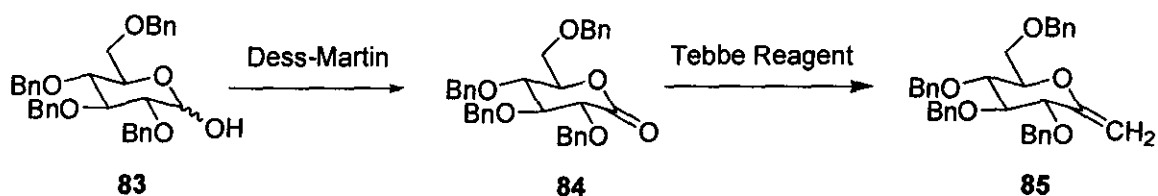
2.3. Results

a. Synthesis of Starting Materials

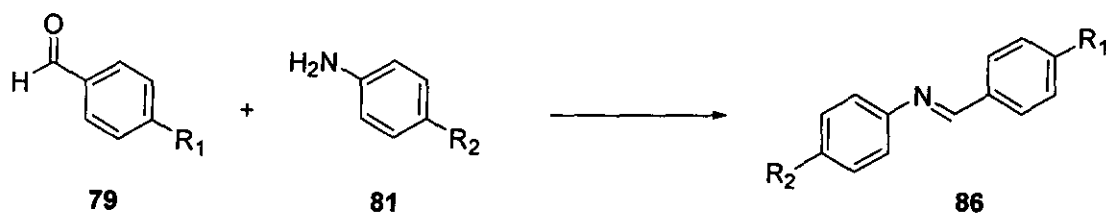
Below we describe our synthetic efforts toward a series of novel, glycosylidene-based quinolines. In order to begin a survey of analogues, we needed to first prepare the common *exo*-glycal intermediate from which we would conduct our research (Scheme 2.11). We began our synthesis with commercially available 2,3,4,6-tetra-*O*-benzyl-D-glucopyranose **83**. Glucose was chosen as the sugar for the carbohydrate scaffold because of its known biological importance. We decided to utilize the benzyl group to protect the hydroxyl functionalities because of the observations that acetyl and silyl protected D-glucals reacted slowly under Povarov conditions and the corresponding products were not particularly stable.⁷⁴ The anomeric hydroxyl group of compound **83** was oxidized with Dess-Martin periodinane,⁷⁵ and lactone **84** was produced in 93% yield. Next we needed to obtain the terminal alkene, and a Tebbe olefination reaction⁷⁶ resulted in a 75% yield of the desired *exo*-glycal **85**. With this crucial intermediate in hand, we then turned our attention to studies involving the Povarov reaction with different imines. We were able to purchase several benzanilines through commercial sources while others

were synthesized according to published literature procedures (Scheme 2.12).⁷⁷ A representative experimental procedure involved a room temperature reaction between derivatives of benzaldehyde **79** and aniline **81** to give imine **86**. Once the required intermediate compounds were synthesized, we began to perform experiments aimed at studying Povarov reaction conditions.

Scheme 2.11. Synthesis of the essential *exo*-glycal intermediate.



Scheme 2.12. Synthesis of benzanilines.

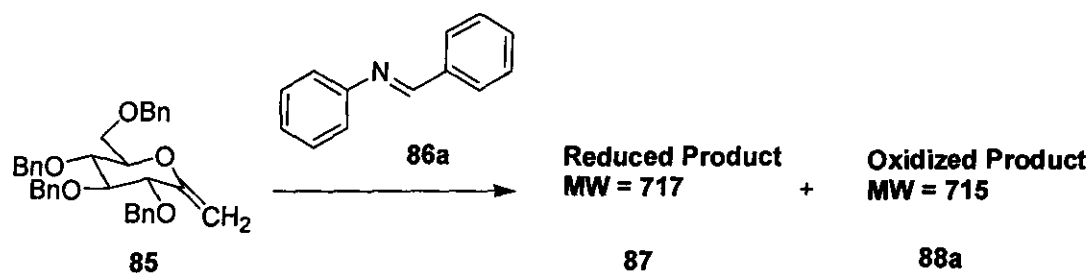


b. Catalyst Screening

In order to investigate conditions for the Povarov reaction between *exo*-glycal **85** and benzaniline **86a**, we screened several rare earth metal triflates as Lewis acid catalysts (Table 2.0). Based on our literature survey, we chose to study Sc(OTf)₃, Yb(OTf)₃, and

Tb(OTf)₃. With all three catalysts (Entries 1-3), we observed the complete conversion of **85** to a mixture of products. In each reaction, we noticed that the molecular weight of the products differed by two amu. We surmised that this difference may correspond to the presence of an oxidized/reduced pair. Of the screened catalysts, Sc(OTf)₃ gave the highest ratio of **88a**:**87** (oxidized to reduced products) as well as the cleanest reaction (Entry 1). Catalysis of the reaction with Yb(OTf)₃ and Tb(OTf)₃ resulted in almost identical ratios of **88a**:**87** (Entries 2 & 3). These preliminary results were encouraging, and we next proceeded to isolate the reaction products and perform structural characterization studies.

Table 2.0. Catalyst and reaction condition screening.



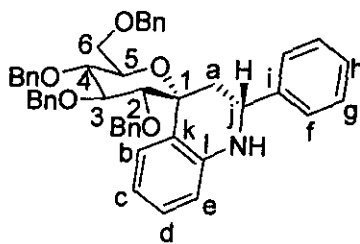
Entry	Catalyst	Reaction Conditions ^a	Ratio of 88a : 87 ^b
1	Sc(OTf) ₃	room temperature, overnight	2.67:1
2	Yb(OTf) ₃	room temperature, overnight	0.92:1
3	Tb(OTf) ₃	room temperature, overnight	0.96:1

^a **85** (1.0 equiv), **86a** (1.0 equiv), and catalyst (0.2 equiv) were dissolved in MeCN and allowed to react under the specified conditions. ^b Determined by HPLC/MS analysis.

c. Structural Determination

A series of 1D and 2D NMR experiments were conducted in order to determine the structural identity of the reaction products. The proton spectra of **87** in CDCl₃ indicated that this reduced product was isolated as a 4:1 mixture of diastereomers. In addition, assignment of both ¹H and ¹³C spectra of the isomeric mixture indicates that the reduced products are two of the four possible glycosylidene-spiroanellated stereoisomers that we predicted to synthesize from the reaction. High resolution mass spectrometry (HRMS) also validated the molecular weight of the products. The signals for the ¹H and ¹³C spectra have been assigned, and Nuclear Overhauser Effect (NOE) experiments have confirmed the stereochemistry of both isomers of **87**. Tables 2.1 and 2.2 summarize the ¹H and ¹³C NMR data and illustrate the assigned structures. For **87Major** (Table 2.1), NOEs were observed between the hydrogens attached to the following carbon atoms: 2 with both j and a, b with both 3 and 5, and 4 with a. These interactions indicate that the stereochemistry is (*R*) at both carbons 1 and j. For **87Minor** (Table 2.2), NOEs were observed between the hydrogens attached to the following carbon atoms: b with both 2 and 4, 3 with a, and 5 with j. The stereochemistry of this isomer is (*S*) at carbon 1 and (*R*) at carbon j. These interactions observed from the advanced NMR experiments definitively confirm the stereochemistry of the glucose-spiro tetrahydroquinolines **87Major** and **87Minor**.

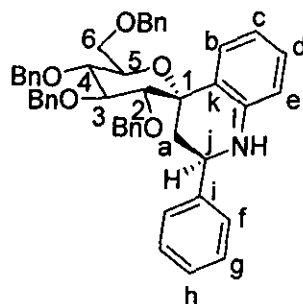
Table 2.1. Spectral analysis for the spiroanellated tetrahydroquinoline **87Major**.⁷⁸



87Major

Atom Label	¹ H Chemical Shift (ppm)	¹³ C Chemical Shift (ppm)
1	-----	76.3
2	4.05	79.9
3	4.14	84.9
4	4.00	78.9
5	4.28	73.3
6	3.80	70.2
a	2.64, 2.19	42.8
b	7.62	129.9
c	6.78	116.9
d	7.16	128.9
e	6.58	113.7
f	7.19	buried under Bn aromatics
g	buried under Bn aromatics	buried under Bn aromatics
h	buried under Bn aromatics	buried under Bn aromatics
i	-----	145.1
j	4.51	55.2
k	-----	123.2
l	-----	144.4

Table 2.2. Spectral analysis for the spiroanellated tetrahydroquinoline **87Minor**.⁷⁸



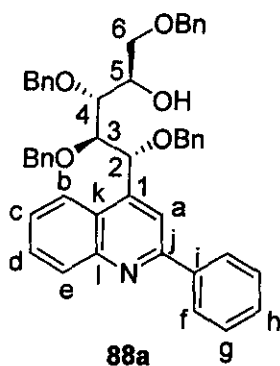
87Minor

Atom Label	¹ H Chemical Shift (ppm)	¹³ C Chemical Shift (ppm)
1	-----	76.3
2	3.67	71.3
3	3.79	87.1
4	4.65	86.6
5	3.87	79.9
6	3.65	69.3
a	2.22, 1.91	44.4
b	7.62	130.8
c	6.71	115.4
d	buried under Bn aromatics	buried under Bn aromatics
e	6.58	114.9
f	7.43	buried under Bn aromatics
g	buried under Bn aromatics	buried under Bn aromatics
h	buried under Bn aromatics	buried under Bn aromatics
i	-----	144.4
j	4.94	52.5
k	-----	117.7
l	-----	145.9

A similar analysis was conducted on the oxidized product **88a** from the Povarov reaction with *exo*-glycal **85**. A variety of advanced NMR experiments were performed in order to assign the structure of the oxidized product as the open-ring glycosylidene-based

quinoline **88a**. Table 2.3 summarizes the ^1H and ^{13}C NMR data and illustrates the assigned structure. Both 1D and 2D NMR experiments, conducted in CD_3CN , were required to confirm the open-ring structure of **88a**. Evidence includes the ^{13}C shift of C1 (145.9 ppm) and the coupling constant for the hydrogen attached to C2 (3.1 Hz). The broad ^{13}C resonance of C2 (78.5 ppm) sharpened upon increased temperature, indicating restricted rotation about the C1-C2 bond. NOEs were observed between the hydrogens attached to the following carbon atoms: 2 with both a and b. COSY and NOESY signals were also observed between the hydrogen and hydroxyl group attached to C5. This evidence, when taken in conjunction with HRMS data, provides strong support for the structural assignment of **88a** as the open-ring, fully aromatized quinoline.

Table 2.3. Spectral analysis for the open-ring glycosylidene-derived quinoline **88a**.⁷⁸



Atom Label	^1H Chemical Shift (ppm)	^{13}C Chemical Shift (ppm)
1	-----	145.9
2	5.56	78.5
3	4.17	81.4
4	3.73	79.2
5	4.04	71.3
6	3.70, 3.56	71.5

OH	3.35	-----
a	8.07	118.4
b	8.22	123.8
c	7.44	126.4
d	7.74	129.6
e	8.13	130.0
f	8.10	127.6
g	7.50	128.5
h	7.48	129.6
i	-----	139.0
j	-----	buried under Bn aromatics
k	-----	125.5
l	-----	148.3

Isolation and structural characterization of the resulting compounds from the Povarov reaction indicated the formation of spiroanellated tetrahydroquinoline **87** as a mixture of diastereomers in addition to the open-ring glycosylidene-based quinoline **88a**. Although the spiro-compound mixture **87** is stable while refrigerated, we observed the slow, partial oxidation to **88a** at room temperature. The aromatization of the tetrahydroquinoline portion of **87** likely drives the opening of the glucopyranose ring. This observation is consistent with the traditional Povarov addition/oxidation sequence (Scheme 2.5) in which elimination of the alkoxy group ultimately leads to ring aromatization to form the dihydroquinoline.

d. Reaction Optimization

In consideration of these initial results, it was therefore our desire to exclusively obtain the oxidized product **88a**, preferably from a one-pot reaction. Of the screened catalysts, Sc(OTf)₃ (Table 2.0, Entry 1) gave the highest ratio of **88a:87** as well as the cleanest reaction. We therefore chose to focus solely on this Lewis acid catalyst. We

decided to monitor the reaction on an hourly basis, and noted that the *exo*-glycal starting material **85** was entirely consumed within one hour when the mixture was stirred at room temperature. In addition, the spiro mixture **87** steadily converted to the open-ring quinoline **88a** until the ratio of ~2.7:1 was reached. Extension of the reaction time to four days (96 hours) did not appreciably change the ratio (Table 2.4, Entry 1). We next altered the experimental conditions by conducting the reaction under the reflux temperature of acetonitrile overnight, and observed the ratio of **88a:87** to be ~2.5:1 (Entry 2). In order to complete our studies of the influence of the reaction's temperature on the ratio of **88a:87**, we conducted the reaction at 0 °C. After three hours of stirring, we observed a mixture of starting material as well as oxidized and reduced products (Entry 3). Allowing the reaction to stir overnight while warming to room temperature resulted in the consumption of the *exo*-glycal starting material **85**. Surprisingly, a majority of the reaction's products was in the reduced form (Entry 4). These reaction temperature optimization studies led to the observation that overnight stirring at room temperature resulted in the highest ratio of **88a:87**. However, we were still unable to completely convert the spiroanellated tetrahydroquinoline mixture **87** to the open-ring glycosylidene-based quinoline **88a**.

Table 2.4. Screening of Povarov reaction conditions involving catalysis by Sc(OTf)₃ at various temperatures.

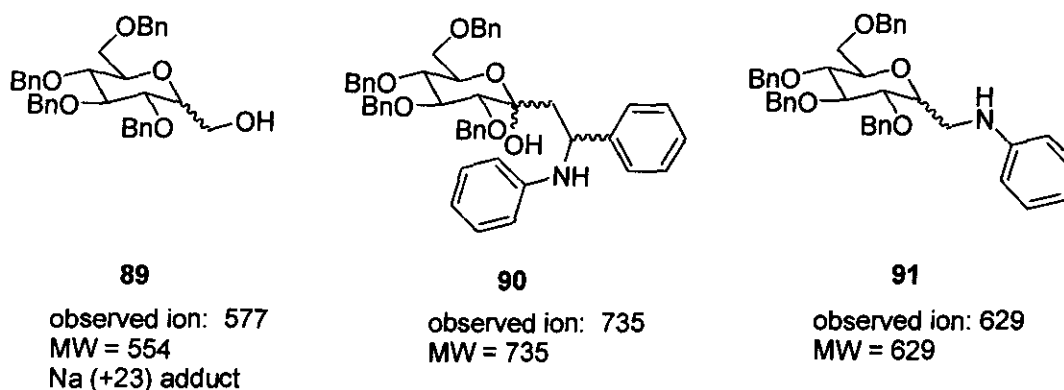
Entry	Conditions ^a	Ratio of 88a :(87Major + 87Minor) ^b
1	room temperature, 4 days	2.67:1
2	reflux, overnight	2.51:1
3	0 °C, up to 3 hours	still mostly <i>exo</i> -glycal 85
4	0 °C for 3 hours, then room temperature overnight	1:1.62

^a **85** (1.0 equiv), **86a** (1.0 equiv), and Sc(OTf)₃ (0.2 equiv) were dissolved in MeCN and allowed to react under the specified conditions. ^b Determined by HPLC/MS analysis.

Throughout our early optimization studies, we were concerned primarily with the ratio of **88a**:**87**. However, we also observed several by-products that resulted from the reaction. In an effort to overcome this limitation, we next turned our attention to minimizing these by-products. We set out to scale up the reaction so that we could obtain compound quantities sufficient for the characterization and identification of the side-products. We allowed 1.0 equiv of *exo*-glycal **85** to react with 1.0 equiv of benzaniline **86a** and 0.2 equiv of Sc(OTf)₃ overnight. Upon chromatographic workup, we isolated three reaction by-products. We assigned tentative structures based on NMR and HPLC/MS data (Figure 2.10). By-product **89** is likely a hydrated version of the starting material, *exo*-glycal **85**. We also isolated addition product **90**, and we tentatively assigned its structure to be a hydrated version of the “pre-cyclization intermediate”. The formation of this compound helps to validate the currently accepted reaction mechanism as a stepwise process rather than a concerted one. Finally, we also observed a minor

amount of a third by-product, compound **91**. Although we were unable to obtain a sufficient amount of pure material for an NMR, HPLC/MS data led us to hypothesize that its identity could be a phenyl amino derivative of **85**. In total, these three by-products accounted for less than one-third of the mass balance. Having identified the by-products, we surmised that we could minimize these side reactions in order to improve upon conversion of *exo*-glycal **85** to desired product **88a**.

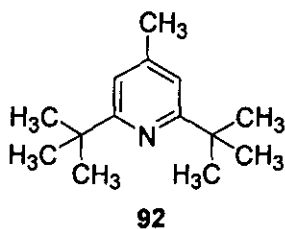
Figure 2.10. Tentative structural assignment of Povarov reaction side-products.



Since the side-products that we primarily observed were hydrated *exo*-glycal **89** and hydrated, pre-cyclization intermediate **90**, we decided to focus on ways in which we could eliminate excess water from the reaction and still promote cyclization. We hypothesized that 4Å molecular sieves may absorb the excess water and help to minimize the formation of these side products. In addition, we theorized that a bulky, non-nucleophilic organic base may help to break the complex between the Lewis acid and the nitrogen of the tetrahydroquinoline system. Therefore, we thought that the addition of

2,6-di-*tert*-butyl-4-methylpyridine **92** (Figure 2.11) could promote cyclization and tetrahydroquinoline formation.

Figure 2.11. Structure of the organic base, 2,6-di-*tert*-butyl-4-methylpyridine.



We designed a series of optimization experiments in order to evaluate the effect of molecular sieves and the organic base **92** on the Povarov reaction with *exo*-glycal **85** (Table 2.5). In general, molecular sieves alone drastically slowed the reaction and limited the conversion to the open-ring sugar based quinoline **88a**. No reaction was observed after stirring for 90 minutes at room temperature, and only one-third of the product mixture consisted of **88a** when the reaction was stirred overnight at room temperature (Entry 1). Even after four days of refluxing, an approximate 1:1 ratio of **88a**:(**87Major** + **87Minor**) resulted from the reaction (Entry 2). This compared to a 2.5:1 ratio when the reaction mixture was refluxed without sieves (Table 2.4, Entry 2). These observations helped to confirm that trace amounts of water are necessary to drive the cyclization, as indicated by the proposed reaction mechanism depicted in Scheme 2.6.

The presence of organic base **92** did not alter the ratio of oxidized to reduced product. No difference was observed between refluxing reactions with and without base (Table 2.5, Entry 3, and Table 2.4, Entry 2). Next we decided to incorporate both

molecular sieves and the pyridine base in one experiment. When run at room temperature for one hour, a 1:2.67 ratio of **88a**:(**87Major** + **87Minor**) was observed (Entry 4). In comparison to the room temperature reaction lacking organic base **92** in which no reaction was observed after 90 minutes, this result marked a substantial improvement in terms of *exo*-glycal consumption. However, refluxing the mixture for three hours did not alter the product ratio (Entry 5). Continuing to reflux the mixture did not result in any additional conversion to the oxidized product **88a**. As a direct result of these experiments, we concluded that molecular sieves slowed the rate of consumption of *exo*-glycal **85** and also resulted in a diminished ratio of **88a**:(**87Major** + **87Minor**). In addition, the pyridine base **92** did not help push the conversion to the oxidized open-ring glycosylidene based quinoline **88a**. The reaction conducted at room temperature in the absence of sieves and organic base **92** (Table 2.0, Entry 1) resulted in the most favorable ratio of **88a**:**87**. Ultimately, these base addition reaction modifications did not entirely eliminate the problem of incomplete cyclization, and side-products **89**, **90**, and **91** were detected by HPLC/MS analysis. After performing this series of experiments, we were still unable to attain 100% conversion to **88a**.

Table 2.5. Reaction optimization experiments involving addition of molecular sieves and/or 2,6-di-*tert*-butyl-4-methylpyridine **92**.

Entry	Conditions ^a	Ratio of 88a :(87Major + 87Minor) ^b
1	sieves ^c , room temperature, overnight	1:2.34
2	sieves, reflux, up to 4 days	1.03:1
3	92 ^d , reflux, overnight	2.53:1
4	92 , sieves, room temperature, 1 hour	1:2.67
5	92 , sieves, reflux, 3 hours	1:2.43

^a **85** (1.0 equiv), **86a** (1.0 equiv), and Sc(OTf)₃ (0.2 equiv) were dissolved in MeCN and allowed to react under the specified conditions. ^b Determined by HPLC/MS analysis.

^c 1.3 mg of activated 4Å molecular sieves per 1 mg of *exo*-glycal **85**. ^d 1.0 equiv added

Next we chose to study the effects of conducting the Povarov reaction in a microwave reactor. We decided to perform these experiments because Jimenez and colleagues reported success with multicomponent Povarov additions that were subjected to microwave irradiation.⁷¹ One of the main advantages of the use of a microwave reactor is the attainment of reaction temperatures which exceed the solvent reflux temperature. These “pressure-cooking” conditions have the potential to enhance reactivity while shortening reaction times.⁷⁹ In our first microwave experiment, we heated the reaction mixture for two minutes at 120 °C (Table 2.6, Entry 1) and observed about a 1:1 ratio of oxidized to reduced products. In a separate experiment, 4Å molecular sieves were added to the reaction mixture. After 20 minutes of heating, however, no product was formed (Entry 2). This observation again confirms the fact that trace quantities of water are required for the cyclization step of the reaction to occur. Finally,

addition of organic base **92** did not enhance the conversion to the open-ring form. After 70 minutes of heating, the ratio of **88a**:(**87Major** + **87Minor**) was still nearly 1:1 (Entry 3). Clearly microwave reaction conditions did not result in enhanced conversion of the spiro mixture **87Major** + **87Minor** to the open-ring sugar based quinoline **88a**.

Table 2.6. Reaction optimization experiments involving a microwave reactor.

Entry	Conditions ^a	Ratio of 88a :(87Major + 87Minor) ^b
1	2 minutes at 120 °C	1:1.12
2	sieves ^c , 20 minutes at 120 °C	still mostly <i>exo</i> -glycal 85
3	92 ^d , 70 minutes at 120 °C	1:1.07, still <i>exo</i> -glycal 85

^a **85** (1.0 equiv), **86a** (1.0 equiv.), and Sc(OTf)₃ (0.2 equiv) were dissolved in MeCN and allowed to react under the specified conditions. ^b Determined by HPLC/MS analysis.

^c 1.3 mg of activated 4Å molecular sieves per 1 mg of *exo*-glycal **85**. ^d 1.0 equiv added

In order to address the issues that we were facing, we next decided to turn our attention to the reaction solvent, acetonitrile. As a result of the scale-up studies, we observed hydrated products, suggesting to us that water was attacking the intermediate that resulted during this stepwise reaction. In the experiments involving molecular sieves, we noted that the reaction's progress was very slow. When we conducted experiments with unopened, Sure/SealTM anhydrous bottles of acetonitrile, we no longer encountered substantial amounts of hydrated side-products. In addition, since the reactions went to completion, enough water must be present in the system to allow for

cyclization of the intermediate to the tetrahydroquinoline. Going forward, all reaction experiments were conducted with unopened Sure/Seal™ bottles of acetonitrile.

Now that the problem with the solvent and excess water was behind us, we decided to explore the synthesis of the spiro compounds in more depth. Interestingly, we observed that predominately spiroanellated tetrahydroquinolines were present when the Sc(OTf)₃ catalyzed reaction was stopped after a period of one hour. We were able to successfully isolate **87Major** + **87Minor** (~4:1 ratio) in 65% yield with only a trace amount (<4%) of **88a**. However, as previously noted, this mixture of isomers is not stable at room temperature and partially converts to the fully aromatized, open-ring compound **88a**. Therefore we set out to study the effect of oxidizing agents on the reaction as another strategy to exclusively obtain the open-ring product. We hypothesized that an inorganic oxidizing agent added to the reaction may help drive the tetrahydroquinoline aromatization and subsequent ring opening of the glucose spiroanellated tetrahydroquinoline **87** to yield the fully aromatized glycosylidene-derived quinoline **88a**. To our delight, we quickly discovered that the addition of 2.0 equiv of manganese (IV) oxide (MnO₂) resulted in the complete conversion of *exo*-glycal starting material **85** to the open-ring glycosylidene-derived quinoline **88a** in high yield. A representative procedure for the synthesis of **88a** is as follows: To a solution of *exo*-glycal **85** (100 mg; 0.186 mmol) in acetonitrile (1 mL, unopened Sure/Seal™ bottle) was added benzaniline **86a** (33.8 mg; 0.186 mmol) followed by Sc(OTf)₃ (18.3 mg; 0.0372 mmol). The reaction was stirred at room temperature under an atmosphere of nitrogen. After two hours, MnO₂ (32.4 mg; 0.372 mmol) was added and the mixture was stirred overnight. The reaction was diluted with ethyl acetate (15 mL), filtered through Celite,

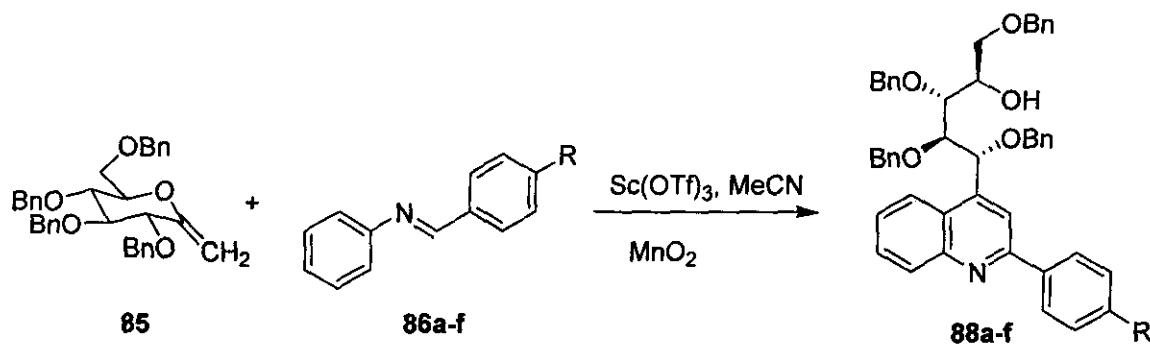
and concentrated *in vacuo*. The crude material was purified over silica gel, eluting with a gradient of 0% - 40% ethyl acetate in hexane to give **88a** as a colorless oil (87 mg; 65% yield).

e. Evaluation of Substituent Effects

We next applied this one-pot Povarov cycloaddition/oxidation procedure to a series of *para*-substituted benzanilines in order to evaluate the electronic effect of substituents on this reaction (Table 2.7). First we chose to examine *para*-substituted benzanilines in which the R-group is derived from the benzaldehyde precursor. In general, the halogen substituted benzanilines (Entries 2 & 3) reacted efficiently to produce the corresponding open-ring glycosylidene-based quinolines. The yields, which exceeded 60%, were very similar when compared to the non-substituted phenyl ring (Entry 1). The electron-withdrawing inductive effect of the halogens is due to their electronegativity values, and it acts in a manner opposite to their electron-donating resonance effects. These properties are counter to each other and result in no net impact on the reaction yields. However, reactions that involved an imine with an electron-withdrawing group, such as a cyano or trifluoromethyl substituent, resulted in moderate yields of the desired product (Entries 4 & 5). The reaction yield also suffered when benzaniline was substituted with an electron-donating methoxy group (Entry 6). These observations suggest that benzanilines containing strongly electron-donating or withdrawing moieties in the *para* position result in diminished reaction yield in

comparison to halogen substituents. Nonetheless, this procedure represents an effective way to access unique carbohydrate-based quinolines.

Table 2.7. Examination of the electronic effect of *para*-substituted, benzaldehyde-derived imines on the one-pot synthesis of glycosylidene-based quinolines.



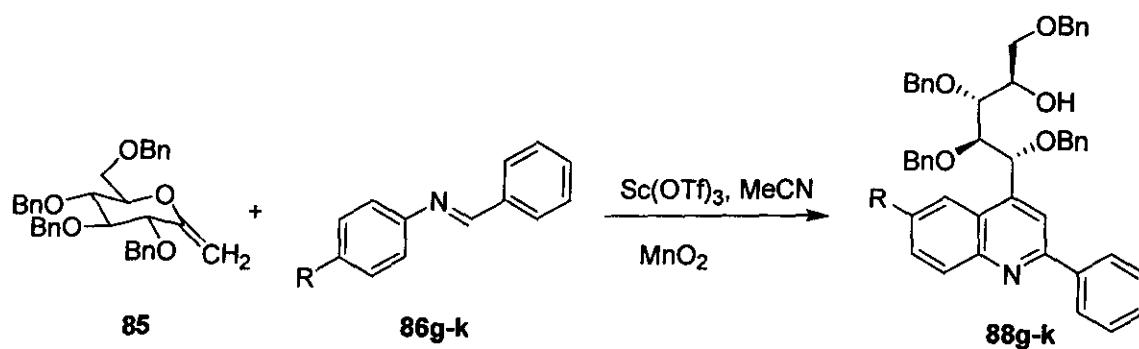
Entry	Benzaniline	Benzaniline R-group	Product	Isolated Yield
1	86a	H	88a	65%
2	86b	F	88b	60%
3	86c	Br	88c	64%
4	86d	CN	88d	43%
5	86e	CF ₃	88e	46%
6	86f	OCH ₃	88f	45%

We then decided to employ this methodology to synthesize compounds in which the aniline-derived phenyl ring is *para*-substituted. In order to accomplish this, we made several imines which are derived from benzaldehyde and a *para*-substituted aniline. We chose to evaluate the same substituents as we studied previously (Table 2.7). In this

series of experiments, reactions of all substituted imines resulted in diminished yields when compared to the non-substituted phenyl ring (Table 2.8, Entries 1-6). Of the substituents evaluated in this series, the imine substituted with the electron-donating methoxy group gave the best cycloaddition/oxidation reaction yield at 55% (Entry 6). This compound marks the only instance in which the yield in this series is higher than its counterpart in the series involving the benzaldehyde-derived phenyl substitutions. The halogen substituted imines gave modest yields in the Povarov cycloaddition/oxidation sequence (Entries 2 & 3). For these benzanilines (**86g** & **86h**), the electron-withdrawing inductive effect of the halogens must have been more influential than the electron-releasing resonance effect. In addition, the experiment involving the benzaniline with the electron-withdrawing trifluoromethyl group gave the lowest yield at 18% (Entry 5). In the case of cyano-substituted imine **86i**, the expected product was not isolated (Entry 4). Instead, the non-cyclized, hydrated adduct was formed in 45% yield. One potential reason for this result is that the electron-withdrawing nature of the cyano group prevented cyclization of the aromatic carbon with the anomeric carbon. Another possible explanation for this result could be that the imine reactant was impure. The condensation reaction between the aldehyde and aniline did not go to completion, and successful recrystallization conditions were not determined. In general, the success of the Povarov cycloaddition/oxidation reaction sequence with this particular series of compounds appears to be negatively affected by the presence of *para* substituents on the aniline ring. This effect was most pronounced with imines containing an electron-withdrawing group in the *para* position. We theorize that removal of electron density from the aniline-derived phenyl group renders the pi-bond electrons of the aromatic ring less available for

attack of the positively charged anomeric carbon (see Scheme 2.6 for generic mechanism). In contrast, release of electron density into the ring by the methoxy group favorably impacts ring closure.

Table 2.8. Examination of the electronic effect of *para*-substituted, aniline-derived imines on the one-pot synthesis of glycosylidene-based quinolines.



Entry	Benzaniline	Benzaniline R-group	Product	Isolated Yield
1	86a	H	88a	65%
2	86g	F	88g	39%
3	86h	Br ^a	88h	38%
4	86i	CN	88i	Not isolated ^b
5	86j	CF ₃ ^a	88j	18%
6	86k	OCH ₃	88k	56%

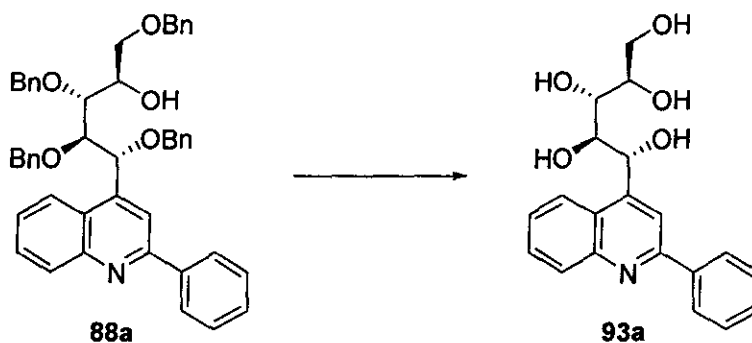
^a Required 8 equiv of MnO₂ for complete conversion. ^b CN analogue of **90** isolated.

The one-pot Povarov cycloaddition/oxidation methodology allows for the preparation of novel glycosylidene-based quinolines. Our studies indicate that the procedure worked best for benzaniline itself. We have determined that *para* substitutions on either phenyl ring of the imine result in diminished yields. However, yields for reactions involving imines with halogen substituents on the benzaldehyde phenyl ring were essentially equal to that benzaniline. Halogen substituted imines in the benzaldehyde-derived series also gave higher yields than the corresponding reaction in the aniline substituted series. The halogen group's electron-donating and withdrawing properties acted in a counteractive manner for the benzaldehyde-derived series. Based upon yields in the aniline-derived benzaniline series, however, the electron-withdrawing inductive effect of the halogen substituent was stronger than the electron-releasing resonance effects. Interestingly, moderate yields were obtained with imines that possess both electron-donating and electron-withdrawing groups on the benzaldehyde-derived phenyl ring. The most dramatic electronic effects were observed with imines substituted in the *para* position of the aniline-derived phenyl ring. Electron-withdrawing groups substantially reduced reaction yields, while the yield with the example involving the electron-releasing methoxy group was rather close to that of benzaniline. These results can be explained by considering the postulated reaction mechanism depicted in Scheme 2.6. Removal of pi-bond electron density makes ring closure more difficult while electron donation into this ring enhances the likelihood of cyclization. Overall, the facile reaction sequence that we developed works well for a variety of benzaniline derivatives, and very respectable product recoveries were obtained from this one-pot procedure.

f. Deprotection Attempts

We next turned our attention to the the final step in our synthetic sequence, the debenzylolation reaction (Scheme 2.13). In order to demonstrate the synthetic utility of the one-pot Povarov addition/oxidation chemistry, we needed to determine conditions to successfully remove the benzyl protecting groups. Traditionally, benzyl ethers are among the most common hydroxyl protective groups used in organic synthesis. In addition, a variety of reliable conditions exist for benzyl ether cleavage.⁹ Our general plan was to first screen the most straightforward conditions with the highest probability of success. If required, we would then progress to the less commonly used procedures. Specifically, our strategy was to start out with room temperature, palladium (Pd)-catalyzed hydrogenolysis conditions before attempting high pressure, high temperature reactions. If those conditions were not successful in removing the benzyl groups, we would move to transfer hydrogenation conditions followed by more specialized chemical methods. Theoretically, the final product produced by the Pd-catalyzed reactions should not require purification other than catalyst filtration and solvent concentration. We predicted that chromatographic purification of the crude material would be difficult due to the polar nature of the final product. The issue of purification provided additional motivation for our rationale of beginning the debenzylolation experiments with standard hydrogenolysis conditions.

Scheme 2.13. Benzyl ether deprotection of glucose-based quinoline **88a**.



Our first attempted debenzylation experiment involved a room temperature reaction under a hydrogen gas balloon catalyzed by Pd/C (5% wet, 1:0.5 wt_{sub}:wt_{cat}) (Table 2.9, Entry 1). Pd-promoted hydrogenolysis is the most common reaction procedure used to remove benzyl ether groups, and Pd is the preferred catalyst because the use of platinum (Pt) often results in ring hydrogenation.⁸⁰ Unfortunately, after overnight stirring, no reaction was observed. We next added Pd(OH)₂/C (Pearlman's catalyst (20% wet)) to give a total catalyst loading of 1:1 wt_{sub}:wt_{cat}. Again, no reaction was observed after overnight stirring at room temperature (Entry 2). The reaction mixture was then heated to 50 °C in an attempt to drive the deprotection (Entry 3). However, only a trace amount of product with one benzyl group removed was observed. As a result of this first pass study, we quickly learned that deprotection of the four benzyl groups would require harsher reaction conditions. Clearly, the standard room temperature and balloon pressure hydrogenolysis procedure followed by catalyst filtration did not apply to our complex glycosylidene-derived quinoline.

Table 2.9. Hydrogen balloon debenzylation experiments.

Entry	Conditions ^a	Results ^b
1	Pd/C (5% wet, 1:0.5 wt _{sub} :wt _{cat}), H ₂ balloon, room temperature	no reaction
2	Entry 1 reaction vessel + Pd(OH) ₂ /C (20% wet) (1:1 wt _{sub} :wt _{cat}), room temperature	no reaction
3	Entry 2 reaction vessel, 50 °C	trace of loss of 1 Bn group

^a Stirred overnight in ethanol. ^b Determined by HPLC/MS analysis.

We next turned our focus to a variety of Pd-based catalysts at conditions involving higher pressure and temperature. In general, for all catalysts attempted at 50 °C and below (Table 2.10, Entries 1-5), we observed no debenzylation by HPLC/MS analysis. Instead we noticed a reduction of two double bonds of the quinoline system to yield isomers of **94a** with a MW of 719 (Figure 2.12a). This result was rather unexpected, as Pd-based catalysts usually do not affect double bonds within an aromatic ring.⁹ We then decided to increase the temperature of the reactions to see if the enhanced temperature would result in deprotection (Entries 6-9). After overnight heating at 60 °C, we did in fact observe complete debenzylation in all screens that we performed. However, by HPLC/MS, we also observed product **94b** with a MW of 365, and this mass likely corresponds to the complete reduction of the quinoline system (Figure 2.12b). While this result is rather interesting, it still did not give us the final compound that we desired. As a result of this series of screens, we learned that high pressure, high

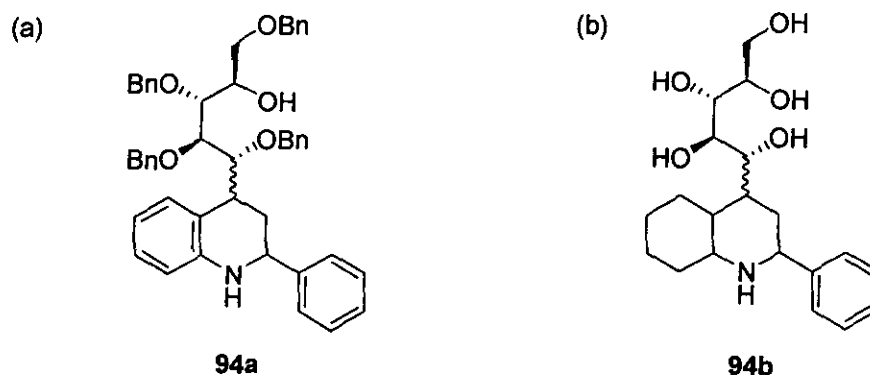
temperature conditions would not remove the benzyl groups while leaving the quinoline system intact. Therefore, we decided to try transfer hydrogenation conditions for the benzyl ether deprotection.

Table 2.10. High pressure, high temperature debenzylation experiments.⁸¹

Entry	Conditions ^a	Results ^b
1	Pd/C (10%, wet) (1:1 wt _{sub} :wt _{cat}), 40 °C, 40 psi H ₂	94a isomers
2	Pd/C (5%, dry) (1:1 wt _{sub} :wt _{cat}), 40 °C, 40 psi H ₂	94a isomers
3	Pd(OH) ₂ /C (20%, wet) (1:1 wt _{sub} :wt _{cat}), 40 °C, 40 psi H ₂	94a isomers
4	Pd(OH) ₂ /C (20%, wet) (1:1 wt _{sub} :wt _{cat}), 40 °C, 40 psi H ₂ , acetic acid charge	94a isomers
5	Pd/C eggshell (10%, wet) (1:0.5 wt _{sub} :wt _{cat}), 50 °C, 50 psi H ₂	94a isomers
6	Entry 1 reaction vessel, 60 °C, 40 psi H ₂ overnight	94b isomers
7	Entry 2 reaction vessel, 60 °C, 40 psi H ₂ overnight	94b isomers
8	Entry 3 reaction vessel, 60 °C, 40 psi H ₂ overnight	94b isomers
9	Entry 4 reaction vessel, 60 °C, 40 psi H ₂ , overnight	94b isomers

^a Stirred overnight in methanol. ^b Determined by HPLC/MS analysis.

Figure 2.12. Tentative structural assignments of the products formed from reaction conditions in (a) entries 1-5 and (b) entries 6-9 of Table 2.10.



Transfer hydrogenation is a reaction strategy in which hydrogen gas is formed *in situ*. It requires a Pd/C catalyst as well as either cyclohexene or ammonium formate to generate the hydrogen gas necessary for the reaction to take place. For our debenzylolation attempts using transfer hydrogenation conditions, we decided to utilize Pearlman's catalyst.⁸² Our initial experiment (Table 2.11, Entry 1) involved cyclohexene, and these conditions successfully cleaved off all of the benzyl protective groups after refluxing the reaction for two days. However, the reaction vessel continually dried out and the solvents needed to be replenished periodically. In order to work around this problem, we tried the same reaction in the microwave reactor. We had also hoped that microwave irradiation could shorten the reaction time. Unfortunately, heating in the microwave for over five hours did not result in complete conversion to the desired product (Entry 2). The experiment was discontinued because the reaction tube broke due to extended heating times. We then modified our transfer hydrogenation conditions by increasing the catalyst loading to 1:1 ($w_{\text{sub}}:w_{\text{cat}}$). We conducted the reaction in a sealed tube as

opposed to a nitrogen-linked condenser. We hypothesized that this modification would prevent the solvents from evaporating. We also thought that the sealed tube approach would keep the generated hydrogen gas within the reaction vessel. These conditions successfully debenzylated compound **88a** (Entry 3). However, we also observed two by-products (MW-16, MW-18) that comprised approximately 25% of the crude reaction mixture. One of these compounds (MW-18) likely corresponds to a dehydration of one of the hydroxyl groups. Purification of the mixture by silica gel chromatography (gradient of 0% to 15% methanol in dichloromethane) did not successfully separate the impurities from the desired product due to the polar nature of the compounds. We also tried similar transfer hydrogenation conditions with ammonium formate⁸³ (Entry 4). However, we only observed a trace amount of compound in which one benzyl group was removed. It is likely that the ammonium formate conditions did not generate enough hydrogen gas required for the reaction to occur. Even portion-wise addition of a large excess of this reagent did not have a favorable effect on the reaction. This series of experiments led us to the conclusion that successful debenylation is possible without reduction of the quinoline system. However, we turned our attention to chemical methods because of the difficulty of separating the desired compound from the side products that formed.

Table 2.11. Transfer hydrogenation debenzylation experiments.

Entry	Conditions ^a	Results ^b
1	Pd(OH) ₂ /C (20%, wet) (1:0.25 wt _{sub} :wt _{cat}), 90 °C (reflux), cyclohexene, 2 days	93a but reaction continually dries out
2	Pd(OH) ₂ /C (20%, wet) (1:0.25 wt _{sub} :wt _{cat}), 120 °C (microwave), cyclohexene, 5 hours	partial conversion to 93a ; tube breaks in microwave
3	Pd(OH) ₂ /C (20%, wet) (1:1 wt _{sub} :wt _{cat}), 90 °C (sealed tube), cyclohexene, overnight	93a but ~25% by-products (MW-18, MW-16)
4	Pd(OH) ₂ /C (20%, wet) (1:1 wt _{sub} :wt _{cat}), 90 °C (sealed tube), ammonium formate, overnight	trace of loss of 1 Bn group

^a Stirred for the time indicated in ethanol. ^b Determined by HPLC/MS analysis.

Numerous chemical conditions are known to remove benzyl ether protecting groups.⁹ However, due to potential purification difficulties, we made this strategy our last resort. For our first debenzylation attempt using chemical methods (Table 2.12, Entries 1 & 2), we tried conditions involving excess methanesulfonic acid. Since no reaction was observed at room temperature, the mixture was heated overnight. Unfortunately, no desired product resulted from the reaction and the compound was instead destroyed. Another deprotection experiment involved the use of excess ferric chloride⁸⁴ (Entry 3). This reagent successfully removed the benzyl protecting groups when stirred at room temperature overnight. However, the reaction was very messy. Given the promising results with ferric chloride, we decided to try another Lewis acid,

boron trichloride⁸⁵ (Entry 4). To our delight, this reagent successfully cleaved the protective groups after one hour of stirring at -78 °C.

Table 2.12. Debenzylation experiments utilizing chemical methods.

Entry	Conditions	Results ^a
1	methanesulfonic acid, DMF, DCM, room temperature, overnight	no reaction
2	Entry 1 reaction vessel, 75 °C, overnight	compound destroyed
3	FeCl ₃ , DCM, room temperature, overnight	93a , messy reaction
4	BCl ₃ , DCM, -78 °C, 1 hour	93a , clean reaction

^a Determined by HPLC/MS analysis.

The crude material generated by the boron trichloride conditions required purification by reverse phase high performance liquid chromatography (HPLC) in order to remove the borane-ligated by-products. Method development resulted in conditions that utilized acetonitrile and water (ammonium hydroxide, pH 10).⁸⁶ The ammonium hydroxide mobile phase modifier does not result in a product counterion, and lyophilization of the solvents yielded the free base in high yield. A representative procedure for the synthesis of **93a** is as follows: To a solution of **88a** (70 mg; 0.098 mmol) in dichloromethane (2.0 mL) at -78 °C was added BCl₃ (1 M in hexane; 0.39 mL; 0.39 mmol). The reaction was stirred at -78 °C under an atmosphere of nitrogen. After one hour, additional BCl₃ (1 M in hexane; 0.195 mL; 0.195 mmol) was introduced, and

the reaction was maintained at -78 °C for one hour. The reaction was quenched with the addition of methanol (2.0 mL). The crude material was concentrated *in vacuo*. The residue was coevaporated twice with methanol, and then purified with a Waters mass directed reverse phase prep HPLC system. The following chromatographic conditions were used: (a) column: Waters Xbridge C-18, 30 x 75 mm, 5 micron; (b) flowrate: 50 mL/min; (c) mobile phase: A = water + ammonium hydroxide (pH 10), B = acetonitrile; (d) mobile phase gradient method: time = 0 min, A = 98, B = 2; time = 11 min, A = 65, B = 35; time = 11.2 min, A = 0, B = 100; time = 14.2 min, A = 98, B = 2; time = 15 min, A = 98, B = 2. Lyophilization of the resulting fractions yielded **93a** as a fluffy white solid (24 mg; 69% yield). These deprotection conditions were also attempted with other perbenzylated compounds. Application of this debenzylation procedure to fluoro analogue **88b** resulted in its deprotected counterpart, **93b**, in 63% yield.

2.4. Summary

We have successfully developed a one-pot synthetic methodology that leads to the preparation of novel glucose-derived quinolines. This Povarov addition/oxidation chemistry takes place between an *exo*-glycal dienophile and a benzaniline diene. We have also shown that this reaction proceeds through the glucose-spiroannellated tetrahydroquinoline intermediates, which subsequently oxidize to the open-ring, fully aromatized forms. Extensive catalyst screening and reaction optimization experiments were performed, and they have led us to the conclusion that Sc(OTf)₃ is the optimal catalyst for the synthesis of the open-ring compound. Careful 1D and 2D NMR experiments have confirmed the structure of both the spiro and open-ring glucose-linked

quinolines. This one-pot methodology has been successfully employed with a series of *para*-substituted benzanilines to access several novel open-ring, glycosylidene-derived quinolines in moderate to good yields. A lengthy set of deprotection experiments was carried out in order to develop conditions to remove the benzyl protective groups. The success of the debenzylating chemistry verifies that this one-pot synthetic methodology is a useful way to obtain carbon-linked glucose-derived quinolines.

Chapter 3

Reaction Scope Expansion

3.1. Introduction

The field of organic synthesis has the impressive ability to construct complex and diverse molecular structures from relatively simple compounds. The tools of total synthesis are the chemical reactions which drive structural transformations. Discovery and development of new reactions is crucial for the invention of strategies that ultimately lead to the synthesis of increasingly complex defined target molecules. Research into the development and expansion of new and improved synthetic methodologies will help to propel studies involving target synthesis. Further reaction scope expansion research provides a strong sense of utility for organic name reactions.

The one-pot Povarov cycloaddition/oxidation reaction sequence that we have developed is a facile and convenient way to synthesize novel glucose-derived quinolines. Successful removal of the benzyl ether protective groups validates this approach as a viable strategy toward sugar-derived quinolines. It was our desire, however, to build upon and expand the scope of the reaction methodology. Practically all of the classical organic name reactions have been extensively studied in an attempt to broaden the general applicability of the chemistry. We wanted to test the effect of other sugar *exo*-glycals on the reaction. In addition to varying the sugar-based dienophiles, we hypothesized that other dienes, such as aliphatic imines and azobenzenes, may be applicable to our newly developed reaction methodology. We also theorized that the

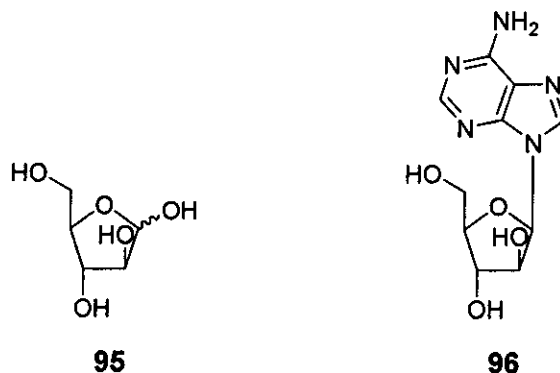
quinoline system could be further transformed through alkylation chemistry. Finally, we desired to study the facial and diastereoselectivity of the addition reaction through both chemical reactions as well as molecular modeling calculations and simulations. In total, this set of experiments is required to more thoroughly understand the extent of the broadness and overall applicability of the reaction. We therefore embarked upon further studies to address the breadth and capacity of this one-pot reaction.

3.2. Background

a. Biological Relevance of Arabinose and Galactose

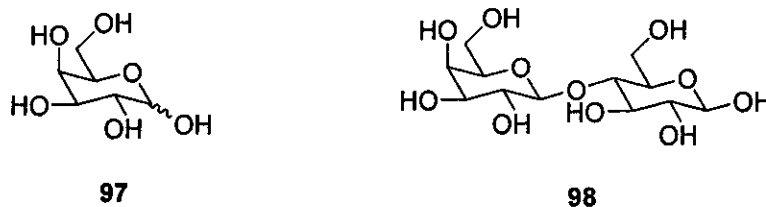
Aside from glucose, several other biologically significant monosaccharides are present throughout nature. Many of these monosaccharides serve as crucial structural components of more complex natural products. For instance, one such example is arabinose **95** (Figure 3.0), a biologically important sugar that is a key monosaccharide of biopolymers such as hemicellulose and pectin.⁶ In addition, this monosaccharide is also a component of the antiviral agent, vidarabine **96** (Figure 3.0).⁸⁷ We therefore surmised that incorporation of an arabinose-based sugar may lead to potentially bioactive compounds.

Figure 3.0. Arabinose and an antiviral derivative.



In addition to arabinose, galactose **97** is also a monosaccharide with biological relevance (Figure 3.1). Aside from D-glucose and 2-deoxy-D-ribose, galactose is one of the few sugars found to any great extent in the animal kingdom.³ Galactose, like arabinose, is a component of the polysaccharide, hemicellulose. Galactose is incorporated into various glycolipids and glycoproteins, and it is also a key component of the determinant saccharides (blood group antigens) that comprise the classical ABO blood group system. More importantly, galactose, along with glucose, are monosaccharides that make up lactose **98** (Figure 3.1). This crucial disaccharide is present in mammalian milk as well as other dairy products.⁶ Given the biological relevance of galactose, we concluded that incorporation of this monosaccharide into our sugar-based quinolines would be worthy of our efforts.

Figure 3.1. Structures of galactose and the disaccharide, lactose.



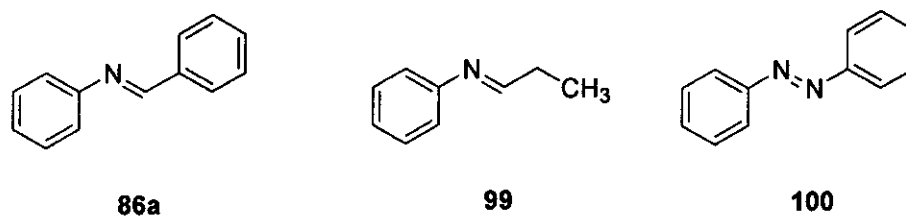
b. Scope Expansion Rationale

The cycloaddition reaction of *N*-aryl imines with nucleophilic olefins is a convenient method of quinoline preparation. This aza-Diels-Alder reaction, also known as the Povarov reaction, involves the reaction between an azadiene and dienophile. Traditionally, the dienophile is an activated vinyl ether or vinyl sulfide. In addition, the Povarov reaction's diene is most frequently a derivative of benzaniline. Although the imine is capable of acting as either a dienophile or azadiene, it is almost always the diene in the Povarov reaction.⁶⁶

There are numerous reports in the literature documenting Povarov reactions conducted with an *N*-aryl imine in which the diene is derived from an aliphatic aldehyde and an aniline analogue.⁶⁶ Reactions with these imines are thought to proceed through the same pathway as their benzaniline counterparts. We envisioned utilizing propionaldehyde-derived imine **99** in our reaction (Figure 3.2). In addition, to the best of our knowledge, there are no reports of Povarov reactions in which an azobenzene derivative acts as a diene in the cycloaddition. Azobenzene **100** is an analogue of

benzaniline in which the nitrogen replaces the imine carbon (Figure 3.2). It also seemed reasonable to attempt to apply this type of diene to our synthetic methodology.

Figure 3.2. Alternate azadienes.



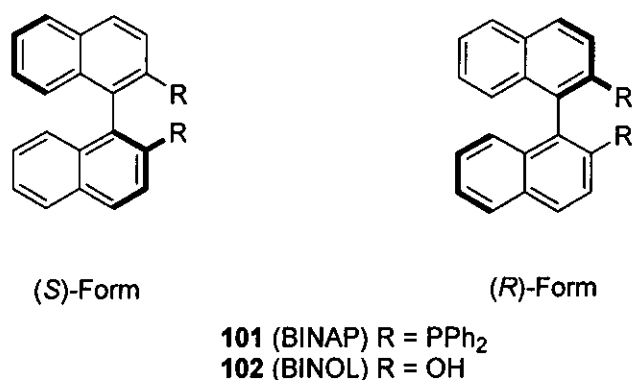
Scope expansion studies are vital to the development of broadly applicable chemical reactions. In fact, the most widely used reaction methods are those which are highly general in nature. Such comprehensive reactions are preferred, especially if the products can serve as synthetically advantageous intermediates. Further derivatization of useful intermediates is both effective and efficient, especially in SAR studies performed by medicinal chemists.

c. Reaction Stereochemistry

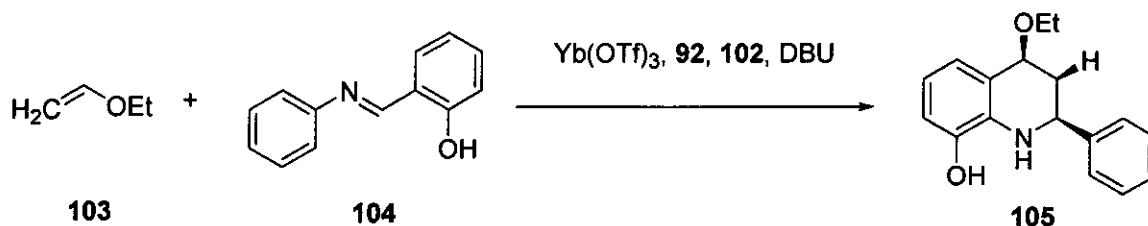
Both the Diels-Alder reaction and the Povarov reaction are synthetically useful reactions that have the potential to be conducted in a stereo- and regio- specific manner. Stereoselective catalysis is frequently promoted by chiral ligands such as BINAP **101**⁸⁸ and BINOL **102**⁸⁹ (Figure 3.3). In fact, there is literature precedent for catalytic asymmetric aza-Diels-Alder reactions involving chiral ligands. Ishanti and Kobayashi

prepared a chiral lanthanide Lewis acid complex from $\text{Yb}(\text{OTf})_3$, (*R*)-(+)-BINOL **102**, DBU, and 2,6-di-*tert*-butyl-4-methylpyridine **92**. The researchers used this chiral ytterbium catalyst to successfully synthesize tetrahydroquinoline derivatives with high diastereo- and enantioselectivities. The group applied this strategy to the Povarov reaction between vinyl ether **103** and benzaniline derivative **104**, and they obtained quinoline derivative **105** (Scheme 3.0).⁹⁰ These favorable results indicate that control over the stereochemistry of Povarov reactions is attainable.

Figure 3.3. Structures of the chiral ligands, BINAP and BINOL.



Scheme 3.0. Ishanti and Kobayashi's stereoselective Povarov reaction.

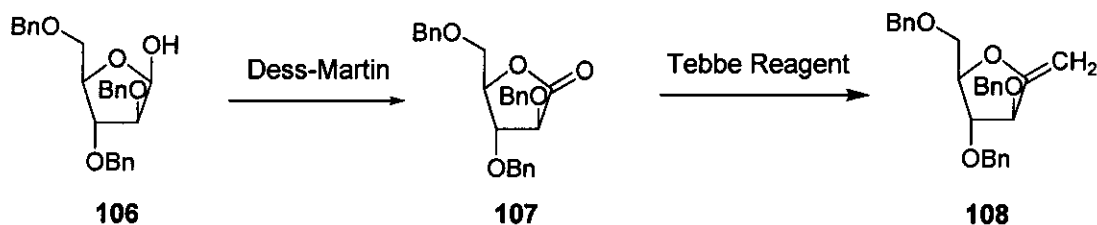


3.3. Results

a. *exo*-Glycal Dienophiles

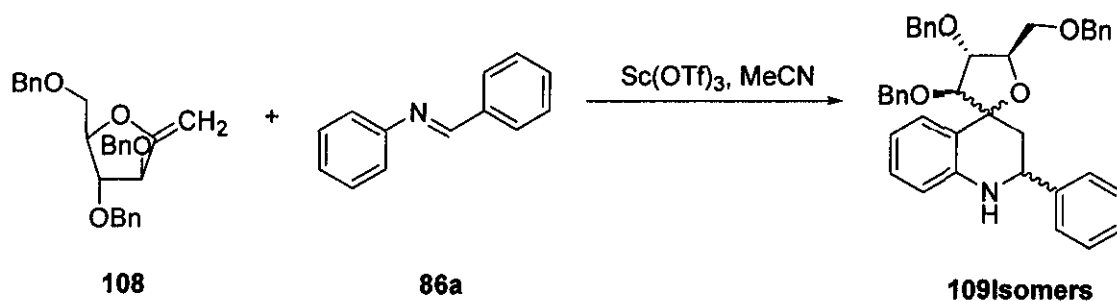
In order to probe the generality of the reaction and further expand our one-pot Povarov cycloaddition/oxidation methodology to other sugars, we chose to target a series of arabinose-based quinolines. We decided to use arabinose **95** as the sugar portion of the compound because we wanted to test the effect of using an *exo*-glycal dienophile that is derived from a five-membered ring sugar. Our synthesis in the arabinose series began with commercially available 2,3,5-tri-*O*-benzyl- β -D-arabinofuranose **106** (Scheme 3.1). We conducted our preparative route in an analogous manner to the synthesis of glucose-derived *exo*-glycal **85**. First the anomeric hydroxyl group was oxidized with Dess-Martin periodinane to give lactone **107** in nearly quantitative yield.⁹¹ Next, the lactone was subjected to Tebbe olefination reaction conditions to give the C1 *exo*-glycal **108** in 43% yield.⁹² With this required terminal alkene in hand, we set out to apply the Povarov addition/oxidation chemistry to synthesize arabinose-derived compounds.

Scheme 3.1. Synthesis of the arabinose-derived *exo*-glycal.



For this series of compounds, we chose to sample several benzanilines (**86a**, **86b**, **86f**, & **86g**) that we utilized in the previous series. Our initial efforts focused on the reaction of *exo*-glycal **108** and benzaniline **86a**. We observed that this reaction also proceeded through the spiroanellated intermediate, just like the reaction with *exo*-glycal **85**. We discovered that *exo*-glycal **108** was consumed within one hour, and we isolated **109Isomers** as a complex mixture of spiro products in 60% yield (Scheme 3.2). However, we were unable to characterize the stereochemistry of the individual components of the mixture and were also unsuccessful in the determination of separation conditions for these compounds.

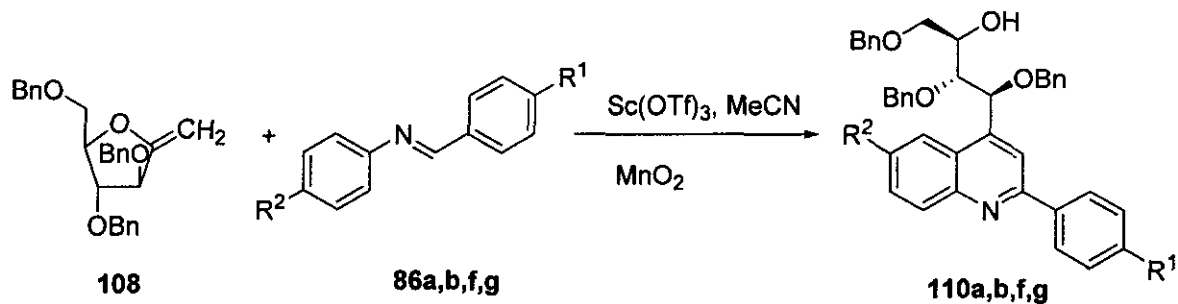
Scheme 3.2. Synthesis of the arabinose-spiroanellated tetrahydroquinoline.



Following our one-pot Povarov cycloaddition/oxidation methodology involving MnO_2 , we synthesized arabinose-derived quinoline **110a** in 57% yield (Table 3.0, Entry 1). We also attempted this reaction with several *para*-substituted benzanilines and isolated open-ring arabinose-derived quinolines in moderate yields (Entries 2-4). In general, the yields for the open-ring products in the arabinose series are similar (within 10%) of the glucose series. However, with exception of the reaction with benzaniline

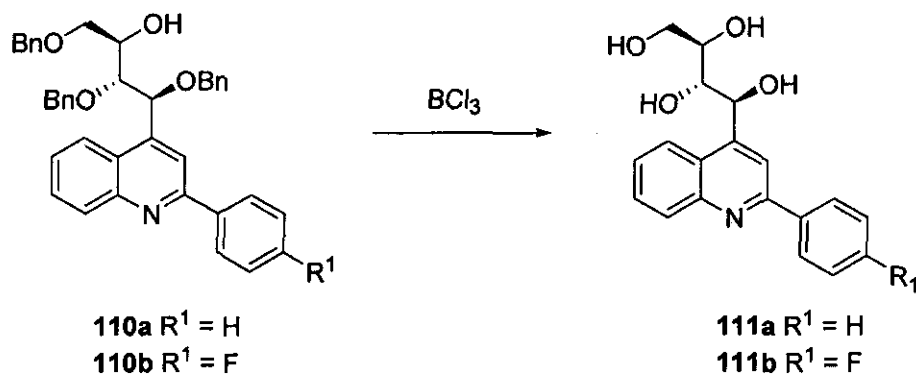
86a, none of the reaction yields exceeded 50%. Interestingly all of the oxidations with arabinose-derived *exo*-glycal **108** ultimately required 8.0 equiv of MnO₂ for complete conversion to the open-ring form. This leads us to surmise that the arabinose-spiroanellated tetrahydroquinoline diastereomers are less susceptible to ring opening than the spiroanellated products in the glucose series. Perhaps this is due to entropic factors, as only three rotatable bonds result from a ring-opening event as compared to four for the glucose series. Nonetheless, our one-pot procedure can still be utilized to effectively synthesize novel carbohydrate-based quinolines. This set of experiments demonstrates that the Povarov cycloaddition/oxidation chemistry successfully works with a pentose *exo*-glycal dienophile. In addition, application of our BCl₃-based debenzylation procedure with **110a** and **110b** produced perhydroxylated compounds **111a** and **111b** in 63% and 48% yield respectively (Scheme 3.3).

Table 3.0. Synthesis of arabinose-based quinolines.



Entry	Benzaniline	R ¹ -group	R ² -group	Product	Isolated Yield
1	86a	H	H	110a	57%
2	86b	F	H	110b	47%
3	86f	OCH ₃	H	110f	44%
4	86g	H	F	110g	49%

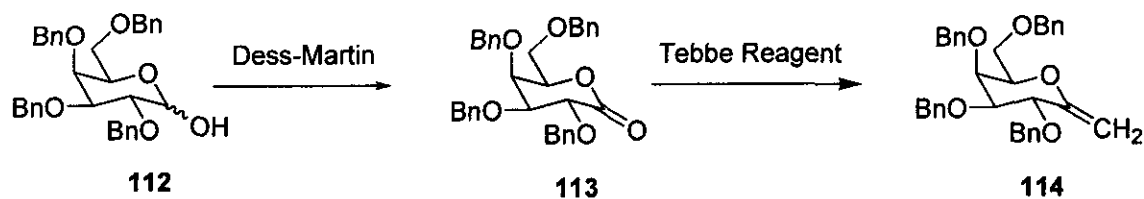
Scheme 3.3. Debenzylation of arabinose-based quinolines **110a** and **110b**.



We also decided to target a small series of galactose-derived quinolines in order to expand upon the breadth of our one-pot Povarov cycloaddition/oxidation methodology that we developed with glucose and successfully applied to arabinose. We selected galactose **97** as the monosaccharide portion of our quinoline derivative because this hexose is a close analogue of glucose, differing only by the configuration of the C4 chiral center. In galactose, the hydroxyl group is in the axial position as opposed to the equatorial position that it occupies in glucose.

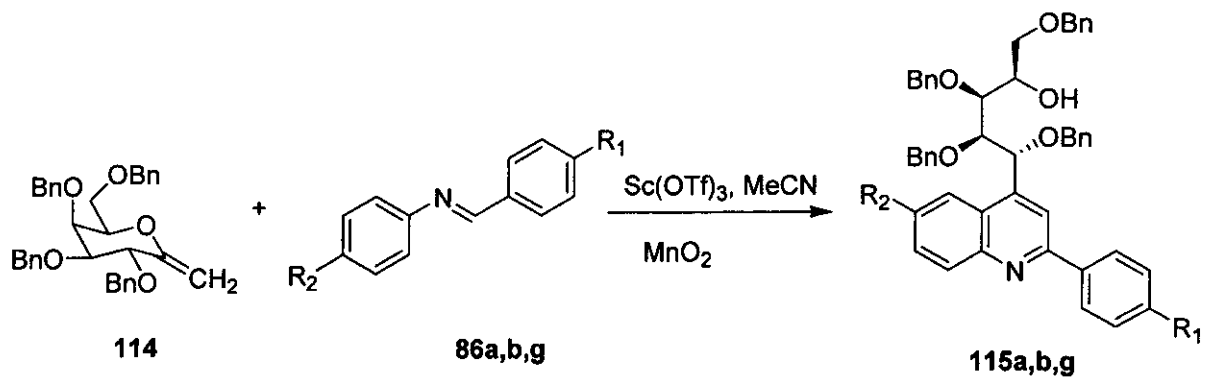
exo-Glycal synthesis in the galactose series required the use of commercially available 2,3,5,6-tetra-*O*-benzyl-D-galactopyranose **112** (Scheme 3.4). We conducted our synthetic route in an analogous manner to the synthesis of glucose-derived *exo*-glycal **85**. Dess-Martin periodinane oxidation of the anomeric hydroxyl group formed lactone **113** in nearly quantitative yield.⁹³ Next, this intermediate was treated with Tebbe reagent to give the C1 *exo*-glycal **114** in 51% yield.⁹⁴ With the necessary galactose-derived dienophile in hand, we set out to apply the addition/oxidation sequence with several benzaniline dienes in order to synthesize galactose-derived quinolines.

Scheme 3.4. Synthesis of the galactose-derived *exo*-glycal.



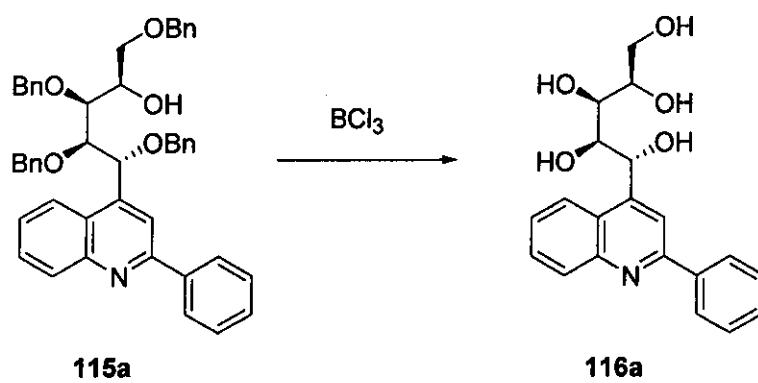
For this series of galactose-based compounds, we performed reactions with several benzanilines (**86a**, **86b**, & **86g**) utilized previously with the glucose and arabinose-based *exo*-glycals. Our initial efforts focused on the addition/oxidation reaction between *exo*-glycal **114** and benzaniline **86a**. We observed the spiroanellated intermediate by HPLC/MS, but did not isolate the isomeric mixture because of a limited supply of **114**. We instead decided to proceed directly to the open-ring quinoline and synthesized **115a** in 51% yield (Table 3.1, Entry 1). We also attempted this reaction with the *para*-fluoro-substituted benzanilines and isolated moderate yields of open-ring galactose-derived quinolines (Entries 2 & 3). As with the arabinose series, the yields for the open-ring products in the galactose series are lower than the glucose series. Although not enough compounds were synthesized in this series to formulate conclusions regarding electronic effects, we did in fact successfully demonstrate that our method works for hexoses other than glucose. In addition, perbenzylated galactose-based quinoline **115a** was subjected to BCl₃, and the deprotected analogue **116a** resulted in 60% yield. The success of the debenylation chemistry once again validates the merit of our strategy directed at the synthesis of sugar-based quinolines.

Table 3.1. Synthesis of galactose-derived quinolines.



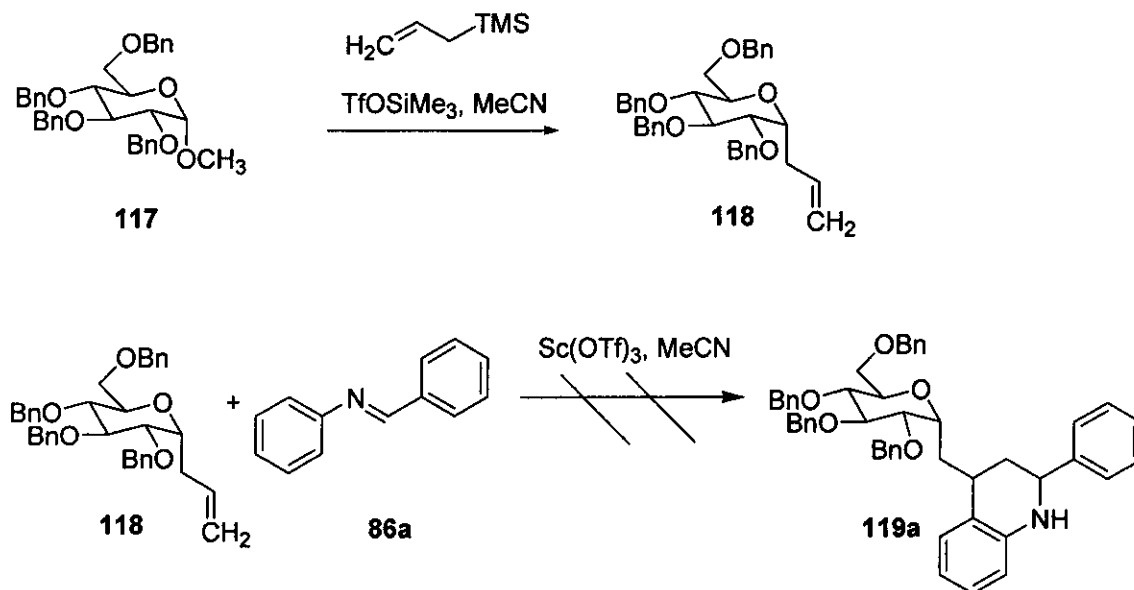
Entry	Benzaniline	R ¹ -group	R ² -group	Product	Isolated Yield
1	86a	H	H	115a	51%
2	86b	F	H	115b	48%
3	86g	H	F	115g	45%

Scheme 3.5. Debenzylation of galactose-based quinoline **115a**.



Another scope expansion idea that we pursued was to use an ethenyl-*exo*-glycal as the Povarov reaction dienophile. This experiment was performed in an attempt to insert a methylene linker in between the quinoline heterocycle and the anomeric carbon of the glucose portion of the molecule. We also thought that this type of system would be less likely to undergo complete aromatization of the tetrahydroquinoline and may therefore avoid ring opening of the sugar. In order to conduct these experiments, we first needed to synthesize the required olefin (Scheme 3.6). Following direct literature procedures developed by Hosomi⁹⁵ and Danishefsky,⁹⁶ we obtained olefin **118** in 63% yield. We next applied our Sc(OTf)₃ catalyzed Povarov cycloaddition reaction conditions with benzaniline **86a**. We did not detect desired product **119a** and instead observed that no reaction occurred when the mixture was stirred overnight at room temperature (no MnO₂). Literature precedent for Povarov reactions involves only vinyl ethers and vinyl sulfides. We concluded that this reaction did not occur because the olefin starting material does not contain a vinylic ether system and is therefore too electron deficient.

Scheme 3.6. Povarov reaction attempts with ethenyl *exo*-glycal **118**.

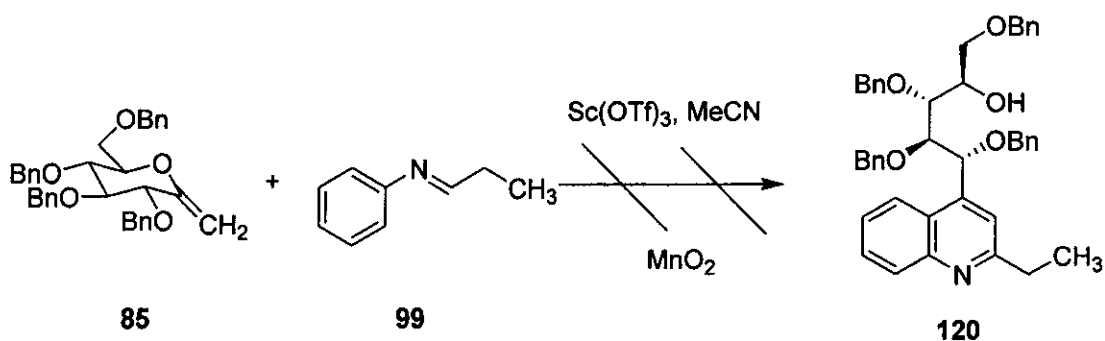


b. Azadienes

We also decided to try the Povarov cycloaddition/oxidation sequence with an imine derived from an aliphatic aldehyde and aniline. Our initial experiments involved the synthesis of imine **99**. We were unable to obtain complete conversion of the reaction between propionaldehyde and aniline, despite carefully following the literature procedure.⁹⁷ Our crude imine **99** was approximately 70% pure by weight, and we used it directly in the one-pot reaction sequence (Scheme 3.7). When subjected to the Povarov addition/oxidation reaction, we observed only a trace quantity of desired product **120** by HPLC/MS. Instead, the major product, identified by mass spectrometry, was a hydrated *exo*-glycal, likely compound **89**. This outcome indicates that the reaction contained too much water content. Further attempts at this reaction, including the use of molecular

sieves and starting reagents azeotroped with toluene, failed to give desired product. These inconclusive results do not allow for an adequate determination regarding the reactivity of *N*-aryl aliphatic aldimines. On the basis of this data, we reasoned that it is unlikely that aliphatic imines can be readily utilized in our addition/oxidation reaction sequence. We therefore did not further pursue experiments in this area of study.

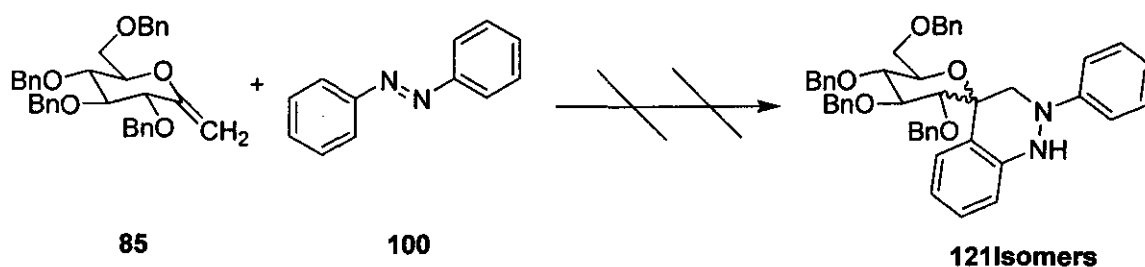
Scheme 3.7. Povarov reaction attempts with imine **99**.



We envisioned substituting azobenzenes for benzanilines in an attempt to expand the scope of the Povarov reaction with *exo*-glycal **85**. We surmised that our previously developed chemistry may be applicable to the addition of azobenzenes. We could easily access a variety of azobenzenes through the reaction of a nitrosobenzene and an aniline derivative as previously documented by Ansporn.⁹⁸ Unfortunately, attempts to apply our Povarov cycloaddition conditions to this reaction expansion idea with azobenzene **100** were unsuccessful. We screened the same rare earth metal triflate catalysts (Sc(OTf)₃, Yb(OTf)₃, & Tb(OTf)₃; Table 3.2) as we did for the Povarov reaction between *exo*-glycal **85** and benzaniline **86a**. In each case, the starting material was consumed, but desired product, **121** isomers, was not formed. According to HPLC/MS data, all three catalysts

produced the same major by-product. Unfortunately, we were unable to structurally identify the major by-product that resulted from these scope expansion experiments. The electronics of this particular reaction are substantially different from that of the Povarov reaction with benzaniline **86a**. In benzaniline, a net electronegativity difference exists between the carbon and nitrogen atoms of the imine, leading to an electron cloud that is distorted toward the nitrogen side of the bond. Since azobenzene is a symmetrical molecule, no such difference exists. This theoretical explanation is a potential reason to account for the failure of the attempted reaction. In addition, to the best of our knowledge, there is no literature precedent for this particular type of transformation. Based upon our observations with this series of experiments, we decided not pursue alternate conditions.

Table 3.2. Catalyst and reaction condition screening with azobenzene **100**.



Entry	Catalyst	Reaction Conditions ^a	Result ^b
1	Sc(OTf) ₃	room temperature, overnight	unidentified by-product MW=659/682(+23)
2	Yb(OTf) ₃	room temperature, overnight	unidentified by-product MW=659/682(+23)
3	Tb(OTf) ₃	room temperature, overnight	unidentified by-product MW=659/682(+23)

^a **85** (1.0 equiv), **100** (1.0 equiv), and catalyst (0.2 equiv) were dissolved in MeCN and allowed to react under the specified conditions. ^b Determined by HPLC/MS analysis.

c. Further Transformations of Sugar-Derived Quinolines

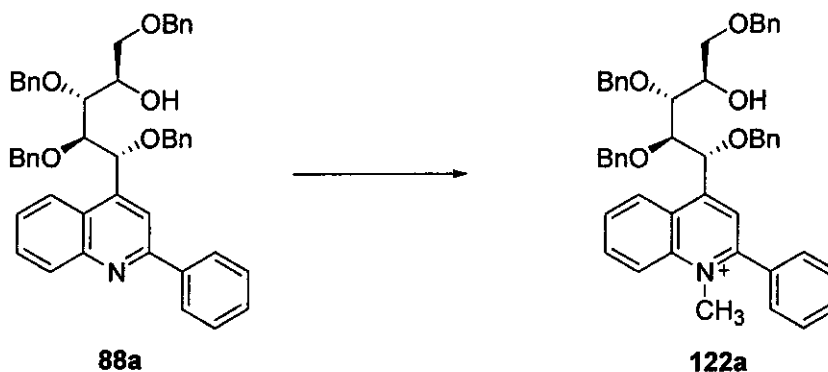
We hypothesized that we could utilize our sugar-derived quinoline as an intermediate for the synthesis of additional novel compounds. For instance, we desired to synthesize the *N*-methyl analogue of **88a** (structure **122a** in Table 3.3). The rationale behind this design was to create a positively charged nitrogen within the quinoline system. We thought that this charge may be a way to help increase the likelihood of the

affinity of the sugar-derived quinoline for DNA. More specifically, we theorized that the positively charged nitrogen may interact electrostatically with the negatively charged phosphate groups on the DNA backbone. Examples of *N*-methylated quinolines as DNA intercalators have been reported in the literature and help to provide further validation for this strategy.⁹⁹

We followed modified literature procedures in order to carry out this synthetic transformation (Table 3.3). Several of our attempts involved iodomethane¹⁰⁰ as the methylating reagent (Entries 1 & 2). Both room temperature and reflux conditions did not give any reaction with the quinoline. This could be due to the volatility of iodomethane as a result of its low boiling point. Our next attempts utilized another common alkylating agent, dimethyl sulfate.¹⁰¹ When allowed to stir at room temperature, no reaction occurred (Entry 3). Refluxing overnight, however, destroyed the glucose-based quinoline starting material (Entry 4). Our final attempts employed methyl triflate as the methylating reagent¹⁰² (Entries 5-8). This reagent initially showed promising results, as we observed nearly 50% conversion to **122a** at room temperature. The reaction, however, was not able to be pushed any further. Increasing the quantity of reagent and heating the mixture to reflux temperature did not enhance the conversion. In addition, an experiment in which a large excess of methyl triflate was added initially did not result in improved conversion. We were unsuccessful in our attempts to consume all of the starting material as well as our efforts to separate the starting material from the methylated product. The associated triflate counterion rendered the separation problematic. Due to the fact that these strategies did not drive the reaction to completion,

we decided not to devote any additional resources to the synthesis of the *N*-methylated quinoline target **122a**.

Table 3.3. Quinoline *N*-methylation attempts.



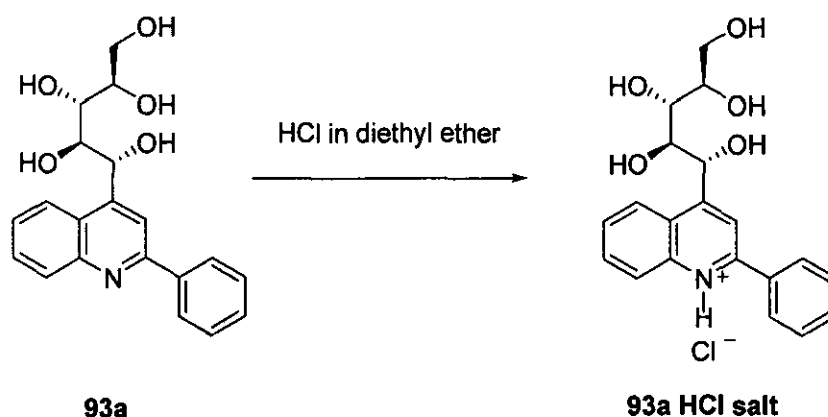
Entry	Conditions ^a	Result ^b
1	Iodomethane (5.0 equiv), room temperature, overnight	no reaction
2	Entry 1 reaction vessel, reflux, overnight	no reaction
3	Dimethyl Sulfate, (10.0 equiv), room temperature, overnight	no reaction
4	Entry 3 reaction vessel, reflux, overnight	compound destroyed
5	MeOTf (1.2 equiv), room temperature, 1 hour	~50% conversion
6	Entry 5 reaction vessel (2.4 equiv total), room temperature, overnight	~50% conversion
7	Entry 5 reaction vessel (10.0 equiv total), reflux, overnight	compound destroyed
8	MeOTf (30 equiv), room temperature, 1 hour	trace product, unknown by-product

^a Reagents were dissolved in MeCN and allowed to react under the specified conditions.

^b Determined by HPLC/MS analysis.

We decided to make a hydrochloride salt of **93a** as a way to install a positive charge on the nitrogen within the quinoline system. The monohydrochloride was easily formed in quantitative yield by treatment of **93a** with excess hydrogen chloride in diethyl ether (1 M solution). The salt stoichiometry was determined by potentiometric titration to be 1:1.¹⁰³ While the charge may be transient depending upon the pH of the surrounding environment, this compound may also prove beneficial because hydrochloride salts are often more soluble in aqueous environments than their free base counterparts.

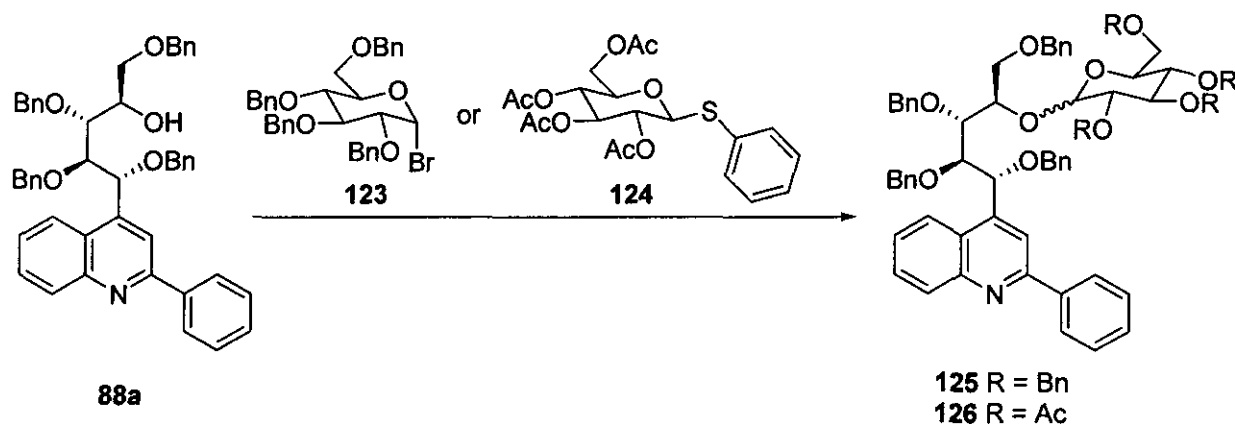
Scheme 3.8. Formation of the hydrochloride salt of **93a**.



We also thought that the hydroxyl group of sugar-based quinoline **88a** could serve as a glycosyl acceptor and lead to the preparation of a compound with two sugar-derived moieties linked together by a glycoside bond. Specifically, we hypothesized that we would be able to perform a Koenigs-Knorr glycosidation reaction between sugar-based quinoline **88a** and glycosyl halide **123**. We made two separate unsuccessful attempts at

target compound **125**. Experiments utilizing the heavy metal salts Ag_2CO_3 ¹⁰⁴ and $\text{Ag}(\text{OTf})$ ¹⁰⁵ resulted in no observed reaction (Table 3.4, Entries 1 & 2). Potential reasons for the failure of these Koenigs-Knorr glycosidation reactions include glycosyl halide hydrolysis as well as 1,2-elimination.¹⁰⁶ We then decided to proceed to thioglycoside conditions¹⁰⁷ in an attempt to form the glycoside bond and access compound **126**. This glycosylation method also did not succeed, as the starting materials failed to react (Entry 3). The lack of success of our first pass condition screening approach toward glycoside bond formation indicates that the hydroxyl group of **88a** is unreactive. This lack of reactivity is likely due to steric hindrance surrounding the hydroxyl functionality. Although a shortage of material prevented us from continuing to pursue these targets, Kahne sulfoxide glycosylation conditions are more likely to yield the desired glycoside product because this type of reaction typically succeeds with unreactive as well as sterically hindered substrates.¹⁰⁶

Table 3.4. Glycosylation attempts.



Entry	Conditions ^a	Result ^b
1	123 , Ag ₂ CO ₃ , MeCN, diethyl ether, room temperature, overnight	no reaction
2	123 , 92 , Ag(OTf), MeCN, room temperature, overnight	no reaction
3	124 , NIS, TfOH, DCM, -40 °C, 30 minutes	no reaction

^a Reactions were run with 4Å molecular sieves under the specified conditions.

^b Determined by HPLC/MS analysis.

d. Stereochemistry of the Povarov Addition Reaction

An interesting aspect of the Povarov addition between glucose-based *exo*-glycal **85** and benzaniline **86a** that warranted further theoretical investigation was the observed facial selectivity and stereocontrol of the reaction. The regiochemistry of addition to the glycal to produce the spiroanellated products is as what would be anticipated based upon mechanistic predictions (Scheme 2.6). According to the non-concerted reaction process,

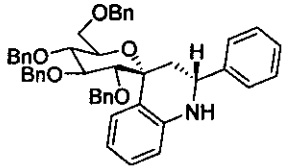
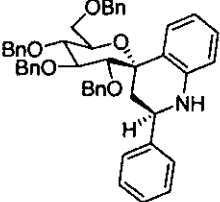
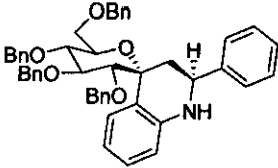
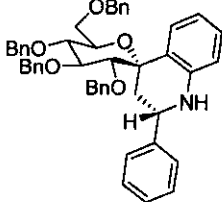
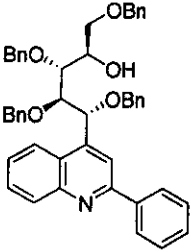
attack of the imine carbon by the more nucleophilic C2 carbon of the vinyl ether occurs first. This is followed by electrophilic attack of the resulting oxonium ion by the ortho carbon of the aniline ring. The two step process has been described by other researchers¹⁰⁸ and was further supported by our isolation of an intermediate addition product. Compound **90** forms when the imine carbon of the benzaniline is added to the C2 carbon of the vinyl ether, and water is added to the C1 carbon of the vinyl ether. The observed axial facial preference for addition to *exo*-glycal **85** leading to the β -substituted methylene group at the anomeric carbon most likely arises because of steric effects experienced by the bicyclic component in the equatorial plane.¹⁰⁹ The steric effects may account for the observation that only 20% of the spiro mixture consists of product (**87Minor**) in which the axial substituent from the anomeric carbon is derived from the C2 carbon of the vinyl ether.

As previously discussed, we observed only two of the four possible tetrahydroquinoline stereoisomers, **87Major** and **87Minor**, from the Povarov cyclization reaction with the glucose-derived *exo*-glycal **85**. Interestingly, neither isomer with the (*S*)-configuration at benzylic carbon j (see Tables 2.1 & 2.2 for the atom labeling system) was formed. This observation led us to utilize molecular modeling calculations to search for an energy trend concerning the product distribution of the spiroanellated compounds. Spartan06 software was used to determine the energy for both molecular mechanics force field (Merck Molecular Force Fields or MMFF) and semi-empirical quantum calculations (Recife Model 1 or RM1).¹¹⁰ MMFF is a family of force fields that is used for the modeling of molecular systems. It involves minimization of a compound's potential in an artificial force field.¹¹¹ RM1, a recently reparameterized version of Austin Model 1 or

AM1, is a semi-empirical method for the quantum calculation of molecular orbital electronic structure that calculates enthalpy of formation.¹¹² Both computational models are highly theoretical in nature and offer a crude approximation for the total energy of the compounds.¹¹³ When comparing calculation results within a simulation model, the compound with the lowest energy value is favored. Although the absolute energy values are not necessarily indicative of actual heat of formation values, a trend may or may not be apparent through comparison of the calculated data for the stereoisomers studied.

The MMFF and RM1 calculations for the four possible spiroanellated stereoisomers do not correlate with the experimentally observed product distribution (Table 3.5). All four spiro stereoisomers have similar MMFF calculated values as well as nearly identical results for the RM1 simulations. These molecular modeling calculations lead us to conclude that the observed distribution of the spiro compounds is not entirely explained by the thermodynamics of all of the possible products. In addition, these models do not account for the absence of the isomers with the (*S*)-configuration at the benzylic carbon. Therefore thermodynamic factors must not be the sole reason that only two of the four possible spiroanellated stereoisomers were produced by the reaction.

Table 3.5. Molecular modeling calculations for both the observed and potential Povarov reaction products.

Compound	Stereochemistry	MMFF potential (kJ/mol)	RMI enthalpy (kJ/mol)
	(<i>R</i>), (<i>R</i>) 87Major	926.4	-209.4
	(<i>S</i>), (<i>R</i>) 87Minor	922.3	-203.8
	(<i>R</i>), (<i>S</i>) Not Observed	937.6	-207.7
	(<i>S</i>), (<i>S</i>) Not Observed	907.0	-207.2
	88a	960.1	-141.1

We next applied the Boltzmann Distribution Law to analyze the simulated energy values for the two observed spiro products that resulted from the reaction in order to look for a correlation between the observed and calculated stereoisomer ratio. This distribution function provides a probability measure for the distribution of the states of a system based on energy differences. The Boltzmann Distribution for a fractional number of particles, N_1/N_2 , occupying a set of states possessing energies E_1 and E_2 is: $N_1/N_2 = e^{(-\Delta E/RT)}$ where R (gas constant) is $8.314510 \text{ J mol}^{-1} \text{ K}^{-1}$ and T is the temperature in Kelvin.¹¹⁴ This distribution equation was used only with the RM1 data set because the potential calculations of the MMFF model did not favor the major observed product. Application to the RM1 simulation data yielded the **87Major:87Minor** ratio of 0.896:0.104. This calculated ratio compares to the 4:1 product ratio that was observed for the reaction and conforms with the trend. However, this correlation is not substantial because the energy difference between **87Major** and **87Minor** (5.6 kJ/mol) is less than the standard error inherent to the model (~25 kJ/mol).¹¹² In addition, the Spartan software simulations cannot be used to explain the absence of the other two potential stereoisomers.

The lack of correlation on the part of these modeling calculations suggests that it is likely that kinetic and/or thermodynamic factors involving a transition state may instead impact the observed product distribution. The energy calculations of the spiro compounds cannot be directly compared to the results for the open-ring products because the molecular formulas of the compounds under consideration are not identical (differ by two hydrogen atoms). Finally, as a general trend, errors in the determination of

conformational energy barriers can be rather large and oftentimes unpredictable, leading to deviations between calculated and experimental results.¹¹³

Despite the inconsistencies with the output of the modeling methods, we confidently contend that **88a** is more favorable from the perspective of Gibb's free energy ($\Delta G = \Delta H - T\Delta S$) than its spiro precursors. We hypothesize that the observed transformation is driven enthalpically by the aromatization of the tetrahydroquinoline to the dihydroquinoline. It is widely accepted that aromatization is an enthalpically favored process, and it confers additional stability to the resulting compound due to the delocalization of the pi electrons within the ring system. In addition to the enthalpic contributions to Gibb's free energy, the oxidized, open-ring form has five additional rotatable bonds which make an entropic contribution to the overall favorability of the process. Clearly the freely rotatable bonds create a more disordered compound. The capacity for bond rotation of the open-ring form contrasts with the conformationally ordered pyranose sugar and spiroanellated ring system. We theorize that the rotational capabilities of the open-ring compound provide for an entropic enhancement to the overall favorability of the process. In consideration of both enthalpy and entropy, the open-ring quinoline product is thermodynamically favored over the spiro forms. The observed lack of stability of the spiro conformers also correlates well with the Povarov addition/oxidation pathway (Scheme 2.5) in which alkoxy group elimination results in an aromatized compound.

While the molecular modeling calculations did not reveal an energy trend concerning the product distribution of the glucose-spiroanellated tetrahydroquinoline stereoisomers, we nonetheless decided to conduct a series of experiments in an attempt to

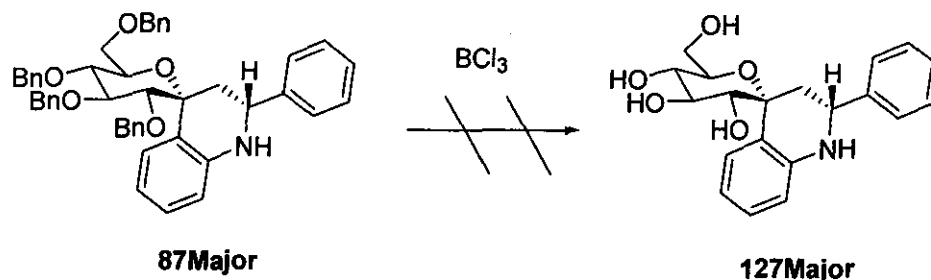
control the stereochemistry of the spiro products. Ligands such as BINAP **101**⁸⁸ and BINOL **102**⁸⁹ are often utilized as part of a general strategy for stereoselective catalysis. We surmised that these chiral auxiliaries may prove useful to us, and we therefore decided to attempt a modified version of the procedure developed by Ishanti and Kobayashi on our system with *exo*-glycal **85** and benzaniline **86a**.

When we applied this strategy to our Povarov reaction involving *exo*-glycal **85** and benzaniline **86a**, no reaction was observed (Table 3.6, Entries 1-3). Unreacted starting material remained after 24 hours of stirring at room temperature. We concluded that either the presence of base (DBU) or the chiral ligand (BINAP or BINOL) prevented the Povarov reaction from taking place by interfering with the action of the lanthanide triflate catalyst. The organic base and chiral ligand were the only reaction condition differences compared to the original cyclization experiments (Table 2.0). Based on these results, we decided not to further pursue stereoselective catalysis conditions.

columns because the chiral stationary phase environment can create non-bonding interactions which may lead to differences in retention and ultimately the separation of the stereoisomers. After a screen involving several chiral columns, we determined that the following analytical conditions successfully separated **87Major** and **87Minor**: ChiralPak IB 4.6 x 250 mm column, 5 micron particle size, 10% ethanol in heptane (isocratic), 0.5 ml/min flowrate, 254 nm wavelength, retention time **87Minor** (8.48 min), **87Major** (13.89 min). We then proceeded to separate the spiro mixture on a prep scale. The fractions containing the compound needed to be concentrated promptly because we observed partial decomposition to the open-ring, fully aromatized form if the fractions sat out on the bench overnight. We successfully separated, concentrated, and characterized each spiro isomer before decomposition occurred. This chromatography work allowed us to isolate individual isomers despite the fact that our attempts to synthesize the spiro isomers stereoselectively failed.

We also attempted to deprotect the perbenzylated spiroannellated tetrahydroquinoline intermediate (Scheme 3.9). When **87Major** was subjected to BCl_3 conditions, we were unable to isolate any debenzylated spiro product. Although the benzyl protective groups were removed, we also observed that the tetrahydroquinoline aromatized to the open-ring, fully aromatized quinoline **93a**, despite the absence of oxidizing agent MnO_2 . Under these reaction conditions, we are led to conclude that the BCl_3 is accelerating the rate of tetrahydroquinoline oxidation. The perhydroxylated spiro tetrahydroquinoline is not stable and its counterpart, the open-ring, dihydroquinoline is clearly favored.

Scheme 3.9. Deprotection of spiroannellated tetrahydroquinoline, **87Major**.



3.4. Summary

We have made progress in our efforts to broaden the scope of the substrates that can be applied to the one-pot methodology that we have developed. Initially our model system was limited to glucose-derived *exo*-glycal **85** and benzaniline **86** analogues. We have succeeded in expanding the capacity of the Povarov chemistry by altering the sugar-derived dienophile involved in the reaction. The addition/oxidation reaction proceeded smoothly with both arabinose and galactose-derived *exo*-glycals, indicating that the chemistry is not limited by the size of the glycal ring or the configuration at the C4 position. However, attempts to apply an ethenyl-*exo*-glycal dienophile were unsuccessful, likely because the Povarov reaction only proceeds with activated alkenes. We also conducted diene modification experiments, but we were unable to substitute azobenzene and an aliphatic aldehyde-derived imine for benzaniline **86** analogues. In addition, we attempted to utilize compound **88a** as an intermediate substrate for further transformations. We explored several conditions for *N*-methylation of the quinoline ring, but were not successful in our efforts to develop a procedure that resulted in complete substrate conversion. On the other hand, we were able to form the monohydrochloride

salt of **93a**. We also unsuccessfully tried to form a glycoside bond by using the hydroxyl group of **88a** as a glycosyl acceptor. Finally, we examined the stereochemistry of the Povarov reaction by studying computer simulations as well as stereoselective reaction conditions. Despite the fact that modified literature procedures involving chiral ligands failed to produce spiro products, we did succeed in separating **87Major** and **87Minor** through chiral chromatography.

Chapter 4

Biological Evaluation of Selected Compounds

4.1. Introduction

The molecular architecture of compounds derived from nature has been, and continues to be, an excellent source of inspiration for the design of drug-like precursors. For instance, nearly 40% of the drugs approved between 1983 and 1994 were natural products or their derivatives. Even a larger percentage of anticancer or antiinfective compounds researched during this period of time fit into the broad category of modified natural products.¹¹⁵ A common strategy for the rapid evaluation of drug candidates that has been employed by drug discovery scientists is to first screen a library of synthetic molecules for potency against a specific target and then follow up by determining the pharmacokinetic properties of several of the most potent compounds. This multifaceted approach to medicinal chemistry allows for a balance to be attained between potency and bioavailability by simultaneously assessing both *in vitro* and *in vivo* properties.

4.2. Background

a. Physicochemical Properties

Yet another important consideration for the development of bioactive compounds as therapeutic agents is the evaluation of pharmacokinetic properties, especially bioavailability. One of the significant goals of drug research and development is to understand the molecular properties that impact a compound's bioavailability. Lipinski's rule of five provides a series of guidelines that can be utilized to predict the oral bioavailability of a drug candidate. This set of principles takes into account such factors as molecular weight (MW), lipophilicity (log P), and the number of hydrogen bond donors and acceptors. In general, Lipinski's rule of five suggests that poor oral absorption is likely when at least two of the following criteria are met: (1) the molecular weight of the compound exceeds 500, (2) the logP is five or greater, (3) the molecule possesses more than five hydrogen bond donors, and (4) the compound has more than ten hydrogen bond acceptors. Since its proposal in the late 1990s, Lipinski's rule of five has helped medicinal chemists to make general estimations regarding the absorption properties of lead structures.¹¹⁶

Although implementation of this analysis has proven useful, there are limitations as it relates to oral bioavailability predictions. For instance, the data that Lipinski analyzed lacked quantitative bioavailability assessment. In addition, numerous scientists, including Veber, noted that poor oral bioavailability can often result in variable dosing. Therefore, in an attempt to further refine Lipinski's guidelines, Veber and colleagues also examined the relationship between the structure of a compound and oral

bioavailability.¹¹⁷ Veber determined that acceptable bioavailability (>20%) was observed for compounds that possessed increased rigidity as measured by the total number of rotatable bonds (single, non-ring bonds that are bound to a non-hydrogen atom). In addition, Veber's analysis also led to the conclusion that total polar surface area (tPSA) is an important consideration in the prediction of oral bioavailability. Veber suggests that a prediction of high oral bioavailability can be made if a compound meets the following two criteria: (1) ten or fewer rotatable bonds are present in the molecule, and (2) the tPSA does not exceed 140 square angstroms. In general, the guidelines developed by both Lipinski and Veber provide a useful set of principles which can be applied by chemists to aid in the process of converting a compound with initially unpromising pharmacokinetic properties into a drug-like lead candidate.

In addition to the molecular properties examined by Lipinski and Veber, there are a plethora of other factors that can have an impact on the overall bioavailability of a compound. Several considerations include protein-assisted active transport, cellular efflux, cellular membrane permeation, and metabolism.¹⁴ Carbohydrates are also known to be assisted across a range of cellular membranes as well as through the blood-brain barrier by glucose transporters, enabling the sugar compounds to act within the cell. These properties are frequently evaluated in the latter stages of the drug discovery process. However, it was our desire to make theoretical predictions regarding absorption and bioavailability parameters while obtaining experimental *in vitro* activity data.

b. Anticancer Screening

The *in vitro* screening approach is a viable strategy to rapidly evaluate the potency values of a large quantity of compounds. In many cases, this data is considered to determine if a compound is worthy of study in live animals. Due to the high throughput nature of rational drug design, resource allocation dictates that it is impossible to conduct *in vivo* analysis of all compounds synthesized for a program. Therefore it is essential to utilize a robust and reliable *in vitro* assay in order to generate preliminary data.

In the late 1980s the US National Cancer Institute (NCI) developed a 60 human tumor cell line anticancer drug screen (NCI60). This *in vitro* screening assay was originally designed as a replacement for transplantable animal tumors. Over the years, this model has become a drug discovery tool and has enabled the screening of compounds submitted by academic scientists who work in the area of cancer research. The aim of the screen is to identify and prioritize the further evaluation of compounds that show selective growth inhibition of particular tumor cell lines. In addition, the program and its associated database have generated experimental data for numerous types of tumors including leukemia, lung, colon, central nervous system, melanoma, ovarian, renal, prostate, and breast cancers. The productivity of the screen is illustrated by the fact that several outcomes have contributed to advances in cancer therapy.¹¹⁸

4.3 Results

a. Physiochemical Property Assessment

In order to maintain control over bioavailability parameters, we utilized the guidelines of both Lipinski and Veber to help us roughly predict absorption and oral bioavailability. Specifically, we calculated the following physiochemical parameters via Advanced Chemistry Development's (ACD) software: molecular weight (MW), number of hydrogen bond acceptors and donors, logP, logD, acidic pKa, the number of rotatable bonds, and the total polar surface area (tPSA). The parameter logD is a measure of the octanol-water partition coefficient that takes into account all ionized forms of the substrate, while logP only considers the neutral species. Although there is no preferred value for pKa, it is widely accepted that charged species are less likely to readily permeate the lipid bilayers of cell membranes.¹⁴ In consideration of this trend, an acceptable logD value for permeation, as predicted by Lipinski, should be under 5.0. A thorough examination of the parameters included in Lipinski's rule of five in conjunction with the properties noted by Veber's analysis will help us to make predictions regarding the oral bioavailability of the novel compounds that we had evaluated for biological activity.

Table 4.0. Calculated physiochemical properties of novel glycosylidene-derived quinolines.

Compound	MW	Hydrogen bond acceptors – donors	clogP	clogD (7.4)	Acidic pKa	Rot. Bonds	tPSA
88a	715.87	6 - 2	10.29	10.29	4.29	19	70.04
93a	355.38	6 - 5	1.01	1.01	4.45	11	114.04
93b	373.37	6 - 5	0.94	0.94	4.34	11	114.04
111a	325.36	5 - 4	1.49	1.48	4.45	9	93.81
127Major	357.40	6 - 5	0.89	0.89	3.67	6	102.18

Of the compounds analyzed by ACD software, only **88a** would be predicted to have poor oral bioavailability. According to Lipinski's rule of five, this perbenzylated intermediate exceeds the threshold limit requirements for the parameters of molecular weight and lipophilicity. This compound also fails Veber's guidelines due to the large number of rotatable bonds. All of the deprotected sugar-based quinolines pass Lipinski's rule of five and would be predicted to possess acceptable oral bioavailability.

Compounds **93a**, **93b**, **111a**, and **127Major** are structurally similar in that they all possess numerous hydroxyl groups as well as a quinoline ring derivative. Glucose-based quinoline **93a** and its fluoro analogue, **93b**, have practically identical values for all fields calculated. Each of these compounds exceeds Veber's requirements for the number of rotatable bonds. However, since both molecules surpass the cutoff by only one rotatable

bond, it is reasonable to conclude that acceptable bioavailability may still be anticipated. In addition, based upon the pKa values, these compounds are also likely to readily permeate cell membranes because they are predicted to be neutral (no net charge) at physiological pH.¹¹⁹ Despite the fact that the spiro compound, **127Major**, was unable to be synthesized, we decided to analyze its calculated properties nonetheless. **127Major** is the only glucose-based compound that passes all of the guidelines as set forth by both Lipinski and Veber. However, this compound has the lowest logD of the series, and a lipophilic modification may be required to boost the values of logD and logP over 1.0. The arabinose-based quinoline, **111a**, displays the most favorable calculated physiochemical properties when compared to the glucose derivatives. This result is due to the fact that it is derived from a five-membered furanose ring as opposed to a six-membered pyranose ring. This seemingly minor difference improves the calculated molecular properties by reducing the molecular weight, polar surface area, and number of rotatable bonds as well as the number of hydrogen bond acceptors and donors. In addition, the higher logD and logP values of nearly 1.5 are in the range of optimum favorability for permeation (1.5 to 3.0).¹⁴ The arabinose-derived quinoline **111a** passes the bioavailability guidelines as set forth by both Lipinski and Veber, and we therefore surmise that this compound will have the most favorable pharmacokinetic profile. Despite these predicted properties, **111a** did not pass the NCI's screening filters and was not assayed for anticancer activity. Overall, the deprotected sugar-derived quinolines represent leads that are predicted to possess potentially favorable oral bioavailability and can therefore be readily modified into drug-like compounds.

b. in vitro Anticancer Activity

The anticancer activity of several novel, open-ring glucose based quinolines was evaluated in NCI's 60 cell line screening model.¹²⁰ Specifically compounds **88a**, **93a**, **93a HCl Salt** and **93b** were tested at a 10 micromolar concentration. NCI reports the data as growth percent of the cell lines, and this number allows for the determination of growth inhibition. For instance, a growth percent value of 100 corresponds to no growth inhibition while a growth percent value of 40 corresponds to a 60% growth inhibition (growth inhibition = 100 – growth percent). Growth percent values greater than 100 indicate cell proliferation and values less than 0 can be interpreted as lethality. Based upon literature precedent of the unique structural attributes of our compounds, we hypothesized that compounds **93a**, **93a HCl Salt** and **93b** are likely to possess anticancer activity.

Perbenzylated compound **88a** displayed the best anticancer profile of the four open-ring, glucose-based quinolines from this project evaluated by the NCI 60 cell line screen (Table 4.1). This compound exhibited more than 40% growth inhibition for eight separate cell lines (values of growth percent are shown in bold). In addition, leukemia cell lines were most susceptible to this compound. Deprotected compounds **93a**, **93a HCl Salt**, and **93b**, on the other hand, displayed an overall similar profile and resulted in little to no growth inhibitory effect for most cell lines. The most favorable results were 20.5% growth inhibition (RXF 393, Renal) for **93a** and 18.8% growth inhibition (SR, Leukemia) for **93b**. The presence of **93b** resulted in substantial proliferation of the following cell lines: NCI-H322M (Non-Small Cell Lung), MALME-3M (Melanoma),

and IGROV1(Ovarian). Interestingly, **93a HCl Salt** was highly effective against the CCRF-CEM leukemia cell line and led to 68.7% cell growth inhibition. Although there is no data for the parent compound **93a** in this cell line, this result seems to deviate from the trend observed for **88a** and **93b**. Perhaps this cell line may be particularly sensitive to the residual hydrochloric acid from this compound. In general, the tested compounds were most effective against leukemia cells and least effective for melanoma cell lines.

Despite the modest anticancer properties of **88a**, this compound was not selected by NCI for dose titration experiments. We anticipated that the deprotected products would possess more favorable anticancer activity than the perbenzylated compounds. Perhaps the highly lipophilic nature of the benzyl groups of **88a** contributes to the activity of this compound. Alternately, the benzyl ether groups of **88a** may be aiding in the intercalation process. Based upon the data, we conclude that the lack of tumor cell growth suppression involving **93a**, **93a HCl Salt**, and **93b** is attributed to insufficient DNA intercalation. Future follow-up studies to determine the DNA binding capacity of compounds **88a**, **93a**, **93a HCl Salt**, and **93b** are planned.

Table 4.1. Results from the NCI60 human tumor cell line anticancer drug screen assay.

Cell Line	88a: Growth Percent at 10 μ M	93a: Growth Percent at 10 μ M	93a HCl salt: Growth Percent at 10 μ M	93b: Growth Percent at 10 μ M
CCRF-CEM (Leukemia)	78.3	----	31.3	91.7
HL-60(TB) (Leukemia)	45.8	----	96.7	98.9
K-562 (Leukemia)	77.7	97.6	82.3	----
MOLT-4 (Leukemia)	40.0	98.5	100.1	99.4
RPMI-8226 (Leukemia)	70.9	107.6	107.0	96.6
SR (Leukemia)	61.1	92.5	----	82.2
A549/ATCC (Non-Small Cell Lung)	88.0	92.9	98.7	99.6
EKVX (Non-Small Cell Lung)	88.7	123.0	120.4	93.3
HOP-62 (Non-Small Cell Lung)	76.7	103.6	107.5	106.3
HOP-92 (Non-Small Cell Lung)	54.3	----	84.8	----
NCI-H226 (Non-Small Cell Lung)	87.9	98.3	106.5	107.4
NCI-H23 (Non-Small Cell Lung)	59.9	99.5	105.2	98.6
NCI-H322M (Non-Small Cell Lung)	104.7	122.8	130.1	151.0
NCI-H460 (Non-Small Cell Lung)	91.6	101.2	108.8	106.1
NCI-H522 (Non-Small Cell Lung)	101.2	----	103.8	86.8
COLO 205 (Colon)	85.3	111.4	102.4	----
HCC-2998 (Colon)	86.5	----	105.6	108.8
HCT-116 (Colon)	58.4	100.7	107.2	106.3
HCT-15 (Colon)	88.2	116.2	100.4	99.2
HT29 (Colon)	70.4	93.5	105.7	97.0
KM12 (Colon)	94.8	104.5	109.6	108.9
SW-620 (Colon)	86.2	99.5	102.1	99.8
SF-268 (CNS)	82.6	102.2	93.8	101.8
SF-295 (CNS)	92.3	127.7	127.7	96.4
SF-539 (CNS)	92.2	103.8	102.7	110.8
SNB-19 (CNS)	70.7	103.7	95.9	97.2
SNB-75 (CNS)	64.9	90.5	100.2	96.2

U251 (CNS)	84.7	100.7	93.7	105.1
LOX IMVI (Melanoma)	75.3	96.3	106.1	----
MALME-3M (Melanoma)	106.4	119.7	114.8	165.0
M14 (Melanoma)	81.8	102.3	107.1	106.5
MDA-MB-435 (Melanoma)	104.9	111.3	106.3	106.2
SK-MEL-2 (Melanoma)	123.3	----	114.4	104.3
SK-MEL-28 (Melanoma)	93.4	103.0	110.7	106.2
SK-MEL-5 (Melanoma)	91.5	101.0	102.5	109.3
UACC-257 (Melanoma)	92.2	----	101.0	101.8
UACC-62 (Melanoma)	104.4	99.4	99.9	100.0
IGROVI(Ovarian)	116.1	-----	119.1	134.2
OVCAR-3 (Ovarian)	83.0	104.2	100.5	110.7
OVCAR-4 (Ovarian)	73.1	103.2	113.0	97.9
OVCAR-5 (Ovarian)	86.8	96.4	99.7	112.6
OVCAR-8 (Ovarian)	100.2	95.5	105.4	109.1
NCI/ADR-RES (Ovarian)	90.9	96.6	113.5	101.1
SK-OV-3 (Ovarian)	85.1	98.7	105.7	114.7
786-0 (Renal)	70.2	105.9	94.8	101.9
A498 (Renal)	60.4	99.0	98.3	91.5
ACHN (Renal)	93.0	105.8	106.0	105.6
CAKI-1 (Renal)	69.6	108.7	100.9	106.8
RXF 393 (Renal)	100.7	79.5	109.1	110.4
SN12C (Renal)	95.5	100.2	96.5	100.7
TK-10 (Renal)	99.9	----	106.5	107.7
UO-31 (Renal)	90.1	----	94.5	112.9
PC-3 (Prostate)	57.1	96.5	91.4	105.4
DU-145 (Prostate)	94.3	105.7	119.9	121.8
MCF7 (Breast)	83.9	98.9	102.2	95.6
MDA-MB-231/ATCC (Breast)	88.4	----	105.2	104.9
HS 578T (Breast)	89.0	105.8	108.6	101.7
BT-549 (Breast)	104.1	----	117.0	98.7
T-47D (Breast)	56.6	94.8	101.0	100.7
MDA-MB-468 (Breast)	58.1	97.3	97.1	109.2

4.4. Summary

The simultaneous assessment of both pharmacokinetic properties and *in vitro* activity is a proven strategy for the evaluation of the drug-like properties of compounds. In order to adhere to this approach, we utilized the data output from ACD Labs software in conjunction with Lipinski and Veber's rules to help us make predictions regarding the bioavailability of the glycosylidene-based quinolines. Based upon our interpretation of the software's physiochemical property calculations, we anticipate that the perhydroxylated compounds should possess favorable bioavailability. In addition, we also submitted several compounds to the NCI (compounds **88a**, **93a**, **93a HCl Salt**, & **93b**) for anticancer screening. We thought that the protected compound **88a** would be less active than the deprotected analogues **93a**, **93a HCl Salt**, and **93b**. Although the perbenzylated precursor displayed moderate anticancer activity against several cell lines, the deprotected compounds that were assayed did not promote growth inhibition of most cell lines. We were particularly surprised by this outcome because we hypothesized that the sugar-based quinolines may behave as DNA intercalators. The only exception to this trend was the 68.7% growth inhibition of CCRF-CEM leukemia cells resulting from treatment with **93a HCl salt**. Overall the tested compounds were most effective against leukemia cell lines. None of the compounds tested possessed sufficient anticancer activity against the cell lines to proceed to the dose titration stage of NCI's evaluation process.

Chapter 5

Conclusions

5.1. Summary

The objective of this research project was to develop a synthetic method for the preparation of novel glycosylidene-based quinolines. Through a survey of the scientific literature, we have noticed that the structural motif of a carbohydrate moiety in combination with an aromatic heterocycle is common among biologically active natural products. As a result of the widespread prevalence and favorable pharmacokinetics of carbohydrates, stable sugar derivatives have attracted attention as scaffolds for drug design. In addition, quinoline-based compounds are also a beneficial class of compounds with therapeutic applications. Our proposed targets integrated the common structural themes associated with some DNA intercalating agents as well as glycosidase inhibitors. These target compounds were chosen, in part, because we anticipated that they may possess favorable biological activities and pharmacokinetic properties. The unique structures would also allow for the investigation of new synthetic methodology strategies.

We have successfully developed a facile one-pot approach toward the synthesis of novel glycosylidene-based quinolines. We hypothesized that carbon-linked glucose-quinoline hybrids could be accessed through a Povarov reaction between benzaniline and a glucose-based *exo*-glycal. We performed extensive screening experiments with several Lewis acids and discovered that scandium triflate is the optimal catalyst for this reaction.

We have also determined through comprehensive NMR studies that the reaction produces an open-ring glucose-based quinoline in addition to diastereomers in which the tetrahydroquinoline portion of the compound is spiroanellated to glucose at the anomeric carbon. These spiro products are not stable at room temperature, and they slowly undergo oxidative ring opening. We presume that the aromatization of the tetrahydroquinoline likely drives the opening of the glucopyranose ring. In addition to the aromatization, the resulting increase in the number of rotatable bonds renders this process favorable from an entropic standpoint. We desired to exclusively obtain the open-ring compound, and soon discovered that addition of 2.0 equiv of manganese dioxide to the reaction mixture drives the complete conversion of the *exo*-glycal into the oxidized product to form a novel C-linked, glycosylidene-based quinoline. In the one-pot reaction, the open-ring compound is accessed through the glucose-spiroanellated tetrahydroquinoline intermediates.

We next applied this one-pot addition/oxidation reaction to a series of *para*-substituted benzanilines in order to evaluate the electronic effect of substituents on the reaction. The highest yield for reactions in this series was 65%, and this result occurred with benzaniline itself. In addition, similar yields (>60%) were obtained when benzaldehyde-derived imines substituted with *para*-halogen groups were reacted with the glucose-based *exo*-glycal. The methoxy-substituted, aniline-derived imine also reacted efficiently to give the desired product. However, yields were diminished when imines with electron-donating and electron-withdrawing groups on the phenyl ring originating from the benzaldehyde were allowed to react with the *exo*-glycal. Perhaps the most dramatic effects were observed with imines in which the aniline-derived phenyl ring was *para*-

substituted with electron-withdrawing groups. The poor reactivity with these benzanilines is likely due to removal of electron density from the aniline-derived phenyl ring. As a consequence, the pi-bond electrons are less available for the ring closure event which takes place upon attack of the positively charged anomeric carbon. Nonetheless, this procedure represents an effective way to access a variety of glucose-derived quinolines with *para*-substituted benzanilines.

The one-pot Povarov cycloaddition/oxidation reaction sequence that we have developed is a convenient route to access C-glycosylated quinolines. Upon consideration of the favorable results of the reaction with the glucose-based *exo*-glycal, we desired to extend this methodology to *exo*-glycals derived from other sugars. When further studies were conducted to address the breadth of this strategy, we were able to successfully apply our reaction to both arabinose and galactose-based *exo*-glycal dienophiles. Overall, the yields were slightly lower with these different sugar *exo*-glycals in comparison to the corresponding *para*-substituted benzanilines in the glucose series. Interestingly, all of the reactions in the arabinose series required 8.0 equiv of manganese dioxide for complete conversion to the open-ring form. We hypothesize that opening of this furanose sugar is not as entropically favorable due to the fact that fewer rotatable bonds result from arabinose, a pentose, than from a hexose such as glucose. Regardless, we have demonstrated that moderate to good yields (40-50%) can be obtained when our one-pot reaction conditions are applied to other sugar *exo*-glycals. This synthetic method is broad enough to permit changes to both the ring size and stereochemistry of the sugar-based dienophile.

A thorough set of debenylation experiments was conducted in order to determine conditions for removal of the protective groups. Attempts using standard hydrogenolysis strategies and high temperature, high pressure palladium-based deprotection procedures were not successful in obtaining the anticipated perhydroxylated product. Transfer hydrogenation conditions involving palladium hydroxide and cyclohexene gave the desired product. However, this procedure was prone to unwanted side reactions which are likely attributed to high catalyst loading and sealed tube heating conditions. Facile deprotection conditions were later identified utilizing the Lewis acid, boron trichloride, and prep scale HPLC conditions were also determined that successfully purified the resulting perhydroxylated material.

Computer software was utilized to calculate the physiochemical properties of several novel, sugar-based quinolines, and this data was interpreted in accordance with Lipinski's and Veber's rules to make predictions regarding bioavailability. In general, the perhydroxylated sugar-derived quinolines are anticipated to possess favorable absorption and distribution properties while the perbenzylated precursor is not. Although several compounds do display modest anticancer efficacy, particularly in leukemia cell lines, the *in vitro* data generated by NCI's 60 cell line screen indicate that the tested compounds do not possess sufficient activity at ten micromolar drug concentrations to proceed to the dose titration stage of the screen.

In conclusion, we have demonstrated that carbon-linked, glycosylidene-derived quinolines can be obtained in moderate to good yields from a one-pot, scandium triflate catalyzed Povarov reaction followed by oxidative tetrahydroquinoline aromatization and sugar ring opening with manganese dioxide. We have also isolated and characterized the

reaction intermediates in which the tetrahydroquinoline is spiroanellated to the sugar's anomeric carbon. The utility of this facile procedure has been effectively employed with a series of *para*-substituted benzanilines as well as several different sugar-derived *exo*-glycal dienophiles to access novel open-ring glycosylidene quinolines. A straightforward deprotection reaction involving boron trichloride was identified to remove the benzyl protective groups. Several of the C-glycosylated quinolines have been evaluated for biological activity in the NCI60 human tumor cell line anticancer drug screen, but the compounds lacked sufficient growth inhibition properties to facilitate dose titration experiments.

5.2. Experimentals

General Remarks

All reactions were performed under a nitrogen atmosphere unless otherwise noted. Anhydrous solvents were purchased from Sigma Aldrich Chemical Company and were used as received. Unless otherwise specified, commercially available reagents were used without further purification. Nuclear magnetic resonance spectra were taken on a Varian Inova (500 or 600 MHz) spectrometer in CDCl₃, CD₃CN, or CD₃OD as solvent using tetramethylsilane as an internal standard. Chemical shifts (δ) are expressed in ppm, coupling constants are expressed in Hz, and splitting patterns are described as follows: s = singlet, d = doublet, t = triplet, q = quartet, dd = doublet of doublets, m = multiplet. High resolving power accurate mass measurement electrospray (ES) mass spectral data were acquired by use of a Bruker Daltonics apex-Qe Fourier transform ion cyclotron

resonance mass spectrometer (FT-ICR MS). External calibration was accomplished with oligomers of polypropylene glycol. IR spectra were obtained as thin films on NaCl plates with use of a Nicolet 380 FT-IR from Thermo Electron Corp. Melting points values (uncorrected) were measured with an Electrothermal MEL-TEMP30 melting point apparatus. Rotation values were obtained through use of a Perkin Elmer 241 Polarimeter. Silica gel column chromatography was carried out using a Combi Flash Companion system and silica gel columns from Teledyne Isco. Thin layer chromatography was carried out with Whatman MK6F silica gel TLC plates. Microwave experiments were conducted with a Biotage Initiator microwave reactor. Prep scale HPLC was conducted with a Waters mass directed reverse phase HPLC system. The following chromatographic conditions were used: (a) column: Waters Xbridge C-18, 30 x 75 mm, 5 micron; (b) flowrate: 50 mL/min; (c) mobile phase: A = water + ammonium hydroxide (pH 10), B = acetonitrile; (d) mobile phase gradient method: time = 0 min, A = 98, B = 2; time = 11 min, A = 65, B = 35; time = 11.2 min, A = 0, B = 100; time = 14.2 min, A = 98, B = 2; time = 15 min, A = 98, B = 2. Analytical HPLC/MS was conducted on an Agilent 1100 Series HPLC system equipped with a 3.0 x 50 mm XTerra C-18 column utilizing solvents buffered with 0.05% TFA. The following method was used: a gradient of 10% to 98% MeCN in H₂O for 3.75 min, then 98% MeCN in H₂O for 1.0 min. Low resolution mass spectrometry electrospray (ES) analysis was performed with a Micromass ZQ by Waters. Prep scale HPLC of chiral samples was carried out with a Gilson Unipoint semi-prep HPLC equipped with a 20 x 250 mm ChiralPak IB column, 5 micron, 9 mL/min flow rate. Screening conditions of chiral samples were performed with a Shimadzu Discovery analytical HPLC.

Lactones

General procedure for the preparation of compounds **84**, **107**, & **113**.⁷⁵

To a solution of anomeric alcohol (500 mg; 0.925 mmol) in dichloromethane (4 mL) was added *tert*-butanol (0.1 mL; 0.999 mmol) followed by Dess-Martin periodinane (408 mg; 0.962 mmol). The reaction was stirred at room temperature under an atmosphere of nitrogen for four hours. The reaction mixture was diluted with diethyl ether (50 mL) and saturated aqueous sodium carbonate solution (50 mL). The layers were separated and the aqueous layer was extracted four times with diethyl ether. The combined organics were washed with brine, dried (Na₂SO₄), and concentrated *in vacuo*. The crude material was filtered through a pad of silica gel, eluting with 40% ethyl acetate in hexane.

(3*R*,4*S*,5*R*,6*R*)-3,4,5-Tris(benzyloxy)-6-[(benzyloxy)methyl]tetrahydro-2*H*-pyran-2-one (84)

Isolated in 93% yield as an off-white solid. ¹H and ¹³C NMR data were consistent with literature values.⁷⁵

(3*R*,4*R*,5*S*)-5-[(Benzyloxy)methyl]-3,4bis(phenoxy)methyl)dihydrofuran-2(3*H*)-one (107)

Isolated in 98% yield as an off-white solid. ¹H and ¹³C NMR data were consistent with literature values.⁹¹

(3*R*,4*S*,5*S*,6*R*)-3,4,5-Tris(benzyloxy)-6-[(benzyloxy)methyl]tetrahydro-2*H*-pyran-2-one (113)

Isolated in 98% yield as a colorless oil. ¹H and ¹³C NMR data were consistent with literature values.⁹³

exo-glycals

General procedure for the preparation of compounds **85**, **108**, & **114**.⁷⁶

To a solution of lactone (195 mg; 0.362 mmol) in toluene (1 mL), THF (0.3 mL), and pyridine (5 μ L) was added Tebbe reagent (0.5 M in toluene, 0.8 mL, 0.398 mmol) at -45 °C. The reaction was stirred at -45 °C under an atmosphere of nitrogen for one hour, and then at 0 °C for one-half hour. The flask was then cooled to -10 to -15 °C, and 15% sodium hydroxide solution (0.15 mL) was slowly added to quench the reaction. The cold bath was removed, and the mixture was diluted with diethyl ether (20 mL), dried (Na_2SO_4), filtered through a pad of Celite, and concentrated *in vacuo*. The crude material was purified over silica gel, eluting with a gradient of 0% to 80% ethyl acetate in hexane.

2,6-Anhydro-3,4,5,7-tetra-O-benzyl-1-deoxy-D-gluco-hept-1-enitol (85)

Isolated in 75% yield as an off-white solid. ^1H and ^{13}C NMR data were consistent with literature values.⁷⁶

1,4-Anhydro-5-O-benzyl-2,3-dideoxy-1-methylidene-2,3-bis(phenoxyethyl)-D-arabinitol (108)

Isolated in 43% yield as an off-white solid. ^1H and ^{13}C NMR data were consistent with literature values.⁹²

2,6-Anhydro-3,4,5,7-tetra-O-benzyl-1-deoxy-D-galacto-hept-1-enitol (114)

Isolated in 51% yield as a colorless oil. ^1H and ^{13}C NMR data were consistent with literature values.⁹⁴

Benzanilines

General procedure for the preparation of compounds **86c**, **86d**, **86e**, **86g**, **86h**, **86i**, **86j**, & **86k**.⁷⁷ (Compounds **86a**, **86b**, & **86f** were obtained from commercial sources).

A mixture of a substituted benzaldehyde derivative (1.105 g; 5.5 mmol) and substituted aniline derivative (511 mg; 5.5 mmol) was vigorously stirred at room temperature under an atmosphere of nitrogen. After a few minutes, solidification of the mixture took place and the resulting product was recrystallized from ethanol.

***N*-[(*E*)-(4-Bromophenyl)methylidene]aniline (**86c**)**

Isolated in 83% yield as a white solid. ¹H and ¹³C NMR data were consistent with literature values.^{121, 122}

4-[(*E*)-(Phenylimino)methyl]benzotrile (86d**)**

Isolated in 68% yield as a yellow solid. ¹H and ¹³C NMR data were consistent with literature values.^{123, 122}

***N*-{(*E*)-[(4-Trifluoromethyl)phenyl]methylidene}aniline (**86e**)**

Isolated in 12% yield as an off-white solid. ¹H and ¹³C NMR data were consistent with literature values.¹²⁴

4-Fluoro-*N*-[(*E*)-phenylmethylidene]aniline (86g**)**

Isolated in 70% yield as an off-white solid. ¹H and ¹³C NMR data were consistent with literature values.¹²⁵

4-Bromo-*N*-[(*E*)-phenylmethylidene]aniline (86h)

Isolated in 42% yield as an off-white solid. ^1H and ^{13}C NMR data were consistent with literature values.^{126, 127}

4-[(*E*)-Phenylmethylidene]amino}benzonitrile (86i)

Recrystallization attempts were unsuccessful. Crude material (90% by wt) was used in the next reaction. ^1H and ^{13}C NMR data were consistent with literature values.¹²⁸

***N*-[(*E*)-Phenylmethylidene]-4-(trifluoromethyl)aniline (86j)**

Isolated in 51% yield as a white solid. ^1H and ^{13}C NMR data were consistent with literature values.¹²⁹

4-Methoxy-*N*-[(*E*)-phenylmethylidene]aniline (86k)

Isolated in 69% yield as a light brown solid. ^1H and ^{13}C NMR data were consistent with literature values.^{130, 127}

Spiroannellated sugar-derived tetrahydroquinolines

Procedure for the preparation and separation of **87Major + **87Minor****

To a solution of *exo*-glycal **85** (100 mg; 0.186 mmol) in acetonitrile (1 mL, unopened Sure/SealTM bottle) was added benzaniline **86a** (33.7 mg; 0.186 mmol) followed by Sc(OTf)₃ (18.3 mg; 0.0372 mmol). The reaction was stirred at room temperature under an atmosphere of nitrogen for one hour. The reaction was concentrated *in vacuo*, and the crude material was purified over silica gel, eluting with a gradient of 0% - 40% ethyl acetate in hexane to give **87Major** + **87Minor** as a colorless oil (4:1 mixture of diastereomers) in 65% yield. The isomers were separated by applying the prep scale

version (20 x 250 mm ChiralPak IB column, 5 micron, 9 mL/min flow rate) of the following analytical chromatography conditions: ChiralPak IB 4.6 x 250 mm column, 5 micron particle size, 10% ethanol in heptane (isocratic), 0.5 mL/min flow rate, 254 nm wavelength, retention time: **87Minor** (8.48 min), **87Major** (13.89 min).

(2*R*,2'*R*,4*S*,5*R*,6*R*)-3,4,5-Tris(benzyloxy)-6-[(benzyloxy)methyl]-2'-phenyl-2',3,3',4,5,6-hexahydro-1*H'*-spiro[pyran-2,4'-quinoline] (87Major)

¹H NMR (500 MHz, CDCl₃): δ 7.62 (d, J = 7.5 Hz, 1 H), 7.42-7.37 (m, 2 H), 7.36-7.25 (m, 19 H), 7.20-7.11 (m, 5 H), 6.78 (t, J = 7.25 Hz, 1 H), 6.58 (d, J = 6.5 Hz, 1 H), 4.73 (d, J = 11.0 Hz, 1 H), 4.67-4.54 (m, 4 H), 4.54-4.43 (m, 2 H), 4.41-4.31 (m, 2 H), 4.31-4.24 (m, 1 H), 4.15-4.12 (m, 1 H), 4.06-4.03 (m, 1 H), 4.02-3.97 (m, 1 H), 3.84-3.75 (m, 2 H), 2.64 (dd, J = 13.25, 4.75 Hz, 1 H), 2.22-2.16 (m, 1 H); ¹³C NMR (126 MHz, CDCl₃): δ 145.1, 144.4, 139.0, 138.8, 138.4, 138.2, 129.9, 128.9, 128.7, 128.6, 128.5, 128.4, 128.1, 128.0, 127.9, 127.9, 127.9, 127.5, 126.9, 123.2, 116.9, 113.7, 84.9, 79.9, 78.9, 76.3, 73.8, 73.6, 73.3, 72.4, 70.2, 55.2, 42.8; IR (NaCl): 3405, 3038, 2911, 2795, 1778, 1607, 1491, 1362, 1094, 698 cm⁻¹; HRMS calcd for C₄₈H₄₈NO₅⁺ [M+H⁺]: 718.3527, found 718.3529; [α]_D²² -13.5° (c 1.0, CHCl₃).

(2*S*,2'*R*,4*S*,5*R*,6*S*)-3,4,5-Tris(benzyloxy)-6-[(benzyloxy)methyl]-2'-phenyl-2',3,3',4,5,6-hexahydro-1*H'*-spiro[pyran-2,4'-quinoline] (87Minor)

¹H NMR (500 MHz, CDCl₃): δ 7.55 (d, J = 7.5 Hz, 1 H), 7.46-7.12 (m, 26 H), 6.68 (t, J = 7.25 Hz, 1 H), 6.60 (d, J = 8.0 Hz, 1 H), 5.07-5.00 (m, 2 H), 4.98-4.88 (m, 3 H), 4.80-4.67 (m, 2 H), 4.68-4.56 (m, 3 H), 3.89-3.85 (m, 1 H), 3.83-3.75 (m, 2 H), 3.68-3.62 (m, 2 H), 2.22 (t, J = 12.75 Hz, 1 H), 1.91 (dd, J = 12.75, 3.75 Hz, 1 H); ¹³C NMR (126 MHz, CDCl₃): δ 145.9, 144.4, 138.9, 138.8, 138.6, 130.8, 129.3, 128.9, 128.7, 128.6, 128.4,

128.3, 128.1, 128.0, 128.0, 127.9, 127.9, 127.8, 127.5, 127.4, 127.2, 117.7, 115.4, 114.9, 87.1, 86.6, 79.9, 76.3, 76.1, 75.8, 75.2, 73.4, 71.3, 69.3, 52.5, 44.4; IR (NaCl): 3405, 3038, 2911, 2795, 1778, 1607, 1491, 1362, 1094, 698 cm^{-1} ; HRMS calcd for $\text{C}_{48}\text{H}_{48}\text{NO}_5^+$ $[\text{M}+\text{H}^+]$: 718.3527, found 718.3529; $[\alpha]_{\text{D}}^{22} +40.2^\circ$ (c 1.0, CHCl_3).

109Isomers was prepared in an analogous manner to **87Major** + **87Minor** and was isolated as a colorless oil in 60% yield by stopping the room temperature, $\text{Sc}(\text{OTf})_3$ catalyzed reaction after one hour. However, separation conditions for the complex mixture of isomers were not found.

(3*S*,4*R*,5*R*)-3,4-Bis(benzyloxy)-5-[(benzyloxy)methyl]-2'-phenyl-2',3',4,5-tetrahydro-1'*H*,3*H*-spiro[furan-2,4'-quinoline] (109Isomers)

^1H NMR (500 MHz, CDCl_3): δ 7.58 (t, $J = 8.0$ Hz), 7.51 (d, $J = 8.0$ Hz), 7.48-7.12 (m), 7.10-7.05 (m), 6.84 (t, $J = 7.0$ Hz), 6.80 (t, $J = 7.0$ Hz), 6.75-6.70 (m), 6.68 (d, $J = 7.5$ Hz), 6.58 (d, $J = 7.5$ Hz), 4.85-4.82 (m), 4.76-4.63 (m), 4.61-4.55 (m), 4.49-4.40 (m), 4.38-4.30 (m), 4.28-4.24 (m), 4.21-4.17 (m), 4.10-3.99 (m), 3.85-3.72 (m), 3.64-3.60 (m), 2.63 (dd, $J = 13.0, 3.0$ Hz), 2.52 (dd, $J = 13.0, 3.0$ Hz), 2.42 (s), 2.35-2.30 (m), 2.25-2.10 (m); ^{13}C NMR (126 MHz, CDCl_3): δ 146.2, 145.2, 144.5, 144.4, 144.0, 143.7, 138.7, 138.7, 138.6, 138.5, 138.5, 138.3, 138.2, 138.2, 138.2, 138.1, 132.5, 130.2, 129.4, 129.0, 128.9, 128.9, 128.8, 128.7, 128.7, 128.6, 128.6, 128.5, 128.5, 128.4, 128.3, 128.2, 128.1, 127.9, 127.9, 127.8, 127.8, 127.7, 127.5, 127.2, 127.0, 126.9, 125.0, 123.0, 120.0, 118.5, 118.4, 118.1, 117.6, 116.0, 115.4, 115.3, 115.2, , 114.6, 113.8, 92.5, 91.2, 90.4, 88.3, 87.9, 85.1, 83.8, 83.5, 82.4, 81.0, 80.7, 80.4, 79.5, 79.4, 79.2, 79.2, 73.7, 73.6, 73.5, 73.1, 72.8, 72.6, 72.4, 72.1, 71.5, 71.0, 70.4, 70.2, 55.5, 55.4, 54.3, 53.1, 45.9, 42.1, 40.8, 40.3;

IR (NaCl): 3376, 3029, 2925, 1724, 1608, 1485, 1096, 747, 699 cm^{-1} ; HRMS calcd for $\text{C}_{40}\text{H}_{40}\text{NO}_4^+$ $[\text{M}+\text{H}^+]$: 598.2957, found 598.2963; $[\alpha]_{\text{D}}^{22} +0.5^\circ$ (c 1.0, CHCl_3).

Open-ring glycosylidene-based quinolines (benzylated)

General procedure for the preparation of compounds **88a**, **88b**, **88c**, **88d**, **88e**, **88g**, **88h**, **88j**, **88k**, **110a**, **110b**, **110f**, **110g**, **115a**, **115b**, & **115g**.

To a solution of *exo*-glycal (100 mg; 0.186 mmol) in acetonitrile (1 mL, unopened Sure/SealTM bottle) was added substituted benzaniline derivative (33.7 mg; 0.186 mmol) followed by $\text{Sc}(\text{OTf})_3$ (18.3 mg; 0.0372 mmol). The reaction was stirred at room temperature under an atmosphere of nitrogen. After two hours, MnO_2 (32.4 mg; 0.372 mmol) was added and the mixture was stirred overnight. If required, additional MnO_2 (up to 6.0 equiv) was added to drive the ring opening to completion. The reaction was diluted with ethyl acetate (15 mL), filtered through Celite, and concentrated. The crude material was purified over silica gel, eluting with a gradient of 0% - 40% ethyl acetate in hexane.

(1R)-1,2,3,5-Tetra-O-benzyl-1-C-(2-phenylquinolin-4-yl)-D-arabinitol (88a)

Isolated in 65% yield as a colorless oil: ^1H NMR (500 MHz, CDCl_3): δ 8.27 (d, J = 8.5 Hz, 1 H), 8.19 (s, 1 H), 8.16 (d, J = 7.0 Hz, 2 H), 8.03 (d, J = 6.5 Hz, 1 H), 7.74 (t, J = 7.75 Hz, 1 H), 7.56-7.49 (m, 3 H), 7.42-7.31 (m, 14 H), 7.30-7.25 (m, 2 H), 7.08 (t, J = 7.5 Hz, 1 H), 7.00 (t, J = 7.5 Hz, 2 H), 6.89 (d, J = 7.5 Hz, 2 H), 5.65 (d, J = 1.5 Hz, 1 H), 4.67-4.56 (m, 6 H), 4.39 (d, J = 11.5 Hz, 1 H), 4.16 (m, 1 H), 4.11-4.03 (m, 2 H), 3.92 (m, 1 H), 3.76 (dd, J = 10.0, 3.75 Hz, 1 H), 3.68 (dd, J = 10.0, 5.0 Hz, 1 H), 3.05 (br s, 1 H); ^{13}C NMR (126 MHz, CDCl_3): δ 157.0, 148.7, 145.7, 139.5, 138.4, 138.3, 137.5,

137.3, 130.8, 129.7, 129.6, 129.1, 128.8, 128.8, 128.7, 128.7, 128.7, 128.3, 128.2, 128.2, 128.1, 128.0, 128.0, 127.9, 126.6, 125.6, 123.1, 118.7, 81.7, 78.0, 77.0, 75.1, 74.0, 73.8, 72.1, 71.9, 71.4; IR (NaCl): 3676, 2836, 2364, 2016, 1724, 1598, 1075, 697 cm^{-1} ; HRMS calcd for $\text{C}_{48}\text{H}_{46}\text{NO}_5^+$ [$\text{M}+\text{H}^+$]: 716.3371, found 716.3377; $[\alpha]_{\text{D}}^{22} +67.3^\circ$ (c 1.0, CHCl_3).

(1*R*)-1,2,3,5-Tetra-*O*-benzyl-1-*C*-[2-(4-fluorophenyl)quinolin-4-yl]-*D*-arabinitol (88b)

Isolated in 60% yield as a colorless oil: ^1H NMR (500 MHz, CDCl_3): δ 8.24 (d, $J = 8.0$ Hz, 1 H), 8.12 (t, $J = 6.7$ Hz, 3 H), 8.03 (d, $J = 7.5$ Hz, 1 H), 7.74 (t, $J = 7.75$ Hz, 1 H), 7.42-7.31 (m, 14 H), 7.30-7.26 (m, 2 H), 7.20 (t, $J = 8.75$ Hz, 2 H), 7.09 (t, $J = 7.5$ Hz, 1 H), 7.00 (t, $J = 7.5$ Hz, 2 H), 6.88 (d, $J = 7.0$ Hz, 2 H), 5.64 (d, $J = 2.0$ Hz, 1 H), 4.68-4.55 (m, 6 H), 4.44 (d, $J = 11.5$ Hz, 1 H), 4.14-4.10 (m, 1 H), 4.10-4.03 (m, 1 H), 4.04 (br s, 1 H), 3.92 (m, 1 H), 3.76 (dd, $J = 9.75, 3.75$ Hz, 1 H), 3.68 (dd, $J = 9.75, 4.75$ Hz, 1 H), 3.05 (br s, 1 H); ^{13}C NMR (126 MHz, CDCl_3): δ 165.1, 163.2, 155.9, 148.6, 145.9, 138.4, 138.3, 137.5, 137.3, 130.6, 129.9, 129.8, 129.7, 128.8, 128.8, 128.7, 128.6, 128.4, 128.3, 128.2, 128.1, 128.1, 128.0, 127.9, 126.7, 125.5, 123.1, 118.3, 116.1, 115.9, 81.9, 78.0, 77.0, 75.1, 74.0, 73.8, 72.1, 71.9, 71.3; IR (NaCl): 3649, 2911, 2537, 2356, 2051, 1502, 1090, 697 cm^{-1} ; HRMS calcd for $\text{C}_{48}\text{H}_{45}\text{FNO}_5^+$ [$\text{M}+\text{H}^+$]: 734.3276, found 734.3276; $[\alpha]_{\text{D}}^{22} +74.2^\circ$ (c 1.0, CHCl_3).

(1*R*)-1,2,3,5-Tetra-*O*-benzyl-1-*C*-[2-(4-bromophenyl)quinolin-4-yl]-*D*-arabinitol (88c)

Isolated in 64% yield as a colorless oil: ^1H NMR (500 MHz, CDCl_3): δ 8.24 (br s, 1 H), 8.11 (s, 1 H), 8.05-7.97 (m, 3 H), 7.74 (t, $J = 7.3$ Hz, 1 H), 7.64 (d, $J = 8.5$ Hz, 2 H), 7.44-

7.32 (m, 14 H), 7.29-7.26 (m, 2 H), 7.09 (t, $J = 7.5$ Hz, 1 H), 7.01-6.96 (m, 2 H), 6.86 (d, $J = 7.0$ Hz, 2 H), 5.64 (d, $J = 2.0$ Hz, 1 H), 4.67-4.56 (m, 6 H), 4.43 (d, $J = 11.5$ Hz, 1 H), 4.14-4.04 (m, 2 H), 4.03 (s, 1 H), 3.93 (m, 1 H), 3.76 (dd, $J = 9.75, 3.75$ Hz, 1 H), 3.67 (dd, $J = 9.75, 5.0$ Hz, 1 H), 3.03 (br s, 1 H); ^{13}C NMR (126 MHz, CDCl_3): δ 155.7, 138.4, 138.3, 137.4, 137.3, 132.2, 130.8, 129.8, 129.5, 128.9, 128.8, 128.7, 128.6, 128.4, 128.3, 128.2, 128.1, 128.1, 128.0, 128.0, 127.9, 126.8, 125.6, 123.1, 118.2, 81.8, 78.0, 77.5, 75.1, 74.0, 73.8, 72.1, 71.9, 71.3; IR (NaCl): 3567, 3030, 2868, 1958, 1596, 1073, 698 cm^{-1} ; HRMS calcd for $\text{C}_{48}\text{H}_{45}\text{BrNO}_5^+$ [$\text{M}+\text{H}^+$]: 794.2476, found 794.2504; $[\alpha]_{\text{D}}^{22} +39.0^\circ$ (c 1.0, CHCl_3).

(1R)-1,2,3,5-Tetra-O-benzyl-1-C-[2-(4-cyanophenyl)quinolin-4-yl]-D-arabinitol (88d)

Isolated in 43% yield as a colorless oil: ^1H NMR (500 MHz, CDCl_3): δ 8.25 (d, $J = 8.5$ Hz, 1 H), 8.20 (d, $J = 8.0$ Hz, 2 H), 8.14 (s, 1 H), 8.05 (d, $J = 8.0$ Hz, 1 H), 7.82-7.74 (m, 3 H), 7.44 (t, $J = 7.5$ Hz, 1 H), 7.40-7.32 (m, 13 H), 7.28 (m, 2 H), 7.07 (t, $J = 7.25$ Hz, 1 H), 6.97 (t, $J = 7.5$ Hz, 2 H), 6.84 (d, $J = 7.5$ Hz, 2 H), 5.66 (d, $J = 1.5$ Hz, 1 H), 4.70-4.54 (m, 6 H), 4.44 (d, $J = 11.50$ Hz, 1 H), 4.10-4.05 (m, 2 H), 4.02 (br s, 1 H), 3.94 (m, 1 H), 3.77 (dd, $J = 10.0, 3.5$ Hz, 1 H), 3.67 (dd, $J = 10.0, 5.0$ Hz, 1 H), 3.01 (br s, 1 H); ^{13}C NMR (126 MHz, CDCl_3): δ 154.6, 148.7, 146.4, 143.7, 138.4, 138.3, 137.4, 137.3, 132.8, 131.0, 130.0, 129.0, 128.8, 128.7, 128.5, 128.4, 128.2, 128.2, 128.1, 127.9, 127.4, 125.9, 123.2, 119.2, 118.4, 113.0, 82.0, 77.9, 76.9, 75.1, 74.1, 73.8, 72.2, 72.0, 71.3; IR (NaCl): 3556, 3030, 2829, 2227, 1779, 1597, 1073, 699 cm^{-1} ; HRMS calcd for $\text{C}_{49}\text{H}_{45}\text{N}_2\text{O}_5^+$ [$\text{M}+\text{H}^+$]: 741.3323, found 741.3322; $[\alpha]_{\text{D}}^{22} +56.3^\circ$ (c 1.0, CHCl_3).

(1*R*)-1,2,3,5-Tetra-*O*-benzyl-1-*C*-{2-[4-(trifluoromethyl)phenyl]quinolin-4-yl]-*D*-arabinitol (88e)

Isolated in 46% yield as a colorless oil: ¹H NMR (500 MHz, CDCl₃) δ 8.26 (d, *J* = 8.5 Hz, 1 H), 8.21 (d, *J* = 8.0 Hz, 2 H), 8.15 (s, 1 H), 8.04 (d, *J* = 8.0 Hz, 1 H), 7.79-7.73 (m, 3 H), 7.45-7.31 (m, 14 H), 7.29-7.26 (m, 2 H), 7.07 (t, *J* = 7.5 Hz, 1 H), 6.97 (t, *J* = 7.5 Hz, 2 H), 6.84 (d, *J* = 7.5 Hz, 2 H), 5.65 (d, *J* = 2.0 Hz, 1 H), 4.68-4.55 (m, 6 H), 4.44 (d, *J* = 11.5 Hz, 1 H), 4.14-4.05 (m, 2 H), 4.03 (s, 1 H), 3.93 (m, 1 H), 3.76 (dd, *J* = 9.75, 3.75 Hz, 1 H), 3.67 (dd, *J* = 10.0, 5.0 Hz, 1 H), 3.01 (br s, 1 H); ¹³C NMR (126 MHz, CDCl₃): δ 155.3, 148.5, 146.4, 142.8, 138.4, 138.3, 137.4, 137.2, 130.8, 129.9, 128.8, 128.8, 128.7, 128.5, 128.4, 128.2, 128.2, 128.1, 128.0, 127.9, 127.2, 125.9, 125.9, 125.8, 123.2, 118.5, 81.8, 77.9, 77.3, 75.1, 74.1, 73.8, 72.2, 72.0, 71.3; IR (NaCl): 3549, 3030, 2865, 1598, 1324, 1107, 698 cm⁻¹; HRMS calcd for C₄₉H₄₅F₃NO₅⁺ [M+H⁺]: 784.3244, found 784.3242; [α]_D²² +53.7° (*c* 1.0, CHCl₃).

(1*R*)-1,2,3,5-Tetra-*O*-benzyl-1-*C*-[2-(4-methoxyphenyl)quinolin-4-yl]-*D*-arabinitol (88f)

Isolated in 45% yield as a colorless oil: ¹H NMR (500 MHz, CDCl₃): δ 8.23 (d, *J* = 8.5 Hz, 1 H), 8.13 (d, *J* = 9.0 Hz, 3 H), 8.02 (br s, 1 H), 7.72 (t, *J* = 8.5 Hz, 2 H), 7.58 (m, 1 H), 7.52-7.47 (t, *J* = 8.5 Hz, 1 H), 7.40-7.31 (m, 12 H), 7.30-7.26 (m, 2H), 7.12-6.97 (m, 4 H), 6.91 (d, *J* = 7.0 Hz, 2 H), 5.63 (br s, 1 H), 4.68-4.53 (m, 6 H), 4.44 (d, *J* = 11.5 Hz, 1 H), 4.20-4.12 (m, 1 H), 4.07 (m, 3 H), 3.94 (s, 3 H), 3.76 (dd, *J* = 10.0, 3.75 Hz, 1 H), 3.68 (dd, *J* = 9.85, 5.0 Hz, 1 H), 3.09 (br s, 1 H); ¹³C NMR (126 MHz, CDCl₃): δ 138.4, 138.3, 137.4, 137.1, 133.2, 132.4, 132.3, 132.2, 128.9, 128.8, 128.7, 128.7, 128.4, 128.2, 128.2, 128.1, 128.1, 128.0, 125.2, 123.1, 118.5, 114.6, 81.6, 77.9, 77.0, 75.0, 74.1, 73.8,

72.2, 72.0, 71.3, 55.7; IR (NaCl): 3555, 2912, 2008, 1601, 1503, 1118, 697 cm^{-1} ; HRMS calcd for $\text{C}_{49}\text{H}_{48}\text{NO}_6^+$ $[\text{M}+\text{H}^+]$: 746.3476, found 746.3478; $[\alpha]_{\text{D}}^{22} +40.2^\circ$ (*c* 1.0, CHCl_3).

(1R)-1,2,3,5-Tetra-O-benzyl-1-C-(6-fluoro-2-phenyl)quinolin-4-yl)-D-arabinitol (88g)

Isolated in 39% yield as a colorless oil: ^1H NMR (500 MHz, CDCl_3): δ 8.26-8.20 (m, 1 H), 8.18-8.09 (m, 3 H), 7.77 (d, *J* = 9.25 Hz, 1 H), 7.56-7.48 (m, 4 H), 7.41-7.28 (m, 15 H), 7.06 (t, *J* = 7.25 Hz, 1 H), 6.97 (t, *J* = 7.5 Hz, 2 H), 6.84 (d, *J* = 7.5 Hz, 2 H), 5.48 (d, *J* = 2.5 Hz, 1 H), 4.69-4.56 (m, 6 H), 4.42 (d, *J* = 11.5 Hz, 1 H), 4.20-4.11 (m, 1 H), 4.09-4.04 (m, 1 H), 4.02-3.97 (m, 1 H), 3.95-3.90 (m, 1 H), 3.75 (dd, *J* = 9.75, 3.75 Hz, 1 H), 3.63 (dd, *J* = 9.75, 5.25 Hz, 1 H), 3.00 (br s, 1 H); ^{13}C NMR (126 MHz, CDCl_3): δ 161.5, 159.6, 156.4, 146.1, 145.0, 144.9, 139.5, 138.3, 138.2, 137.4, 137.1, 133.3, 133.3, 129.7, 129.1, 128.8, 128.8, 128.7, 128.4, 128.3, 128.3, 128.2, 128.1, 127.9, 127.8, 126.2, 126.1, 119.7, 119.5, 119.3, 107.2, 107.0, 81.3, 77.8, 77.6, 75.0, 74.1, 73.7, 72.1, 71.9, 71.2; IR (NaCl): 3419, 2927, 2360, 1724, 1625, 1073, 697 cm^{-1} ; HRMS calcd for $\text{C}_{48}\text{H}_{45}\text{FNO}_5^+$ $[\text{M}+\text{H}^+]$: 734.3276, found 734.3300; $[\alpha]_{\text{D}}^{22} +48.9^\circ$ (*c* 1.0, CHCl_3).

(1R)-1,2,3,5-Tetra-O-benzyl-1-C-(6-bromo-2-phenyl)quinolin-4-yl)-D-arabinitol (88h)

Isolated in 38% yield as a colorless oil: ^1H NMR (500 MHz, CDCl_3): δ 8.30 (s, 1 H), 8.17-8.06 (m, 4 H), 7.80 (dd, *J* = 9.0, 2.0 Hz, 1 H), 7.57-7.49 (m, 3 H), 7.40-7.28 (m, 15 H), 7.06 (t, *J* = 7.25 Hz, 1 H), 6.98 (t, *J* = 7.25 Hz, 2 H), 6.85 (d, *J* = 7.5 Hz, 2 H), 5.53 (d, *J* = 2.5 Hz, 1 H), 4.70-4.62 (m, 3 H), 4.61-4.55 (m, 3 H), 4.43 (d, *J* = 11.5 Hz, 1 H), 4.16-4.08 (m, 2 H), 3.99-3.96 (m, 1 H), 3.93-3.89 (m, 1 H), 3.74 (dd, *J* = 9.75, 3.75 Hz, 1 H), 3.63 (dd, *J* = 9.75, 5.25 Hz, 1 H), 3.04 (s, 1 H); ^{13}C NMR (126 MHz, CDCl_3): δ 157.3, 147.6, 144.7, 139.3, 138.3, 137.4, 137.1, 132.9, 132.6, 129.9, 129.1, 128.8, 128.8, 128.7,

128.5, 128.4, 128.3, 128.2, 128.0, 127.9, 126.8, 125.7, 120.6, 119.5, 81.4, 77.5, 77.3, 74.9, 73.9, 73.8, 72.2, 71.9, 71.3; IR (NaCl): 3442, 2927, 2091, 1643, 1072, 697 cm^{-1} ; HRMS calcd for $\text{C}_{48}\text{H}_{45}\text{BrNO}_5^+$ [$\text{M}+\text{H}^+$]: 794.2476, found 794.2513; $[\alpha]_{\text{D}}^{22} +59.8^\circ$ (c 1.0, CHCl_3).

(1*R*)-1,2,3,5-Tetra-*O*-benzyl-1-*C*-[2phenyl-6-(trifluoromethyl)quinolin-4-yl]-*D*-arabinitol (88j)

Isolated in 18% yield as a colorless oil: ^1H NMR (500 MHz, CDCl_3): δ 8.49 (s, 1 H), 8.31 (d, $J = 8.5$ Hz, 1 H), 8.20 (s, 1 H), 8.17-8.14 (m, 2 H), 7.91-7.87 (m, 1 H), 7.57-7.52 (m, 3 H), 7.40-7.29 (m, 13 H), 7.27-7.24 (m, 2 H), 7.02 (t, $J = 7.25$ Hz, 1 H), 6.93 (t, $J = 7.5$ Hz, 2 H), 6.81 (d, $J = 7.5$ Hz, 2 H), 5.58 (d, $J = 2.5$ Hz, 1 H), 4.73-4.49 (m, 6 H), 4.43 (d, $J = 11.5$ Hz, 1 H), 4.20-4.14 (m, 1 H), 4.10-4.05 (m, 1 H), 4.01-3.97 (m, 1 H), 3.89-3.84 (m, 1 H), 3.70 (dd, $J = 9.75, 3.5$ Hz, 1 H), 3.58 (dd, $J = 9.75, 5.5$ Hz, 1 H), 2.99 (d, $J = 4.5$ Hz, 1 H); ^{13}C NMR (126 MHz, CDCl_3): δ 159.0, 150.0, 146.6, 139.1, 138.3, 138.2, 137.3, 137.0, 132.0, 130.2, 129.2, 128.8, 128.7, 128.6, 128.4, 128.2, 128.1, 128.0, 128.0, 127.9, 125.1, 124.7, 121.6, 119.8, 81.2, 77.5, 77.3, 77.0, 74.9, 73.9, 73.7, 72.3, 71.5; IR (NaCl): 3555, 2927, 1727, 1274, 1073, 698 cm^{-1} ; HRMS calcd for $\text{C}_{49}\text{H}_{45}\text{F}_3\text{NO}_5^+$ [$\text{M}+\text{H}^+$]: 784.3244, found 784.3267; $[\alpha]_{\text{D}}^{22} +47.0^\circ$ (c 0.5, CHCl_3).

(1*R*)-1,2,3,5-Tetra-*O*-benzyl-1-*C*-(6-methoxy-2-phenyl)quinolin-4-yl]-*D*-arabinitol (88k)

Isolated in 56% yield as a colorless oil: ^1H NMR (500 MHz, CDCl_3): δ 8.21-8.13 (m, 4 H), 7.54 (t, $J = 7.5$ Hz, 2 H), 7.53-7.47 (m, 1 H), 7.45-7.33 (m, 15 H), 7.28-7.24 (m, 2 H), 7.14 (t, $J = 7.25$ Hz, 1 H), 7.07 (t, $J = 7.25$ Hz, 2 H), 6.99 (d, $J = 7.0$ Hz, 2 H), 5.58 (d, $J = 3.0$ Hz, 1 H), 4.70-4.54 (m, 6 H), 4.43 (d, $J = 11.5$ Hz, 1 H), 4.31-4.23 (m, 1 H), 4.14-

4.07 (m, 2 H), 3.90-3.84 (m, 1 H), 3.74 (dd, $J = 9.5, 3.5$ Hz, 1 H), 3.69-3.64 (m, 4 H), 3.00 (d, $J = 4.0$ Hz, 1 H); ^{13}C NMR (126 MHz, CDCl_3): δ 158.0, 154.8, 145.1, 143.8, 139.9, 138.6, 138.3, 137.7, 137.6, 132.3, 129.2, 129.0, 129.0, 128.8, 128.7, 128.6, 128.3, 128.3, 128.2, 128.1, 128.0, 127.9, 127.7, 126.7, 122.0, 119.0, 101.9, 81.9, 77.7, 77.6, 77.1, 75.4, 73.7, 72.2, 71.7, 71.5, 55.6; IR (NaCl): 3418, 2930, 2015, 1622, 1497, 1073, 697 cm^{-1} ; HRMS calcd for $\text{C}_{49}\text{H}_{48}\text{NO}_6^+$ [$\text{M}+\text{H}^+$]: 746.3476, found 746.3508; $[\alpha]_D^{22} +56.0^\circ$ (c 1.0, CHCl_3).

(2*R*,3*R*,4*S*)-1,3,4-tris(benzyloxy)-4-(2-phenylquinolin-4-yl)butan-2-ol (110a)

Isolated in 57% yield as a colorless oil: ^1H NMR (500 MHz, CDCl_3): δ 8.31-8.27 (m, 2 H), 8.21 (d, $J = 7.5$ Hz, 2 H), 7.98 (d, $J = 8.0$ Hz, 2 H), 7.78 (t, $J = 7.0$ Hz, 1 H), 7.59-7.47 (m, 4 H), 7.61-7.14 (m, 10 H), 7.07 (t, $J = 7.5$ Hz, 1 H), 6.98 (t, $J = 7.5$ Hz, 2 H), 6.76 (d, $J = 7.0$ Hz, 2 H), 5.69 (s, 1 H), 4.75 (d, $J = 12.0$ Hz, 1 H), 4.56 (s, 2 H), 4.41 (d, $J = 12.0$ Hz, 1 H), 4.31-4.27 (m, 1 H), 4.11 (d, $J = 11.0$ Hz, 1 H), 3.86 (d, $J = 7.5$ Hz, 1 H), 3.77-3.65 (m, 3 H), 2.70 (s, 1 H); ^{13}C NMR (126 MHz, CDCl_3): δ 157.2, 148.8, 145.3, 139.8, 138.0, 137.6, 137.0, 131.0, 129.7, 129.5, 129.3, 129.1, 129.0, 129.0, 128.8, 128.8, 128.8, 128.7, 128.5, 128.3, 128.2, 128.0, 127.9, 126.7, 125.6, 122.8, 118.5, 80.7, 75.5, 74.8, 73.8, 72.2, 71.3, 70.2; IR (NaCl): 3449, 3027, 2983, 1723, 1597, 1484, 1075, 745, 696 cm^{-1} ; HRMS calcd for $\text{C}_{40}\text{H}_{38}\text{NO}_4^+$ [$\text{M}+\text{H}^+$]: 596.2801, found 596.2812; $[\alpha]_D^{22} -44.9^\circ$ (c 1.0, CHCl_3).

(2*R*,3*R*,4*S*)-1,3,4-tris(benzyloxy)-4-[2-(4-fluorophenyl)quinolin-4-yl]butan-2-ol (110b)

Isolated in 47% yield as a colorless oil: ^1H NMR (500 MHz, CDCl_3): δ 8.26 (d, $J = 8.5$ Hz, 1 H), 8.21 (s, 1 H), 8.19-8.16 (m, 2 H), 7.97 (d, $J = 8.5$ Hz, 1 H), 7.80 (t, $J = 7.5$ Hz, 1

H), 7.50 (t, $J = 7.5$ Hz, 1 H), 7.40-7.33 (m, 9 H), 7.21 (t, $J = 8.5$ Hz, 2 H), 7.08 (t, $J = 7.5$ Hz, 2 H), 6.98 (t, $J = 7.5$ Hz, 2 H), 6.74 (d, $J = 7.5$ Hz, 2H), 5.69 (s, 1 H), 4.74 (d, $J = 11.5$ Hz, 1H), 4.56 (s, 2 H), 4.41 (d, $J = 12.0$ Hz, 1H), 4.31-4.27 (m, 1 H), 4.12 (d, $J = 11.0$ Hz, 1 H), 3.84 (dd, $J = 7.75, 1.75$ Hz, 1 H), 3.7-3.68 (m, 3 H), 2.68 (s, 1 H); ^{13}C NMR (126 MHz, CDCl_3): δ 165.1, 163.1, 156.1, 148.7, 145.5, 137.9, 137.6, 137.0, 136.0, 130.9, 129.8, 129.8, 129.7, 129.0, 128.8, 128.8, 128.6, 128.5, 128.3, 128.2, 128.0, 126.8, 125.4, 122.7, 118.1, 116.1, 115.9, 80.7, 75.4, 74.8, 73.8, 72.2, 71.3, 70.1; IR (NaCl): 3448, 3030, 2962, 2360, 1724, 1598, 1450, 1073, 737, 698 cm^{-1} ; HRMS calcd for $\text{C}_{40}\text{H}_{37}\text{FNO}_4^+$ [$\text{M}+\text{H}^+$]: 614.2706, found 614.2707; $[\alpha]_D^{22}$ -43.0° (c 1.0, CHCl_3).

(2*R*,3*R*,4*S*)-1,3,4-tris(benzyloxy)-4-[2-(4-methoxyphenyl)quinolin-4-yl]butan-2-ol (110f)

Isolated in 44% yield as a colorless oil: ^1H NMR (500 MHz, CDCl_3): δ 8.25-8.23 (m, 2 H), 8.18 (d, $J = 9.0$ Hz, 2 H), 7.95 (d, $J = 8.5$ Hz, 1 H), 7.75 (t, $J = 7.5$ Hz, 1 H), 7.46 (t, $J = 7.25$ Hz, 1 H), 7.39-7.33 (m, 10 H), 7.08-7.06 (m, 3 H), 6.98 (t, $J = 7.5$ Hz, 2 H), 6.76 (d, $J = 7.5$ Hz, 2 H), 5.67 (s, 1 H), 4.74 (d, $J = 12.0$ Hz, 1 H), 4.55 (s, 2 H), 4.40 (d, $J = 12.0$ Hz, 1 H), 4.16 (s, 1 H), 4.08 (d, $J = 10.5$ Hz, 1 H), 3.94 (s, 3 H), 3.85 (m, 1 H), 3.74-3.68 (m, 3 H), 2.68 (br s, 1 H); ^{13}C NMR (126 MHz, CDCl_3): δ 161.1, 156.7, 148.8, 145.0, 138.0, 137.6, 137.0, 132.4, 130.8, 129.4, 129.3, 129.0, 128.8, 128.8, 128.7, 128.4, 128.3, 128.2, 128.2, 127.9, 126.3, 125.3, 122.7, 118.0, 114.4, 80.7, 75.4, 74.8, 73.8, 72.1, 71.3, 70.2, 55.7; IR (NaCl): 3450, 3033, 2927, 1723, 1599, 1453, 1072, 737, 698 cm^{-1} ; HRMS calcd for $\text{C}_{41}\text{H}_{40}\text{NO}_5^+$ [$\text{M}+\text{H}^+$]: 626.2906, found 626.2918; $[\alpha]_D^{22}$ -31.9° (c 1.0, CHCl_3).

(2R,3R,4S)-1,3,4-tris(benzyloxy)-4-(6-fluoro-2-phenylquinolin-4-yl]butan-2-ol (110g)

Isolated in 49% yield as a colorless oil: ¹H NMR (500 MHz, CDCl₃): δ 8.28-8.21 (m, 2 H), 8.16 (d, J = 7.0 Hz, 2 H), 7.63 (d, J = 9.0 Hz, 1 H), 7.58-7.48 (m, 5 H), 7.40-7.31 (m, 9 H), 7.05 (t, J = 7.5 Hz, 1 H), 6.96 (t, J = 7.5 Hz, 2 H), 6.74 (d, J = 7.5 Hz, 2 H), 5.51 (s, 1 H), 4.70 (d, J = 12.0 Hz, 1 H), 4.62-4.51 (m, 2 H), 4.39 (d, J = 12.0 Hz, 1 H), 4.28-4.23 (m, 1 H), 4.18-4.12 (m, 1 H), 3.82-3.65 (m, 4 H); ¹³C NMR (126 MHz, CDCl₃): δ 161.6, 159.6, 156.5, 145.9, 145.1, 145.0, 139.4, 137.8, 137.4, 136.8, 133.3, 133.2, 129.7, 129.1, 128.9, 128.8, 128.7, 128.5, 128.3, 128.2, 128.2, 127.9, 127.8, 126.2, 126.1, 119.8, 119.6, 119.2, 106.9, 106.7, 80.5, 76.0, 74.7, 73.9, 72.3, 71.1, 70.1; IR (NaCl): 3461, 3031, 2925, 2363, 1723, 1623, 1496, 1072, 738, 697 cm⁻¹; HRMS calcd for C₄₀H₃₇FNO₄⁺ [M+H⁺]: 614.2706, found 614.2731; [α]_D²² -21.3° (c 1.0, CHCl₃).

(5R)-1,2,3,5-Tetra-O-benzyl-5-C-(2-phenylquinolin-4-yl)-D-arabinitol (115a)

Isolated in 51% yield as a colorless oil: ¹H NMR (500 MHz, CDCl₃): δ 8.34 (s, 1 H), 8.22 (s, 1 H), 8.16 (d, J = 6.5 Hz, 2 H), 8.03 (s, 1 H), 7.79 (t, J = 7.5 Hz, 1 H), 7.58-7.48 (m, 4 H), 7.40-7.27 (m, 13 H), 7.20 (d, J = 6.5 Hz, 2 H), 7.08 (t, J = 7.5 Hz, 1 H), 6.99 (t, J = 7.5 Hz, 2 H), 6.90 (d, J = 7.0 Hz, 2 H), 5.56 (s, 1 H), 4.70 (d, J = 12.0 Hz, 1 H), 4.58 (d, J = 12.0 Hz, 1 H), 4.51 (d, J = 12.0 Hz, 1 H), 4.46-4.42 (m, 2 H), 4.34-4.22 (m, 3 H), 4.09-4.07 (m, 2 H), 3.83-3.76 (m, 1 H), 3.68-3.63 (m, 1 H), 3.58-3.53 (m, 1 H), 2.56 (br s, 1H); ¹³C NMR (126 MHz, CDCl₃): δ 156.9, 138.2, 138.1, 137.6, 137.0, 130.6, 129.9, 129.1, 128.8, 128.8, 128.7, 128.7, 128.3, 128.2, 128.2, 128.1, 128.0, 127.9, 127.0, 125.6, 122.9, 118.6, 80.4, 78.0, 77.3, 75.4, 74.3, 73.5, 71.7, 71.6, 69.5; IR (NaCl): 3674, 2835, 2364, 2015, 1724, 1598, 1073, 697 cm⁻¹; HRMS calcd for C₄₈H₄₆NO₅⁺ [M+H⁺]: 716.3371, found 716.3405; [α]_D²² -6.9° (c 1.0, CHCl₃).

(5R)-1,3,4,5-Tetra-O-benzyl-5-C-[2-(4-fluorophenyl)quinolin-4-yl]-D-arabinitol (115b)

Isolated in 48% yield as a colorless oil: ¹H NMR (500 MHz, CDCl₃): δ 8.27 (d, J = 8.5 Hz, 1 H), 8.15-8.06 (m, 3 H), 8.02 (s, 1 H), 7.78 (t, J = 7.75 Hz, 1 H), 7.53 (t, J = 7.75 Hz, 1 H), 7.40-7.27 (m, 13 H), 7.23-7.16 (m, 4 H), 7.08 (t, J = 7.0 Hz, 1 H), 7.00 (t, J = 7.5 Hz, 2 H), 6.89 (d, J = 7.5 Hz, 2 H), 5.56 (s, 1 H), 4.67 (d, J = 12.0 Hz, 1 H), 4.58 (d, J = 12.0 Hz, 1 H), 4.55-4.39 (m, 3 H), 4.33-4.27 (m, 2 H), 4.27-4.21 (m, 1 H), 4.13-4.03 (m, 2 H), 3.75-3.71 (m, 1 H), 3.67-3.64 (m, 1 H), 3.58-3.55 (m, 1 H), 2.55 (br s, 1 H); ¹³C NMR (126 MHz, CDCl₃): δ 165.2, 163.2, 155.8, 138.2, 137.6, 137.1, 130.7, 129.9, 128.8, 128.7, 128.7, 128.6, 128.3, 128.2, 128.2, 128.1, 128.0, 127.9, 127.0, 125.5, 123.6, 118.2, 116.1, 115.9, 80.5, 78.0, 77.3, 75.4, 74.4, 73.6, 71.8, 71.6, 69.5; IR (NaCl): 3549, 2915, 2360, 1725, 1503, 1080, 697 cm⁻¹; HRMS calcd for C₄₈H₄₅FNO₅⁺ [M+H⁺]: 734.3276, found 734.3306; [α]_D²² -6.6° (c 1.0, CHCl₃).

(5R)-1,3,4,5-Tetra-O-benzyl-5-C-(6-fluoro-2-phenylquinolin-4-yl)-D-arabinitol (115g)

Isolated in 45% yield as a colorless oil: ¹H NMR (500 MHz, CDCl₃): δ 8.25-8.21 (m, 1 H), 8.18 (s, 1 H), 8.14-8.10 (m, 2 H), 7.67 (br s, 1 H), 7.55-7.49 (m, 4 H), 7.40-7.27 (m, 13 H), 7.19 (d, J = 7.0 Hz, 2 H), 7.07 (t, J = 6.75 Hz, 1 H), 7.00 (t, J = 7.5 Hz, 2 H), 6.91 (d, J = 7.0 Hz, 2 H), 5.36 (s, 1 H), 4.65 (d, J = 12.0 Hz, 1 H), 4.56 (d, J = 12.0 Hz, 1 H), 4.51 (d, J = 12.0 Hz, 1 H), 4.47-4.42 (m, 2 H), 4.28-4.21 (m, 3 H), 4.07 (d, J = 7.5 Hz, 1 H), 4.00 (d, J = 9.0 Hz, 1 H), 3.81 (d, J = 10.5 Hz, 1 H), 3.66-3.62 (m, 1 H), 3.57-3.53 (m, 1 H), 2.58-2.54 (m, 1 H); ¹³C NMR (126 MHz, CDCl₃): δ 156.4, 146.1, 144.7, 139.4, 138.2, 138.1, 137.5, 137.0, 133.4, 133.4, 129.7, 129.1, 128.8, 128.8, 128.7, 128.4, 128.2, 128.1, 128.0, 128.0, 127.7, 119.9, 119.6, 119.1, 82.2, 80.3, 77.9, 75.4, 74.3, 73.5, 71.7,

71.6, 69.4; IR (NaCl): 3543, 2913, 2360, 1724, 1524, 1073, 697 cm^{-1} ; HRMS calcd for $\text{C}_{48}\text{H}_{45}\text{FNO}_5^+$ $[\text{M}+\text{H}^+]$: 734.3276, found 734.3307; $[\alpha]_{\text{D}}^{22}$ -5.4° (c 1.0, CHCl_3).

Open-ring glycosylidene-based quinolines (debenzylated)

General procedure for the preparation of compounds **93a**, **93b**, **111a**, **111b**, & **116a**.

To a solution of perbenzylated intermediate (70 mg; 0.098 mmol) in dichloromethane (2.0 mL) at -78°C was added BCl_3 (1 M in hexane; 0.39 mL; 0.39 mmol). The reaction was stirred at -78°C under an atmosphere of nitrogen. After one hour, additional BCl_3 (1 M in hexane; 0.195 mL; 0.195 mmol) was introduced, and the reaction was maintained at -78°C for one hour. The reaction was quenched with the addition of methanol (2.0 mL). The crude material was concentrated *in vacuo*. The residue was coevaporated twice with methanol, and then purified with a Waters mass directed reverse phase prep HPLC system. The following chromatographic conditions were used: (a) column: Waters Xbridge C-18, 30 x 75 mm, 5 micron; (b) flowrate: 50 mL/min; (c) mobile phase: A = water + ammonium hydroxide (pH 10), B = acetonitrile; (d) mobile phase method: time = 0 min, A = 98, B = 2; time = 11 min, A = 65, B = 35; time = 11.2 min, A = 0, B = 100; time = 14.2 min, A = 98, B = 2; time = 15 min, A = 98, B = 2. The resulting fractions that contained the desired compound were lyophilized.

(1R)-1C-(2-Phenylquinolin-4-yl)-D-arabinitol (93a)

Isolated in 69% yield as a white solid: ^1H NMR (500 MHz, CD_3OD): δ 8.34 (d, $J = 8.0$ Hz, 1 H), 8.21 (s, 1 H), 8.17-8.13 (m, 3 H), 7.77 (t, $J = 7.75$ Hz, 1 H), 7.61 (t, $J = 7.75$ Hz, 1 H), 7.56 (t, $J = 7.5$ Hz, 2 H), 7.53-7.48 (m, 1 H), 5.73 (d, $J = 5.0$ Hz, 1 H), 4.24 (dd, $J = 5.0, 2.0$ Hz, 1 H), 3.78-3.72 (m, 2 H), 3.60-3.55 (m, 1 H), 3.52 (dd, $J = 8.0, 1.5$ Hz, 1

H); ^{13}C NMR (126 MHz, CD_3OD): δ 157.6, 150.0, 148.1, 139.7, 129.6, 129.5, 129.1, 128.7, 127.7, 126.4, 125.3, 123.8, 118.2, 72.9, 72.5, 71.9, 71.7, 63.6; IR (NaCl): 3631, 2822, 1794, 1599, 1554, 1415, 1027, 697 cm^{-1} ; HRMS calcd for $\text{C}_{20}\text{H}_{22}\text{NO}_5^+$ $[\text{M}+\text{H}^+]$: 356.1492, found 356.1496; $[\alpha]_{\text{D}}^{22} +22.3^\circ$ (c 1.0, CH_3OH); mp 178-180 $^\circ\text{C}$.

(1R)-1C-[2-(4-Fluorophenyl)quinolin-4-yl]-D-arabinitol (93b)

Isolated in 63% yield as a white solid: ^1H NMR (CD_3OD): δ 8.32 (d, $J = 8.5$ Hz, 1 H), 8.23-8.17 (m, 3 H), 8.13 (d, $J = 8.5$ Hz, 1 H), 7.76 (t, $J = 7.25$ Hz, 1 H), 7.60 (t, $J = 7.5$ Hz, 1 H), 7.29 (t, $J = 8.75$ Hz, 2 H), 5.72 (d, $J = 5.0$ Hz, 1 H), 4.24 (dd, $J = 5.0, 2.0$ Hz, 1 H), 3.78-3.72 (m, 2 H), 3.58 (dd, $J = 8.0, 2.0$ Hz, 1 H), 3.53-3.50 (m, 1 H); ^{13}C NMR (126 MHz, CD_3OD): δ 156.4, 149.7, 148.3, 129.8, 129.7, 129.6, 129.3, 126.4, 125.2, 123.8, 117.8, 115.5, 115.3, 72.9, 72.4, 71.9, 71.6, 63.6; IR (NaCl): 3630, 2820, 1793, 1598, 1554, 1503, 1412, 1027, 697 cm^{-1} ; HRMS calcd for $\text{C}_{20}\text{H}_{21}\text{FNO}_5^+$ $[\text{M}+\text{H}^+]$: 374.1404, found 374.1417; $[\alpha]_{\text{D}}^{22} +22.0^\circ$ (c 0.5, CH_3OH); mp 188-189 $^\circ\text{C}$.

(1S,2S,3R)-1-(2-Phenyl)quinolin-4-yl)-butane-1,2,3,4-tetrol (111a)

Isolated in 64% yield as a white solid: ^1H NMR (500 MHz, CD_3OD): δ 8.28 (s, 1 H), 8.18 (d, $J = 8.50$ Hz, 1 H), 8.15 (d, $J = 8.5$ Hz, 3 H), 7.76 (t, $J = 7.25$ Hz, 1 H), 7.60 (t, $J = 7.25$ Hz, 1 H), 7.56 (t, $J = 7.5$ Hz, 2 H), 7.50 (t, $J = 7.25$ Hz, 1 H), 5.99 (s, 1 H), 4.00-3.95 (m, 1 H), 3.88 (dd, $J = 11.5, 3.5$ Hz, 1 H), 3.78 (d, $J = 9.0$ Hz, 1 H), 3.70 (dd, $J = 11.5, 5.5$ Hz, 1 H); ^{13}C NMR (126 MHz, CD_3OD): δ 157.6, 150.8, 148.0, 140.0, 129.3, 129.3, 128.7, 127.7, 126.3, 124.8, 123.1, 117.7, 73.8, 72.0, 67.6, 64.0; IR (NaCl): 3632, 2821, 1794, 1599, 1553, 1505, 1415, 1027, 697 cm^{-1} ; HRMS calcd for $\text{C}_{19}\text{H}_{20}\text{NO}_4^+$ $[\text{M}+\text{H}^+]$: 326.1392, found 326.1402; $[\alpha]_{\text{D}}^{22} -16.6^\circ$ (c 0.5, CH_3OH); mp 175-176 $^\circ\text{C}$.

(1*S*,2*S*,3*R*)-1-[2-(4-Fluorophenyl)quinolin-4-yl]-butane-1,2,3,4-tetrol (111b)

Isolated in 48% yield as a white solid: ¹H NMR (500 MHz, CD₃OD): δ 8.25 (s, 1 H), 8.23-8.10 (m, 4 H), 7.75 (t, J = 7.0 Hz, 1 H), 7.59 (t, J = 7.25 Hz, 1 H), 7.29 (t, J = 8.75 Hz, 2 H), 5.98 (s, 1 H), 4.00-3.95 (m, 1 H), 3.88 (dd, J = 11.5, 3.5 Hz, 1 H), 3.77 (d, J = 9.0 Hz, 1 H), 3.69 (dd, J = 11.25, 5.75 Hz, 1 H); ¹³C NMR (126 MHz, CD₃OD): δ 156.3, 151.0, 148.1, 136.3, 129.8, 129.7, 129.4, 129.3, 126.3, 123.1, 117.3, 115.5, 115.3, 73.8, 72.0, 67.5, 64.0; IR (NaCl): 3632, 2822, 1793, 1599, 1553, 1505, 1414, 1025, 697 cm⁻¹; HRMS calcd for C₁₉H₁₉FNO₄⁺ [M+H⁺]: 344.1298, found 344.1308; [α]_D²² -13.4° (c 0.5, CH₃OH); mp 185-187 °C.

(5*R*)-5-*C*-(2-Phenylquinolin-4-yl)-*D*-arabinitol (116a)

Isolated in 60% yield as a white solid: ¹H NMR (500 MHz, CD₃OD): δ 8.29 (s, 1 H), 8.20 (d, J = 8.0 Hz, 1 H), 8.17-8.14 (m, 3 H), 7.76 (t, J = 8.25 Hz, 1 H), 7.62-7.54 (m, 3 H), 7.52-7.48 (m, 1 H), 6.01 (s, 1 H), 4.01-3.92 (m, 3 H), 3.74-3.70 (m, 2 H); ¹³C NMR (126 MHz, CD₃OD): δ 157.6, 151.2, 148.0, 140.0, 129.3, 129.2, 128.7, 127.8, 126.3, 124.8, 123.2, 117.7, 115.3, 72.9, 70.7, 70.6, 67.5, 64.0; IR (NaCl): 3630, 2823, 1795, 1599, 1555, 1415, 1027, 697 cm⁻¹; HRMS calcd for C₂₀H₂₂NO₅⁺ [M+H⁺]: 356.1492, found 356.1506; [α]_D²² -4.8° (c 0.5, CH₃OH); mp 158-162 °C.

Ethenyl-*exo*-glycal

Procedure for the preparation of **2,6-Anhydro-1,3,4,5-tetra-*O*-benzyl-7,8,9-trideoxyl-*D*-glycero-*L*-*gulo*-non-8-enitol (118)**.

To a solution of methyl-2,3,4,6-tetra-*O*-benzyl- α -*D*-glucopyranoside (200 mg; 0.361 mmol) in acetonitrile (5 mL) was added allyl trimethylsilane (61.8 mg; 0.542 mmol) and trimethylsilyl trifluoromethanesulfonate (41 mg; 0.181 mmol) at room temperature

under an atmosphere of nitrogen. The reaction was stirred overnight and quenched with the addition of saturated aqueous bicarbonate solution (1 mL). The mixture was extracted three times with ethyl acetate, and the combined organics were washed with brine, dried (Na_2SO_4), and concentrated *in vacuo*. The crude material was purified over silica gel, eluting with a gradient of 5% to 100% ethyl acetate in hexane to give the olefin as a colorless oil (128 mg; 63% yield). The ratio of α : β anomers was ~10:1. ^1H and ^{13}C NMR data were consistent with literature values.¹³¹

The NCI60 human tumor cell line anticancer drug screen¹²⁰

The human tumor cell lines of the cancer screening panel are grown in RPMI 1640 medium containing 5% fetal bovine serum and 2 mM L-glutamine. For a typical screening experiment, cells are inoculated into 96 well microtiter plates in 100 μL at plating densities ranging from 5,000 to 40,000 cells/well depending on the doubling time of individual cell lines. After cell inoculation, the microtiter plates are incubated at 37 $^\circ\text{C}$, 5% CO_2 , 95% air and 100% relative humidity for 24 hours prior to addition of experimental drugs. After 24 hours, two plates of each cell line are fixed *in situ* with trichloroacetic acid (TCA), to represent a measurement of the cell population for each cell line at the time of drug addition (Tz). Experimental drugs are solubilized in dimethyl sulfoxide at 400-fold the desired final maximum test concentration (10 μM) and stored frozen prior to use. At the time of drug addition, an aliquot of frozen concentrate is thawed and diluted to twice the desired final maximum test concentration with complete medium containing 50 $\mu\text{g}/\text{mL}$ gentamycin. Aliquots of 100 μL of this different drug dilution are added to the appropriate microtiter wells already containing 100 μL of

medium, resulting in the required final drug concentrations. Following drug addition, the plates are incubated for an additional 48 hours at 37 °C, 5% CO₂, 95% air, and 100% relative humidity. For adherent cells, the assay is terminated by the addition of cold TCA. Cells are fixed *in situ* by the gentle addition of 50 µL of cold 50 % (w/v) TCA (final concentration, 10% TCA) and incubated for 60 minutes at 4 °C. The supernatant is discarded, and the plates are washed five times with tap water and air dried.

Sulforhodamine B (SRB) solution (100 µL) at 0.4% (w/v) in 1 % acetic acid is added to each well, and plates are incubated for 10 minutes at room temperature. After staining, unbound dye is removed by washing five times with 1% acetic acid and the plates are air dried. Bound stain is subsequently solubilized with 10 mM trizma base, and the absorbance is read on an automated plate reader at a wavelength of 515 nm. For suspension cells, the methodology is the same except that the assay is terminated by fixing settled cells at the bottom of the wells by gently adding 50 µL of 80% TCA (final concentration, 16% TCA). Using the seven absorbance measurements [time zero, (Tz), control growth, (C), and test growth in the presence of drug at concentration level (Ti)], the percentage growth is calculated.

References

- (1) Nelson, D. L.; Cox, M. M. *Lehninger Principles of Biochemistry*, 3rd ed., Worth Publishers, New York, 2000.
- (2) Silverman, R. B. *The Organic Chemistry of Drug Design and Drug Action*, 2nd ed., Elsevier Academic Press, New York, 2004.
- (3) Collins, P. M.; Ferrier, R. J. *Monosaccharides: Their Chemistry and Their Roles in Natural Products*, John Wiley and Sons, New York, 1995.
- (4) O'Neil, M. J.; Heckelman, P. E.; Koch, C. B.; Roman, K. J., Eds. *The Merck Index*, 14th ed., Merck and Co., Inc., Whitehouse Station, NJ, 2006.
- (5) Stick, R. V. *Carbohydrates: The Sweet Molecules of Life*, Academic Press, New York, 2001.
- (6) Lindhorst, T. K. *Essentials of Carbohydrate Chemistry and Biochemistry*, 2nd ed., Wiley-VCH, Weinheim, Germany, 2003.
- (7) Edward, J. T. *Chem Ind.* **2005**, 1102.
- (8) (a) Lemieux, R. U. In *Molecular Rearrangements*, de Mayo, P. Ed., Interscience Publishers, John Wiley and Sons, New York, 1964; (b) Lemieux, R. U. *Pure Appl. Chem.*, **1971**, *25*, 527.
- (9) Greene, T. W.; Wuts, P. G. M. *Protective Groups in Organic Synthesis*, 2nd ed., John Wiley and Sons, New York, 1999.
- (10) Brown, W. H.; Foote, C. S. *Organic Chemistry*, 2nd ed., Saunders College Publishing, New York, 1998.
- (11) Varki, A. *Glycobiology* **1993**, *3*, 97.
- (12) Sharon, N.; Lis, H. *Scientific American* **1993**, *268*, 82.
- (13) Witczak, Z. J. *Curr. Med. Chem.* **1995**, *1*, 392.
- (14) Brunton, L. L.; Lazo, J. S.; Parker, J. L., Eds. *Goodman & Gilman's The Pharmacological Basis of Therapeutics*, 11th ed., McGraw-Hill, New York, 2006.
- (15) Drinnan, N. B.; Vari, F. *Mini-Reviews in Medicinal Chemistry* **2003**, *3*, 633.

- (16) (a) Levine, M. *N.Engl. J. Med.* **1986**, *314*, 892; (b) Sauberlich, H. E. *Ann. Rev. Nutr.* **1994**, *14*, 371.
- (17) (a) Maryanoff, B. E. *J. Med. Chem.* **1987**, *30*, 880; (b) Silberstein, S. D. *Headache* **2007**, *47*, 170.
- (18) Koch, W. L. *Anal. Profiles Drug Subs.* **1979**, *8*, 159.
- (19) Williams, K. N.; Bishai, W. R. *Expert Opin. Pharmacother.* **2005**, *6*, 2867.
- (20) Weiss, R. B. *J. Org. Chem.* **1978**, *44*, 9.
- (21) Sethi, M. L. *Anal. Profiles Drug Subs.* **1991**, *20*, 729.
- (22) Pearson, M. S. M.; Mathe-Allainmat, M.; Fargeas, V.; Lebreton, J. *Eur. J. Org. Chem.* **2005**, 2159.
- (23) Kato, A.; Kato, N.; Kano, E.; Adachi, I.; Ikeda, K.; Yu, L.; Okamoto, T.; Banba, Y.; Ouchi, H.; Takahata, H.; Aasano, N. *J. Med. Chem.* **2005**, *48*, 2036.
- (24) El Ashry, E. S. H.; Rashed, N.; Shobier, A. H. S. *Pharmazie* **2000**, *55*, 251.
- (25) Griffith, D.; Danishefsky, S. *J. Amer. Chem. Soc.* **1991**, *113*, 5863.
- (26) Kobayashi, Y. *Carbohydr. Res.* **1999**, *315*, 3.
- (27) Robertus, D. J.; Stephen, E.; Monzigno, A.; Bortone, K. *J. Mol. Biol.* **2002**, *320*, 293.
- (28) Inovye, S.; Tsuruoka, T.; Niida, T. *J. Antibiot.* **1966**, *19*, 288.
- (29) (a) Rhinehart, L.; Robinson, K. M.; King, C. H.; Liu, P. S. *Biochem. Pharmacol.* **1990**, *39*, 1537; (b) Sunkara, P. S.; Bowlin, T. L.; Liu, P. S. *Biochem. Biophys. Res. Commun.* **1987**, *148*, 206.
- (30) Fleet, G. W.; Petursson, S.; Campbell, A. L.; Mueller, R. A.; Behling, J. R.; Babiak, K. A.; Ng, J. S.; Scaros, M. G. *J. Chem. Soc., Perkin Trans. 1.* **1989**, 665.
- (31) Andrew, D. M.; Bird, M. I.; Cunningham, M. M.; Ward, P. *Bioorg. Med. Chem. Lett.* **1993**, *3*, 2533.
- (32) van den Broek, L. A. G. M.; Vermaas, D. J.; Heskamp, B., M.; van Boeckel, C. A. A.; Tan, M. C. A. A.; Bolscher, J. G. M.; Ploegh, H. L.; van Kemenade, F. J.; deGroede, R. E. Y.; Miedema, F. *Rec. Trav. Chim. Pays-Bass.* **1993**, *112*, 82.
- (33) Dennis, J. W. *Cancer Res.* **1986**, *46*, 5131.

- (34) (a) Saul, R. *Arch. Biochem. Biophysics*. **1983**, *221*, 593; (b) Walker, B. D. *Proc. Natl. Acad. Sci. USA* **1987**, *84*, 8120.
- (35) Scott, L. J.; Spencer, C. M. *Drugs* **2000**, *59*, 521.
- (36) Sailor, D.; Roger, G. *Arzneim.-Forsch.* **1980**, *30*, 2182.
- (37) (a) Nakajima, M; Itoi, K.; Takamatsu, Y.; Kinoshita, T.; Okazaki, T.; Kawakubo, K; Shindo, M; Honma, T.; Tohjigamori, M.; Haneishi, T. *J. Antibiot.* **1991**, *44*, 293; (b) Haruyama, H.; Takayama, T.; Kinoshita, T.; Kondo, M.; Nakajima, M.; Haneishi, T. *J. Chem. Soc. Perkin Trans.* **1991**, 1637.
- (38) Osz, E.; Szilagyi, L.; Somsak, L.; Benyei, A. *Tetrahedron* **1999**, *55*, 2419.
- (39) Frankowshi, A.; Seliga, C.; Bur, D.; Streith, J. *Helv. Chim. Acta* **1991**, *74*, 934.
- (40) Burgess, K.; Chaplin, D.A. *Heterocycles* **1994**, *37*, 673.
- (41) Tatsuta, K.; Niwata, Y.; Umezawa, K.; Toshima, K.; Nataka, M. *Tetrahedron Lett.* **1990**, *31*, 1171.
- (42) Granier, T.; Vasella, A. *Helv. Chim. Acta* **1995**, *78*, 1738.
- (43) For reviews, see: (a) Katritzky, A. R.; Rachwal, S.; Rachwal, B. *Tetrahedron* **1996**, *52*, 15031; (b) Madapa, S.; Tusi, Z; Batra, S. *Curr. Org. Chem.* **2008**, *12*, 1116.
- (44) For a review, see: Campoli-Richards, D. M.; Monk, J. P.; Price, A.; Benfield, P.; Todd, P. A.; Ward, A. *Drug* **1988**, *35*, 373.
- (45) Shaikh, I. A.; Johnson, F.; Grollman, A. P. *J. Med. Chem.* **1986**, *29*, 1329.
- (46) Wink, M. *Alkaloids* **2007**, *64*, 1.
- (47) Paris, D.; Cottin, M.; Demonchaux, P.; Augert, G.; Dupassieux, P.; Lenoir, P.; Peck, M. J.; Jasserand, D. *J. Med. Chem.* **1995**, *38*, 669.
- (48) Normand-Bayle, M.; Benard, C.; Zouhiri, F.; Mouscadet, J.-F.; Leh, H.; Thomas, C.-M.; Mbemba, G.; Desmaele, D.; d'Angelo, J. *Bioorg. Med. Chem. Lett.* **2005**, *15*, 4019.
- (49) Polanski, J.; Zouhiri, F.; Jeanson, L.; Desmaele, D.; d'Angelo, J.; Mouscadet, J.-F.; Gieleciak, R.; Gasteiger, J.; Le Bret, M. *J. Med. Chem.* **2002**, *45*, 4647.
- (50) Liu, L.F. *Annual Rev. Biochem.* **1989**, *58*, 351.

- (51) Marie, P.; Teulade, F.; Jean, P.V. In *Small Molecule DNA and RNA Binders: From Synthesis to Nucleic Acid Complexes*. Demeunynck, M.; Bailly, C.; Wilson, W.D. Eds. Wiley-VCH Verlag GmbH & Co. KGaA, Weinheim, 2003.
- (52) Byler, K. G.; Wang, C.; Setzer, W. N. *J. Mol. Model.* **2009**, *15*, 1417.
- (53) Li, W.; Zhang, Z.-W.; Wang, S.-X.; Ren, S.-M.; Jiang, T. *Chem. Biol. Drug Des.* **2009**, *74*, 80.
- (54) Taillefumier, C. A.; Chapleur, Y. *Chem. Rev.* **2004**, *104*, 263.
- (55) Knapp, S.; Amorelli, B.; Doss, G. A. *Synlett.* **1997**, 435.
- (56) Knapp, S.; Kirk, B. A.; Vocadlo, D.; Withers, S. G. *Tetrahedron Lett.* **2004**, *45*, 8507.
- (57) DeCastro, M. Ph.D. Dissertation, Seton Hall University, **2006**.
- (58) Lemieux, R. U.; Hendriks, K. B.; Stick, R. V.; James, K. J. *J. Am. Chem. Soc.* **1975**, *97*, 4056.
- (59) Thiem, J.; Karl, H.; Schwentner, J. *Synthesis* **1978**, 696.
- (60) DeCastro, M.; Marzabadi, C. H. *J. Carbohydr. Chem.* **2005**, *24*, 179.
- (61) Talisman, I. J. Ph.D. Dissertation, Seton Hall University, **2008**.
- (62) Osz, E.; Somsak, L.; Szilagyi, L.; Dinya, Z. *Tetrahedron* **1997**, *53*, 5813.
- (63) Osz, E.; Szilagyi, L.; Somsak, L.; Benyei, A. *Tetrahedron* **1999**, *55*, 2419.
- (64) Gasch, C.; Pradera, M. A.; Salameh, B. A. B.; Molina, J. L.; Fuentes, J. *Tetrahedron: Asymmetry* **2001**, *12*, 1267.
- (65) (a) Povarov, L. S.; Grigos, V. I.; Karakhanov, R. A.; Mikhailov, B. M. *Russ. Chem. Bull., Int. Ed. (Engl. Transl.)* **1965**, 344; (b) Povarov, L. S.; Grigos, V. I.; Mikhailov, B. M. *Russ. Chem. Bull., Int. Ed. (Engl. Transl.)* **1966**, 120.
- (66) For reviews, see: (a) Povarov, L. S. *Russ. Chem. Rev.* **1967**, *36*, 656; (b) Glushkov, V. A.; Tolstikov, A. G. *Russ. Chem. Rev.* **2008**, *77*, 137; (c) Kouznetsov, V. V. *Tetrahedron* **2009**, *65*, 2721.
- (67) (a) Makioka, Y.; Shindo, T.; Taniguchi, Y.; Takaki, K.; Fujiwara, Y. *Synthesis* **1995**, 801; (b) Cheng, D.; Zhou, J.; Saiah, E.; Beaton, G. *Org. Lett.* **2002**, *4*, 4411.

- (68) (a) Kametani, T.; Takeda, H.; Suzuki, Y.; Kasai, H.; Honda, T. *Heterocycles* **1986**, *24*, 3385; (b) Lucchini, V.; Prato, M.; Scorrano, G.; Stivanello, M.; Valle, G. *J. Chem. Soc., Perkin Trans. 1* **1989**, 2245.
- (69) Srinivas, K. V. N. S.; Das, B. *Synlett* **2004**, 1715.
- (70) Cabral, J.; Laszlo, P. *Tetrahedron Lett.* **1989**, *30*, 7237.
- (71) Jimenez, O.; de la Rosa, G.; Lavilla, R. *Angew. Chem., Int. Ed.* **2005**, *44*, 6521.
- (72) Scheffler, G.; Montavon, F.; Henning, M.; Wessel, H. P. *J. Chem. Soc. Perkin Trans. 1* **2000**, 753.
- (73) Yadav, J. S.; Reddy, B. V. S.; Srinivas, M.; Padmavani, B. *Tetrahedron* **2004**, *60*, 3261.
- (74) Brogden, K. N.; Marzabadi, C. H. Personal communication of unpublished data.
- (75) Csuk, R.; Dorr, P. *J. Carb. Chem.* **1995**, *14*, 35.
- (76) RajanBabu, T. V.; Reddy, G. S. *J. Org. Chem.* **1986**, *51*, 5458.
- (77) Bigelow, L. A.; Eatough, H. *Org. Synth.* **1928**, *8*, 22. NMR spectra of synthetic benzanilines matched literature values. See associated references denoted in benzaniline experimental section. With the exception of **86e**, yields were >40% and were not negatively impacted by the nature of the *para*-substituent.
- (78) PHD thanks Dr. George A. Doss and Dr. Mihkail Reibarkh of Merck Research Laboratories for their assistance with NMR experiments.
- (79) Galena, S. A. *Chemical Society Reviews* **1997**, *26*, 233.
- (80) Heathcock, C. H.; Ratcliffe, R. *J. Am. Chem. Soc.* **1971**, *93*, 1746.
- (81) PHD thanks Dr. R. Scott Hoerrner of Merck Research Laboratories for his assistance with experiment entries 1-4, 6-9 and Dr. Setrak K. Tanielyan of Seton Hall University for his assistance with experiment entry 5.
- (82) Hanessian, S.; Liak, T. J.; Vanesse, B. *Synthesis* **1981**, 396.
- (83) Bieg, T.; Szeja, W. *Synthesis* **1985**, 76.
- (84) Rodenbaugh, R.; Debenham, J. S.; Fraser-Reid, B. *Tetrahedron Lett.* **1996**, *37*, 5477.
- (85) Williams, D. R.; Brown, D. L.; Benbow, J. W. *J. Am. Chem. Soc.* **1989**, *111*, 1923.

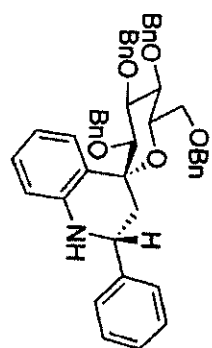
- (86) PHD thanks Eric C. Streckfuss of Merck Research Laboratories for his assistance with chromatographic method development and prep scale purification of deprotected perhydroxylated quinoline compounds.
- (87) Hong, W.-H.; Chang, T.; Daly, R. E. *Anal. Profiles Drug Subs.* **1986**, *15*, 647.
- (88) For a review, see: Brunel, J. M. *Chem. Rev.* **2005**, *405*, 857.
- (89) For a review, see: Akutagawa, S. *Appl. Catalysis A: General* **1995**, *128*, 171.
- (90) Ishitani, H.; Kobayashi, S. *Tetrahedron Lett.* **1996**, *37*, 7357.
- (91) NMR spectra matched previously reported data; see: Meng, Q., Hesse, M. *Helv. Chim. Acta* **1991**, *74*, 445.
- (92) NMR spectra matched previously reported data; see: Csuk, R., Glanzer, B. I. *Tetrahedron* **1991**, *47*, 1655.
- (93) NMR spectra matched previously reported data; see: Dondoni, A., Scherrmann, M.-C. *J. Org. Chem.* **1994**, *59*, 6404.
- (94) NMR spectra matched previously reported data; see: Yang, W.-B., Yang, Y.-Y.; Gu, Y.-F.; Wang, S.-H.; Chang, C.-C.; Lin, C.-H. *J. Org. Chem.* **2002**, *67*, 3773.
- (95) Hosomi, A.; Sakata, Y.; Sakurai, H. *Tetrahedron Lett.* **1984**, *22*, 2383.
- (96) Danishefsky, S.; Kerwin, J. F. *J. Org. Chem.* **1982**, *47*, 3803.
- (97) Crampton, M. D.; Lord, S. D.; Millar, R. *J. Chem. Soc., Perkin Trans. 2* **1997**, *5*, 909.
- (98) Ansporn, H. D. *Org. Synth.* **1945**, *25*, 86.
- (99) Martinez, R.; Chacon-Garcia, L. *Curr. Med. Chem.* **2005**, *12*, 127.
- (100) Castle, S. L.; Buckhaults, P. J.; Baldwin, L. J.; McKenney, J. D. Jr.; Castle, R. N. *J. Heterocyclic Chem.* **1987**, *24*, 1103.
- (101) Chrobak, E.; Maslankiewicz, A. *Heterocycles* **2004**, *63*, 2329.
- (102) Vitry, C.; Vasse, J.-L.; Dupas, G.; Levacher, V.; Queguiner, G.; Bourguignon, J. *Tetrahedron* **2001**, *57*, 3087.
- (103) PHD thanks Dorothy A. Levorse of Merck Research Laboratories for her assistance with this experiment.

- (104) Schmidt, R. R.; Wegmann, B.; Jung, K.-H. *Liebigs Ann. Chem.* **1991**, 121.
- (105) Joisen-Lefebvre, D.; Le Drian, C. *Helv. Chim. Acta* **2003**, *86*, 661.
- (106) Kurti, L.; Czako, B. *Strategic Applications of Named Reaction in Organic Synthesis*, Elsevier Academic Press, New York, 2005.
- (107) Kuzsmann, J.; Medgyes, G.; Boros, S. *Carbohydr. Res.* **2004**, *339*, 2407.
- (108) (a) Hermitage, S.; Jay, D. A.; Whiting, A. *Tetrahedron Lett.* **2002**, *43*, 9633; (b) Hermitage, S.; Howard, J. A. K.; Jay, D. A.; Pritchard, R. G.; Probert, M. R.; Whiting, A. *Org. Biomol. Chem.* **2004**, *2*, 2451; (c) Beifuss, U.; Ledderhose, S.; Ondrus, V. *Arkivoc* **2005**, v, 147; (d) Alves, M. J.; Azoia, N. G.; Fortes, A. G. *Tetrahedron* **2007**, *63*, 727; (e) Mayr, H.; Ofial, A. R.; Sauer, J.; Schmied, B. *Eur. J. Org. Chem.* **2000**, 2013.
- (109) Similar α -facial selectivity has been reported for other addition reactions for *exo*-glycals; see: (a) Colinas, P.; Jager, V.; Lieberknecht, A.; Bravo, R. D. *Tetrahedron Lett.* **2003**, *44*, 1071; (b) Enderlin, G.; Taillefumier, C.; Didierjean, C.; Chapleur, Y. *Tetrahedron Assym.* **2005**, *16*, 2459; (c) Taillefumier, C.; Chapleur, Y. *Chem. Rev.* **2004**, *104*, 263.
- (110) PHD thanks Dr. Mikhail Reibarkh of Merck Research Laboratories for his assistance with Spartan molecular modeling simulations.
- (111) (a) Halgren, T. A. *J. Comput. Chem.* **1996**, *17*, 490; (b) Halgren, T. A.; Nachbar, R. B. *J. Comput. Chem.* **1996**, *17*, 587.
- (112) Rocha, G. B.; Freire, R. O.; Simas, A. M.; Stewart, J. J. P. *J. Comput. Chem.* **2006** *27*, 1101.
- (113) Ramachandran, K. I.; Gopakumar, D.; Namboori, K. *Computational Chemistry and Molecular Modeling*, Springer-Verlag, Berlin, 2008.
- (114) Levine, I. N. *Physical Chemistry*, 5th ed., McGraw-Hill, New York, 2002.
- (115) Cragg, G. M.; Newman, D. J.; Snader, K. M.; *J. Nat. Prod.* **1997**, *60*, 52.
- (116) Lipinski, C. A.; Lombardo, F.; Dominy, B. W.; Feeny, P. *Adv. Drug Del. Rev.* **1997**, *23*, 3.
- (117) Veber, D. F.; Johnson, S. R.; Cheng, H.-Y.; Smith, B. R.; Ward, K. W.; Kopple, K. D. *J. Med. Chem.* **2002**, *45*, 2615.
- (118) Shoemaker, R. H. *Nat. Rev. Cancer* **2006**, *6*, 813.

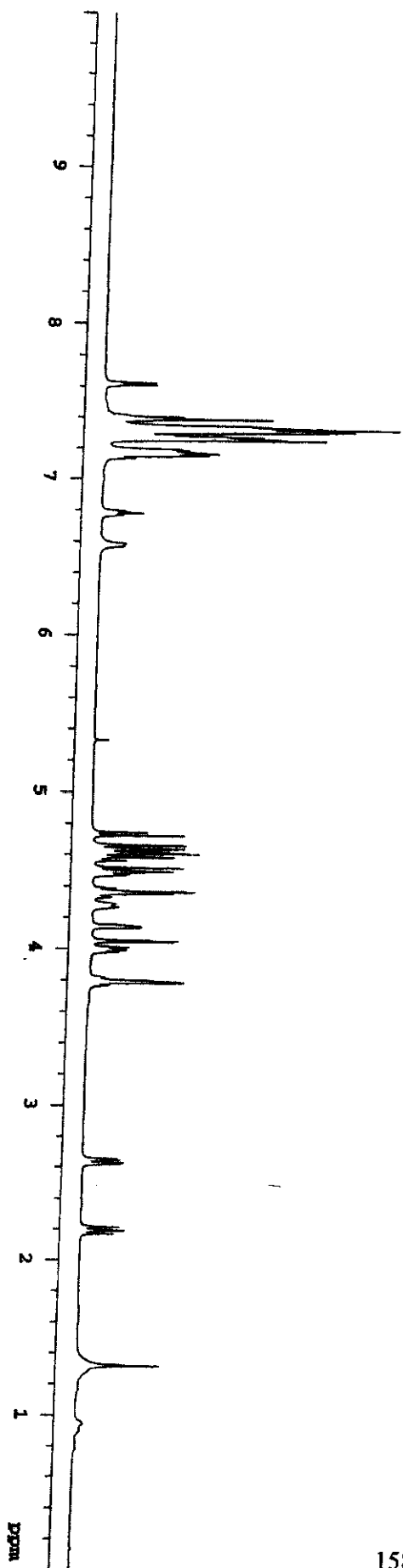
- (119) The pKa of **93a** was experimentally determined to be 4.42 in 0.15 M KCl in H₂O at 25 °C. This value correlates well with ACD software's calculated value of 4.45. PHD thanks Dorothy A. Levorse of Merck Research Laboratories for conducting this pKa determination experiment.
- (120) We thank the National Cancer Institute for evaluating our compounds. For a thorough description of the assay protocol, visit the following websites:
http://dtp.nci.nih.gov/branches/btb/onedose_interp.html and
<http://dtp.nci.nih.gov/branches/btb/ivclsp.interp.html>
- (121) Iovel, I.; Golomba, L.; Fleisher, M.; Popelis, J.; Grinberga, S.; Lukevics, E. *Chem. of Heterocycl. Compd (N. Y. NY, U. S.)* **2004**, *40*, 701.
- (122) Akaba, R.; Sakuragi, H.; Tokumaru, K. *Bull. Chem. Soc. of Jpn.* **1985**, *58*, 1186.
- (123) Grigg, R.; Mitchell, T. R.B.; Tongpenyai, N. *Synthesis* **1981**, 442.
- (124) Hasegawa, A.; Naganawa, Y.; Fushimi, M.; Ishihara, K.; Yamamoto, H. *Org. Lett.* **2006**, *8*, 3175.
- (125) Hwu, J. R.; Tseng, W. N.; Patel, H. V.; Wong, F. F.; Horng, D.-N.; Liaw, B. R.; Lin, L. C. *J. Org. Chem.* **1999**, *64*, 2211.
- (126) Naeimi, H.; Sharghi, H.; Salimi, F.; Rabiei, K. *Heteroat. Chem.* **2008**, *19*, 43.
- (127) Echevarria, A.; Miller, J.; Nascimento, M. G. *Magn. Reson. Chem.* **1985**, *23*, 809.
- (128) Ruano, J. L. G.; Aleman, J.; Alonso, I.; Parra, A.; Marcos, V.; Aguirre, J. *Chem. Eur. J.* **2007**, *13*, 6179.
- (129) Imhof, W.; Goebel, A.; Ohlmann, D.; Flemming, J.; Fritzsche, H. *J. Organomet. Chem.* **1999**, *584*, 33.
- (130) Nongkunsarn, P.; Ramsden, C. A. *Tetrahedron* **1997**, *53*, 3805.
- (131) Yokoyama, M.; Toyoshima, H.; Shimizu, M.; Mito, J.; Togo, H. *Synthesis* **1998**, 409.

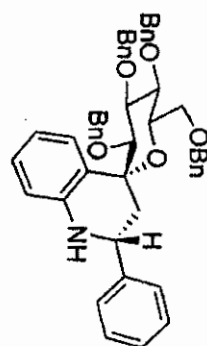
5.4. *Appendix*

^1H and ^{13}C NMR Spectra of Novel Compounds

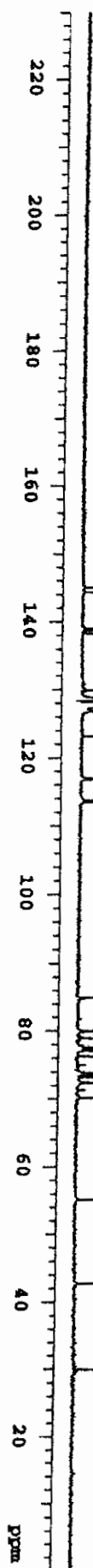


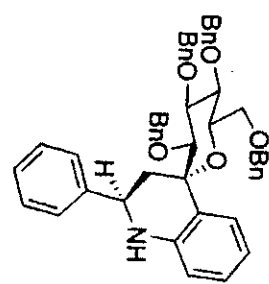
87Major



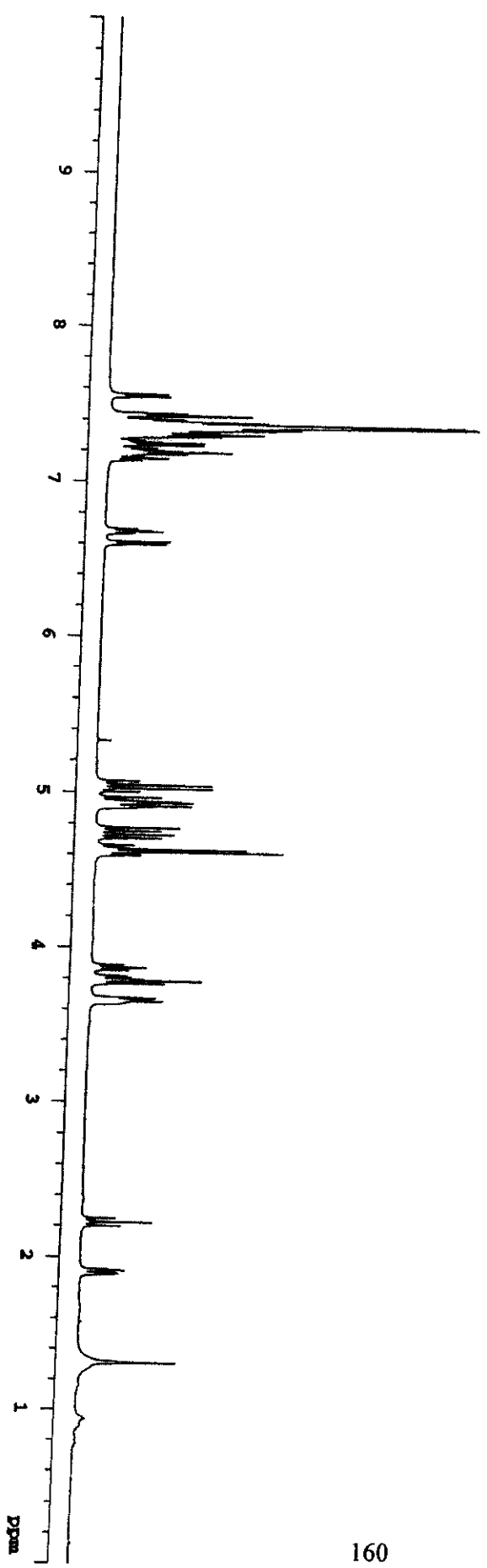


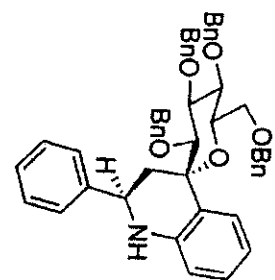
87Major



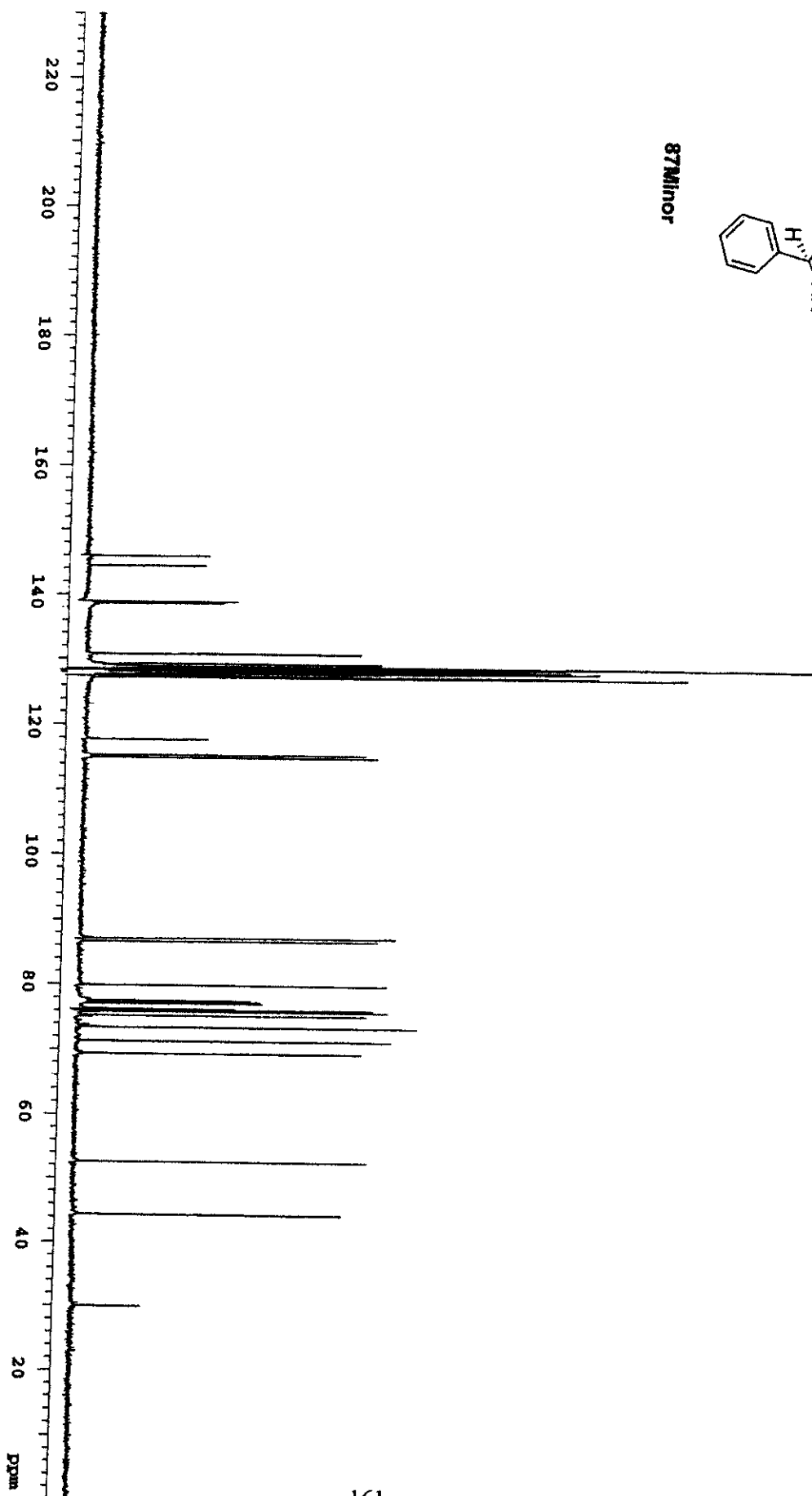


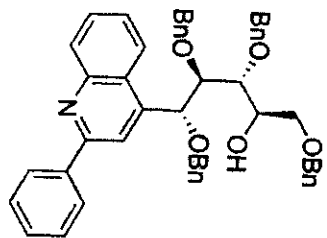
87MInor



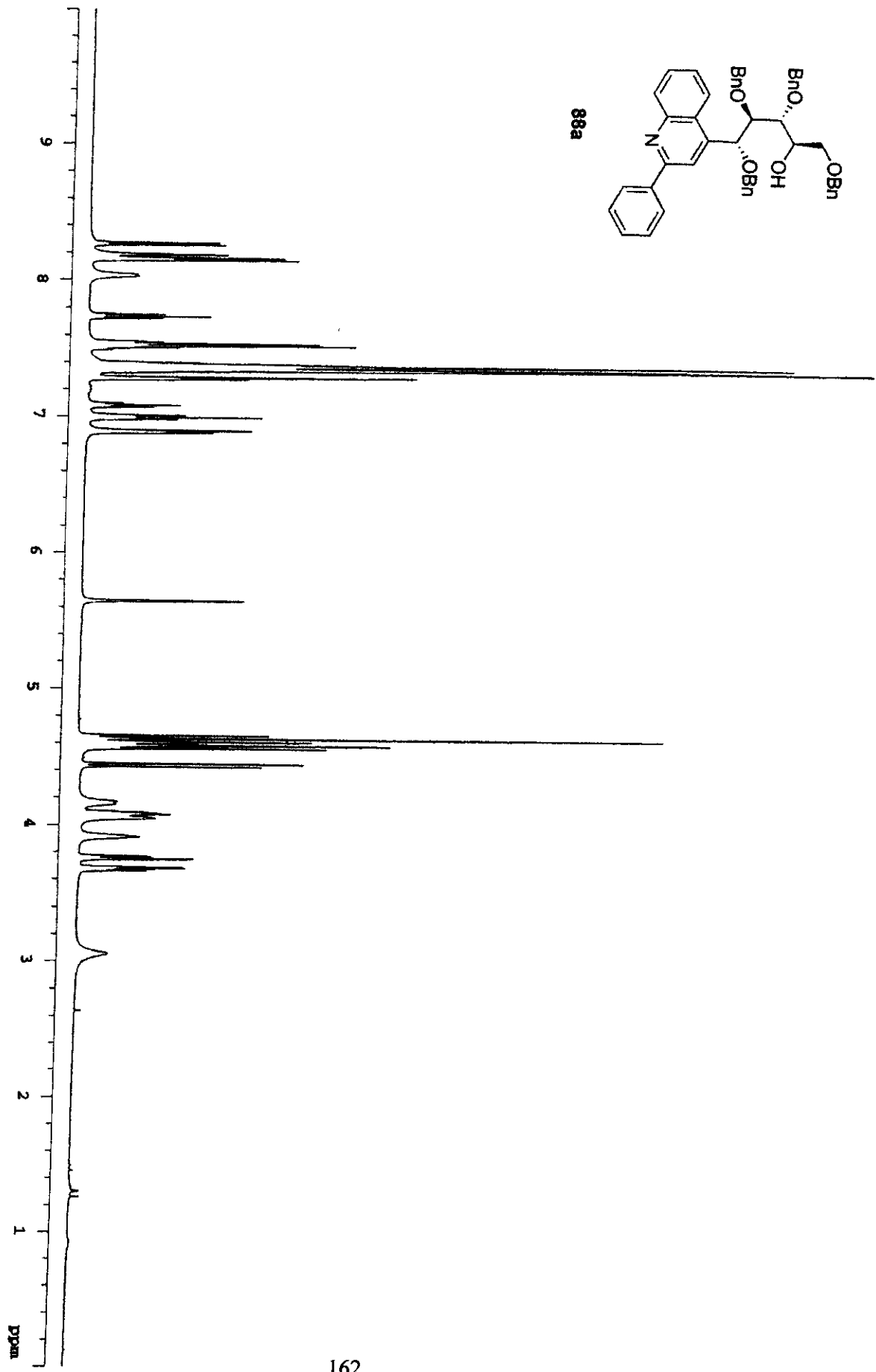


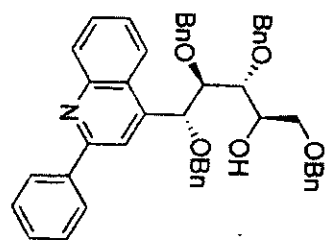
87MInor



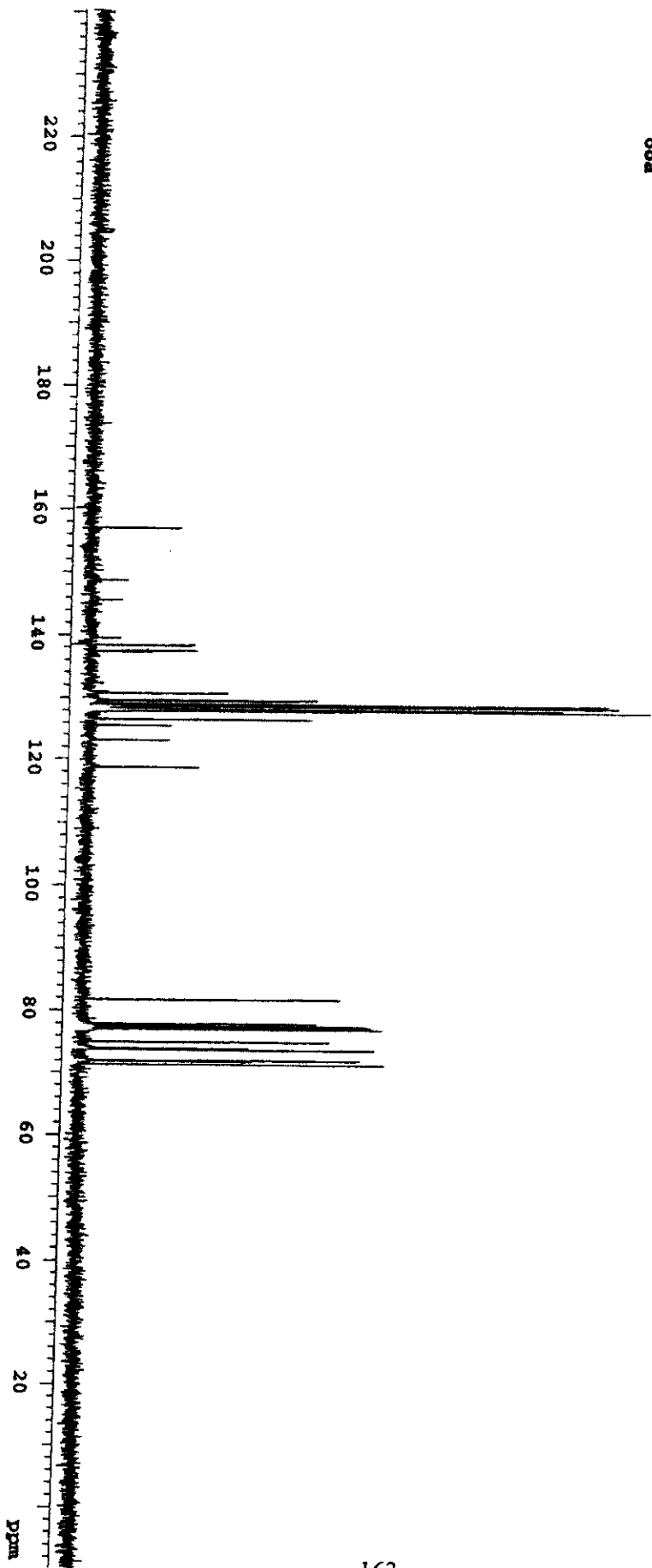


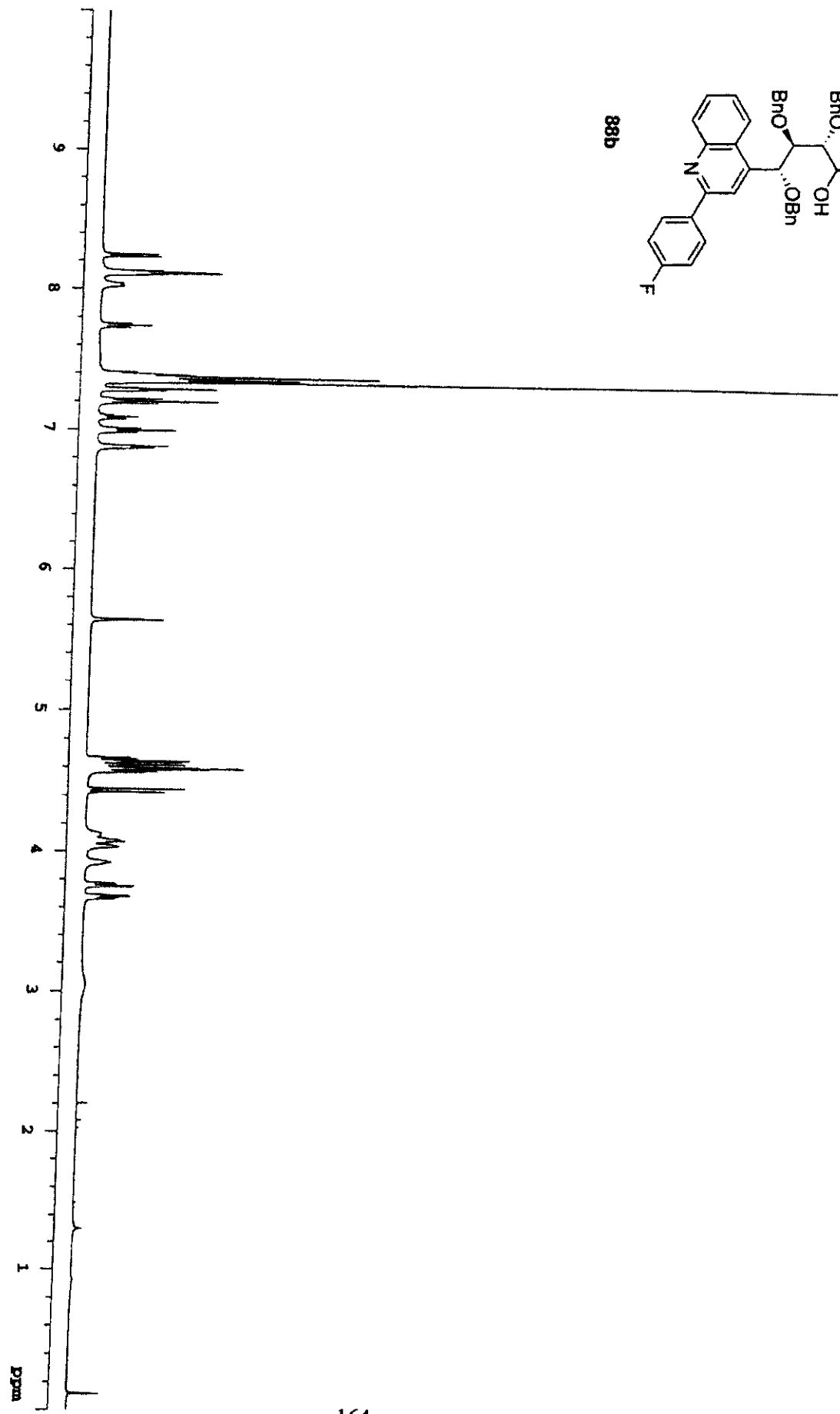
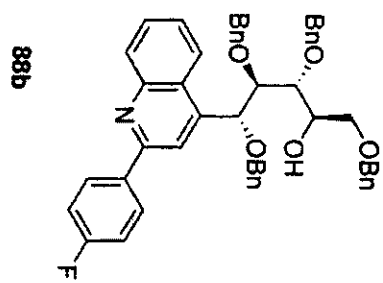
88a

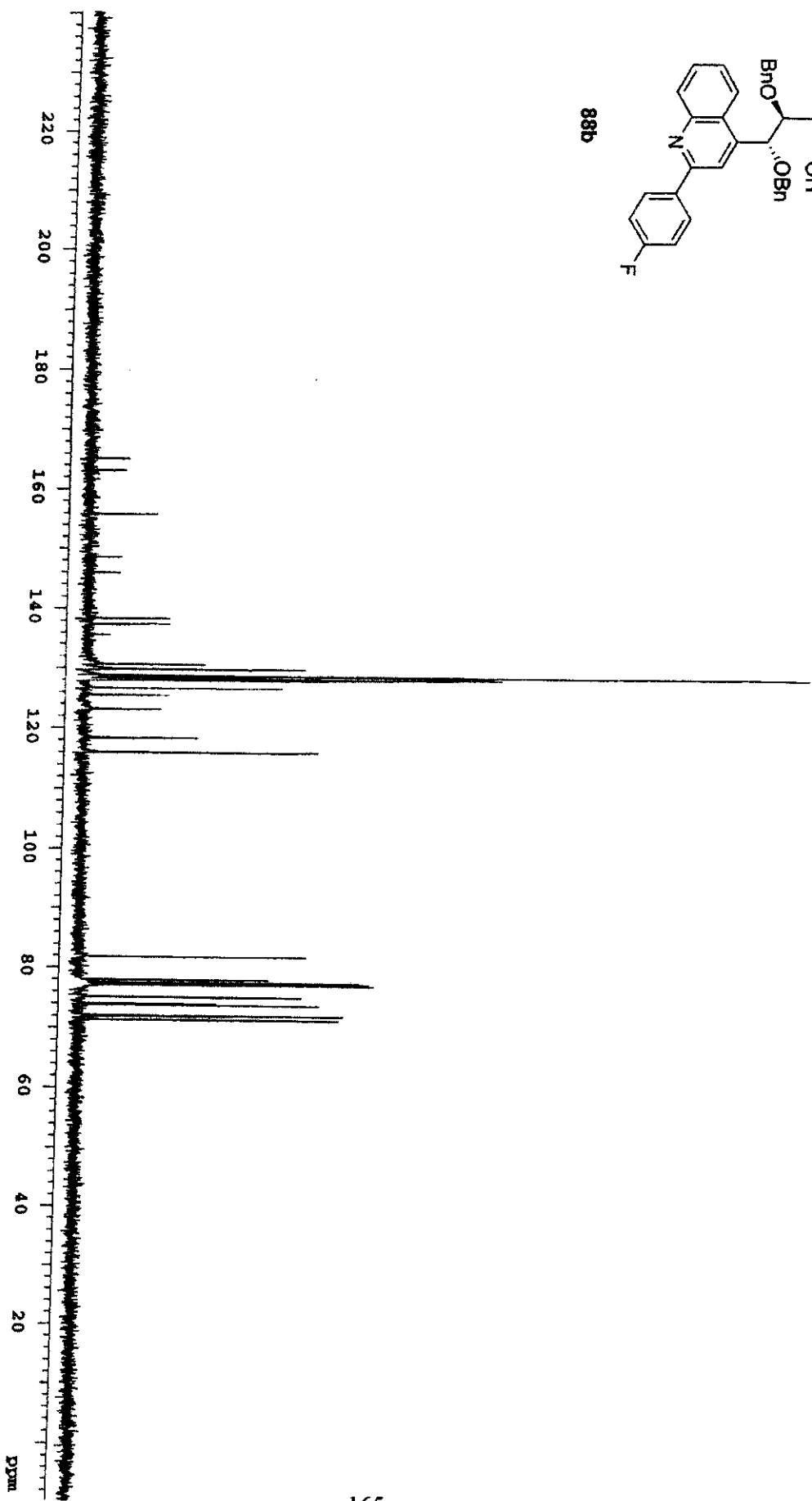
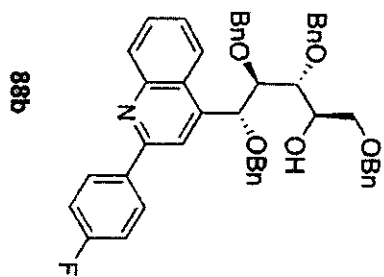


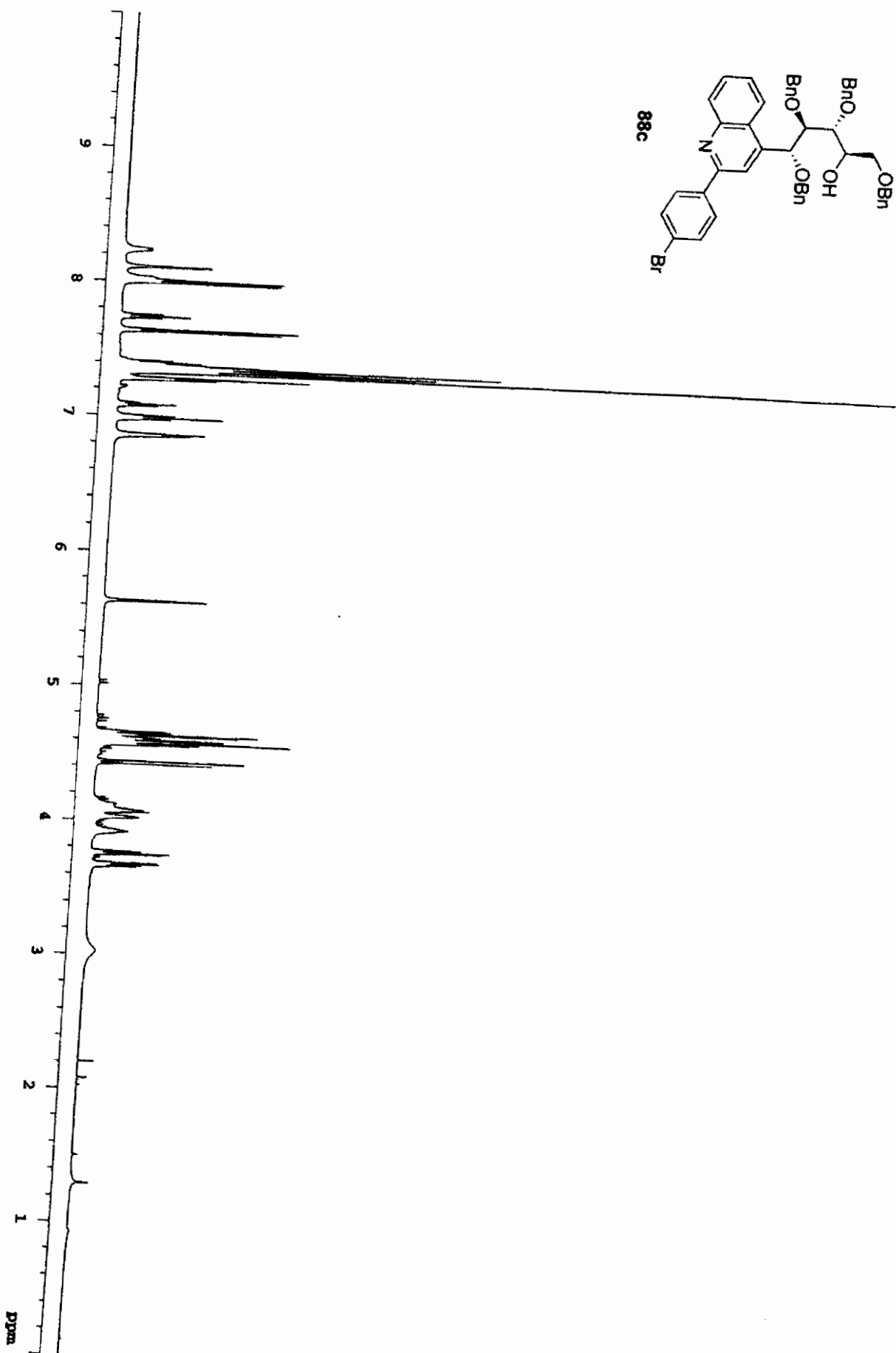
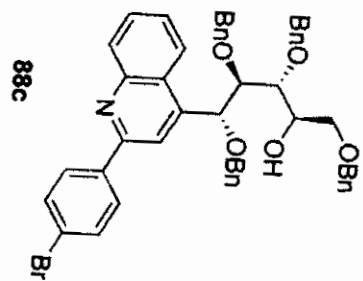


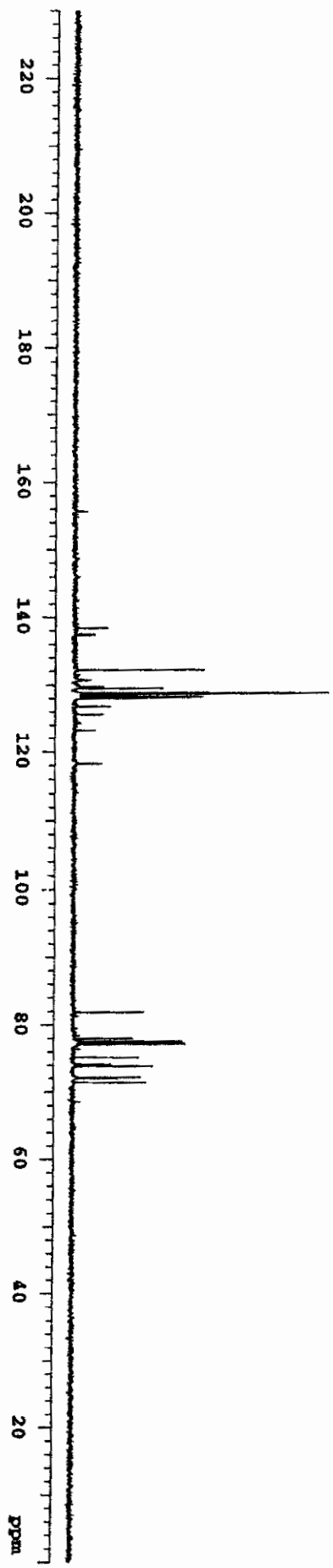
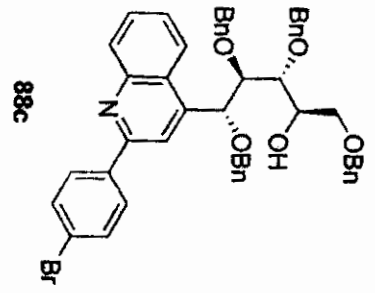
88a

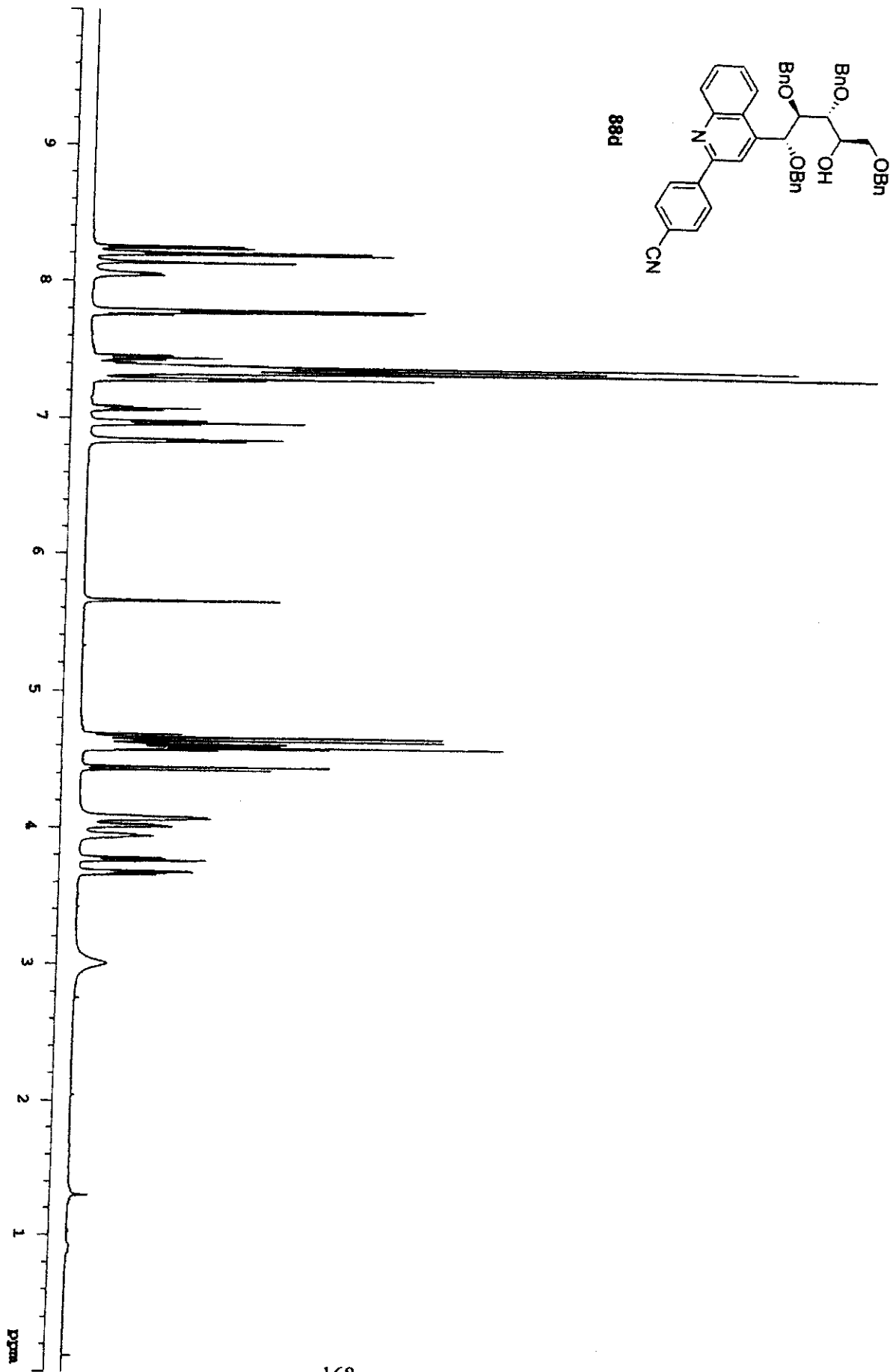
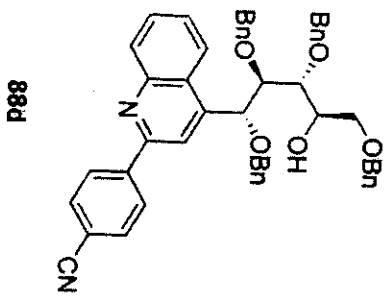


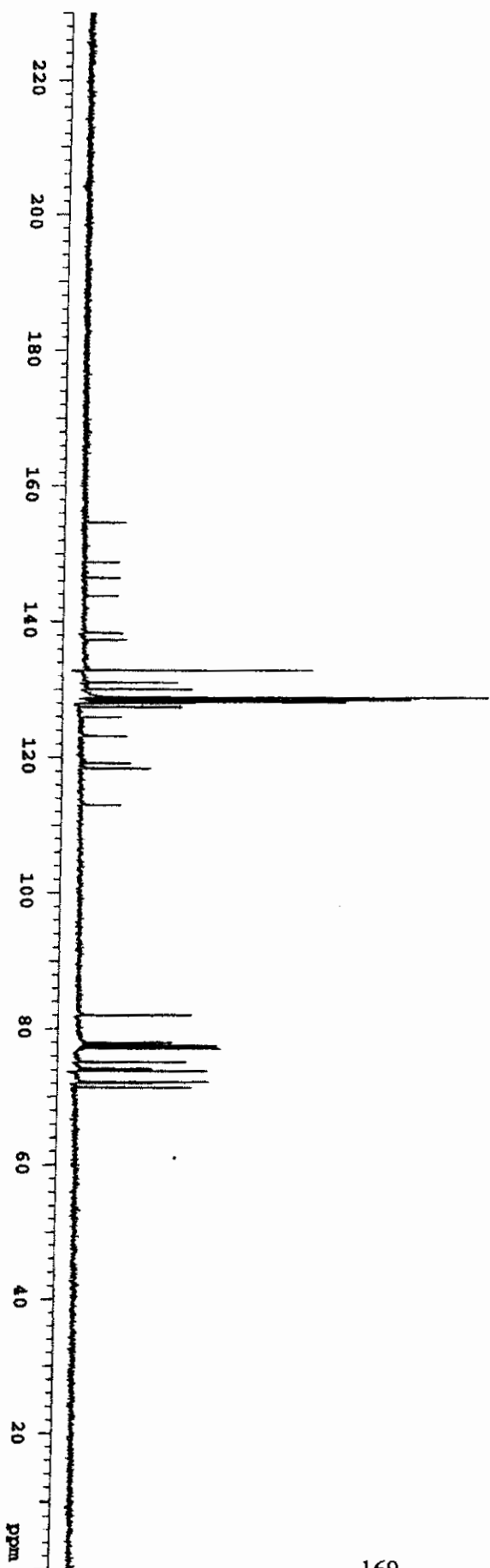
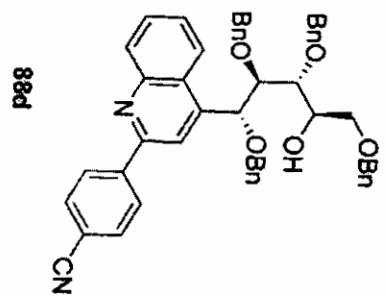


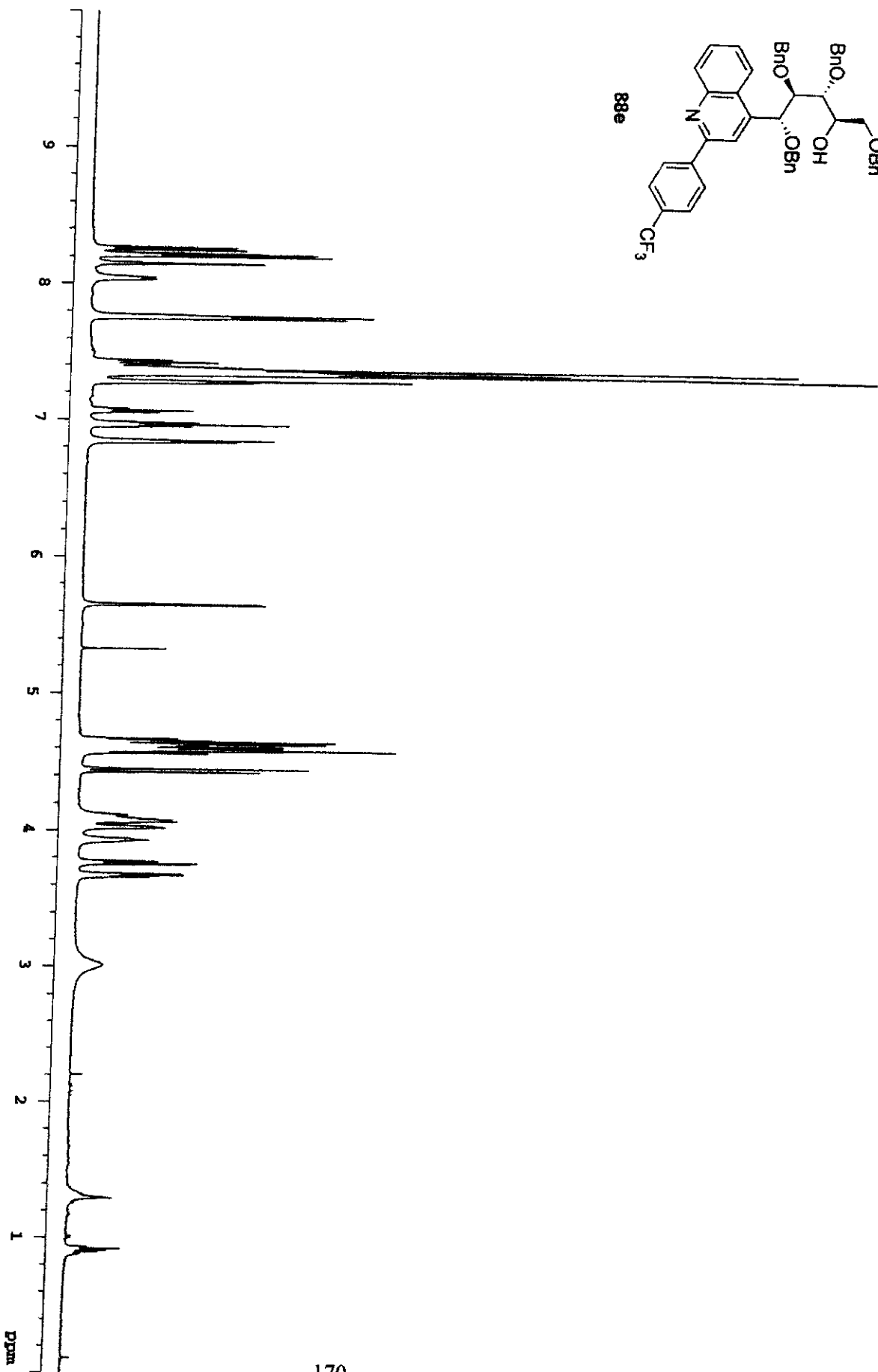
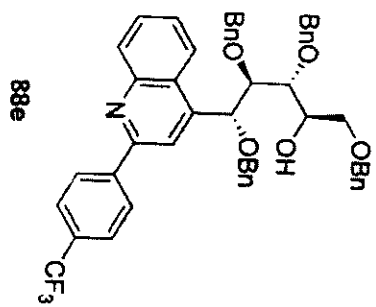


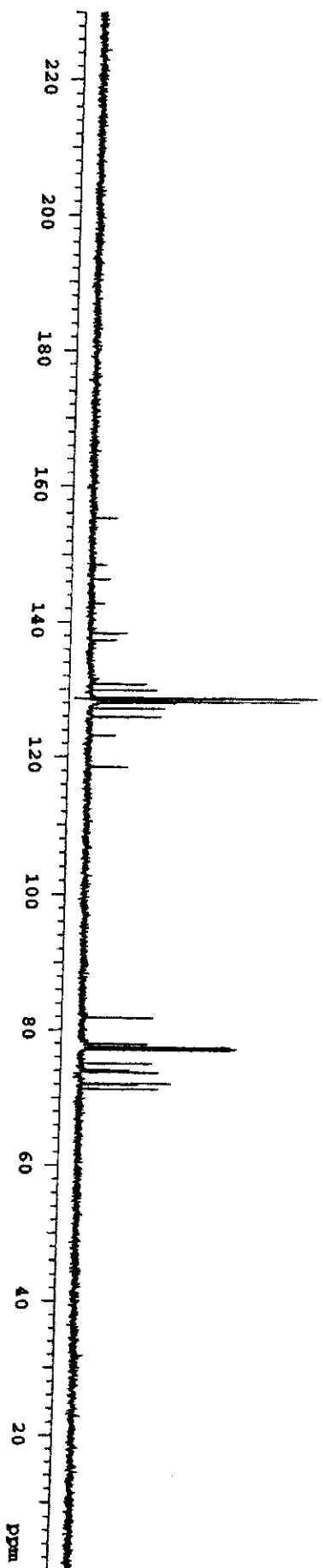
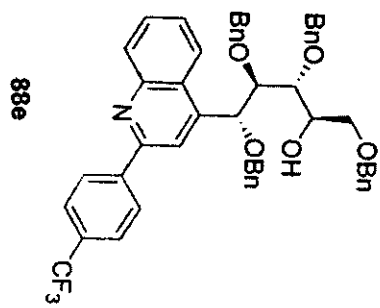


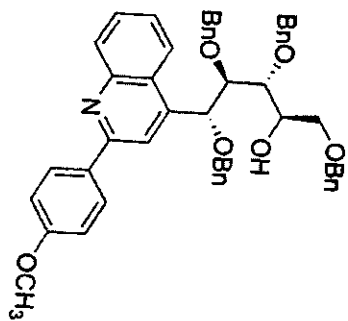




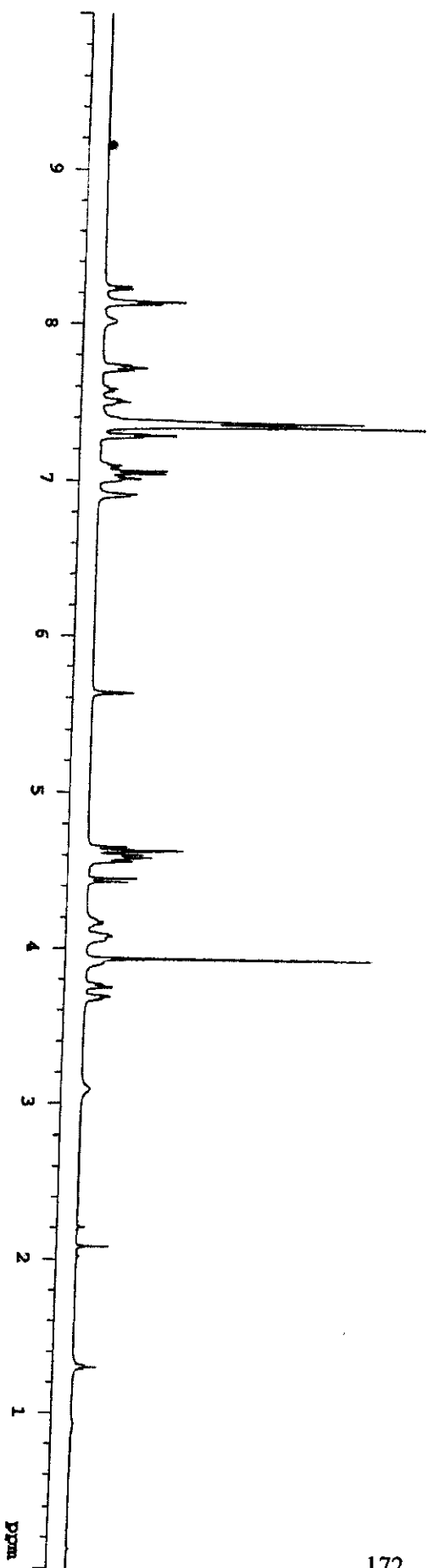


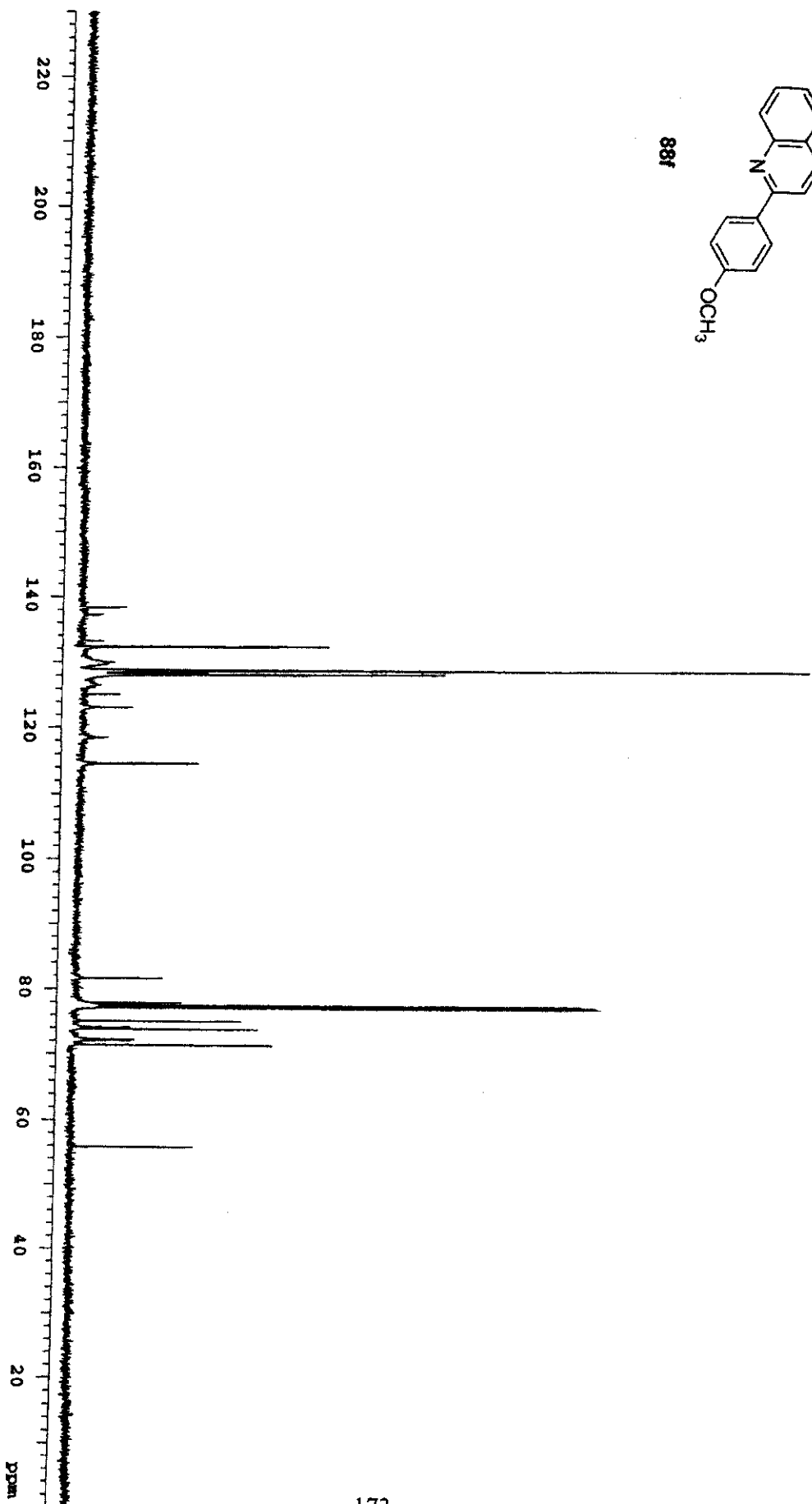
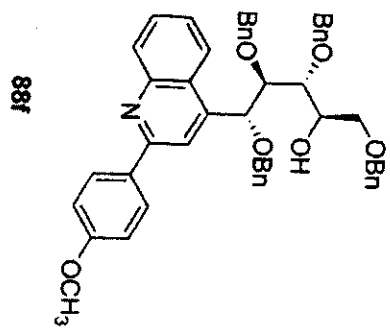


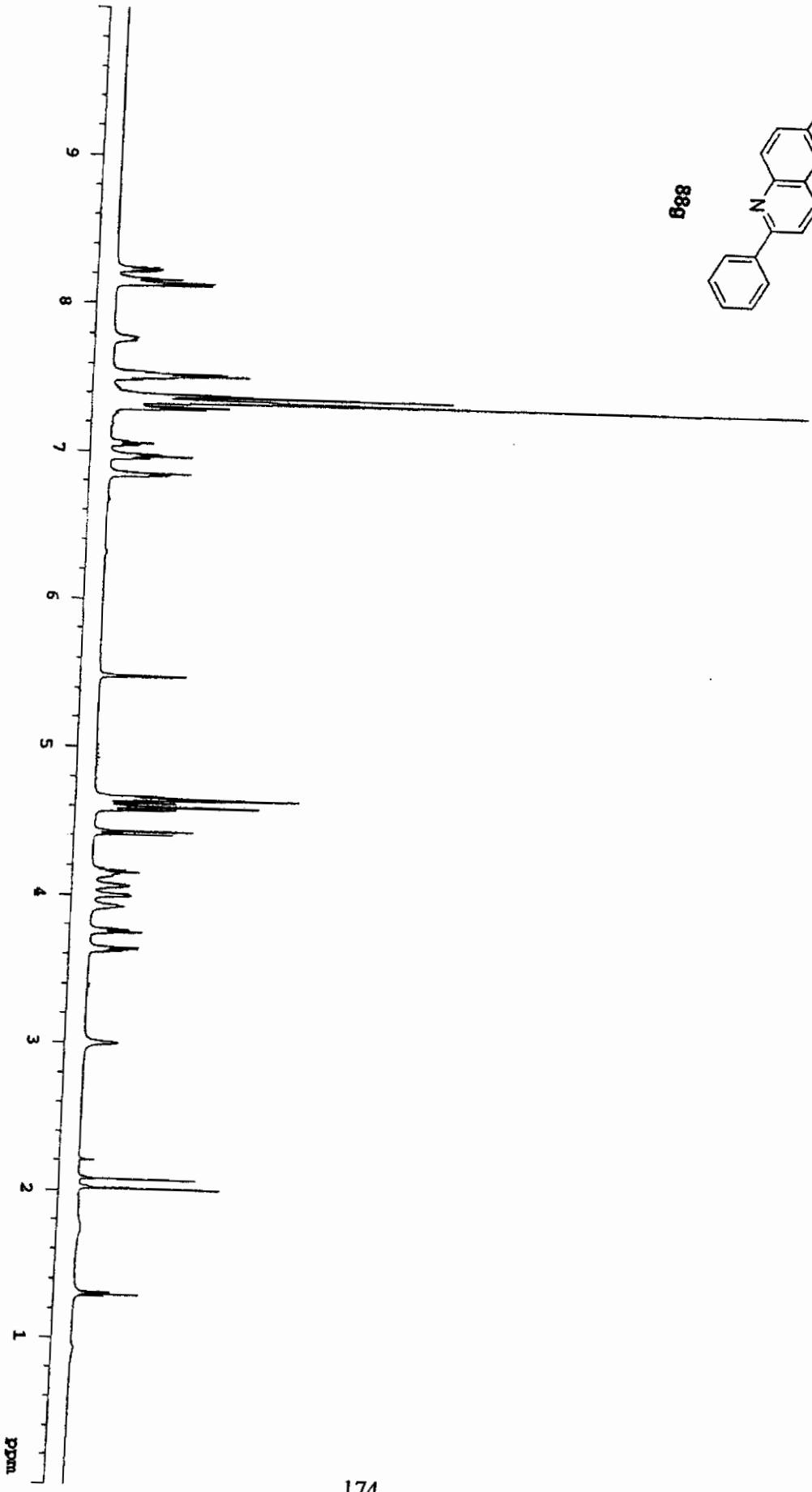
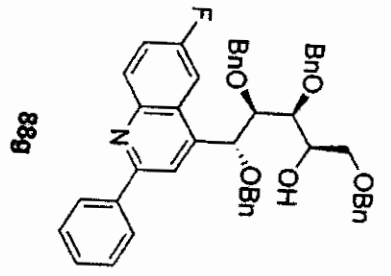


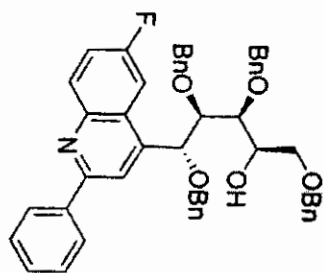


88f

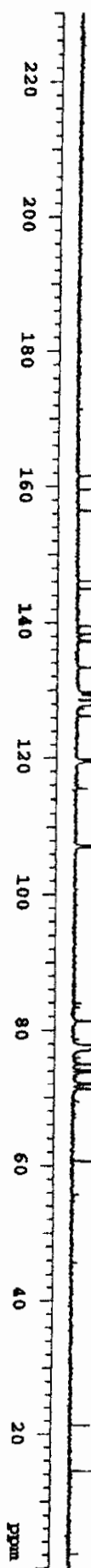


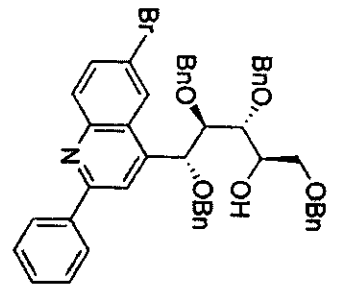




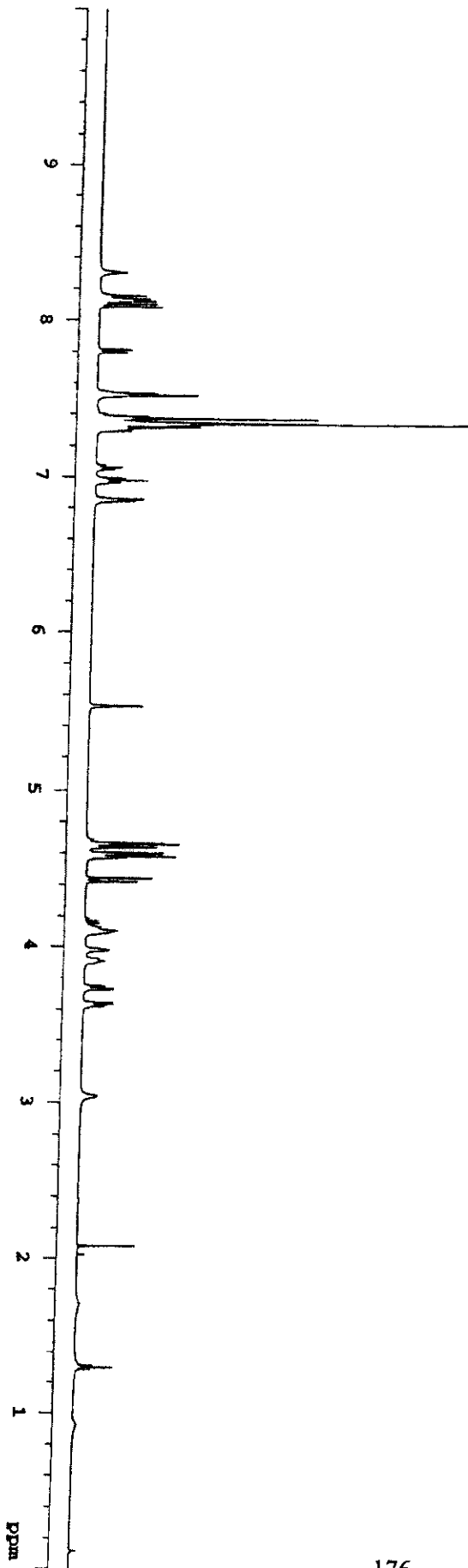


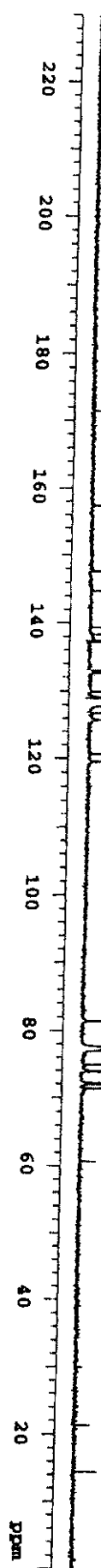
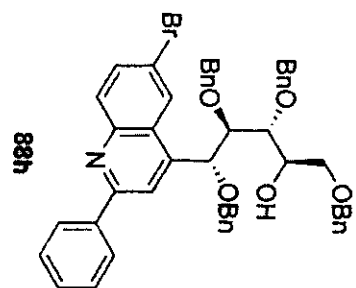
88g

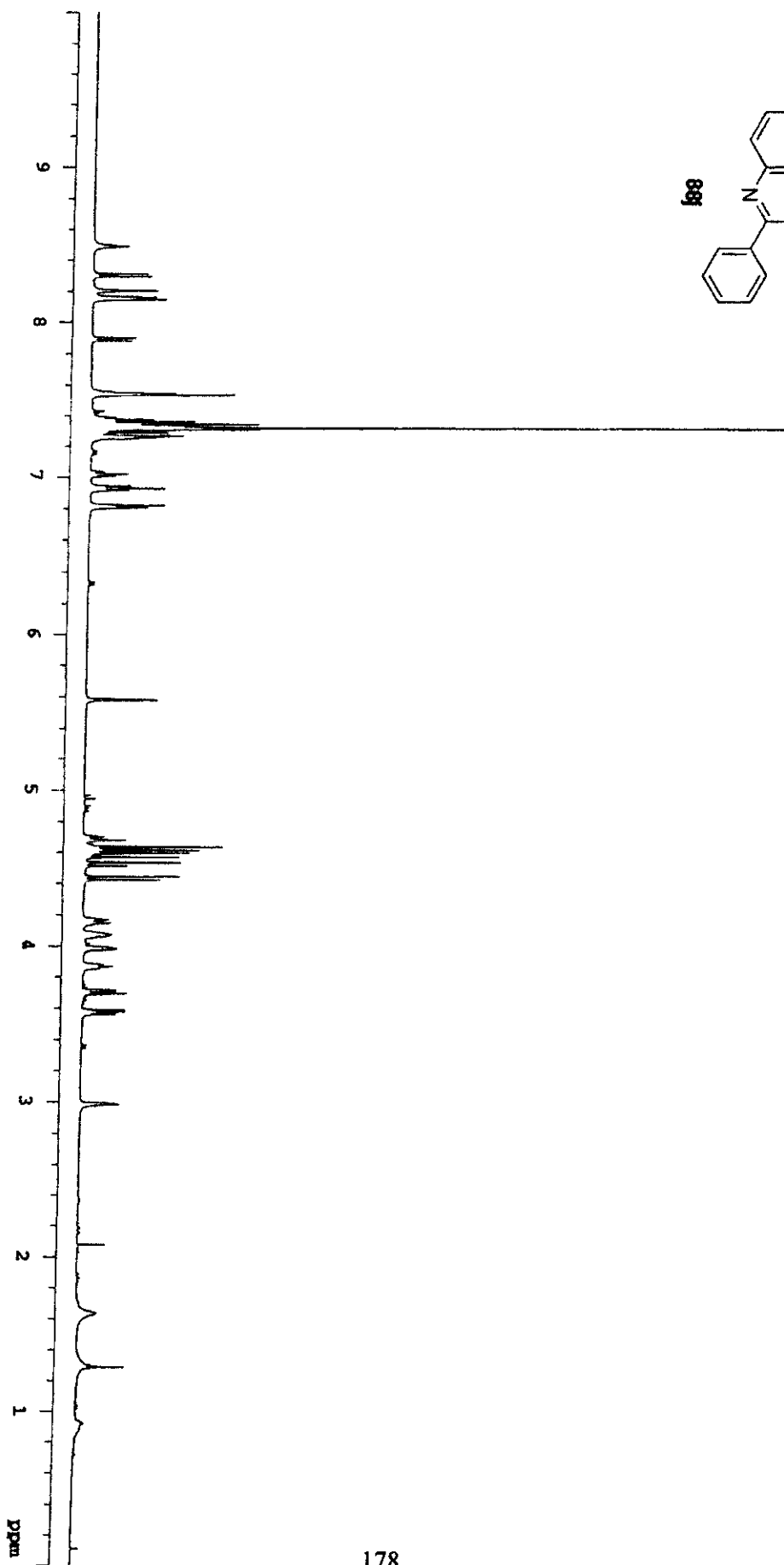
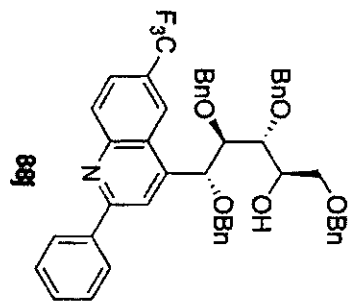


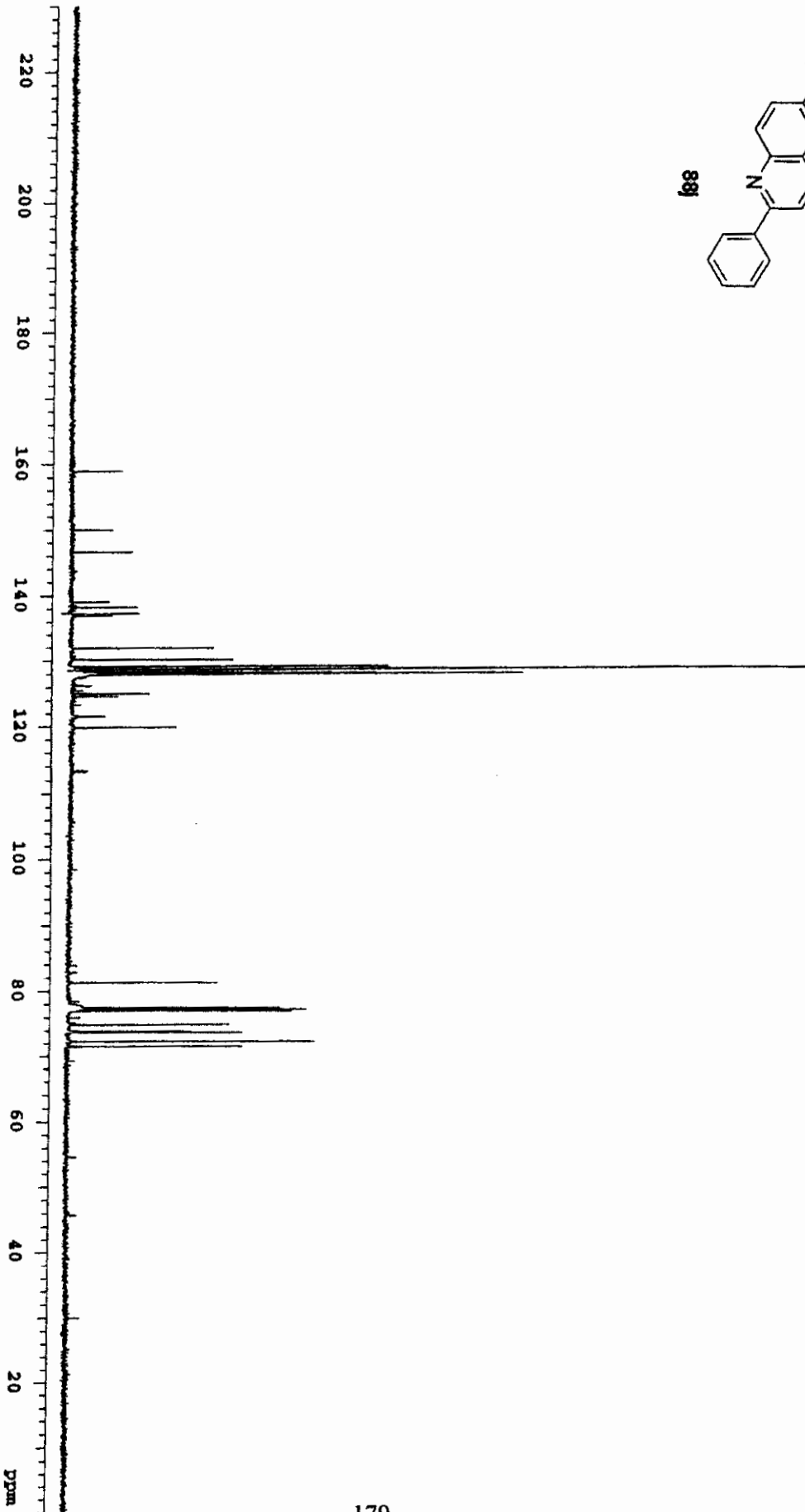
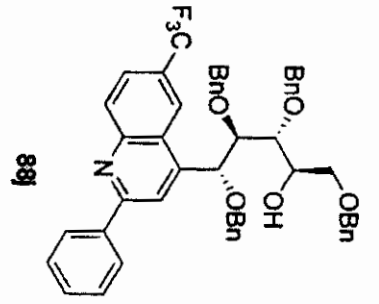


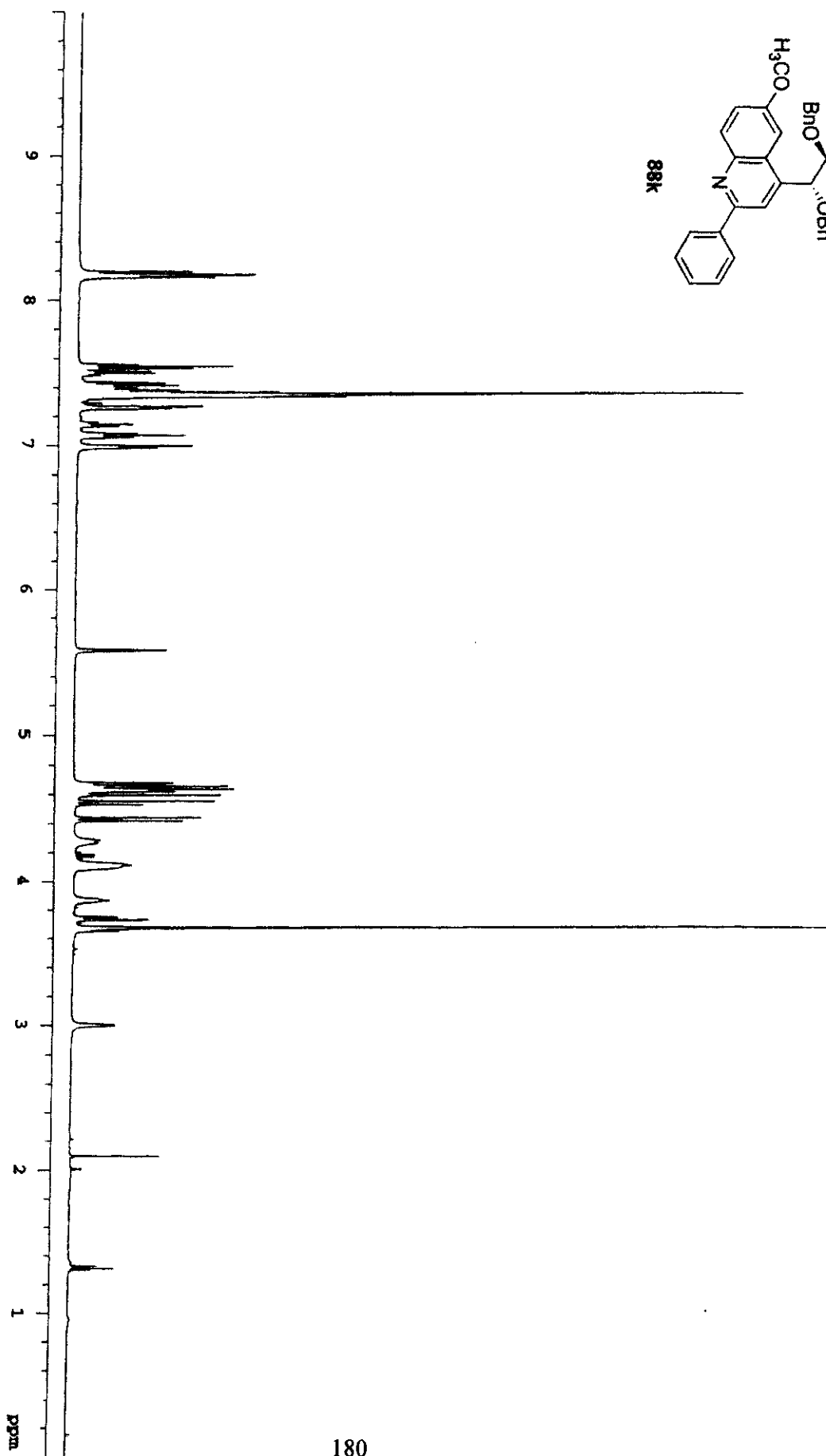
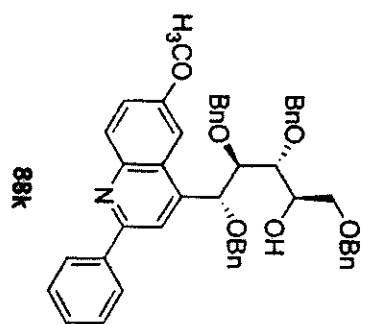
88h

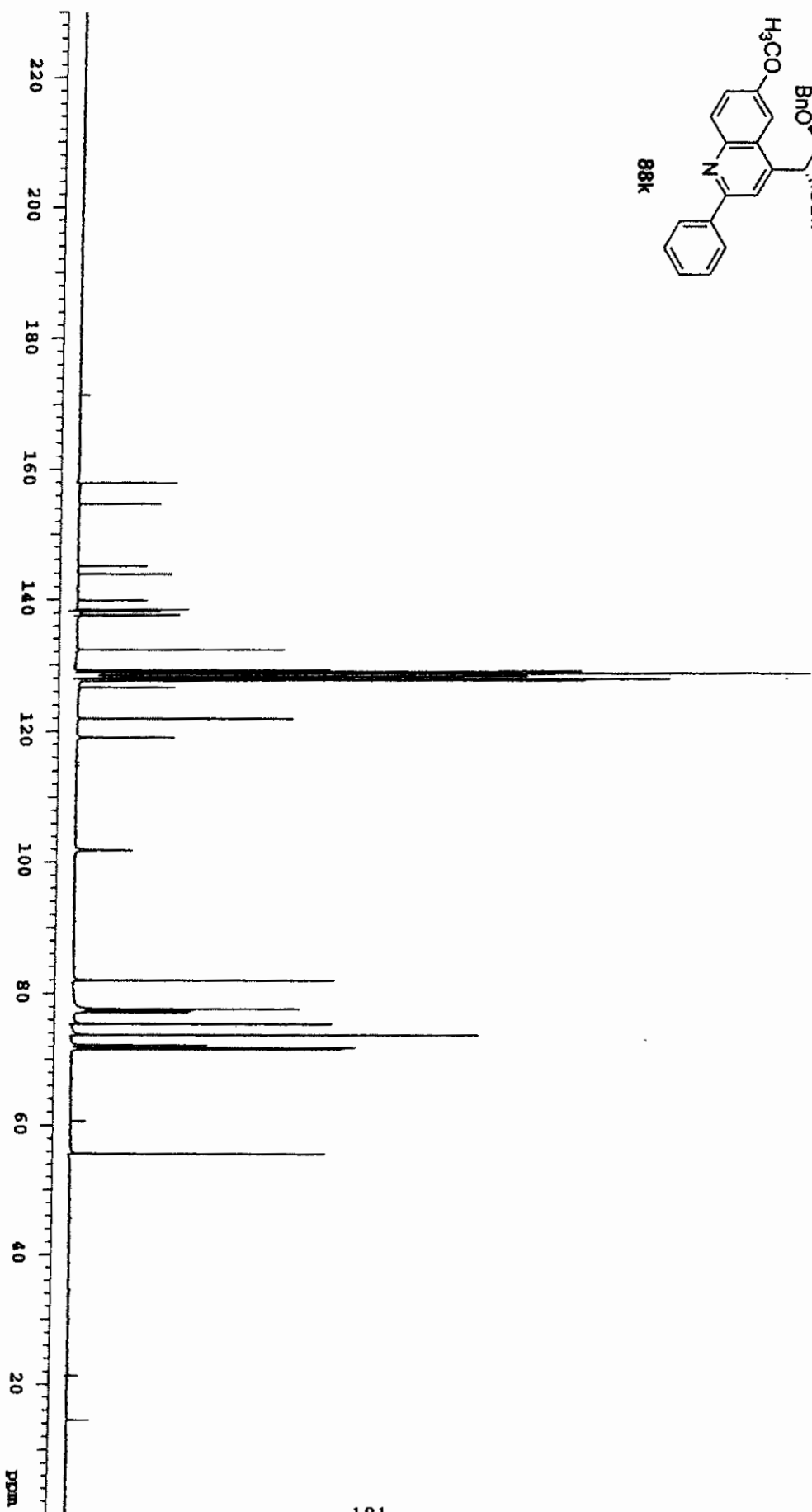
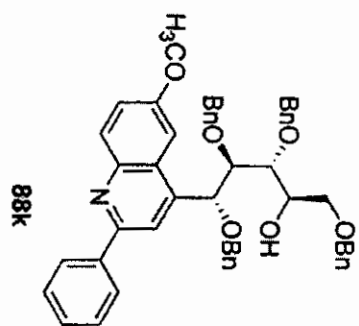


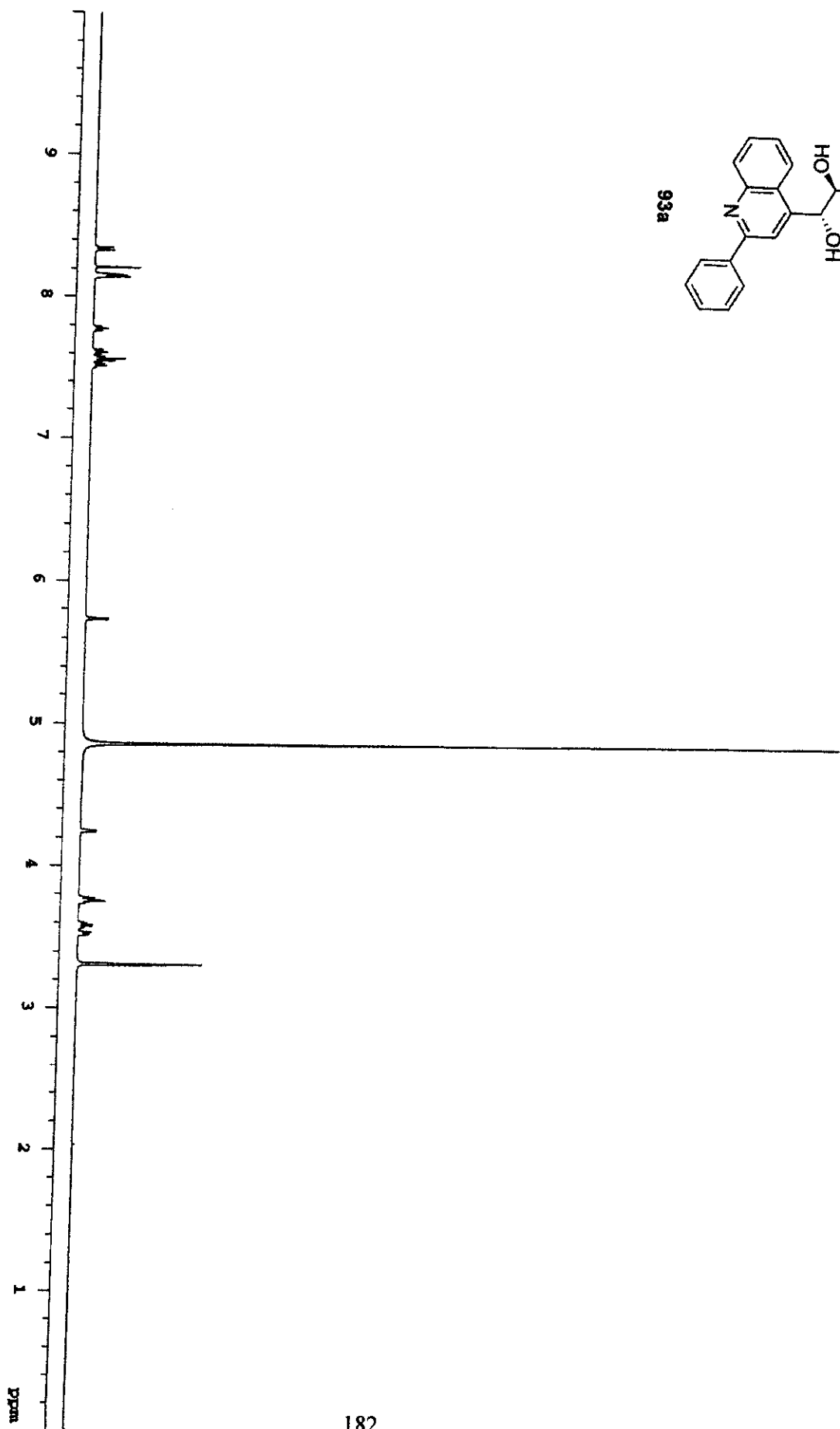
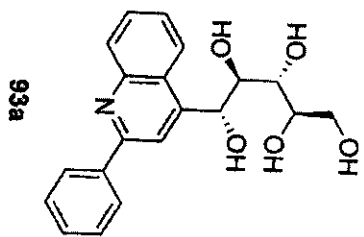


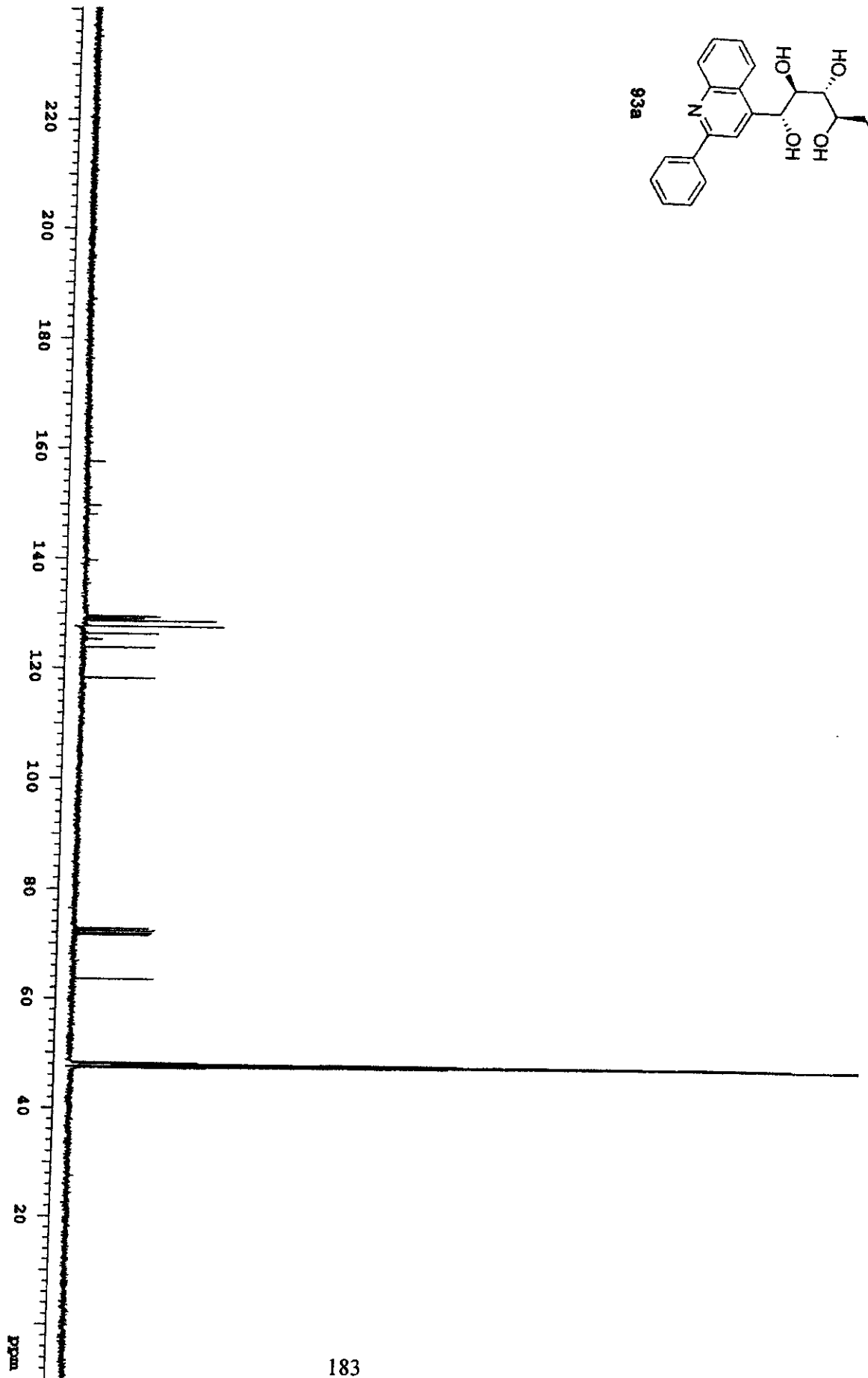
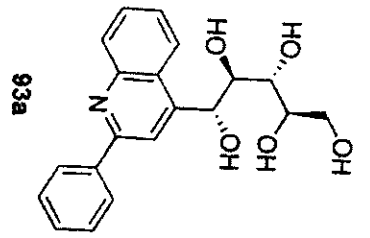


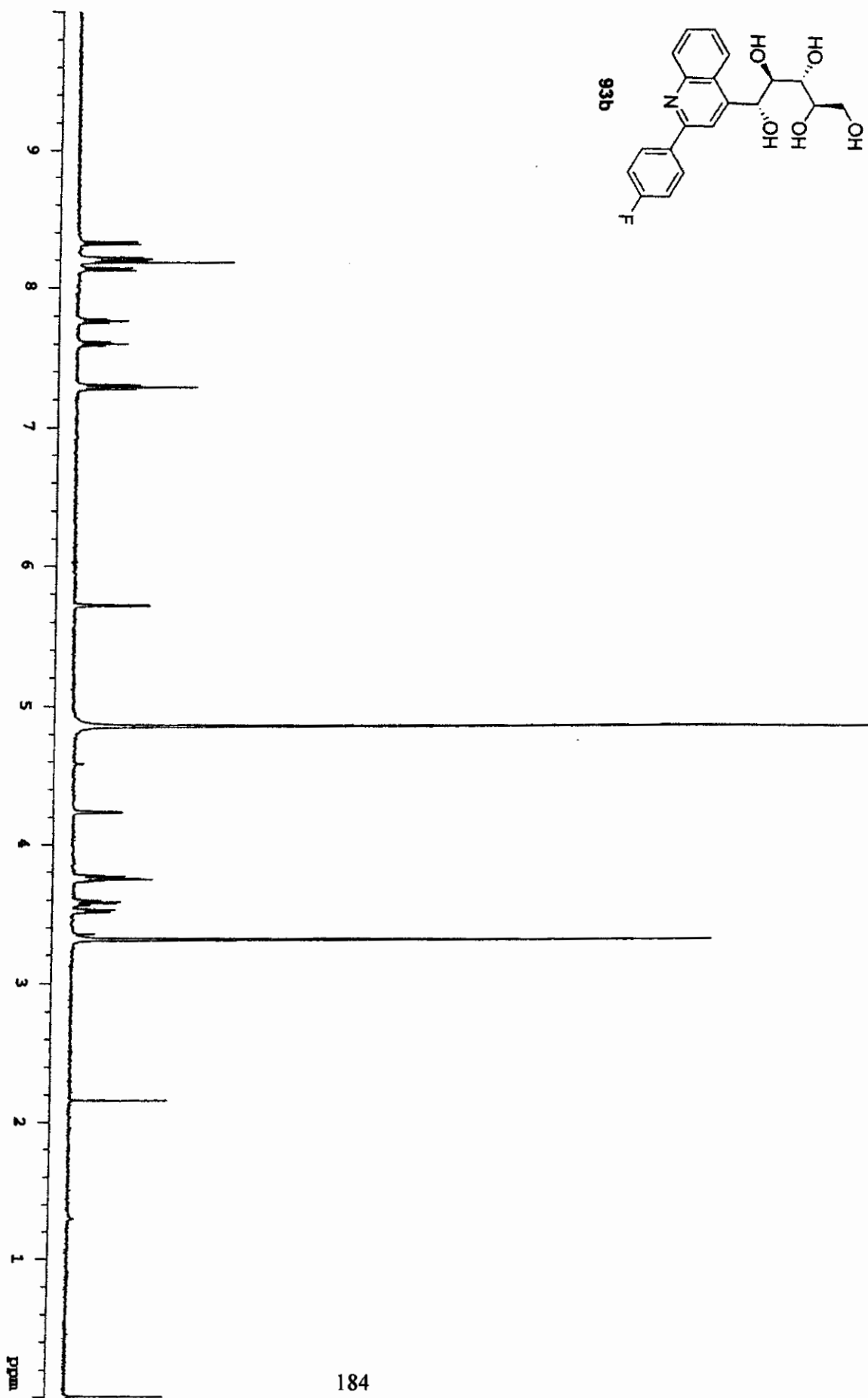
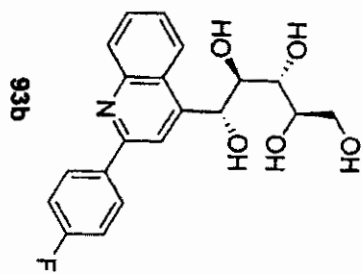


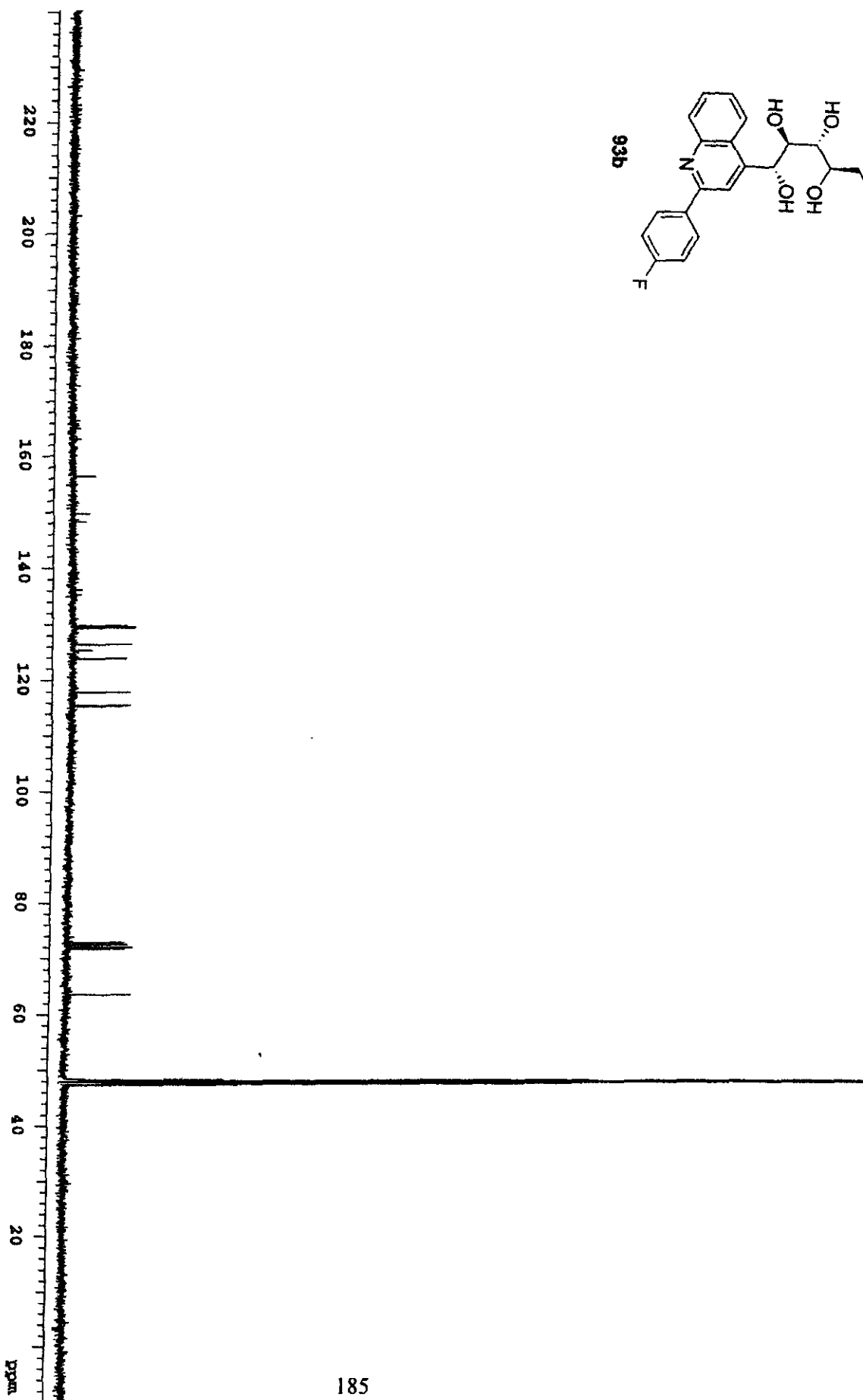
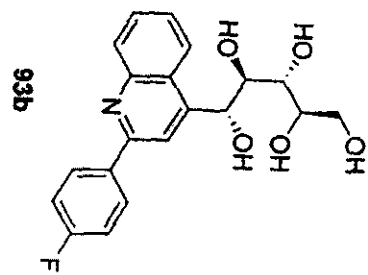


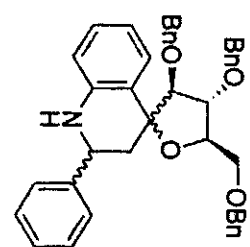




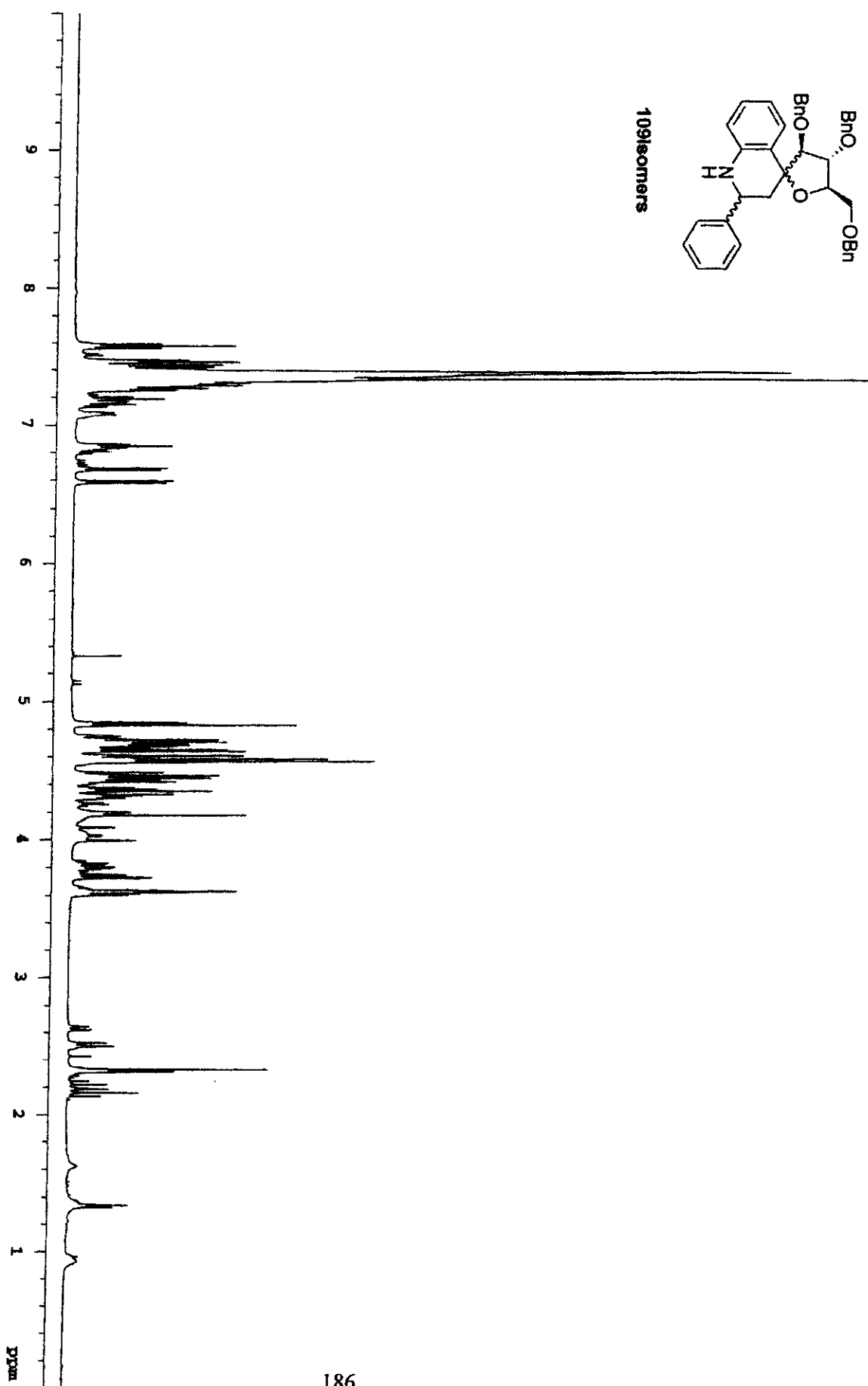


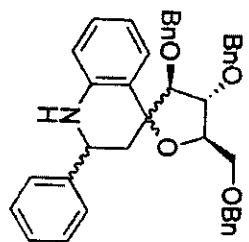




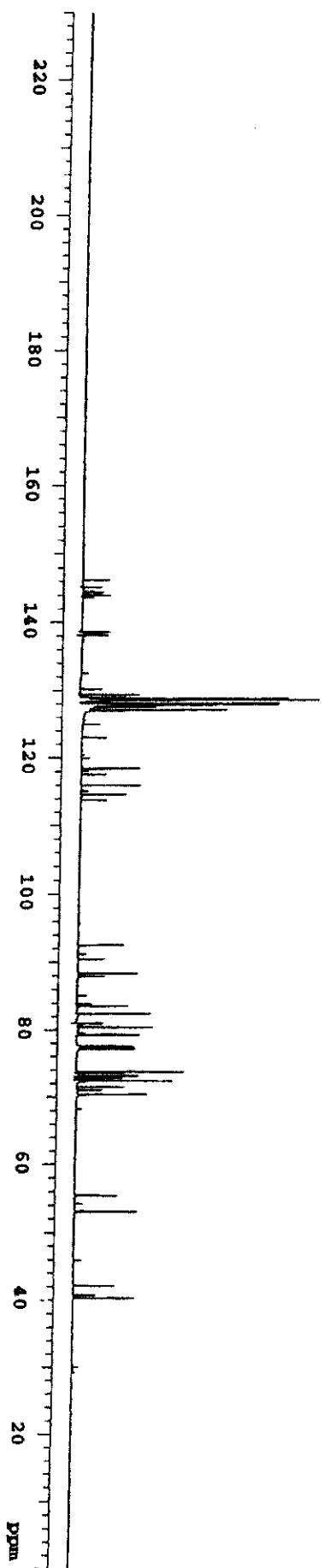


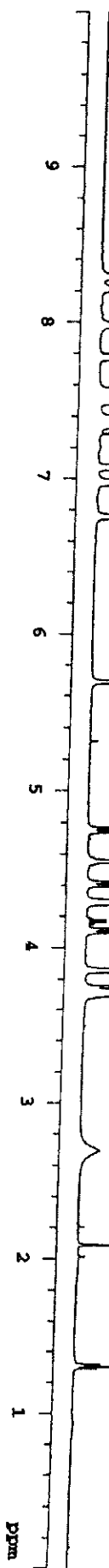
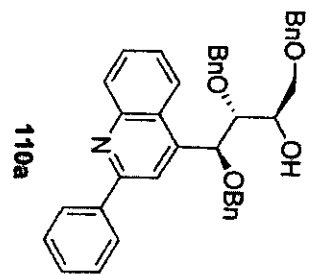
109 isomers

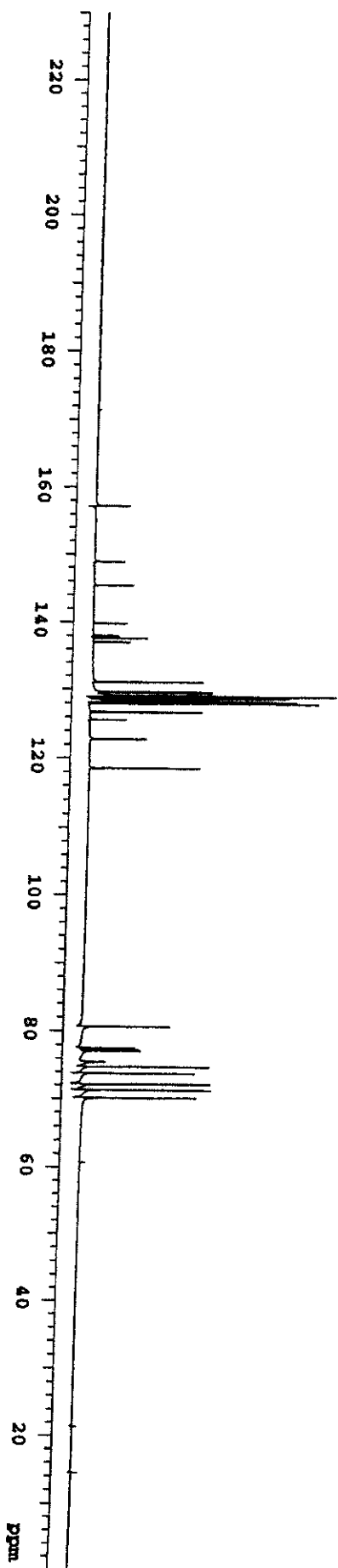
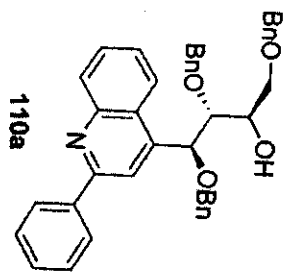


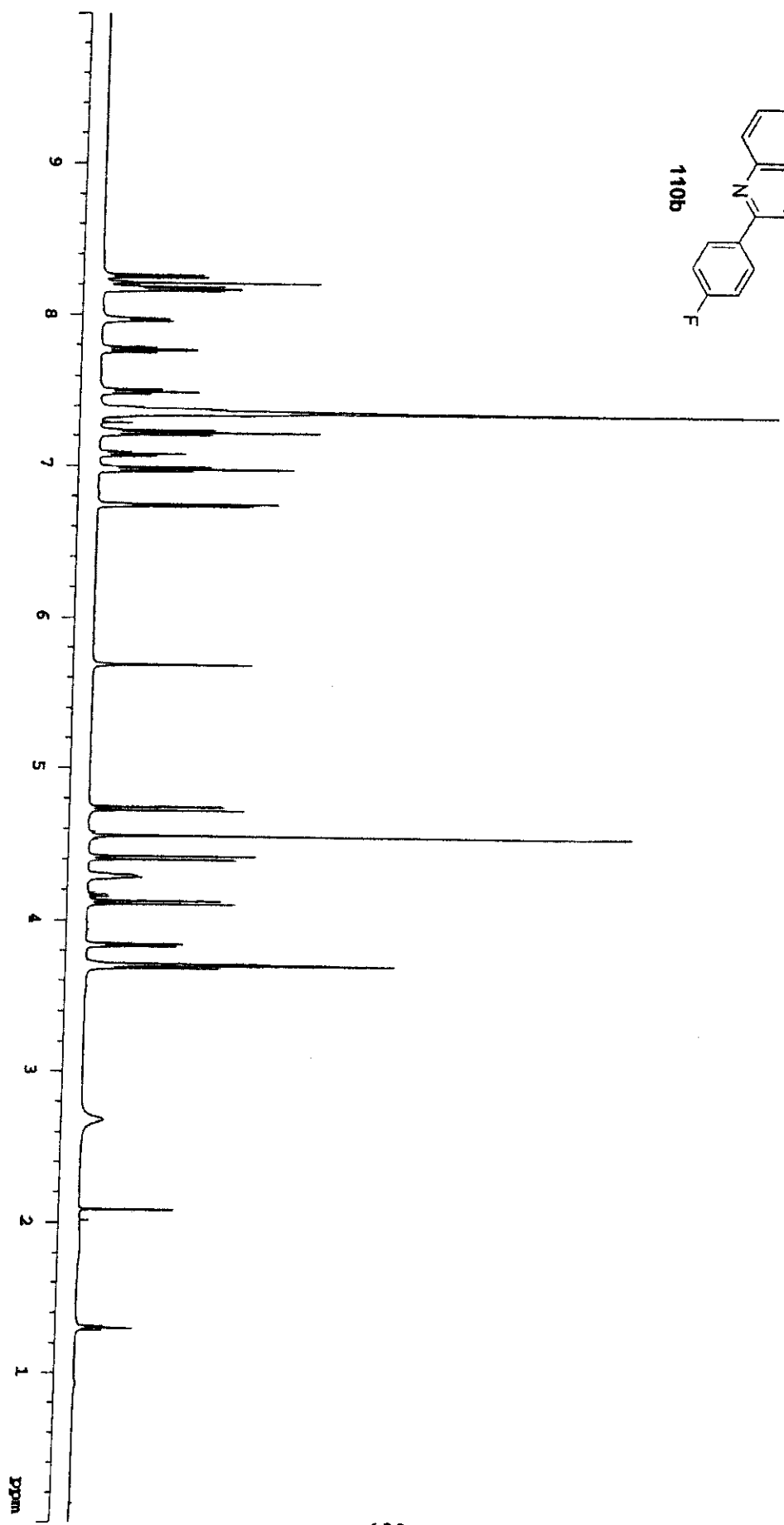
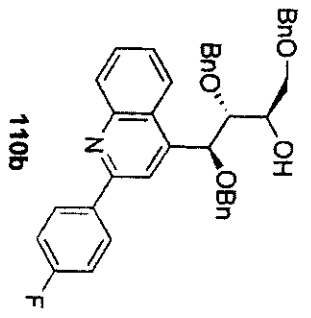


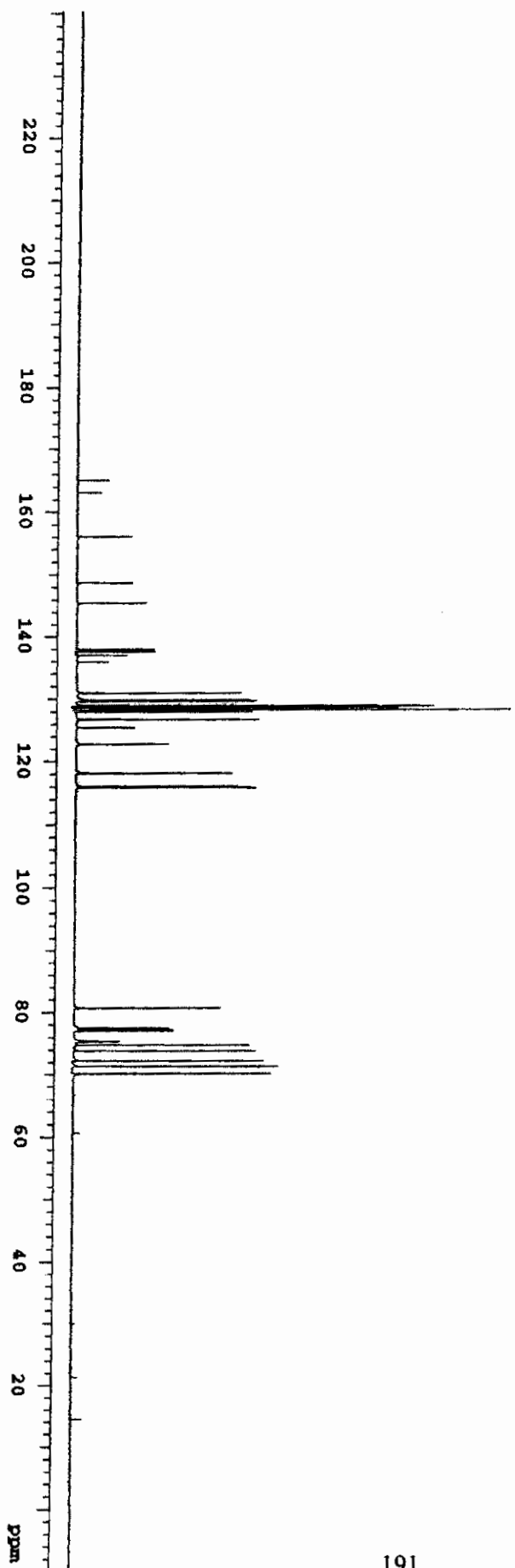
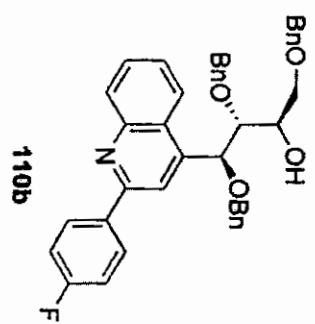
109 isomers

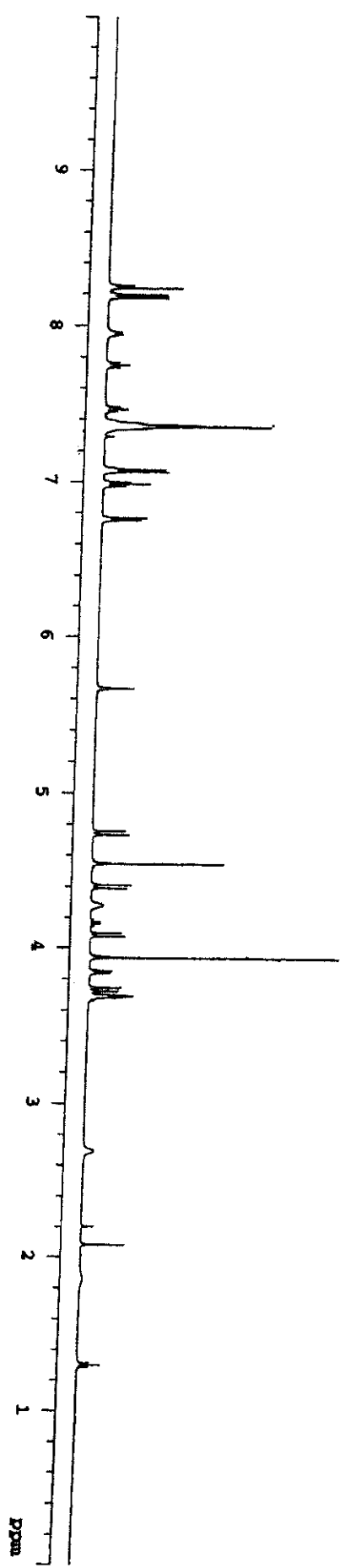
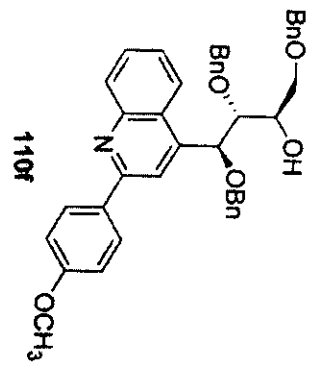


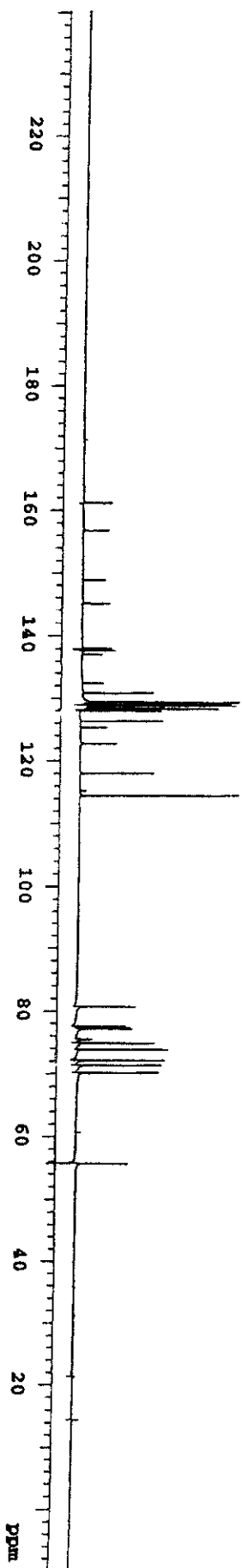
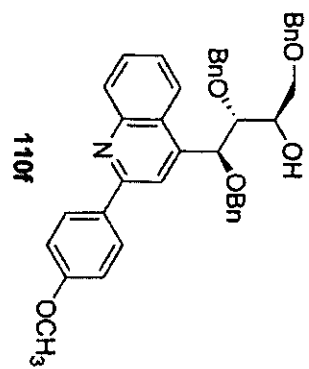


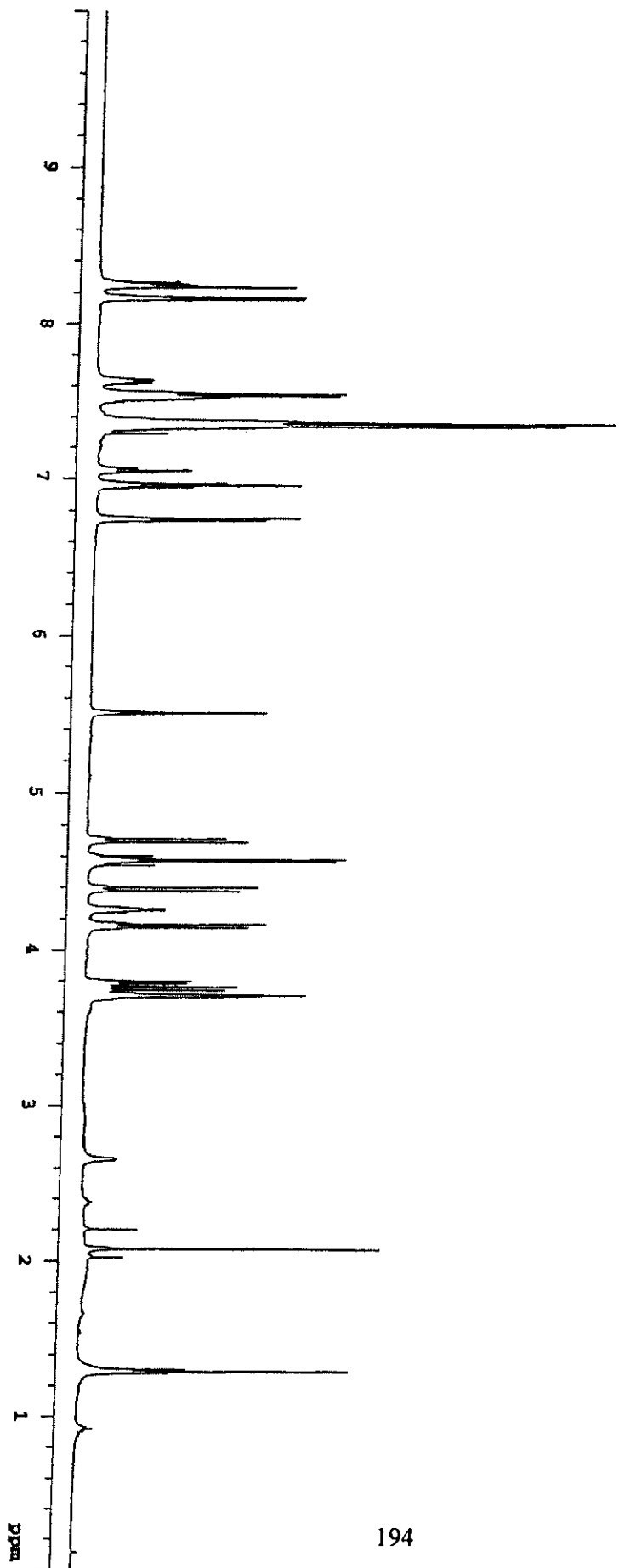
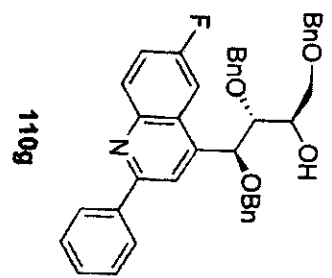


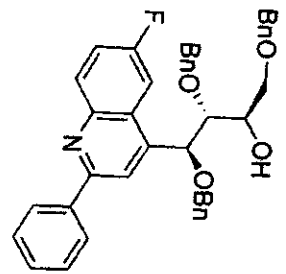












110g

